Molecular genetics and biochemistry of quantitative resistance against *Pyrenopeziza brassicae* in *Brassica napus*

Ajisa Muthayil Ali, BSc., MSc.

Student number: 16017526

Submitted to the University of Hertfordshire in partial fulfilment of the requirements of the degree of Doctor of Philosophy

Research supervisors:

Dr Henrik U Stotz (UH)

Prof Bruce D L Fitt (UH)

Prof Frederic Beaudoin (Rothamsted Research)

School of Life and Medical Sciences, University of Hertfordshire

Hatfield, Hertfordshire AL10 9AB

March 2023

Abstract

The aim of this project was to better understand the molecular genetics and the biochemical components involved in quantitative resistance against *Pyrenopeziza brassicae* in *Brassica napus*. In addition, pathogenicity variations in *P. brassicae* populations and isolates from Aberdeen, Scotland and Hertfordshire, England were assessed to enhance knowledge about the regional sub-populations. Furthermore, resistance of *B. napus* accessions against *P. brassicae* was phenotyped, quantitative disease resistance (QDR) genes against *P. brassicae* were identified by qPCR and potential biochemical components of resistance such as glucosinolates (GSL), cuticular wax and cutin were quantified. To identify novel QDR genes, the resistance phenotyping of 72 *B. napus* accessions done during this study helped to provide complementary data to that from the original test panel, which included 195 *B. napus* accessions. This is the first study which reveals the gene expression patterns of QDR genes associated with resistance and/or susceptibility against *P. brassicae* in *B. napus*.

The results from this study showed that there is a variation in pathogenicity between Aberdeen and Hertfordshire *P. brassicae* populations/isolates. It will be beneficial to analyse sequence variations between isolates from different regions to enhance the current knowledge about the pathogenicity factors in *P. brassicae*. Furthermore, a gene knockdown of the mating type genes of *P. brassicae* can reveal if they are involved in spore size dimorphism and pathogenicity.

The current study helped to provide information about the QDR genes, their potential signalling pathways and the proteins encoded to enhance resistance and or susceptibility against *P. brassicae* in *B. napus*. An early induction of the vesicle trafficking protein, *β-adaptin* and universal stress protein in resistant lines was seen to potentially limit the germination and penetration of *P. brassicae*. Furthermore, *Pathogenesis related protein (PR1)* and *Cinnamate 4 hydroxylase* genes were upregulated to reduce branching and colonisation respectively. In addition, the association of *HXXXD-type acyl transferase* with enhanced pathogenicity of *P. brassicae* in susceptible lines of *B. napus* such as Cabriolet was shown in this study.

This research showed a significantly greater glucosinolate (GSL) concentration in resistant *B. napus* lines/cultivars (Cubs Root, POSH and Dwarf Essex) than in susceptible lines (Cabriolet, Sansibar and Laser). Additionally, concentrations of aliphatic compounds (7-methyl sulfinyl heptyl: 7msh, 3-butenyl: 3but, 4-pentenyl: 4pent, 6-methyl sulfinyl hexyl: 6msh and 5 methylthio propyl:5mtp); indolic compounds (4-methoxy-indolyl-3-methyl: 4moi3m, indolyl-3-methyl: i3m) and an aromatic compound (2pe) were significantly greater in resistant *B. napus* lines/cultivars than in susceptible lines/cultivars.

Epicuticular wax load, its components and their structural variation and cutin monomers enhanced the host resistance against *P. brassicae*. The alkane forming pathway of wax products is negatively correlated with LLS disease severity. This was confirmed by alternate alcohol forming pathway product (1^0 alcohol) content remaining constant in *B. rapa* and *B. napus* resistant lines/cultivars after inoculating with *P. brassicae*. The results indicate a potential involvement of the minor component C30 aldehyde in the signalling defence response to limit the sporulation by the *P. brassicae*. Furthermore, a possible association of cutin monomers with *P. brassicae* pathogenicity was identified.

This study revealed many likely genetic resources in *B. napus,* such as lines POSH, Laser, Moana, Dwarf Essex, SWU Chinese 1 and Cubs Root, which can be used to breed *B. napus* cultivars resistant against *P. brassicae*. All these *B. napus* lines/cultivars showed significantly less LLS disease severity with greater GSL content/higher induction of QDR genes/higher wax and cutin contents. Furthermore, this study confirms the possibility of enhancing the narrow genetic diversity of *B. napus* available to breed for cultivars resistant against *P. brassicae* by introgressing resistance from *B. rapa*.

Acknowledgements

Bismillah-ir-Rahman-ir-Rahim: in the name of God, the merciful and compassionate.

List of publications

Papers in refereed journals:

Fell, H., **Ali, A.M.,** Wells, R., Mitrousia, G.K., Woolfenden, H., Schoonbeek, H., Fitt, B. D. L., Ridout, C.J., Stotz, H. U. (2023), Novel gene loci associated with susceptibility or cryptic quantitative resistance to *Pyrenopeziza brassicae* in *Brassica napus*. *Theoretical and Applied Genetics.* Appendix 29.1.

Stotz, H. U., **Ali, A. M**., de Lope, L. R., Rafi, M. S., Mitrousia, G. K., Huang, Y. J., & Fitt, B. D. L. (2023). *Leptosphaeria maculans* isolates with variations in *AvrLm*1 and *AvrLm4* effector genes induce differences in defence responses but not in resistance phenotypes in cultivars carrying the *Rlm7* gene. *Pest Management Science*, 10.1002/ps.7432. Appendix 29.2.

Paper published in conference proceedings:

Ali, A.M., Fell, H., Fitt, B. D. L., Stotz, H. U., Beaudoin, F., Genetic basis of partial resistance against *Pyrenopeziza brassicae* in oilseed rape. Proceedings AFCP conference: Management of Oilseed Rape Diseases and Pests. 16th June 2021, P 41-42. Appendix 29.3.

Abstracts of presentations at conferences:

1. **Ali, A. M.,** Stotz H.U. & Fitt, B.D.L., (2019). Genetic basis of partial resistance against *Pyrenopeziza brassicae* in oilseed rape. School of Life and Medical Sciences Research Conference, University of Hertfordshire, Hatfield, UK. Poster presentation. 16th April 2019. Appendix 29.4a, b.

2. **Ali, A. M.,** Stotz H.U. & Fitt, B.D.L., (2019). Genetic basis of partial resistance against *Pyrenopeziza brassicae* in oilseed rape. International Rapeseed Congress, Berlin, Germany. 16th- 19th June 2019, Poster presentation. Abstract number 508. Appendix 29.4a, b.

3. **Ali, A. M.,** Stotz H.U. & Fitt, B.D.L., (2019). Genetic basis of partial resistance against *Pyrenopeziza brassicae* in oilseed rape. British Society for Plant Pathology Conference, University of the West of England, Bristol, UK. Arms race, evolution of plant pathogens and their hosts. P17. 2nd-3rd September 2019, Poster presentation. Appendix 29.4a, b.

4. **Ali, A. M.,** Stotz H.U., Beaudoin, F., & Fitt, B.D.L., (2021). Genetic basis of partial resistance against *Pyrenopeziza brassicae* in oilseed rape. School of Life and Medical Sciences Research Conference, University of Hertfordshire, Hatfield, UK. 22nd June 2021, Poster presentation. Appendix 29.5a, b.

5. **Ali, A. M.,** & Stotz H.U., (2021). Genetic basis of partial resistance against *Pyrenopeziza brassicae* in oilseed rape. British Society for Plant Pathology Conference, University of Birmingham, UK. Our plants, our future. 6th-8th December 2021, Oral presentation and poster. P13. Appendix 29.5a, b.

Table of contents

List of figures

List of figures

List of acronyms

AHDB	Agriculture and Horticulture Development Board
BLAST	Basic local alignment search tool
cv.	Cultivar
cvs	Cultivars
dpi	Days post inoculation
df	Degrees of freedom
°C	Degree Celsius
h	Hour
HR	Hypersensitive response
LLS	Light leaf spot
lsd	Least significant difference
MEA	Malt extract agar
MEGA	Molecular evolutionary genetics analysis
μL	Microlitre
min	Minute
mL	Millilitre
1^0 Alcohol	Primary alcohol
2^0 Alcohol	Secondary alcohol
PCR	Polymerase chain reaction
PDA	Potato dextrose agar
qPCR	Quantitative polymerase chain reaction
s	Second
Sd	Standard deviation
SDW	Sterile distilled water
TILLING	Targeting Induced Local Lesions in Genomes
USA	United States of America
UV	Ultraviolet
UK	The United Kingdom of Great Britain and Northern Ireland

| vs | Versus |
| WT | Wild type |

Chapter 1: General introduction

The global food security index is alarming as the global population is forecast to reach 9.1 bn by 2050 (The Economist Group, 2018). World-wide annual crop losses caused by plant pathogens amount to 16% and, of this, 70 to 80% of losses are due to fungal pathogens (Moore *et al.*, 2011; Evans *et al.*, 2010). To meet the food demand, crop production must increase by more than 50% in the next 25 years (Second world seed conference, 2009). Breeding for cultivar resistance to pathogens significantly contributes to alleviate the problems of food security and world hunger.

Light leaf spot (LLS) caused by *Pyrenopeziza brassicae* is the most damaging disease of oilseed rape (*Brassica napus*) in the UK. The disease accounts for up to £160 M yield loss annually in England, despite expenditure of £20M on fungicides, and the severity of the disease is much greater in Scotland (Karandeni Dewage *et al.*, 2018a; Ashby, 1997). In the UK, the disease has been increasing as a national problem in recent decades rather than just being confined to Scotland and Northern England.

LLS is currently controlled by a combination of cultivar resistance, fungicide applications and cultural practices. However, resistance mechanisms of the oilseed rape plant against *P. brassicae* are not understood well. Furthermore, fungicide control is problematic as the pathogen has developed insensitivity to benzimidazole and triazole fungicides (Carter *et al.*, 2014). Carter *et al.* (2014) have reported decreased azole fungicide sensitivity in UK *P. brassicae* isolates. This is concerning, as 75% of the fungicides used contain triazoles. Moreover, in the UK 80% of the oilseed rape crop area receives fungicide applications to control diseases. Thus, it is necessary to understand pathogenicity factors of *P. brassicae* and host resistance of *Brassica napus* to design an improved and durable control strategy against LLS.

1.1 *Brassica napus*: a significant part of UK and world agriculture

Oilseed rape is the third most important arable crop in the UK and second largest source of vegetable oil in the world (Fitt *et al.*, 2006). Rapeseed is currently grown in the northern hemisphere in China, Canada, Europe and India and in the southern

hemisphere in Australia, South Africa and South America as a source of healthy vegetable oil, protein, animal feed and biodiesel.

Rapeseed is one of the most profitable crops in the UK and is an important part of crop rotation, mainly with cereals such as wheat and barley. Since rapeseed is not a host to major cereal pathogens, e.g. *Gaeumannomyces graminis* (take-all), it is an excellent choice for crop rotation. Furthermore, the roots of canola have a bio-fumigation effect as they release biocidal glucosinolates, which is beneficial for the following cereal crops (Norton *et al.*, 1999). *B. napus* tissues contain glucosinolates. When tissues are crushed, they are hydrolysed by the endogenous enzyme myrosinase to oxazolidinethiones, nitriles, epithionitriles, isothiocyanates and various forms of volatile isothiocyanates (Stotz *et al.*, 2014). These products, especially isothiocyanates, have broad insecticidal, nematicidal, fungicidal, antibiotic and phytotoxic effects (Kirkegaard & Sarwar, 1998). Natural isothiocyanates act against development and maturation of *Pseudomonas aeruginosa* biofilm (Kaiser *et al.*, 2017). Glucosinolate breakdown product isothiocyanates inhibit *Arabidopsis* growth (Urbancsok *et al.*, 2017).

Beneficial effects of rapeseed on soil structure and soil moisture infiltration contribute to its important role in crop rotation (West *et al.*, 2001). The large taproot aids in increased water infiltration, whereas the extensive fine root system creates more stable soil aggregates and therefore improves soil structure (Norton *et al.*, 1999).

Rapeseed oil sale in the UK had increased by 24% in March 2017 compared to the previous year (The Daily Telegraph, 2017). However, sales of other popular oils, such as sunflower oil, vegetable oil and the extra virgin olive oil, have decreased by 3%, 12% and 8%, respectively. In addition, rapeseed oil has a lower saturated fat content than any other cooking oil. The smoking point is high compared to olive oil and therefore it is more suitable for frying and roasting. Furthermore, it is rich in vitamin E, omega-3 and omega-6 fatty acids. All these factors contribute to the increasing popularity and the demand for much cheaper and healthier rapeseed oil, in comparison to the other oils such as olive oil. The Kantar World panel, a consumer research group, also confirms the increasing demand for rapeseed oil.

The worldwide production of rapeseed has increased six-fold between 1975 and 2007. Between 1994 and 2017, rapeseed area harvested and crop production increased greatly in global agriculture (Figure 1.1). Europe is the second largest producer of rapeseed (Figure 1.2) and it is an economically important crop in Germany, France, the UK and Poland. (Figure 1.3) (FAOSTAT, 2019).

1.2 Light leaf spot: an economically important disease

Many studies indicate that wet, cold weather favours *P. brassicae* development (Karandeni Dewage *et al.,* 2018a; Figueroa *et al.,* 1995; Fitt *et al.,* 1998b; Gilles *et al.*, 2000). However, the Department for Environment, Food and Rural Affairs (Defra) survey shows that the incidence and severity of LLS has increased progressively in the UK (Figure 1.4) with a substantial yield loss (Figure 1.5), regardless of recent global warming and increasing temperature in the UK and Europe.

P. brassicae is not only pathogenic to *Brassica napus* (oilseed rape) but also infects *Brassica juncea* (Indian mustard), *Brassica oleracea* (Brussels sprouts), *Brassica rapa* subsp*. oleifera* (turnip rape) and *Brassica oleracea* var*. capitata* (cabbage) (www.plantwise.org). LLS can reduce oilseed rape yield by a third, i.e. 30% yield loss for 90% plants affected. Therefore, it is essential to understand the factors that favour disease progression in order to control LLS efficiently.

1.3 Complex life cycle of *Pyrenopeziza brassicae*

P. brassicae is a heterothallic ascomycete with mating types *MAT1* and *MAT2* (Gilles *et al.*, 2001). Figure 1.6 shows a schematic representation of the *P. brassicae* polycyclic life cycle. In the summer after harvest, the infected crop debris becomes the source of primary inoculum for the disease epidemics. The pathogen, which survives as a saprophyte on senesced debris, undergoes sexual reproduction to produce ascospores from mature apothecia. The ascospores are dispersed by wind, land on the leaves of *B. napus* in autumn and initiate polycyclic LLS epidemics. Germinated ascospores enter the host directly through the cuticle (Gilles *et al.,* 2001; Rawlinson *et al.*, 1978). The pathogen then enters a long asymptomatic phase during which it proliferates and colonises subcuticular spaces between the cuticle and epidermal cells.
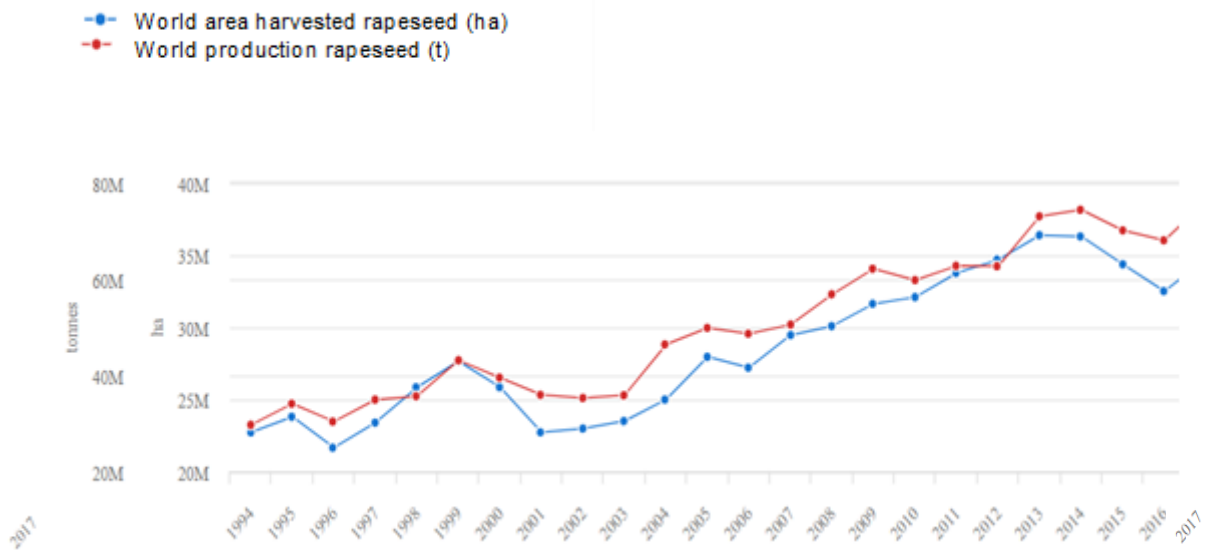
Figure 1.1: Rapeseed area harvested and yield globally between 1994 and 2017 (FAOSTAT, 2019).
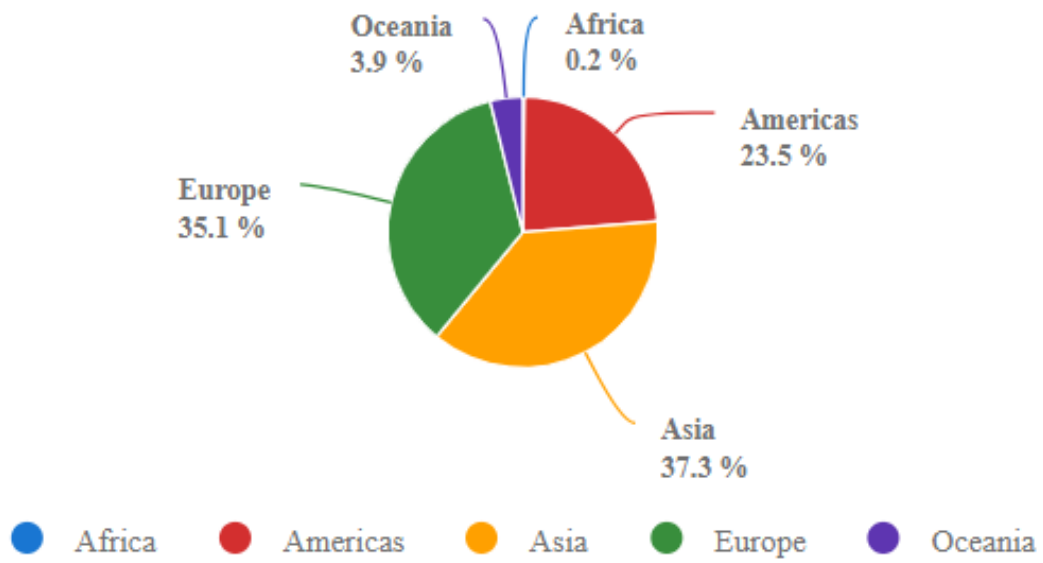
Figure 1.2: Proportion of worldwide rapeseed production by region between 1994 and 2017 (FAOSTAT, 2019).
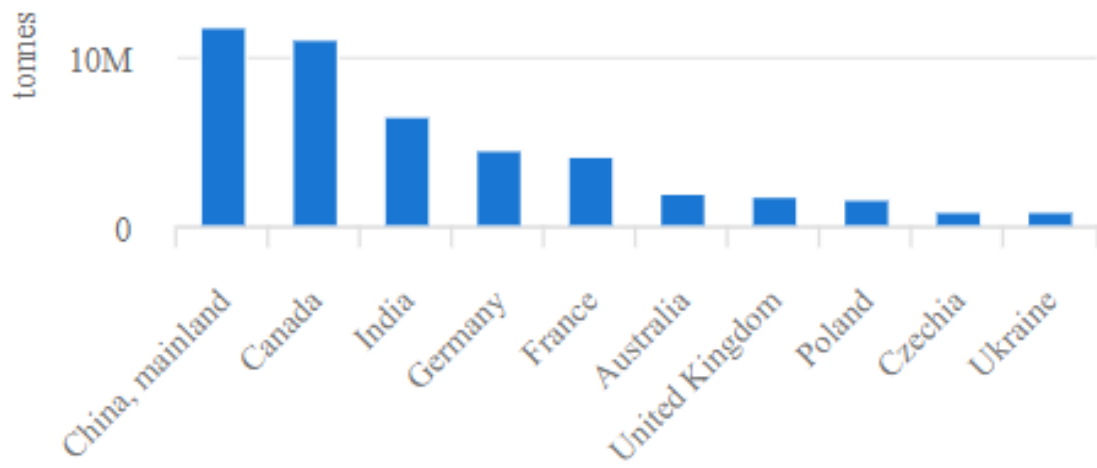
Figure 1.3: Top 10 rapeseed producing countries between 1994 and 2017 (FAOSTAT, 2019).

Figure 1.4: Forecast of light leaf spot incidence (% of plants affected in a region) from 2013 until spring 2020 (West, 2021).
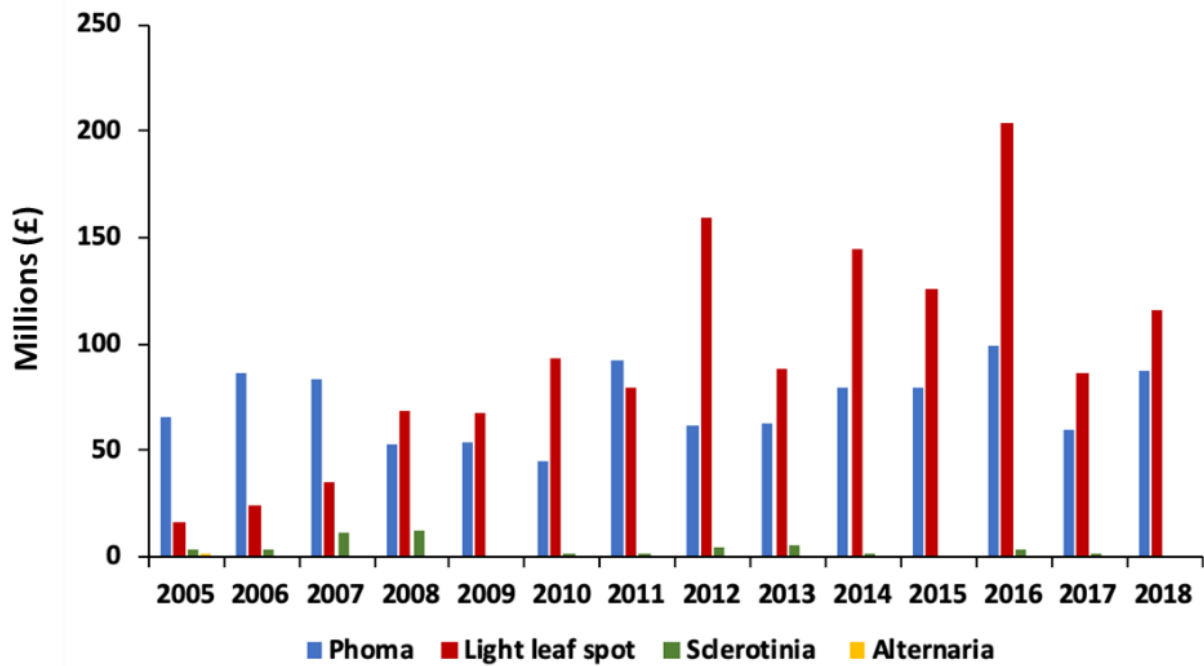
Figure 1.5: Winter oilseed rape yield losses caused by major diseases in England (Phoma in blue, Light leaf spot in red, Sclerotinia in green and Alternaria in yellow) between 2005 and 2018 in millions (£). From 2008 yield loss caused by LLS remains the greatest except for in 2011. CropMonitor; www.cropmonitor.co.uk, oilseed rape pest and disease, The Monitor information service, 2019.
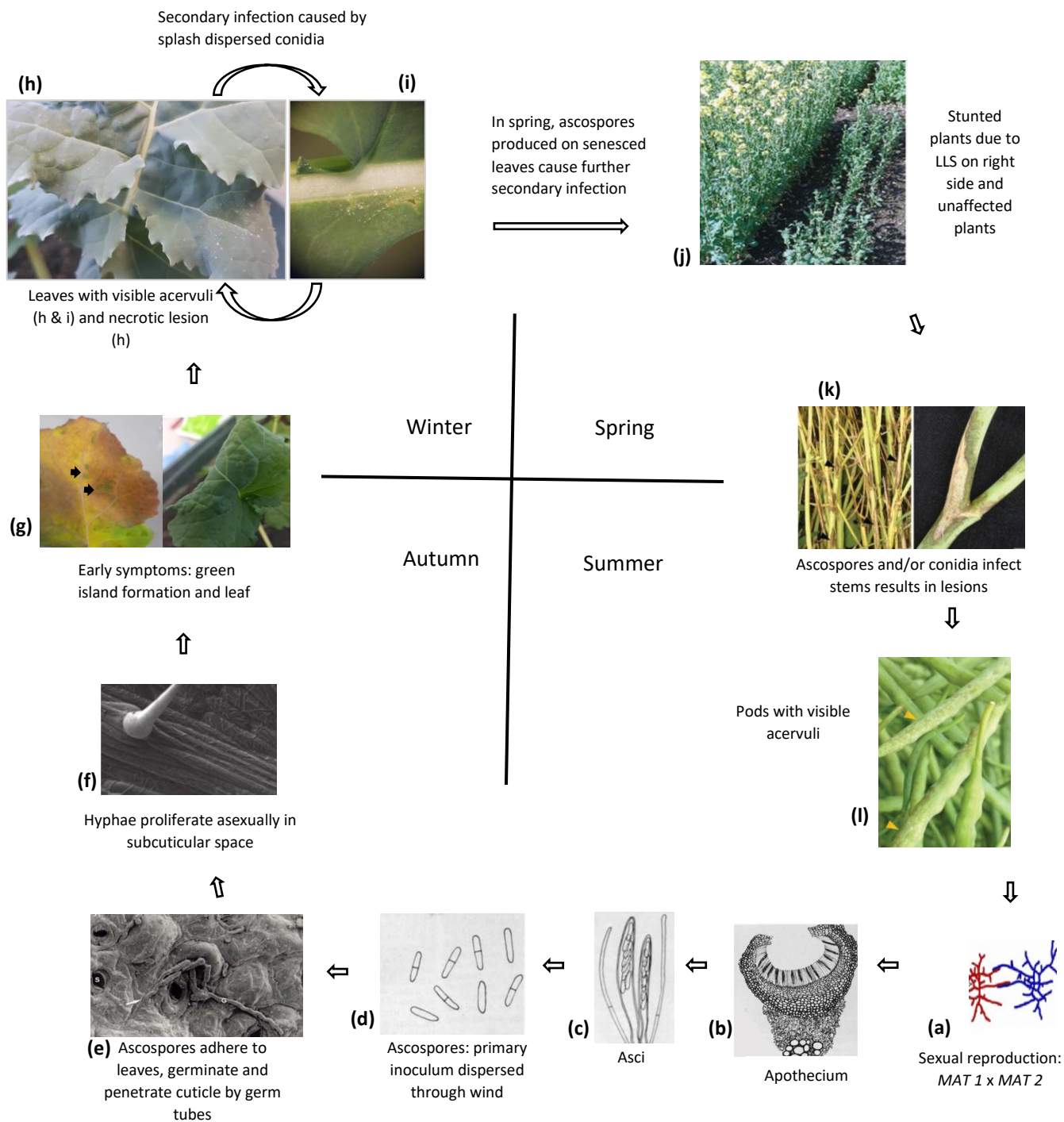
Figure 1.6 Life cycle of *P. brassicae* on winter oilseed rape in Europe (adapted from Cheah *et al.*, 1980; Karandeni Dewage *et al.*, 2018a; Boys *et al.*, 2007). (a) In summer after harvest, the pathogen undergoes sexual reproduction (*MAT 1* x *MAT 2*) on infected crop debris; (b) sexual fruiting body apothecium; (c) asci bearing ascospores; (d) ascospores are released and dispersed by wind; (e) germinated ascospores directly penetrate cuticle; (f) *P. brassicae* proliferates and colonises between cuticle and epidermal cells; (g) leaves showing early symptoms such as green island formation and leaf distortion in susceptible cultivar Cabriolet; (h) susceptible cultivar Eurol with visible acervuli; (i) acervuli on susceptible cultivar Bristol near leaf petiole; (j) LLS infected plants showing stunted growth on the right side uninfected comparison to control plants with normal height on left; (k) infected stems with visible lesions; (l) diseased pods with acervuli.

In winter, when enough biomass has accumulated, the conidiomata rupture through the cuticle and release asexual conidia from acervuli. The acervuli can be visible as white spots arranged in circles, and therefore the anamorph is known as *Cylindrosporium concentricum*.

Rain-splash dispersed conidia serve as secondary inoculum. Furthermore, ascospores produced on infected leaves in spring also promote secondary infection (Boys *et al.* 2007, 2012; Karandeni Dewage *et al.* 2018a). Early ascospore infections in autumn and winter result mainly in leaf distortion, stunting, green island formation and leaf spots (Ashby, 1997). In spring, secondary infection from conidia and ascospores produces stem lesions, premature ripening and pod shattering, which results in yield loss (Fitt *et al.* 1998b; Rawlinson *et al.*, 1978). *P. brassicae* not only infect *B. napus* but also affect *B. oleracea, B. rapa* and other related *Brassica* species or subspecies. These include Brussels sprouts (*B. oleracea* var. *gemmifera*), cabbage (*B. oleracea* var. *capitata*), cauliflower (*B. oleracea* var. *botrytis*), broccoli (*B. oleracea* var. *italica*), kale (*B. oleracea* var. *acephala*), turnip (*B. rapa* ssp. *rapa*), swede (*B. rapa* ssp. *rapifera*), Chinese cabbage (*B. rapa* ssp. *pekinensis*) and black mustard (*B. nigra*) (Karandeni Dewage *et al.*, 2018a)

1.4 Control measures and limitations

In the UK, the disease is mainly controlled by fungicide applications and host resistance (Fitt *et al.*, 1998a). Due to the subtle onset of the disease, it is extremely difficult to optimise the fungicide treatment timing. A study done in 2017-2018, with aid from the Agricultural Development and Advisory Service (ADAS) and the Association of Independent Crop Consultants (AICC), showed that both growers and ADAS identified LLS in 23% of samples. However, another 33% of the samples, which were not initially identified by the growers, were later confirmed to have the disease (Bayer, 2018).

Double fungicide treatment, once in late-autumn (November/December) followed by second application at the beginning of stem extension (January-March), has been found to give efficient control of LLS. However, there are many reports of fungicide insensitive isolates of *P. brassicae* (Boys *et al.*, 2007; Carter *et al.*, 2013; Carter *et al.*, 2014; Fitt *et al.*, 1998a; Gilles *et al.*, 2000).

The most effective and environmentally friendly way to control the disease is by deploying resistance genes. Qualitative resistance can work mainly in a 'boom and bust' manner. Substantial increases in the cultivation of lines/cultivars with specific resistances moulded pathogen populations to evolve and emerge as virulent. In addition, the polycyclic *P. brassicae* life cycle, with sexual reproduction and a wide host-range, increases the potential to produce genetic variation and virulent races quickly. Cultivar resistance shifts have been observed in the past. For example, resistant Recital and Bristol suddenly changed to susceptible; whereas cultivar Apex gradually lost its resistance (Boys *et al.*, 2007). In 2012-2014, the resistance of cultivar Cracker had broken down in Scotland. Quantitative disease resistance (QDR) also known as minor gene resistance is more durable than *R* gene-mediated resistances and exerts less selection on pathogen. Therefore, exploiting QDR will be the way forward to efficiently control the disease.

1.5 Quantitative and qualitative resistance in *Brassica napus*

Use of cultivar resistance is the most important and economical method to control LLS. In *B. napus,* both multi-genic QDR and mono-genic qualitative resistance against *P. brassicae* have been identified. Table 1.1 summarises the quantitative and qualitative resistances identified so far. Pilet *et al.* (1998) identified six environmentally stable quantitative trait loci (QTLs) in a doubled haploid (DH) population derived from the cross between moderately resistant Darmor-bzh and susceptible Yudal lines. Bradburne *et al.* (1999) reported two major resistance loci named as *PBR1* and *PBR2*, positioned on linkage groups A01 and C06 respectively. The resistance was introgressed into winter oilseed rape from wild accessions of *B. oleracea* and *B. rapa*. *PBR1* derived from *B. rapa* gave a phenotype with no apparent symptoms, while *PBR2* from *B. oleracea* showed black necrotic flecking and reduced asexual sporulation. Furthermore, Boys *et al.* (2012) characterized a major *R* gene-mediated resistance phenotype against *P. brassicae* in a DH mapping population. Resistance from Bradburne *et al.* (1999) materials was introgressed into the cultivar Imola and the resistance further used to develop a DH population. This *R* gene (*PBR1*) mediated resistance resulted in black flecking by 8 days post inoculation (dpi) and no asexual sporulation. However, this did not prevent sexual reproduction once the leaves had senesced. Karandeni Dewage *et al.* (2022) identified four QTLs involved in QDR of

Table 1.1: Known resistances against *P. brassicae* in *Brassica napus*

Resistances in *B. napus*
o Pilet *et al.* (1998) identified 6 QTLs involved in field resistance to *P. brassicae* at linkage groups A02, A06, A07, A09 and C04.
o Bradburne *et al.* (1999) identified 2 major resistance loci on chromosomes A01 and C06.
o Boys *et al.* (2012) characterised a major resistance locus on chromosome A01.
o Karandeni Dewage *et al.* (2022) identified 4 QTLs at C01, C06, C09. Two of these QTLs were identified on the same chromosome (C06).

B. napus against *P. brassicae* where the C01 QTL reduce the asexual sporulation of the fungus significantly.

1.6 Pathogenicity factors in *Pyrenopeziza brassicae*

Li *et al.* (2003) demonstrated the involvement of *P. brassicae Pbc1* in cuticle penetration and disease symptom development or pathogenicity. Batish *et al.* (2003) showed the presence of an extracellular protease *Psp1* during the growth of *P. brassicae* in *B. napus*. *Psp1* may promote pathogenicity by breaking down *B. napus* intercellular matrices and thereby facilitating space for subcuticular growth. Other potential roles of *Psp1* include degrading plant signalling proteins involved in resistance responses or degrading host cell wall or cell membrane proteins to derive nutrients from the apoplast. Ashby (1997) reported the possible involvement of cytokinins as pathogenicity factors by providing nutrients to the pathogen by altering host metabolism and diverting nutrients to the infection site. Furthermore, Ashby (2000) showed rapid pathogen growth and premature cuticular rupture in hosts with constitutive expression of iso-pentenyl transferase (*ipt*) in *P. brassicae* from *Agrobacterium*, an enzyme involved in cytokinin synthesis. Potential pathogenicity factors in *P. brassicae* are shown in Table 1.2.

1.7 Potential resistance mechanisms in *B. napus* against *P. brassicae*

QDR may act during ascospore adhesion, germination or cuticular penetration. Since this is the very first stage of the interaction between the host and the pathogen, QDR may be related to pathogen associated molecular pattern triggered immunity (PTI). Host cuticular wax composition may affect the germination and penetration of the pathogen. *P. brassicae* does not induce a hypersensitive response in the host soon after pathogen invasion (Stotz *et al.*, 2014). During its subcuticular growth (between cuticle and epidermal cells), major gene-mediated resistance/s or QDR may inhibit hyphal proliferation. *R* gene-mediated resistance may act to prevent production of acervuli or asexual reproduction. Finally, either quantitative and or qualitative resistance may be able to inhibit or to reduce the sexual reproduction. Figure 1.7 illustrates the potential operation of quantitative and qualitative resistance in *B. napus* during various stages of the *P. brassicae* life cycle.

Table 1.2: Known pathogenicity factors in *Pyrenopeziza brassicae* operating against brassicas.

Pathogenicity factors in *P. brassicae*
○ Extracellular cutinase *Pbc1* (Li *et al.*, 2003).
○ Extracellular protease *Psp1* (Batish *et al.,* 2003).
○ Cytokinin produced by *P. brassicae* to suppress the host cell death (Ashby, 1997)

QDR? possible phytotoxins in cuticular wax inhibit *P. brassicae* ascospore adhesion, germination and cuticle penetration. Cutinase inhibitor expression inhibits cutinase activity and cuticular penetration. Some individual lines from Q doubled haploid mapping population have shown reduced fungal sub-cuticular colonisation and growth, indicating reduced penetration (Karandeni Dewage, 2018b).

Ascospore adhesion,
germination and
cuticular penetration

QDR? Proteases/plant cytokinins (Ashby *et al.*, 2000) prevent growth of the pathogen.
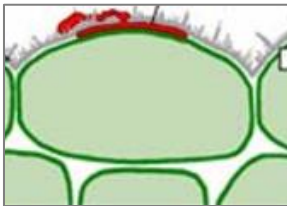
P. brassicae subcuticular growth
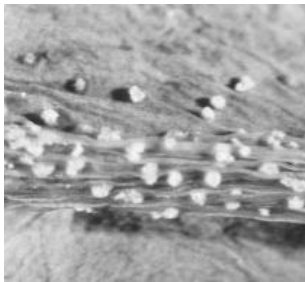
R? Possible major gene/s act to prevent asexual sporulation. Cultivar Imola showed reduced asexual sporulation and black flecking resistant phenotypes (Boys *et al.*, 2012).

Asexual sporulation (conidia)

QDR? quantitative and/or qualitative resistance may be involved in preventing sexual reproduction and ascospore formation.
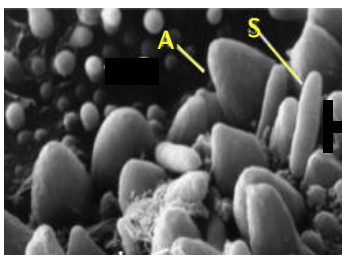
Sexual reproduction and
ascospore formation
(A) Asci and (S) ascospores

Figure 1.7: Operation of possible sources of quantitative (QDR) and qualitative (R gene) resistance in *B. napus* against *P. brassicae* life cycle progression. Images adapted from Boys *et al.* (2007) and Gilles *et al.* (2001).

1.8 Aims and objectives

LLS is an economically important disease in Northern Europe. Yet little is known about the genetic variation in the pathogen or the genetic basis of host resistance. This project will benefit UK and European agriculture by decreasing risk of LLS epidemics through improved understanding of resistance against *P. brassicae.* Breeders and growers will be able to breed and select lines with efficient resistance against *P. brassicae.* In addition, this project will enlighten other researchers about host resistance mechanisms against apoplastic fungi. Thus, this project aims to improve the current knowledge of crop resistance mechanisms against *P. brassicae.* This will further benefit breeders, growers and ultimately the community through reduced use of fungicides.

The specific objectives are:

1. To understand *P. brassicae* population and isolate variation between Hertfordshire, England and Aberdeen, Scotland.
2. To better understand the genes involved in quantitative resistance operating against *P. brassicae* in *B. napus.*
3. To study the role of the biochemical compounds such as glucosinolates and cuticular wax/cutin in resistance of *B. napus* against *P. brassicae.*

Chapter 2: General materials and methods

2.1 Media preparation for *P. brassicae* germination and growth

All media were autoclaved at 121 °C for 15 min and prepared in a fume hood.

2.1.1 Malt extract agar (MEA)

7.5 g of malt extract (Oxoid LP0039, UK) and 15 g of agar powder (Oxoid LP0011) were mixed in a glass bottle with a screw cap and autoclaved. When it had cooled down to 50°C, streptomycin and penicillin (50 µg/mL or 500 µL each) were added, and then poured into 9cm diameter labelled Petri-dishes.

2.1.2 Potato dextrose Agar (PDA)

39 g PDB (Sigma Aldrich 70139, UK) was mixed in 1L deionized water and autoclaved. 50 µg/mL each of streptomycin and penicillin were added once it had cooled down to 50°C.

2.2 Growing *Brassica napus* in a controlled environment for true leaf inoculation experiments

2.2.1 *B. napus* seed germination

In a labelled Petri-dish Whatman filter paper was laid and soaked with deionized water. The seeds were placed on filter paper by using an aseptic tweezer and incubated for 48 h in the dark at $20^{°C}$.

2.2.2 Planting of pre-germinated seeds into soil

A 50:50 ratio of Arthur Miracle-Gro and John Innes 3 composts (UK) was mixed and clots were broken to make it smooth. A 40 well seed tray was filled with the compost mixture and a small hole was made in each well with a small finger. Pre-germinated seeds were sown and covered with vermiculite to increase soil aeration and porosity. The wells were placed in an outer tray with soaked capillary sheets to maintain the water content. Content labels showing the name, date and experiment were attached

to the trays. Plants were incubated in a controlled environment cabinet (FITOCLIMA D1200; ARALAB, Portugal) at 20$^{\circ C}$ in light for 18 h and 18$^{\circ C}$ in dark for 6 h. This long daylight setting increased growth rate of the plants. Seedlings reached growth stage 1,0-1,1 (Sylvester-Bradley *et al.* 1984) and were transferred into 9 cm diameter pots with the same compost mixture. They were incubated at the same temperature and light settings until they reached growth stage 1,3-1,4 or 1,4-1,5 and were ready for inoculation. Appendix 1 illustrates the key growth stages in oilseed rape.

2.3 Diseased leaf washing and *P. brassicae* population conidial suspension preparation

B. napus leaves with light leaf spot symptoms were chosen, discarding leaves with any other disease symptoms. To induce the sporulation, leaf samples were covered in a wet tissue and then sealed in a labelled polyethylene bag and incubated at 4 °C for 3-6 days (Figure 2.1a). Visible conidia were washed into a 500 mL beaker by pipetting 1 mL (varied depending on amount of sporulation) of sterile distilled water. Spores were collected, based on the location (Rothamsted, UK in 2019). Collected spore suspensions were filtered using autoclaved Whatman filter paper (Figure 2.1b) and the spores were counted using a Bright-Line haemocytometer under a stereomicroscope (GX Microscopes, XTC-3A1) to determine concentration. Inoculum was diluted to 10^5 spores/mL with sterile distilled water and stored at -20 °C as 10 mL aliquots, until required. A few aliquots were stored at -20 °C with 20% sterile glycerol.

2.4 *P. brassicae* spray inoculation method

10^5 spores/mL conidial inoculum were used for spray inoculation. A surfactant Tween 80 (0.005%) was added to the suspension before spraying onto the leaves. Each plant was sprayed with 1.2 mL suspension using a spray bottle until the leaves were covered (Figure 2.2a). Sprayed plants were covered with transparent polyethylene sheets (Figure 2.2b) and incubated for 48 h to enhance humidity to facilitate *P. brassicae* infection. Plants were incubated at 16 °C for 12 h in daylight and 14 °C for 12 h in the dark. Furthermore, to check the germination rate, 100 μL and 200 μL of 10^5 spores/mL conidial suspension were spread onto MEA plates and incubated at 15 °C in the dark.

Figure 2.1: Conidial inoculum preparation. (a) Harvested leaf samples covered in wet tissue to induce asexual sporulation and incubated at 4 °C for 3-6 days. (b) Sterile Whatman filter paper fitted into autoclaved funnel to filter conidial suspension prepared from diseased leaf wash

Figure 2.2: Spray inoculation with *P. brassicae* conidial suspension (a) *B. napus* lines spray inoculated with 10^5 spores/mL *P. brassicae* conidial inoculum (b) Spray inoculated plants covered with transparent polyethylene sheets for 48 h to increase humidity to facilitate *P. brassicae* conidial germination and infection.

2.5   Spore counting

After 21 dpi, infected leaves were selected and incubated at 4 °C for 3-6 days to induce sporulation. Conidia produced on leaves were washed by adding 1 mL sterile distilled water. Spore suspensions were filtered through sterile Miracloth (Merck Millipore, Watford, UK) and the concentration of each spore suspension was measured using a Bright-Line haemocytometer.

2.6   Spot inoculation

A 10^5 spores/mL conidial suspension was prepared (section 2.3). Sterile Whatman filter paper was cut into squares of 0.8 mm x 0.8 mm and they were immersed in the conidial suspension using a sterile tweezer. These were placed onto the marked spaces of third or fourth *B. napus* true leaves. Plants were covered with polyethylene sheets to increase the humidity.

2.7 Growing *Arabidopsis thaliana* in a controlled environment and spray inoculation with *P. brassicae*

A. thaliana ecotypes were transferred into small pots with a 50:50 ratio of Arthur Miracle-Gro and John Innes 3 compost mix using a P20 pipette. Water was pipetted onto each seed, which was kept in a glass bowl (Figure 2.3 a, Figure 2.3 b). Seed trays with wet capillary matting to facilitate watering were incubated at 4 °C for 4 days or until germinated (Figure 2.3c). Plants were grown in a controlled environment cabinet (FITOCLIMA D1200; ARALAB) for 21 days (Figure 2.4 a) and spray inoculated. Inoculated plants were covered with tray covers sprayed with water to increase humidity for 48 h (Figure 2.4 b) and incubated at 16 °C for 12 h in the daylight and 14 °C for 12 h in the dark for analysis.

2.8 Trypan blue staining

An ethanol and chloroform mixture (3:1, v/v) was added to labelled 55mm diameter Petri dishes. Spot inoculated *B. napus* leaf discs or whole spray inoculated *Arabidopsis thaliana* leaves were put into the Petri dishes (Figure 2.5a) and left for 16 h to remove chlorophyll. Figure 2.5b shows the leaves after removal of the pigments.

Leaves or leaf discs were removed using forceps, washed with sterile water (Figure 2.5c), dried with Whatman filter paper (Figure 2.5d) and immersed in 0.025% trypan blue solution in 55mm diameter Petri dishes for 4 h (Figure 2.5e). Stained leaves were washed, dried, mounted on a labelled glas slide with 70% droplet of glycerol and covered with a cover slip (Figure 2.5f).

2.9   DNA extraction for regular PCR and qPCR assays

Infected leaf samples freeze-dried in liquid nitrogen were ground into fine powder using a mortar and pestle. Genomic DNA (gDNA) was extracted from 20 mg powdered sample using a DNA extraction kit (DNAMITE plant kit, Microzone Ltd., UK). An extra step was added to the manufacture's protocol at the beginning (1 mL cell lysis solution/solution LA and three metal beads of 3 mm diameter each were added into the leaf samples, vortexed and procesed in a FastPrep machine (MP Biomedicals, UK) at speed level 4 for 30 s). Based on the DNA pellet size, samples were re-suspended in 40-80 µL of sterile nuclease free water (Promega). The DNA concentration was calculated using a Nanodrop ND-1000 spectrophotometer (Labtech International, UK) and samples were diluted to a final concentration of 50 ŋg µL with sterile distilled water and and stored at -20 °C for further qPCR analysis.

2.10 qPCR to quantify pathogen DNA

To quantify *P. brassicae* DNA from infected plants, 50 ng of DNA from each leaf sample and PbITSF and PbITSR primers (Karolewski *et al.*, 2006) were used. A reaction mixture of 20 µL was prepared (Table 2.1). To plot a standard curve, five *P. brassicae* DNA dilutions, ranging from 1pg to 10000pg, were included as standards. Sterile distilled water was used as negative control instead of DNA template and as a positive control 1ng *P. brassicae* DNA was used. Well plates were covered with cap strips and centrifuged for 1 min before running in a Mx3005 qPCR instrument (Agilent technologies, UK). PCR conditions were as follows:

Segment 1: An initial denaturation temperature for 2 min at 95°C.

Segment 2: 50 cycles each of 15 s at 95°C, 45 s at 58°C, 45 s at 72°C and a data collection step of 15 s at 84°C.

Segment 3: Final extension step at 95°C for 1 min, 58°C for 30 s and 95°C for 30 s.

Internal transcribed space region primer sequences with an expected amplicon size of 461 bp are given below (Karolewski *et al.*, 2006).

PbITS (F): 5′-ttg aac ctc tcg aag aag ttc agt ct-3′

PbITS (R): 5′-aga ttt ggg ggt tgt tgg cta a-3′

2.11 Scanning electron microscopy (SEM)

Sample preparation: For low temperature investigation, samples were prepared by using a 2100 Galton Alto cryo preparation system according to the manufacturer's protocol (Gatan, UK). From the spot inoculated area, 0.5 – 1 cm^2 discs were dissected out using a sterile blade and mounted with a 1:1 mixture of colloidal graphite (TAAB) and Tissue Tek (Sakura) onto a SEM stub. The samples were freeze-dried using liquid nitrogen and transferred into the preparation chamber using a vacuum transfer device. Samples were fixed at -90°C for two min and coated with gold for one min.

SEM imaging: A JEOL 6360 Low Vacuum Scanning Electron Microscope at 10kV accelerating voltage, spot size of 38, and a working distance of 15mm and signal detected with a sary electron detector was used to image the samples. Digital micrographs were produced using JEOLSEM Control User Interface Version 6.04.

2.12 Plant RNA extraction and cDNA synthesis for qPCR assessments

Leaf samples were freeze-dried in liquid nitrogen and ground into powder by shaking for 1 min at 27.5 frequency in a FastPrep crushing machine (MP Biomedicals, UK) with three sterile metal beads (3 mm diameter). E.Z.N.A.® Plant RNA kit from Omega Bio-tek was used to extract total RNA from inoculated leaves following manufacturer's instructions. RNA samples were treated with RNase-free DNase set (Omega Bio-tek, UK) to avoid DNA contamination and concentration was determined using a nanodrop. cDNA synthesis was done using a qPCR Bio cDNA synthesis kit (PCR biosystems).

2.13 Agarose gel electrophoresis

2% agarose gel was prepared in 1xTE buffer and 10 µl of each sample (PCR products), 5 µL of the 100 bp DNA ladder (Sigma Aldrich) and a negative control were loaded into each well. Gel was run for 90 min at 75 V and the Gel Red Nucleic acid gel stain (Agilent) was added before visualising under UV light.

Figure 2.3: Sowing *Arabidopsis thaliana* into compost. (a) *A. thaliana* seeds. (b) *A. thaliana seeds* in a glass bowl to prevent sticking, water and pipette to aid transferring seeds into compost. (c) Germinated *A. thaliana* ecotypes after 4 days.

Figure 2.4: Spray inoculation of *Arabidopsis thaliana* (a) *A. thaliana* ecotypes (Ws-0, Nd-1 and Col) ready for spray inoculation (b) Spray inoculated *Arabidopsis thaliana* plants covered with tray cover to increase humidity.
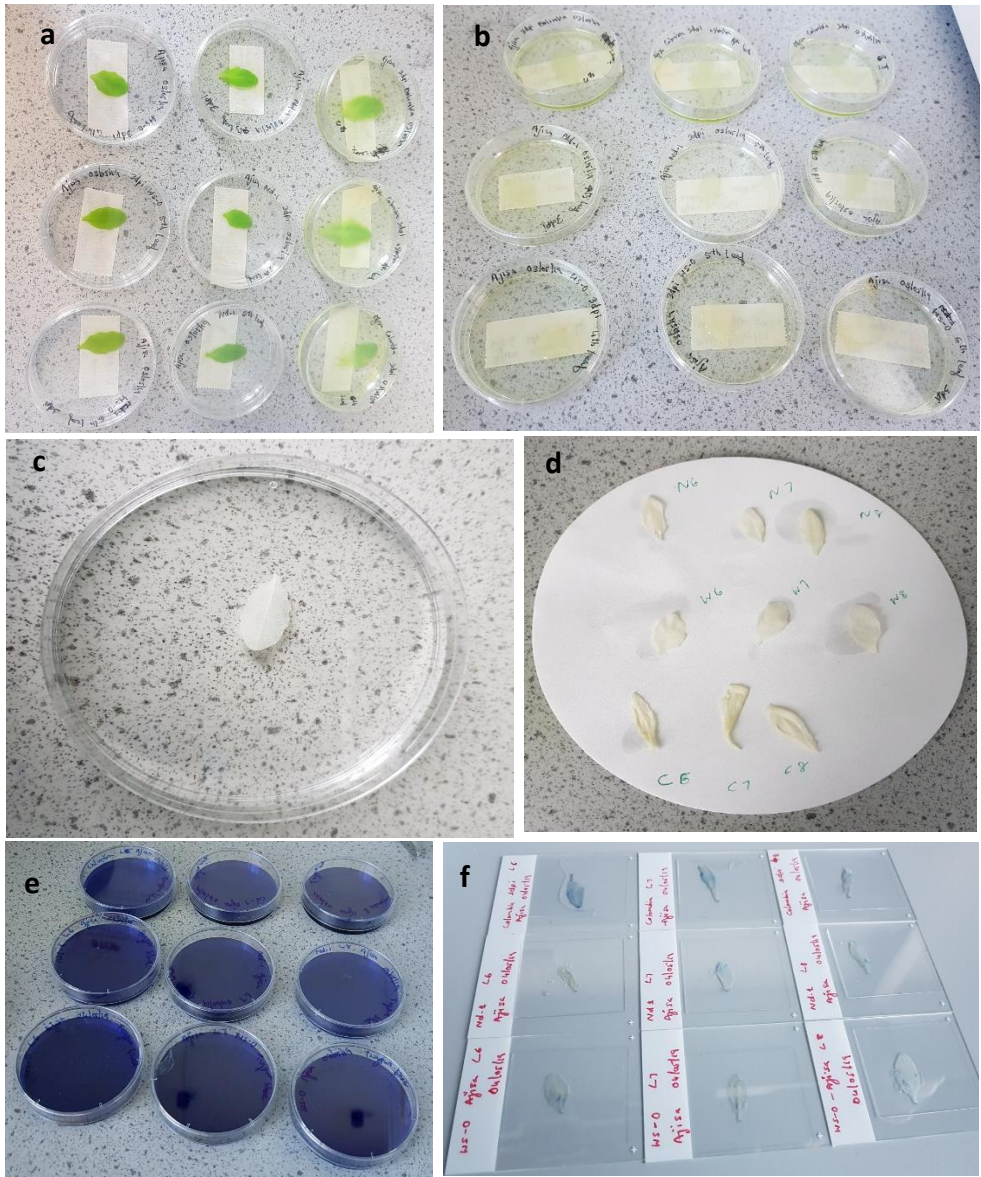
Figure 2.5: Trypan blue staining (a) *A. thaliana* leaves immersed in an ethanol-chloroform mixture to remove the chlorophyll (b) *A. thaliana* leaves after removal of chlorophyll using an ethanol-chloroform mixture. (c) leaves with pigment removed were washed using sterile water and (d) dried on Whatman filter paper (e) *A. thaliana* leaves in trypan blue stain (0.025%) to stain *P. brassicae* hyphae (f) Trypan blue stained *A. thaliana* leaves mounted onto glass slides with a drop of 70% sterile glycerol for analysis under a microscope.

Table 2.1: *P. brassicae* DNA qPCR, amounts of qPCR reagents added in each 96 well plate to quantify *P. brassicae* DNA from plant gDNA (final reaction mixture volume of 20 µL).

Reagents/Samples	Amount in µL
Brilliant III ultra-fast SYBR Green qPCR mix	10 µL
sterile distilled water	6.3 µL
Primers (PbITSF and PbITSR)	0.3 µL each (10 µM)
Template DNA	2.5 µL (20 ɳg µL)

Chapter 3: Regional variation in pathogenicity of *Pyrenopeziza brassicae* populations

3.1 Introduction

Despite use of many control practices, the incidence and severity of the light leaf spot disease and subsequent yield loss have substantially increased in England from 2005 – 2018 (Figure 1.5). In England, LLS became the cause of greatest yield loss in oilseed rape in 2008 and it has remained the most damaging disease of oilseed rape in the UK since then (Figure 1.5). Plant pathogen populations continually adapt to survive in changing environments, and are affected by factors such as crop resistance, fungicides, crop rotation, climate change and irrigation. Pathogen populations with high evolutionary potential can greatly affect durability of crop resistance against them (McDonald & Linde., 2002b). *P. brassicae* has both asexual and sexual reproduction systems, a large population size and is polycyclic; all these factors contribute to a high evolutionary potential for this pathogen (Karandeni Dewage *et al.*, 2018a; McDonald & Linde., 2002a). The evolutionary history of a population determines the genetic structure of individual populations. Disease resistance breakdown is due to the evolution of pathogen populations because of natural selection of mutants, recombinants and/or immigrants that can circumvent host resistance. Better understanding of pathogen evolution will generate more information on genetic mechanisms underlying resistance breakdown (McDonald & Linde., 2002b). Expansion of geographical distribution and increased virulence are major reasons for recent plant disease outbreaks (Hubbard *et al.*, 2015). Therefore, understanding population genetics of a pathogen is crucial for developing durable resistance breeding.

3.1.1 Factors affecting geographical variation in LLS severity

3.1.1.1 Variations in pathogen populations

An important factor that may affect the geographical variation in severity of LLS epidemics, apart from weather conditions, is variation in populations of the pathogen. Pathogen population genetics deal with allele or genotype frequencies within or among

populations in a species. They unravel genetic developments, such as mutation, gene flow, genetic drift, mating systems and natural systems, that lead to evolution or genetic change in populations over time and space (Sork, 2016). Evolutionary forces, such as mutation, genetic drift, gene flow, natural selection and mating systems of pathogens influence the pathogen population structure and genetics (McDonald & Linde., 2002b; Barrett *et al.*, 2008).

Gene flow and natural selection are the main but opposing causes of genotypic and phenotypic differenes in a pathogen population at various geograpical locations (Sork, 2016). Gene flow maintains the genetic variation through distribution and homogenization. However, natural selection minimises variants by selecting one that can survive and reproduce. A pathogen can mutate or alter its nucleotide sequence spontaneously and randomly. Natural selection favours the survival of these mutants to circumvent host plant resistance. Thus, mutation plays an important role in evolution as it introduces new alleles into a population. Larger populations tend to have larger numbers of mutations and allelic variations. Genetic diversity increases with the sexual reproduction system. Therefore, overall genetic diversity of a pathogen population decreases if one or two isolates are selected by natural or artificial selection (McDonald & Linde, 2002b). Pathogens with both sexual and asexual reproduction systems and high degrees of gene flow have a high potential to become virulent. Deploying quantitative resistance will be the best strategy to control this type of pathogen, including *P. brassicae* (McDonald & Linde, 2002b).

Majer *et al.* (1998) showed that *P. brassicae* tends to form subpopulations between geographical regions within UK, even though gene flow can be amplified with wind dispersed ascospores and rain-splash dispersed conidia. This suggests the absence of long-distance movement of *P. brassicae* conidia. Furthermore, the study using neutral markers showed that there was no significant population variation between England and Scotland. However, differences in disease progression across various locations and between growing seasons have been observed (Karandeni Dewage *et al.*, 2018a). Furthermore, the AHDB Cereals and Oilseeds (2017) Recommended List advises deployment of different lines in the East/West and North regions of the UK (http://cereals.ahdb.org.uk/ varieties/running-the-recommended-lists.aspx). This
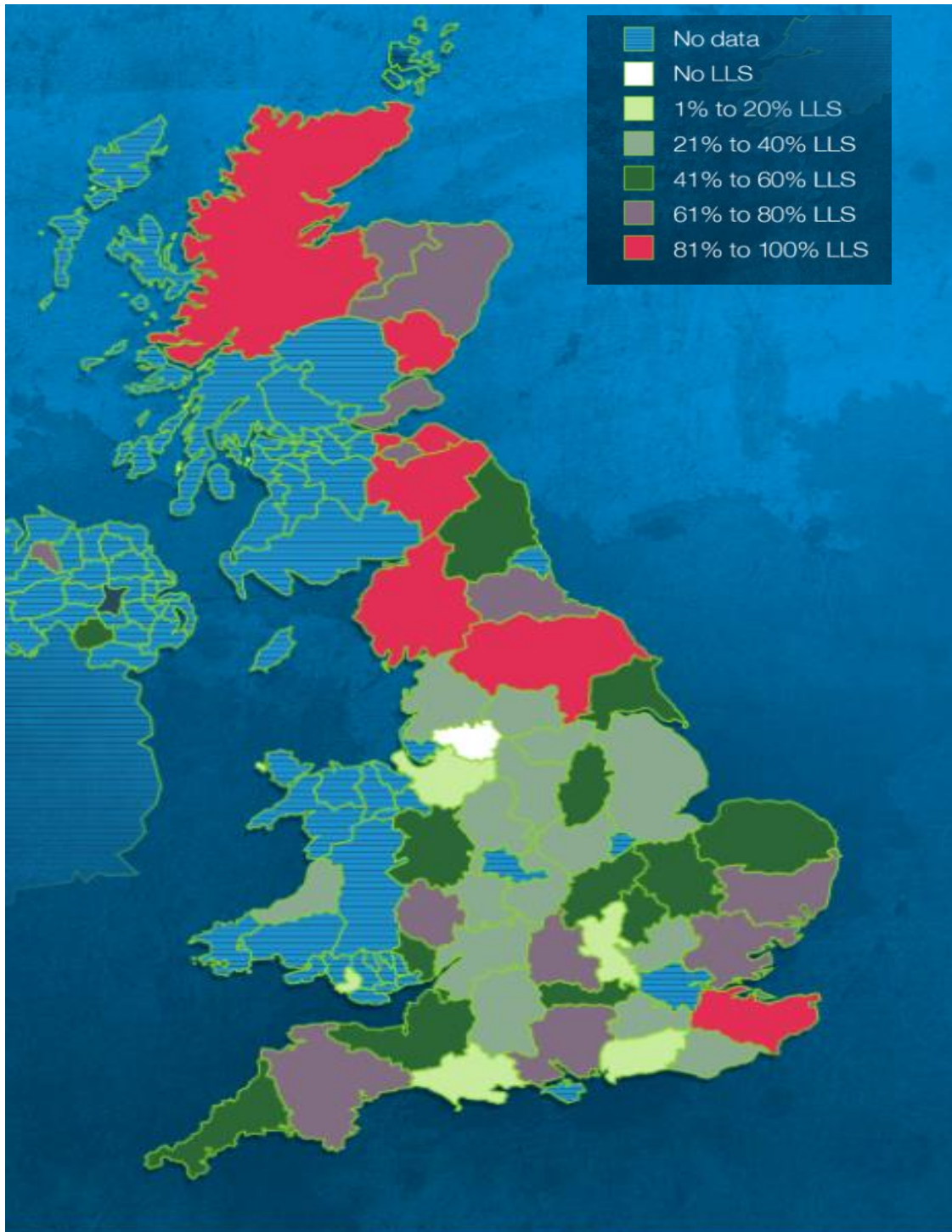
Figure 3.1 Regional variation in light leaf spot incidence (% plants affected) in the UK from October 2021 untill March 2022 (www.cropmonitor.co.uk).

indicate that there may be *P. brassicae* population variations across the UK (Evans *et al.*, 2017). Figure 3.1 shows the variation in LLS incidence between England and Scotland. Therefore, this chapter aims to analyse the pathogenicity differences between *P. brassicae* populations and isolates from different regions. It is important to understand regional isolate and or population pathogenicity differences to develop a rational method to control the entire national pathogen population.

3.1.2.2 Weather differences

Geographical variation in LLS incidence and severity are clearly influenced by weather. Southern parts of UK have higher temperatures and lower rainfall than Northern regions. Figure 3.2 shows the annual mean average temperature and days of rainfall with >=0.2mm from 1991 until 2021 for different regions. Papastamati *et al.* (2002) showed that the seasonal temperature variations had a major effect on the severity of disease caused by *P. brassicae,* especially when the temperatures were less than $5°C$. Low temperatures and wet leaf surfaces aid germination of *P. brassicae* conidia and may be the reason for the greater LLS incidence in Scotland than England (Majer *et al.*, 1998). Therefore, it is clear that weather differences may contribute towards the regional differences in LLS severity.

3.1.2.3 Agronomic practices

Agronomic practices, such as selection of lines/cultivars and fungicides, may result in LLS severity differences between Scotland and England. Oilseed rape lines/cultivars with a good resistance rating for phoma stem canker caused by *Leptoshaeria maculans* and *L. biglobosa* are usually recommended by AHDB in the South, while in the North a good resistance rating against *P. brassicae* is advised. In addition, differences in choice of fungicides between England and Scotland affect the *P. brassicae* isolates and populations and thus influence the epidemic severity. The current recommended fungicides for oilseed rape are SDHI, QoI and DMI (AHDB fungicide performance for cereals and oilseed rape, 2022).
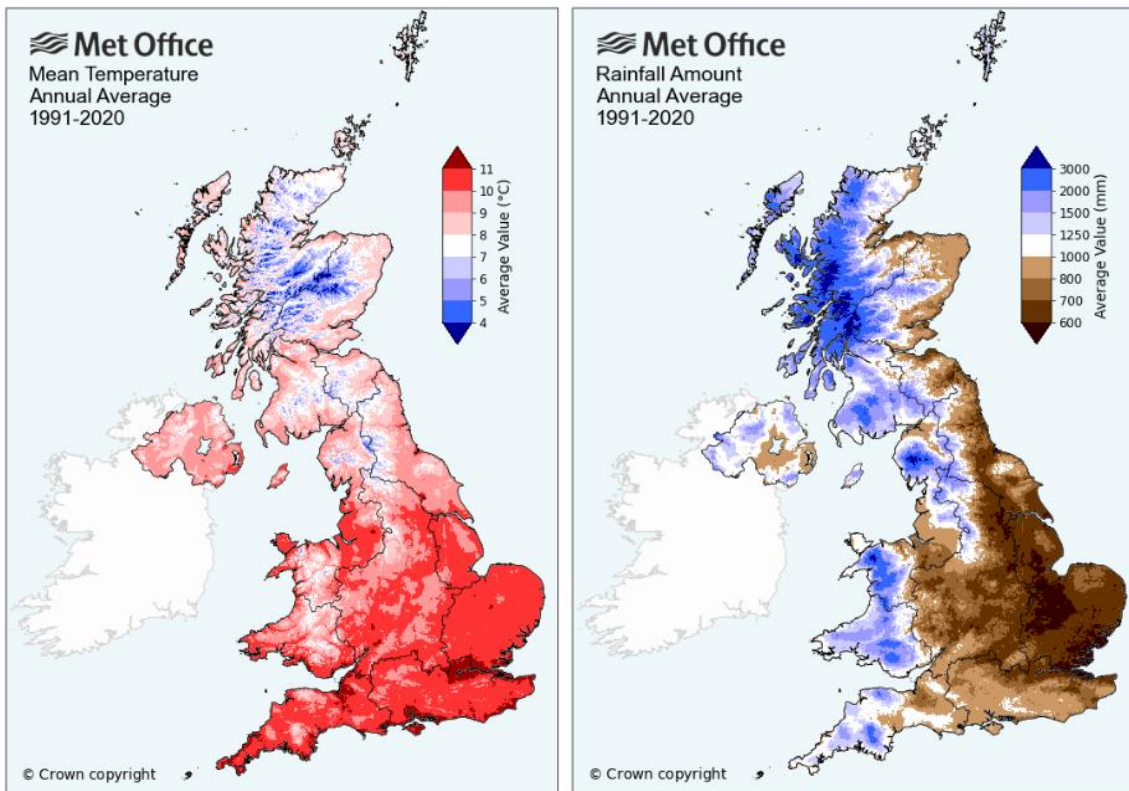
Fig 3.2 Mean annual temperature (°C) and average annual rainfall amount, UK: for the period 1991-2020. © Crown copyright 2021, used with the permission of the Meteorological Office.

3.1.2. Aims and objectives

Light leaf spot is a major problem for oilseed rape production, but there is limited knowledge about the *P. brassicae* population structure. This study will generate knowledge about regional variation in *P. brassicae* populations and isolates, and this will add knowledge to guide the strategy for breeding for durable resistance against *P. brassicae*.

Hypothesis

- o Regional pathogenicity differences between *P. brassicae* populations cause regional differences in LLS severity.

Aim:

- o To assess the pathogenicity differences between Hertfordshire, England and Aberdeen, Scotland *P. brassicae* populations.

Objective:

- o To score light leaf spot (1-6 scale) on three susceptible and three resistant *B. napus* lines inoculated with Hertfordshire and Aberdeen *P. brassicae* isolates or populations under controlled environment conditions.

3.2 Materials and methods

P. brassicae single conidial isolates and populations from Aberdeen were kindly provided by Chinthani Karandeni Dewage and Coretta Klöppel, respectively. Rothamsted isolates were isolated from the Rothamsted KWS field trial site by myself. The pathogen populations and isolates were collected from Aberdeen in Scotland (57.149715, -2.094278) in the 2014-2015 cropping season and English samples were collected from a KWS trial site at Rothamsted, Hertfordshire (51.813125, -0.382005) in the 2018-2019 cropping season. Unfortunately, the Hertfordshire isolates from 2014-2015 had been contaminated and therefore could not be used in the same cropping season as the Aberdeen isolates. *P. brassicae* populations included conidial suspensions collected from diseased leaves from oilseed rape crops, including *B. napus* lines Recital, Cuillin, Rivalda, Catana, Imola, Bristol, Marathon and Anastasia (Aberdeen) and Cuillin, Express and Barbados (Rothamsted). *P. brassicae* populations were prepared for spray inoculation as explained in section 2.3.

From the 2018-2019 Rothamsted population, single conidial isolates (R1, R2 and R3) were cultured by using single acervuli harvested from infected *B. napus* leaves incubated at 4°C for 5 days to increase asexual sporulation (Cullin, Express and Barbados, respectively). Both Rothamsted and Aberdeen single spore isolates are representatives of respective populations. Single acervuli were vortexed with 30 µL sterile distilled water to release conidia and 30 µL suspension was spread onto a PDA plate (section 2.1.2) and incubated at 15 °C in the dark for 1 week. Individual colonies were sub-cultured and isolate suspension was prepared by adding 10 mL of sterile distilled water followed by scraping off the pathogen mycelium. The spore suspension was filtered using Miracloth (Calbiochem, USA) and spore numbers were counted with a Bright-Line haemocytometer (Sigma Aldrich, UK) and spore suspensions were diluted to a concentration of 10^5 spores/mL. Spore suspensions were stored at -20 °C until needed. Five replicates of susceptible *B. napus* (Cabriolet, Laser and Sansibar) and resistant (Cubs Root, Posh and SWU Chinese 1) lines/cvs were arranged in a randomised α-design and used for light leaf spot scoring. The Hertfordshire *P. brassicae* population was produced from mixed lines/cvs of infected *B. napus* leaves collected from Rothamsted in 2019. Aberdeen isolates were prepared in similar way by Chinthani Karandeni Dewage and Coretta Klöppel collected the Aberdeen population of *P. brassicae* in 2015.

3.2.1 PCR detection of mating type of *P. brassicae* isolates

To identify the mating type of the *P. brassicae* isolates, a three primer PCR technique was used (Foster *et al.*, 2002). Table 3.1 shows the 20 µl reaction volume breakdown and the thermal cycling parameters were: initial denaturation at 10 min at 95 °C, 30 cycles of 1 min at 95 °C, 1 min at 56 °C and 1 min at 72 °C with final extension step of 3 min at 72 °C. PCR products were analysed using 2% agarose gel prepared in 1x TBE buffer. 10 µL of each sample, a negative control and 5 µl of the 100 bp DNA ladder (Sigma cat. no. P1473, PCR 100 bp low ladder, Sigma Aldrich, UK) were loaded into each well and run for 90 min at 75 V. Ethidium bromide-stained DNA bands were visualised under UV light.

Table 3.1: Mating type detection of *P. brassicae* isolates using qPCR, 20 µl PCR final volume reagents.

Reagents	Amount	Primer sequence and band size
Redtaq ready mix	10 µL	
Sterile nuclease free water	1 µL	
PbM-1-3 (10 µmol)	2 µL	5'-gat caa gag acg caa gac caa g-3' *MAT1-1*: 687 bp
PbM-2 (10 µmol)	2 µL	5'-ccc gaa atc att gag cat tac aag-3 *MAT1-2*: 858 bp
Mt3 (10 µmol)	4 µL	5'-cca aat cag gcc cca aaa tat g-3'
P. brassicae genomic DNA	1 µL	

3.2.2 Variation in pathogenicity between Aberdeen and Hertfordshire *P. brassicae* isolates

Single spore isolates were prepared from the diseased leaves. Six single spore field isolates of *P. brassicae* were analysed and Table 3.2 shows the details of the isolates. Three susceptible cvs Cabriolet, Laser and Sansibar and three resistant lines/cvs Cubs Root, POSH and SWU Chinese1 were grown under controlled environment conditions (CE experiment 1, 2). 10^5 spores/mL isolate suspensions from Aberdeen (A1, A2 and A9) and Hertfordshire (R1, R2 and R3) were sprayed (section 2.4) onto 1,4 and 1,5 leaf stage *B. napus* cvs and light leaf spot as scored using a 1-6 scale (Fell *et al.*, 2023) (Appendix 29.1a). A visual disease scoring for 1-6 scale at 21 dpi is showed in Fell *et al.*, (2023). Mock inoculation was done as a negative control in five biological replicates.

3.2.3 Variation in pathogenicity between Aberdeen and Hertfordshire *P. brassicae* populations

B. napus lines (three susceptible cvs Cabriolet, Laser and Sansibar and three resistant cvs/lines Cubs Root, POSH and SWU Chinese1) were grown in a controlled environments (CE experiment 3, 4) (section 2.2) and spray inoculated with *P. brassicae* populations from Aberdeen and Hertfordshire (section 2.4) for disease scoring using a 1-6 scale. The whole experiment was repeated twice.

3.2.4 Statistical analysis

Homogeneity of variance and normal distribution were tested using a Bartlett's test and a Shapiro's-test, respectively, to decide whether to apply parametrical or non-parametrical statistical analysis. The mean disease scores of three leaves per plant for each replication were analysed using analysis of variance (ANOVA) in R. Negative control data were excluded from the ANOVA as the plants did not develop any symptoms with those treatments. A Tukey HSD test was done to check the effect of individual factors (i.e. line/isolate) on the disease score.

Table 3.2: List of *P. brassicae* isolates and populations, their lines of origin and their AHDB Recommended List (RL) resistance score. A1, A2 and A9 were isolated from the population collected from Aberdeen in 2015. R1, R2 and R3 were isolated from the *P. brassicae* population collected from three different lines, Rothamsted in 2019.

ID	Isolate	Year Isolation	*B. napus* lines/cultivars	AHDB RL rating	Location	County	Country
A1	SS15OSR17.1	2015	Anastasia	6	Aberdeen	Aberdeenshire	UK
A2	SS15OSR11.1	2015	Marathon	5	Aberdeen	Aberdeenshire	UK
A9	SS15OSR14	2015	Recital	7	Aberdeen	Aberdeenshire	UK
R1	SS19R1	2019	Cuillin	7	Rothamsted	Hertfordshire	UK
R2	SS19R2	2019	Express	7	Rothamsted	Hertfordshire	UK
R3	SS19R3	2019	Barbados	7	Rothamsted	Hertfordshire	UK
AP1		2015	Recital, Cuillin, Rivalda, Catana, Imola, Bristol, Marathon and Anastasia		Aberdeen	Aberdeenshire	UK
RP1		2019	Cuillin, Express and Barbados		Rothamsted	Hertfordshire	UK

3.3 Results

3.3.1 PCR detection of mating type for *P. brassicae* isolates

Gel electrophoresis results identified all isolates from both Aberdeen and Hertfordshire (A1, A2, A9, R1 and R3) except R2 as *MAT 1-2* (Figure 3.3).

3.3.2 Variation in pathogenicity between Aberdeen and Hertfordshire *P. brassicae* isolates

All the six isolates from Aberdeen (A1, A2, A9) and Hertfordshire (R1, R2, R3) that were tested for pathogenicity on the *B. napus* susceptible and resistant lines/cvs caused asexual sporulation. However, lines/cvs Laser, Cubs Root, POSH and SWU Chinese 1 developed significantly fewer acervuli in comparison to cvs Cabriolet and Sansibar. Symptoms were absent on the mock-treated plants. Figure 3.4 shows the light leaf spot score of isolates from Aberdeen and Hertfordshire on *B. napus* lines.

Two-way ANOVA showed that there was a significant effect of isolate ($P = 0.008$ **) and cultivar ($P = $ 2e-16 ***) on the light leaf spot score. However, there were no significant differences between the isolates from Aberdeen and those from Hertfordshire ($P = 0.503$) (Figure 3.5). Good significant variation was shown between A2-A1 ($P < 0.05$) and A9-A1 ($P = 0.05$). However, a strong significant difference was found between isolates R3 and A1 ($P = 0.007$). There was a clearly significant difference in disease severity between all susceptible and all resistant *B. napus* lines/cvs.

3.3.3 Variation in pathogenicity between Aberdeen and Hertfordshire *P. brassicae* populations

All the susceptible and resistant lines/cvs developed disease symptoms after being treated with Aberdeen and Hertfordshire *P. brassicae* populations (Figure 3.6). Two-way ANOVA showed a significant effect of cultivar ($P = $ 2e^{-16} ***) and pathogen population ($P = 0.00015$ ***) on light leaf spot severity. Aberdeen and Hertfordshire *P. brassicae* populations showed a significant difference in susceptible cvs Cabriolet and Sansibar (Figure 3.7).
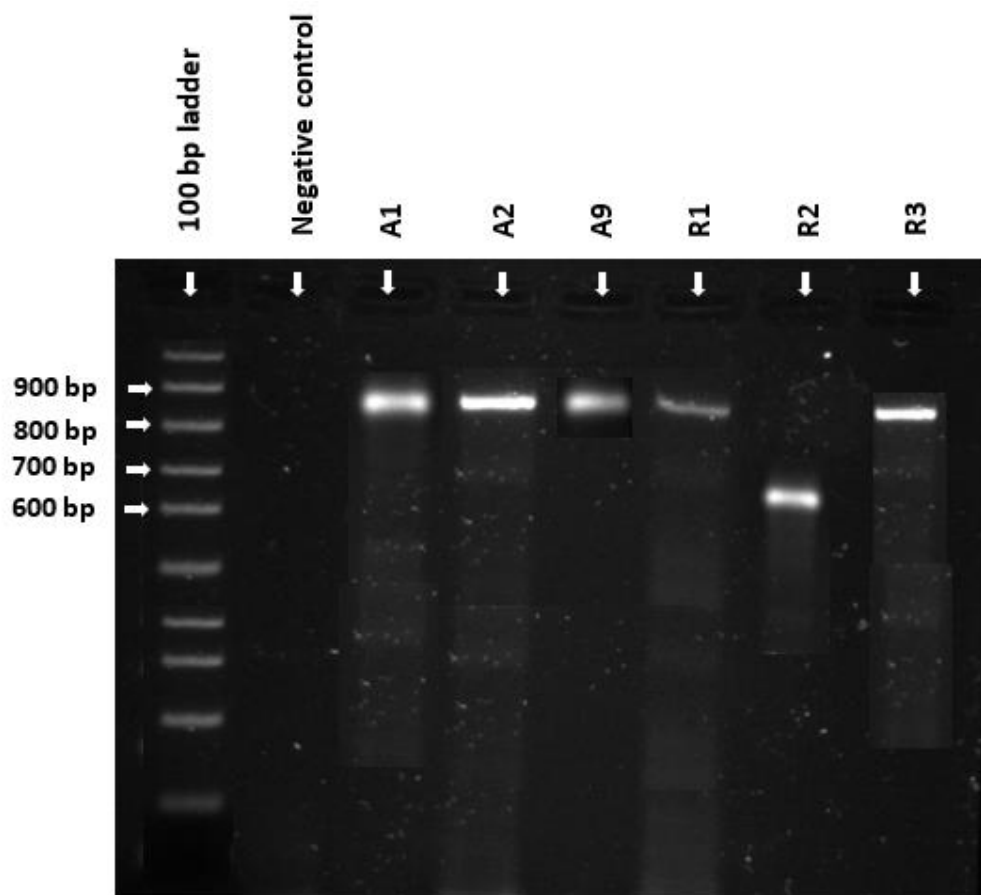
Figure: 3.3 Gel electrophoresis image showing mating types of *P. brassicae* isolates. Isolates A1, A2, A9, R1 and R3 were *MAT 1-2* (858 bp) and R2 was *MAT 1-1* (687 bp).
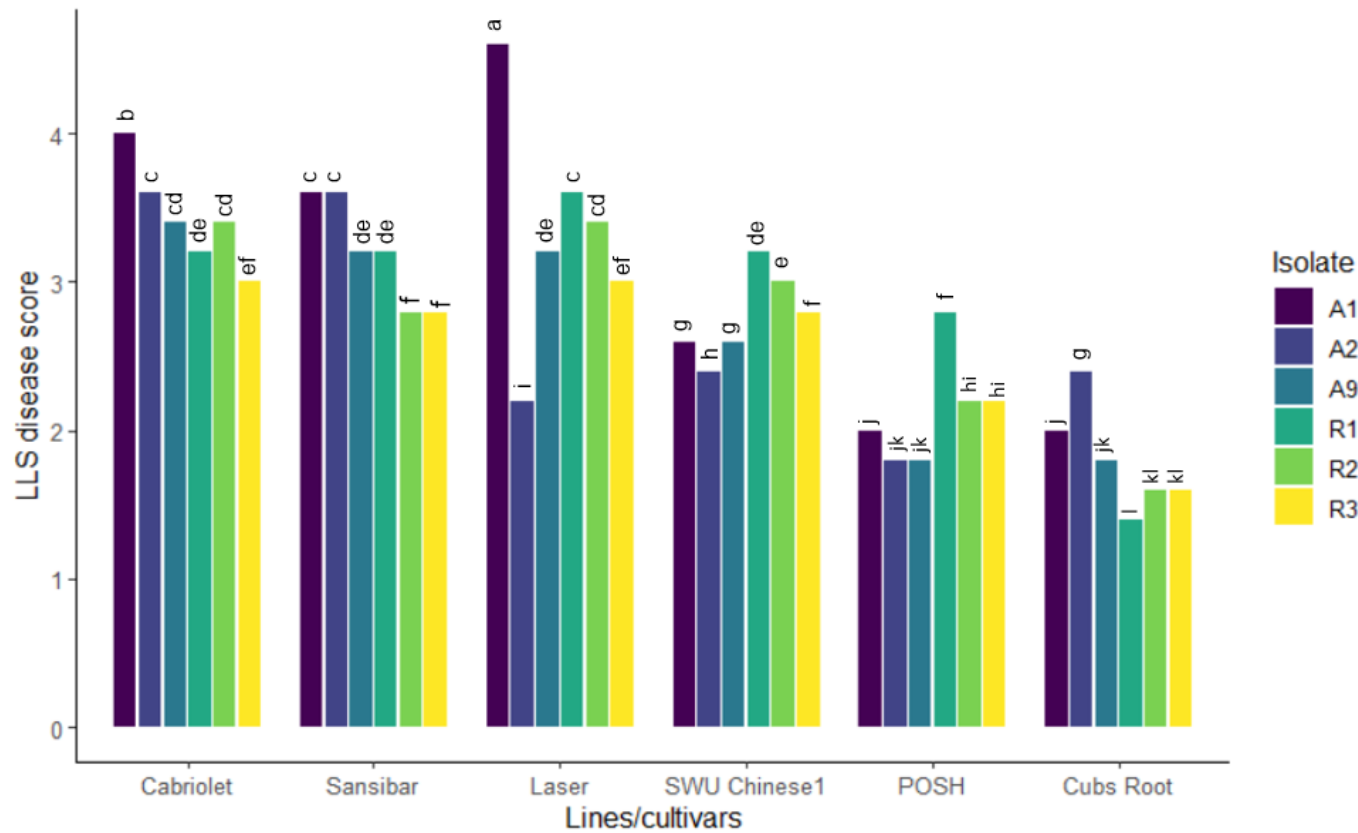
Figure: 3.4 Light leaf spot score: LLS severity scored using a 1-6 scale on three susceptible (Cabriolet, Laser and Sansibar) and three resistant (Cubs Root, POSH and SWU Chinese1) *B. napus* lines/cvs treated with Aberdeen or Hertfordshire *P. brassicae* isolates. Mean from five biological replicates each from two independent experiments. Same alphabetic letter bars do not differ significantly (df 35).
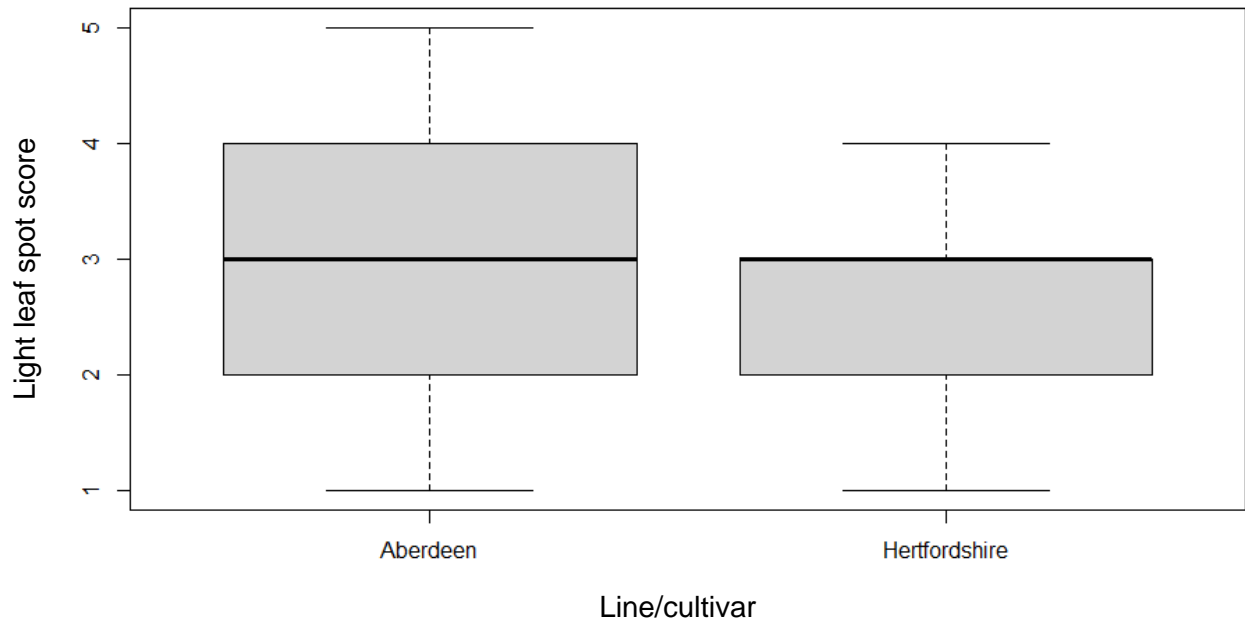
Figure 3.5: Difference between Aberdeen and Hertfordshire *P. brassicae* isolates in pathogenicity. No significant differences were observed between overall Aberdeen and Hertfordshire isolates (P = 0.503).
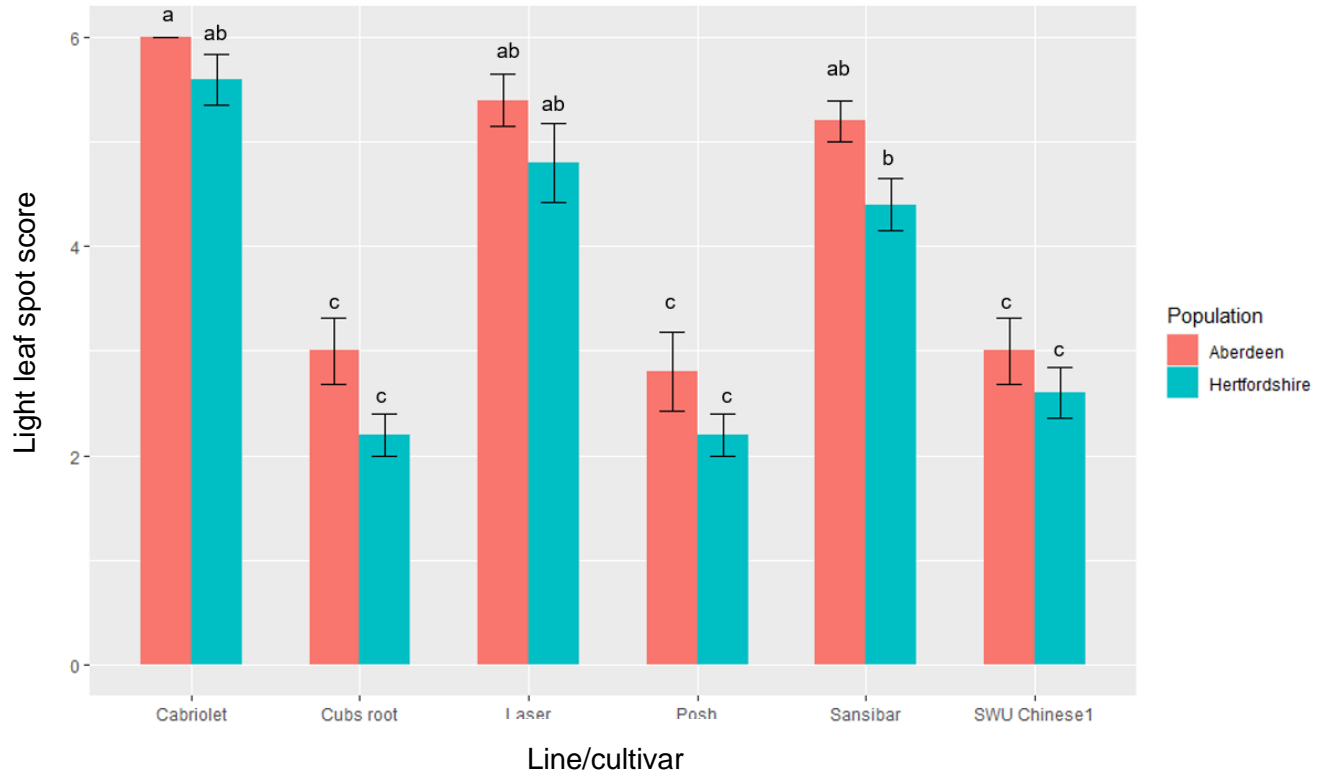
Figure 3.6 Light leaf spot score (1-6 scale) of Aberdeen and Hertfordshire *P. brassicae* populations on three susceptible (Cabriolet, Laser and Sansibar) and three resistant (Cubs Root, POSH and SWU Chinese1) *B. napus* lines/cvs. Mean and sd of five biological replicates from two independent experiments. Same alphabetic letter bars do not differ significantly (TukeyHSD) (df=11).
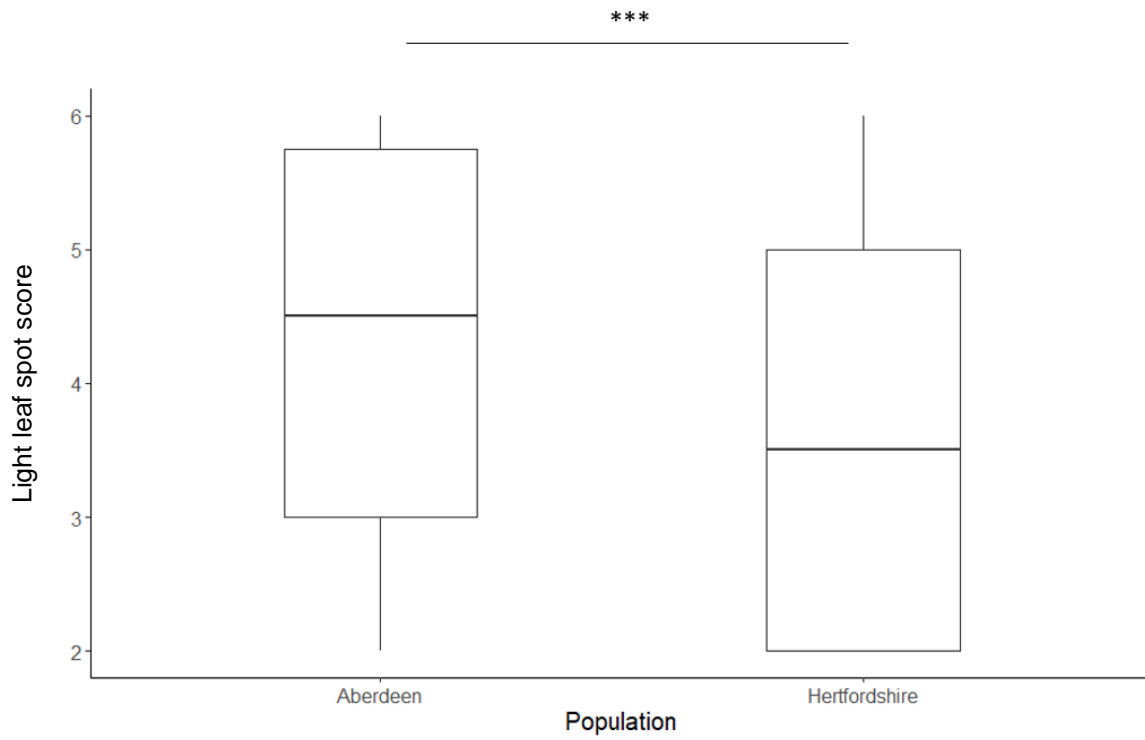
Figure 3.7 Effect of pathogen population on disease score: Tukey HSD analysis showing a significant difference in LLS severity ($P < 0.001$ ***) between Aberdeen and Hertfordshire *P. brassicae* populations.

.

However, resistant lines/cvs Cubs Root, POSH, SWU Chinese 1 and susceptible cv. Laser did not show any significant difference between Aberdeen and Hertfordshire populations.

3.4 Discussion

B. napus lines/cvs tested did not show any complete resistance against *P. brassicae* isolates or populations. However, there were significant variations in severity of the disease in these lines/cvs. This study not only showed significant differences between isolates/populations and between lines/cvs, but also between cultivar-isolate and cultivar-population interactions. Therefore, severity of LLS was significantly affected by differences between isolates and between populations of *P. brassicae*. Differences in LLS score were evident between Aberdeen and Hertfordshire populations. Regional variation in the severity of LLS was also influenced by interactions between host, pathogen and abiotic factors such as weather, cultivar choice and choice of fungicide (azole or non-azole). It will be beneficial to screen more *P. brassicae* isolates and test them in natural conditions to better understand these interactions and their combined effect on the LLS severity. It is interesting that, out of the six *P. brassicae* isolates examined for mating type, five were *MAT1-2* and it will be useful to test if there are pathogenicity gene variations between the mating types. Furthermore, frequencies of *MAT1-2* type *P. brassicae* isolates greater than 50% were also seen in studies done by Carmody *et al*. (2020) and Karandeni Dewage *et al*. (2021).

Mating type loci are involved in sexual reproduction as well as vegetative incompatibility and spore size dimorphism (Singh & Ashby.,1998). Li *et al*. (2011) reported that the sporangiospore size dimorphism is associated with the virulence of *Mucor circinelloides.* A positive correlation was observed between larger spores and greater virulence. *MAT1-1* of *Magnaporthe oryzae* isolated from rice was more prevalent than *MAT1-2* in East Africa (Onaga *et al.,* 2015). Furthermore, *MAT1-1* showed greater pathogenicity than the latter. Yong *et al*. (2020) showed that a *MAT1-1-1* knockout mutant resulted in impaired in hyphal growth, conidial morphogenesis, sexual development and increase in the tolerance to salt and osmotic stress. And *MAT1-1-2* reduced the production of conidia, caused defects in the sclerotia formation and pathogenicity of *Villosiclava virens* in rice.

Singh & Ashby. (1998) cloned the mating type loci and revealed that the *MAT 1-1* locus contains a single gene encoding a putative high-mobility group (HMG) domain protein. The *MAT 1-2* locus has three open reading frames (ORFs) encoding a putative HMG domain, an α-1 domain and metallothionein-like proteins. They have suggested that *B. napus* leaves during senescence express higher amounts of metalliothionein which may activate the putative *P. brassicae PMT1* gene, which may, in turn, stimulate sexual morphogenesis. The prevalence of *P. brassicae MAT 1-2* during this study and previous studies suggest that the sexual morphogenesis and possibly pathogenicity may be affected by the mating type loci. However, the result cannot be conclusive, considering the small number of isolates tested.

Isolates A1 and R3 showed greater disease scores in susceptible cvs/lines than in resistant ones. Susceptible cv. Laser did not show a significant difference in LLS disease score between Aberdeen and Hertfordshire. This indicates that the differences in genotype influence the differences in the severity of the disease. Therefore, the resistant lines/cvs identified can be studied further to map a potential resistance gene or quantitative resistance locus/loci. Furthermore, assessing the gene expression profile using RNA sequencing upon infection of lines with significant differences, such as Cabriolet and other resistant cvs, will help to understand the host resistance mechanism. In addition, screening for other pathogens such as *Leptosphaeria maculans* and *L. biglobosa* can also aid growers to choose a cultivar resistant against several pathogens. Majer *et al.* (1998) reported the existence of a high level of genetic diversity between England and Germany/France *P. brassicae* populations. However, no significant difference was observed between Scotland and England using amplified fragment length polymorphism (AFLP) markers. However, the isolates from 1994 were used for their study and the incidence has increased since 1998 and the LLS has been the most damaging disease in oilseed rape since 2008 (Figure 1.5). This suggests that *P. brassicae* might have undergone mutations and a possible genetic drift exists currently between Scotland and England. Furthermore, as the current study was done under controlled environment conditions, the effect of weather conditions was eliminated or limited. Therefore, the differences in severity of *P. brassicae* populations and isolates observed were mainly due to genetic variations rather than temperature/rainfall differences.

There is limited information available on the genetic diversity and population genetics of *P. brassicae*. It will be useful to study *P. brassicae* population genetics from various locations in Scotland and England, along with weather conditions, cultivar information and choice of fungicide. Population genetics studies not only reveal evolutionary history of pathogens but also aid in identifying factors contributing towards pathogenicity (Barrett *et al.*, 2008). Plant resistance against pathogens tends to be rendered ineffective within a few years in agricultural cultivation; this indicates rapid evolution of agricultural pathogens (Plissonneau *et al.*, 2017). *P. brassicae* is a complex apoplastic fungal pathogen with a mixed reproductive system and very large population sizes. Therefore, it poses a high risk of host resistance being rendered ineffective. Pathogens tend to secrete secondary metabolites, effectors and cytokinins to change the host physiology and to promote growth and colonisation by the pathogen. Therefore, these rapidly evolving, conserved genes are potential prime targets of diversification selection during evolution (Penselin *et al.*, 2016). It is important to understand the genetic basis of pathogenicity to design an effective breeding strategy against LLS. Novel information on structure characterisation, function and evolutionary dynamics of effector proteins can guide breeding processes to maximise the efficiency of breeding resistance against pathogens.

Analysis of variance results showed a significant interaction of cultivar with both isolate and populations. Out of these interactions, the large effect was due to cultivar (with smaller *P*), which indicates that the resistance against *P. brassicae* is mainly due to the *B. napus* genotypic variation. Further investigation with a large panel of *B. napus* lines/cvs will provide valuable information for breeders and, therefore, efficient deployment of cultivar resistance to manage LLS. Chapter four involves screening of *B. napus* lines for resistance to *P. brassicae* and assessment of candidate genes potentially accountable for host resistance against the LLS pathogen.

3.5 Conclusion

There is a higher frequency of mating type *MAT 1-2* of *P. brassicae* (observed during this PhD thesis) and it was consistent with the results reported by Carmody *et al.* (2020) and Karandeni Dewage *et al.* (2021). However, further screening of large number of isolates from different regions needs to be done to make conclusive remarks.

Significant variations in LLS disease score were observed in different genotypes of *B. napus* inoculated with both isolates and populations from Aberdeen and Hertfordshire. These results showed that the pathogen is adapted well to penetrate and colonise *B. napus* lines/cvs, especially cvs Cabriolet and Sansibar. However, Cubs Root, POSH, SWU Chinese 1 and Laser showed smaller LLS disease scores. Therefore, a potential resistance mechanism is operating in these lines/cvs to limit colonisation and asexual reproduction. Further studies to better understand the gene/s involved in the resistance against *P. brassicae* in these lines will be crucial to breed effective resistant *B. napus* lines.

Chapter 4: Molecular genetics and biochemical components of quantitative resistance against *Pyrenopeziza brassicae* in oilseed rape

4.1 Introduction

Oilseed rape (*Brassica napus*) is an important crop cultivated world-wide for edible oil, industrial oil, biodiesel and animal feed (Karandeni Dewage *et al.*, 2018a). Brassicas are also consumed as leafy vegetables, especially in developing countries. Light leaf spot (LLS) is a major disease in the UK, limiting yield. LLS symptoms appear from the true-leaf stage until harvest and the pathogen affects all plant organs. It is an urgent priority to improve LLS disease control. Quantitative disease resistance (QDR) is considered to be effective against most if not all races of a pathogen species. Furthermore, QDR is more durable than *R* gene-mediated qualitative resistance as pathogens adapt and overcome major gene-mediated resistance quickly (Corwin *et al.*, 2017). Thus, recently quantitative resistance has gained interest to address the major challenge of durability of disease resistance.

4.1.1 Quantitative disease resistance (QDR)

QDR is controlled by several genes and is linked to quantitative trait loci (QTL) on specific genomic regions, which contribute to the resistance phenotype against a pathogen but each with variable effect. QDR often reduces the growth of and colonisation by the pathogen. However, Niks *et al.* (2015) showed that complete resistance can be achieved by combining several QTL. Furthermore, the effects of QDR are influenced by environmental conditions and epistatic interactions (Calenge *et al.*, 2005). Study of QDR is challenging as it is difficult to infer genotype from phenotype. Several studies suggest potential relationships between QDR and the defence responses activated by pathogen associated molecular pattern (PAMP) triggered immunity (PTI) (Boyd *et al.* 2013). Association of multiple defence-related genes including receptor-like kinases (RLKs) with QTLs was identified after genome-wide nested association mapping in maize for resistance against the maize southern leaf blight pathogen (Kump *et al.*, 2011). Nested association mapping is a special technique which combines both linkage and association mapping to study especially

designed maize populations. However, how these different resistance loci act together or what would be the best combination to achieve effective resistance is not known. Cloning of QTL genes will generate more knowledge about the genetic mechanism behind each source of resistance and allow a better resistance combination strategy against pathogens. QTL that have been cloned so far encode various proteins including a putative ABC transporter, a serine hydroxymethyl transferase and cell wall associated kinases (Pilet-Nayel *et al.*, 2017).

4.1.2 Genome-wide association study (GWAS) analysis

GWAS involves scanning genetic markers across genetically diverse parental lines and exploiting recombination events that happened historically. GWAS identifies markers in linkage disequilibrium (where recombination between loci happens rarely) with disease resistance genetic loci (Harper *et al.*, 2012). The main limitations of GWAS are the requirement for a large number of polymorphic markers and a sequenced reference genome. However, it is possible to use an associative transcriptomics approach, where a single mRNA sequence data set can be used to identify variations in gene sequences (SNP markers) and expression of genes (gene expression markers/GEMs). Thus, this method was adapted to identify resistance genetic loci against *P. brassicae* in the complex polyploid genome of *B. napus,* where association of genetic and trait variations can be analysed simultaneously. Initial results of GWAS are usually illustrated in a Manhattan plot with a negative $\log_{10}$ base of the *P* values ($-\log_{10}P$) of SNP and GEM polymorphisms on the Y-axis and the corresponding chromosome locations on the X-axis. SNPs and GEMs with Bonferroni level of significance of an arbitrary threshold (*P* value $< 5\times10^{-6}$ – dashed horizontal line) can be considered as associated and require further analysis (Fell *et al.*, 2023; Reed *et al.*, 2015).

4.1.3 Associative transcriptomics

Associate transcriptomics can be adapted to overcome the difficulty to identify molecular markers associated with traits in allo-tetraploid *B. napus.* It uses RNA sequencing to identify and score markers which vary in both sequence and expression in relation to association with trait variation (Harper *et al.*, 2012). The associative

transcriptomics approach has been successfully used to identify genes involved in low glucosinolate (GSL) content in *Brassicaceae* family seeds (Chalhoub *et al.*, 2014; Harper *et al.*, 2012; Lu *et al.*, 2014).

4.1.4 Genes involved in quantitative resistance against *P. brassicae*

The results obtained from glasshouse experiments 1, 2 and 3 obtained from this study were combined with those from 123 lines/cvs assessed previously by Heather Fell, to identify candidate resistant locus/loci operating against *P. brassicae*. Transcriptomics RNA data available from the York knowledgebase (http://yorknowledgebase.hosted.york.ac.uk/resources.html) and the phenotic traits were combined and expression marker association was assessed. Analysis was done by Dr Rachel Wells, John Innes Centre, to identify candidate genes. A Manhattan plot was generated and eight candidate genes were identified through comparative analysis of GWAS data and transcriptome data (Dr Rachel Wells, John Innes Centre).

Fell *et al.* (2023) identified eight GEMs (Appendix 29.1b) highly correlated with LLS disease score ($P > 1.6 \times 10^{-7}$) from the transcriptome data for the 195 lines assessed using GWAS. The putative functions of these GEMs (Fell *et al.*, 2023) show that seven genes impart resistance against *P. brassicae* in *B. napus*, while one gene (*Acyl transferase*) adds to the susceptibility.

The majority of the resistance QTL cloned include *receptor like kinases* (*RLKs*), which suggest that the genes within the loci control pathogen detection (Corwin *et al.*, 2017). Some of the QDR genes encode defence proteins such as defensins and pathogenesis-related proteins/defence proteins and proteins that affect cell wall thickening. In addition, some genes produce transcription factors which can influence the response to defence hormones such as ethylene and salicylic acid (Corwin *et al.*, 2017). Furthermore, QDR genes are involved in secondary metabolite production and signalling processes (Cowger and Brown., 2019).

GSLs are nitrogen and sulphur containing secondary metabolites found in the *Brassicaceae* family. GSL and glucosinolate hydrolysis products (GHP) produced by the enzyme myrosinase can confer resistance against pathogens in *Brassica* crops (Giamoustaris & Mithen., 1997; Rahmanpour *et al.*, 2009). *Serine carboxypeptidase-like (SCPL) acyltransferase* mutants of *Arabidopsis thaliana scpl17* and *scpl19/sng2*

are linked to reduced glucosinolate synthesis through non-conversion of the benzoylated GSL precursors (Lee *et al*., 2012). The *A. thaliana* mutant (*eps1*) showed enhanced susceptibility to *Pseudomonas syringae*. The *EPS1* gene encodes a BAHD acyltransferase superfamily protein that is involved in the SA pathway (Zheng *et al*., 2009).

An enhanced resistance to *Erwinia carotovora* and *P. syringae* in *A. thaliana* is reported with GSL accumulation (Brader *et al*., 2006). Furthermore, a dose-dependent *in vitro* inhibitory effect of GSL, GHP and methanolic leaf extracts on the growth of four *Brassica* pathogens (two bacterial: *Xanthomonas campestris* and *Pseudomonas syringae*, and two fungal: *Alternaria brassicae* and *Sclerotinia scletotiorum* (Stotz *et al*., 2011a; Sotelo *et al*., 2015). GSLs are classified into three main groups, based on the amino acid precursor namely, aliphatic, aromatic and indolic.

β-adaptin proteins are involved in the formation of intracellular transport vesicles and these vesicles are a potential medium to accumulate apoplastic lipophilic metabolites. These metabolites include wax, cutin, sporopollenin, suberin and lignin, which protect the plants from both biotic and abiotic stresses (Ichino *et al*., 2022).

Polyadenylate RNA binding proteins regulate plant immune responses (Woloshen *et al*., 2011). The RNA binding protein which regulates 3′-end mRNA polyadenylation increases susceptibility of *A. thaliana* to *Pseudomonas syringae* (Lyons *et al*., 2013). *Phosphatidylinositol-specific phospholipase C4* (*PLC4*) genes are involved in disease resistance and hypersensitive responses. Silencing of *SlPLC4* in tomatoes increased susceptibility to *Cladosporium fulvum* (Vossen *et al*., 2010). A large number of universal stress proteins (*USPs*) is found in *B. napus* (total 142). They are involved in abiotic and biotic stress control. *USPs* in *A. thaliana (HRU1)* and *Solanum lycopersicum* both result in ROS generation during defence responses (Chi *et al*., 2019). *Ribosomal protein s24e* was upregulated in *Vanilla planifolia* at 2 days post inoculation (dpi) with *Fusarium oxysporum* as a result of a biotic stress response (Solano *et al*., 2019*)*.

The enzyme cinnamate-4-hydroxylase (*C4H*) plays a vital role in lignin biosynthesis (phenylpropanoid pathway) by hydroxylating trans-cinnamic acid to p-coumaric acid (Fang *et a*l., 2018). Over-expression of the soybean *C4H* gene *GmC4H1* in *Nicotiana benthamiana* enhanced resistance to both *Verticillium dahliae* and *Phytophthora*

parasitica, along with increased accumulation of lignin. Furthermore, silencing of *GmC4H1* in soybean hairy roots caused reduced resistance to *Phytophthora sojae* (Yan *et al*., 2019). Becker *et al*. (2017) showed that the salicylic acid regulated gene *pathogenesis-related 1* (*PR1*) expression was increased significantly in resistant *B. napus* lines in comparison to susceptible ones at 3 dpi after inoculating with *Leptosphaeria maculans.*

4.1.5 Cross-talk between quantitative resistance genes

Many genes involved in quantitative resistance are inter-connected and many signalling pathways affect each other, both positively and negatively. Schoch *et al*. (2002) showed that an inhibition of *C4H* can result in reduced lignin production, which results in induction of the SA pathway and *PR1* expression. Figure 4.1 shows a trade-off between *HXXXD-type acyl transferase*, *C4H* and *PR1*. Phenylalanine ammonia-lyase (PAL) is degraded by the Kelch Domain F-Box genes (KFBs) and stops the lignin and SA pathways. Acyl transferases, which are involved in GSL or SA production are also partially sensitive to KFBs (Kim *et al*., 2020). In *A. thaliana,* mutants with *reduced epidermal fluorescence (ref) 5-1* and *ref5-2* showed defects in lignin and indole GSL biosynthesis (Kim *et al*., 2015)*.* Furthermore, phenylpropanoid production and lignin synthesis is reduced by accumulation of GSL intermediates (Kim *et al*., 2020).

4.1.6 Aims and objectives

To analyse multigenic resistance against *P. brassicae*, the following hypothesis has been formulated. In addition, specific aims and objectives have been developed to test the hypothesis.

Hypotheses

1. GSL components have a role in QDR against *P. brassicae* in *B. napus.*
2. Most candidate genes identified in *B. napus* from GEM analysis do affect resistance against *P. brassicae.*

Aim:

To better understand the molecular genetics and GSL components involved in QDR against *P. brassicae* in *B. napus*.

Objectives:

1. To contribute to GWAS analysis by characterising the susceptibility to *P. brassicae* of an additional 72 *B. napus* lines using glasshouse experiments.

2. To study the susceptibility of commercial *B. napus* lines against *P. brassicae*

3. To examine the *B. napus* – *P. brassicae* interactions using trypan blue staining and scanning electron microscopy (SEM).

4. To determine infection-related expression of seven candidate genes identified from GEMs in susceptible and resistant *B. napus* lines/cvs.

5. To compare glucosinolate content and composition in leaf samples of the four most resistant and four most susceptible accessions to better understand the role of GSL in defence against *P. brassicae*.

4.2 Materials and methods

4.2.1 GWAS mapping

A total of 72 cvs/lines were phenotypically assessed in three different glasshouse experiments (experiments 1, 2 and 3) laid out in randomised replicated α-designs (Appendix 2 shows the layout). *B. napus* growing method, spray inoculation with *P. brassicae* and environmental conditions during glasshouse experiments for testing susceptibility of *B. napus* to *P. brassicae,* were as shown in Fell *et al*. (2023) (Appendix 29.1c). Cvs Cabriolet, Temple, Imola and Tapidor were used as controls. The details of 195 cvs/lines screened in total are shown in Fell *et al*. (2023).

Light leaf spot severity was scored at 60 days post germination using a 1-6 scale (Fell *et al.*, 2023). Appendix 3 shows the glasshouse experiment 1 done at Rothamsted Research (a) randomised replicated α-design 1 x 5 replicates ready to be inoculated; (b) Spray inoculated cultivar Surpass 400; (c) Inoculated *B. napus* lines/cvs covered with a polyethylene sheet to increase humidity and (d) Inoculated *B. napus* plants ready for sampling.

PIP

C4H → Benzoic acid → SA → PR1 → SAR

Phenylalanine → t-cinnamic acid → p-coumaric acid → coumaroylcoA → lignin

PAL

KFBs —| HXXXD-type acyl transferase → SA
↘ GSL
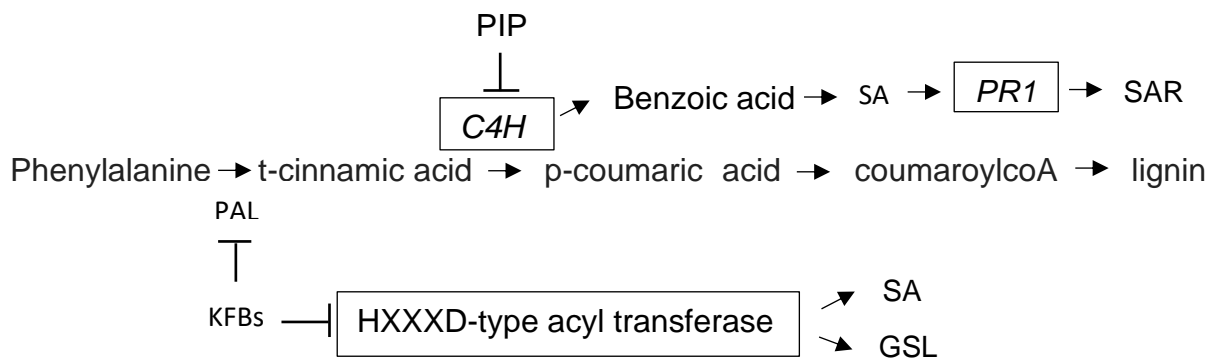
Figure 4.1: Schematic diagram (adapted from Schoch *et al.*, 2002 and Kim et al., 2020) showing *C4H* and *PR1* relationship. *C4H* converts cinnamic acid to coumaric acid in the lignin synthetic pathway. *C4H* inhibitors such as piperonylic acid (PIP) re-direct the lignin pathway to the SA pathway, result in *PR1* expression and lead to systemic acquired resistance (SAR) in plants (Schoch *et al.*, 2002). Kelch Domain F-Box genes (KFBs) encode proteins that degrade phenylalanine ammonia-lyase (PAL) involved in phenyl propanoid metabolism, and partially inhibit acyl transferase, which catalyse glucosinolate (GSL) synthesis or SA biosynthesis (Kim *et al.*, 2020).

4.2.2 Assessment of commercial lines/cultivars

Two separate glasshouse experiments (4 and 5) were done and measured the disease severity (five biological replicates each), spore production (three replicate each) and pathogen DNA (three replicates each). Appendix 4 shows the lines/cvs and the glasshouse layout used to score the disease severity and spore count. Disease was scored using a 1-6 scale (Fell *et al.*, 2023) and the spores were counted as explained in section 2.6.

P. brassicae DNA was quantified from the inoculated *B. napus* leaves. DNA was extracted from leaf samples inoculated with *P. brassicae* (section 2.9) and *P. brassicae* DNA from 50 ng extracts was quantified (section 2.10). For a negative control, sterile distilled water was used and the positive control was 1 ng of *P. brassicae* DNA. Two technical replicates of the qPCR were done with the non-template control, positive control, five standards and DNA from inoculated plant.

4.2.3 Detailed analysis of *P. brassicae* using the most susceptible and most resistant *B. napus* lines/cultivars

From the previous experiments, the four most susceptible and four most resistant lines/cvs were selected for further screening (glasshouse experiments 6 and 7). Disease scoring, spore counting and *P. brassicae* DNA quantification were done to assess any significant differences. Table 4.1 shows the lines/cvs chosen, along with their resistance phenotype and crop type.

4.2.4 Visualisation of *P. brassicae* in infected *B. napus* leaves

Susceptible *B. napus* cv. Cabriolet and resistant cv. Cubs Root were grown under controlled environments (CE experiment 5) in three biological replicates. Plants were spot-inoculated (section 2.7) and leaf discs were taken at different time points (20 min pi, then every hour pi until 15 h pi and every day pi until 8 dpi). Leaf discs were stained with trypan blue (section 2.8) and visualised using a GXM-L2800 microscope (GT vision, UK) and micrographs were taken for analysis. *P. brassicae* penetration and endophytic growth were assessed.

Table 4.1: *B. napus* cvs/lines, their respective crop type and resistance phenotype, used for glasshouse experiments 6 and 7.

Cultivar	Crop type	Phenotype
Cabriolet	Winter OSR	Susceptible
Sansibar	Modern winter OSR	Susceptible
Moana	Fodder brassica type	Susceptible
Laser	Modern winter OSR	Susceptible
SWU Chinese 1	Semi winter OSR	Resistant
Cubs Root	Spring OSR	Resistant
POSH	Modern winter OSR	Resistant
Dwarf Essex	Forage rape	Resistant

4.2.5 Scanning electron microscopy (SEM)

4.2.5.1 SEM to study the *B. napus* - *P. brassicae* pathosystem

Spot inoculated *B. napus* susceptible cultivar Cabriolet was used to assess the initial interaction between host and pathogen (controlled environment experiment 6). Time points included were 8, 10, 12, 16, 20, 24 and 48h pi and they were chosen based on the results obtained from trypan blue staining. Sample preparation and SEM imaging (section 2.11) was done at the Bioimaging facility at Rothamsted Research, Harpenden, United Kingdom by Eudri Venter.

4.2.5.2 SEM using susceptible cultivar (Cabriolet) and resistant cultivar (Cubs Root)

SEM imaging (section 2.11) was done at 2, 4, 6 and 8 dpi using Cabriolet WOSR (susceptible) and Cubs Root SOSR (resistant), to determine if there are any differential interactions between susceptible and resistant lines (controlled environment experiment 7). Furthermore, the total length of hyphae was calculated using ImageJ software to assess significant differences in colonisation between lines at 4 dpi and 8 dpi. Three images each from cvs Cabriolet and Cubs Root with the scale bar 100 µm were used for calculation.

4.2.6 Gene expression profiling of GEMs

4.2.6.1 Identification of homologous gene in *B. napus*

B. oleracea (*Bo5g052100.1, Bo2g028420.1 and Bo7g093320.1*) gene IDs were assessed using Ensembl Plants to generate gene trees. For *cab* genes from *B. rapa* (*Cab002134.1, Cab042707.1, Cab000575.1* and *Cab046181.1*)*,* sequences were taken from Yorknowledgebase – Resources. *Cab* gene sequences were BLASTed against *B. rapa* and *B. napus* genomes and gene trees were generated. Coding sequences for homologs in *B. napus* and *B. rapa* and paralogs within species of *B. oleracea* were downloaded from each gene tree created. Coding sequences of closely related homologs and paralogs were aligned using MEGA phylogenetic comparison with bootstrap values generated. Phylogenetic trees were compared using MEGA software with information from Chalhoub *et al.* (2014) to determine the most closely

related homolog or ortholog in *B. napus.* Candidate genes were further assessed using Ensembl Plants. Gene trees were constructed with homolog genes from *B. napus* and other species within the *Brassicaceae* family, including *A. thaliana*.

4.2.6.2 Primer validation and optimisation

Pre-designed, validated gene-specific TaqMan multiplex assays (primer with dye and labelled probes) from Thermo Fisher were used (Appendix 8).

To confirm the efficiency of the primers, a pool of cDNAs was prepared and a 10-fold serial dilution was made to cover six logs. For each primer pair, a standard curve and a melt curve analysis was done using the serially diluted cDNA pool as the template. In addition, the qPCR products of all primers/assays were analysed using gel electrophoresis (section 2.13). Before the duplex qPCR was done, each primer/assay was assessed, based on the Ct values obtained from single and duplex qPCR results.

4.2.6.3 Taqman multiplex qPCR to study GEMs

B. napus cvs/lines that are susceptible (Cabriolet, Sansibar and Laser) or resistant (Cubs Root, POSH and SWU Chinese 1) to *P. brassicae* were grown under controlled environment conditions (CE experiments 8, 9) (Section 2.2). Leaf samples were spot inoculated with *P. brassicae* spore suspension and discs were taken out using a sterile hole punch for RNA extraction at 1 dpi, 2 dpi, 4 dpi and 8 dpi. Mock-inoculated (0.005% silwet) leaf discs at 0 dpi were used as negative controls. Three biological replicates and two technical replicates were included in these experiments.

Gene expressions of candidate genes were assessed using Taqman multiplex qPCR (Applied Biosystems 7500 real time PCR systems, UK) to confirm expression profiles in both susceptible and resistant lines. Total RNA was extracted from inoculated leaf samples and cDNA was synthesised (section 2.12). Custom made Taqman multiplex gene expression assays with both primers and probes attached were used, along with TaqMan Multiplex Master Mix (Thermofisher Scientific). Assays were run on an ABI 7700 real time PCR System in 96-well plates using the following cycling conditions: 95 °C for 20 s, followed by 40 cycles of 95 °C for 3 s and 60 °C for 30 s. Duplex real-time PCRs were done in a 20 µL reaction, consisting of 10 µL Taqman multiplex

mastermix (2x), 1 μL each (2 μL in total) Custom Taqman gene expression assay (20x), 2 μL cDNA (50ng), and the rest were supplemented with nuclease free water.

4.2.6.4 Normalisation of data

To normalise the gene expression data, *Actin* was used as a reference gene. Using the qRT-PCR computer package (ABI 7500 SDS), primer efficiency was calculated by utilising the linear phase of all the individual reaction amplification curves (Ramakers *et al.*, 2003). ANOVA was done to determine significant variation in primer efficiency. From the primer efficiency calculated by the qPCR machine, the 'window of linearity' method was implemented using the LinRegPCR computer package and the efficiency of each primer was calculated (Ramakers *et al.*, 2003).

Normalised relative quantification (NRQ) was determined using the following equation adapted from Rieu *et al.* (2009)

$$NRQ = \frac{(E_X)^{-CT,X}}{(E_R)^{-CT,R}}$$

Where;

Ex= primer efficiency of target gene

ER= primer efficiency of reference gene

CT,X= Ct value of target gene

CT,R= Ct value of reference gene

NRQ was used for visualisation and statistical analysis. From the NRQ, areas under gene expression curve (AUGEC) were calculated and the total expressions of genes at 8dpi were used to assess the significant differences between the cvs/lines and between the resistant phenotypes. An area under the disease-progress curve (AUDPC) method was adapted to calculate AUGEC (Jeger *et al.*, 2001).

4.2.7 Quantification of glucosinolates

Total and individual GSL from each sub-group of GSL (aliphatic, indolic and aromatic) were quantified using high-performance liquid chromatography (HPLC) LC-MS. Model

specifications are given in next section. Table 4.2 shows the compounds from each group of GSL quantified.

The four most resistant (lines/cvs SWU Chinese1, Cubs Root, POSH and Dwarf Essex) and four most susceptible cvs (Cabriolet, Sansibar, Moana and Laser) were grown in a controlled environment cabinet (FITOCLIMA D1200; ARALAB, Portugal) (CE experiment 10) at a 20$^{°C}$ day for 12 h and 18$^{°C}$ night for 12 h in a randomised block design with five replicates. Leaves were collected from 30-day old plants (1,5 or 1,6 true leaf stage) (Sylvester-Bradley *et al.* 1984). One leaf from each plant was collected. From first plant, true leaf number one was collected, from the second plant true leaf number two was collected and so on. Leaf one was the oldest and leaf five was the youngest true leaf. Leaf samples were freeze dried for three days and GSL were quantified at Copenhagen University, Denmark with the help of Barbara Halkier.

Freeze dried leaf samples were prepared by separating insoluble plant material and extracting glucosinolate samples as desulfo-glucosinolates (dsGSL) by treating with sulfatase solution as described in Jensen *et al.* (2015). dsGSL components were seperated with Agilent HP1200 Series high-pressure liquid chromatography (HPLC) followed by UV detection, identification and quantification. C18 reversed-phase column [Zorbax SB-Aq, 25 cm × 4.6 mm, 5 μm particle size (Agilent) or Lichrospher RP18-5, 25 cm × 4.6 mm, 5 μm particle size (Supelco)] were used (Crocoll *et al.*, 2016; Jensen *et al.*, 2015).

4.2.8 Statistical analysis

For statistical analysis, log$_{10}$ transformed values were used and R programming software was implemented. Bartlett's tests and Shapiro's tests were done, respectively, to confirm homogeneity of variance and normality of distribution. Density plots and qqplots were plotted to visualise the normal distribution. In the case of data with variance and an abnormal distribution, non-parametrical tests (Kruskal Wallis) were done to investigate the significant differences. Analysis of variance (ANOVA) was applied on normally distributed data with homogenous variance and post-hoc tests (TUKEY Hsd) were used to determine significant differences for those which showed *P* values < α = 0.05 with ANOVA.

Table 4.2: Compounds quantified from each sub-group (aliphatic, indolic and aromatic) of glucosinolates using HPLC. Chemical name, abbreviation and common name are listed. *B. napus* susceptible (Cabriolet, Sansibar, Moana and Laser) and resistant (SWU Chinese 1, Cubs Root, POSH, Dwarf Essex) lines/cvs were grown until 1,5 or 1,6 true leaf stage in a controlled environment cabinet. True leaves number 1 to 5 were collected and the following GSL compounds were quantified.

Aliphatic	Indolic	Aromatic
3methylthiopropyl (3mtp): Glucoiberverin	Indolyl-3-methyl (i3m)	2-phenylethyl (2pe):
3methylsulfinylpropyl (3msp): Glucoiberin	4-methoxy-indolyl-3-methyl (4moi3m)	Gluconasturtiin
4 methylthiobutyl (4mtb): Glucoerucin	N-methoxy-indolyl-3-methyl (nmoi3m)	
4-methylsulfinylbutyl (4msb): Glucoraphanin		
5 methylthiopropyl (5mtp)		
5 methylsulfinylpropyl (5msp)		
6-Methyl sulfinyl hexyl (6msh)		
7-Methyl thio heptyl (7mth)		
7-Methyl sulfinyl heptyl (7msh): Glucoibarin		
8-Methyl thio octyl (8mto)		
8-Methyl sulfinyl octyl (8mso): Glucohirsutin		
3-hydroxybutyl (3ohb)		
4-hydroxybutyl (4ohb)		
4-Pentenyl (4pent)		
3-butenyl (3but): Gluconapin		
2-R-hydroxy-3-butenyl (2R-2OH-3but): Progoitrin		

For gene expression data, an analysis of co-variance (ANCOVA) model was used to consider the effect of the internal reference gene *Actin.* Area under gene expression curve (AUGEC) was calculated to check the overall gene expression differences between resistant phenotypes and also between genotypes using the following models respectively:

lm (target gene AUGEC~Genotype*Actin AUGEC)

lm (target gene AUGEC~Resistant phenotype*Actin AUGEC)

To assess the statistical difference between time points within each genotype, a Dunnett test was applied and compared between control (0 dpi) and other time points. For those genes that showed abnormal distribution and non-homogenous variances (*BnaA04g20860*, *BnaC07g38240* and *BnaC08g24910*), a Kruskal Wallis test was done and compared with lm results to make final conclusions.

4.3 Results

4.3.1 GWAS mapping

This experiment was crucial to complete the GWAS analysis as 123 *B. napus* lines were assessed previously and the GWAS population had 195 lines in total. The combined LLS scoring results helped to identify four loci and eight GEMs in *B. napus* associated with QDR against *P. brassicae* (Fell *et al.*, 2023) (Appendix 29.1b).

A total of 72 *B. napus* cvs/lines were scored (Figure 4.2). Results obtained were consistent with the previous data (Fell *et al.*, 2023) and the control cultivar Cabriolet scored the highest. Furthermore, additional control lines Temple and Imola were in the resistant category while Tapidor was intermediate. Cultivars Moana and Sansibar scored as susceptible and the most resistant line identified from these experiments was SWU Chinese 1.

4.3.2 Assessment of commercial lines/cultivars

Commercial cvs/lines were screened as in previous studies (Karandeni Dewage *et al.*, 2018a; Karandeni Dewage *et al.*, 2021) and results indicate that many cvs appeared susceptible despite having high resistance scores in the AHDB Recommendation List.
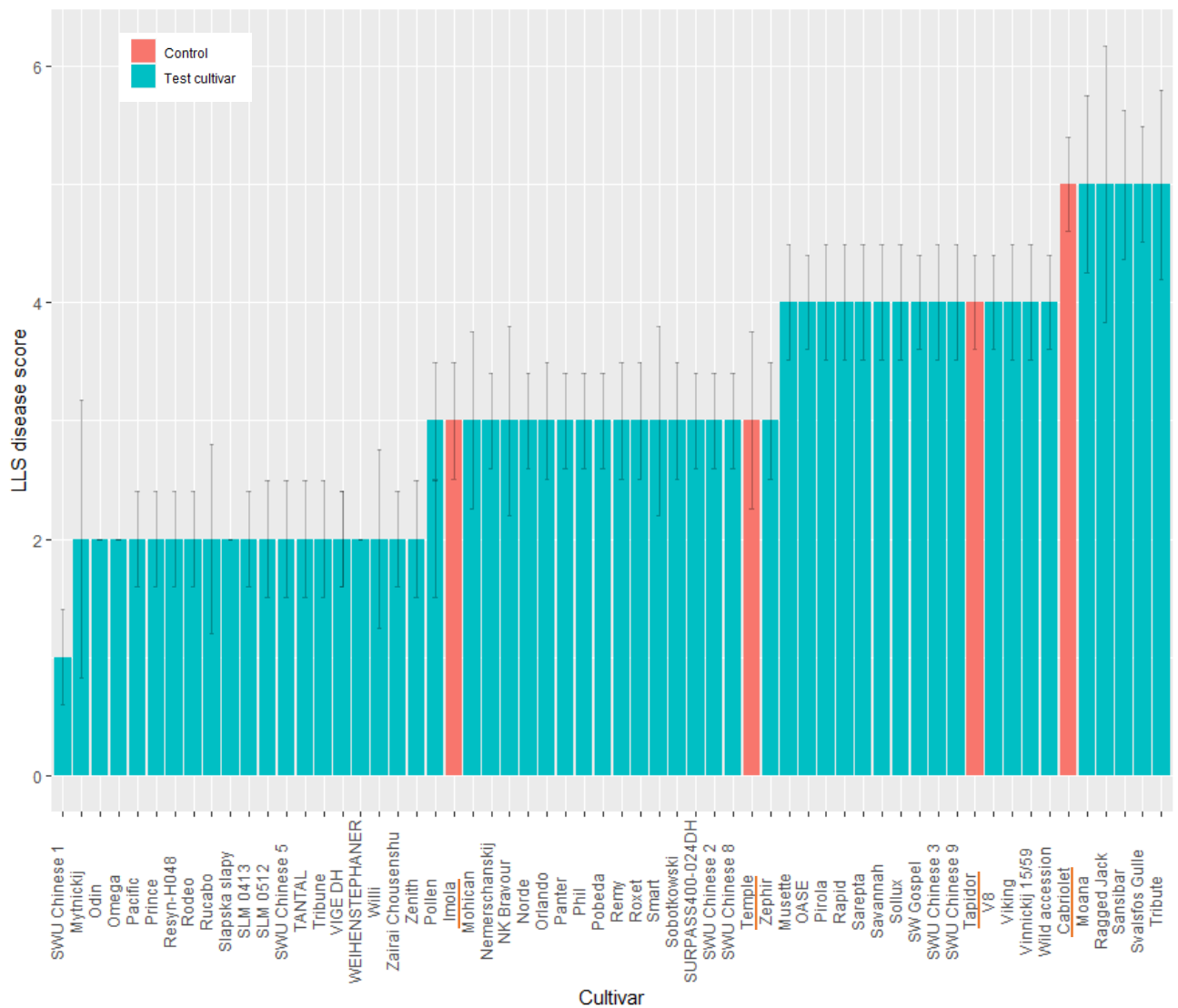
Figure 4.2: Glasshouse experiments on combined disease scores (three experiments) with cvs Imola, Temple, Tapidor and Cabriolet as controls. Imola and Temple appeared more resistant against *P. brassicae*, control Cabriolet was very susceptible and Tapidor was moderately susceptible. SWU Chinese 1 was the line that was most resistant against *P. brassicae*. Error bars represent means and standard deviations of five biological replicates each from two independent experiments (df 59).

DH lines assessed showed a greater resistance against *P. brassicae* than commercial lines (Karandeni Dewage *et al.*, 2021). Furthermore, Boys *et al.* (2007) suggested that widespread commercial deployment of cv. Bristol in the early 1990s resulted in the breakdown of major *R* gene mediated resistance. In addition, the GWAS mapping showed that the commercial cultivar Temple with a good Recommended List score of 7 appeared more susceptible (Fell *et al.*, 2023).

Figure 4.3 illustrates the combined LLS disease scores of commercial *B. napus* cvs/lines. Cultivar Barbados, which is recommended for the North, has a Recommended List LLS resistance score of 8 (AHDB Cereals & Oilseeds, 2016). However, under the glasshouse conditions, it appeared more susceptible and was in the intermediate category. Cultivar Ambassador, which is classified as a high yield cultivar, and cv. Nikita both have a Recommended List resistance score of 7. But cv. Ambassador seemed more susceptible and Nikita was resistant. Cultivar Aurelia has a Recommended List score of 8 and the results agree with that. Therefore, Nikita, Aurelia and Barbados were resistant under glasshouse conditions. A positive correlation was shown between LLS disease score and *P. brassicae* spore count (Figure 4.4). Cultivars Nikita, Aurelia and Barbados appeared resistant with low disease scores and small spore counts. Cultivar Ambassador appeared highly susceptible.

4.3.3 Detailed analysis of *P. brassicae* in the most susceptible and most resistant *B. napus* cvs/lines

To better understand the QDR in *B. napus*, assessments (LLS disease score, *P. brassicae* spore count, *P. brassicae* DNA quantification) were done using the most susceptible and most resistant cvs/lines. Scoring of disease in *B. napus* susceptible and resistant cvs/lines was consistent with previous results (Fell *et al.*, 2023). Susceptible cvs/lines showed greater *P. brassicae* spore counts than resistant lines except for cvs Moana and Dwarf Essex which appeared intermediate. There was a significant difference in *P. brassicae* spore count between susceptible and resistant cvs/lines (Figure 4.5).

Similar patterns were observed with quantity of *P. brassicae* DNA. Amounts of *P. brassicae* DNA from Moana and Dwarf Essex cvs did not vary much and were intermediate relative to the other cvs/lines (Figure 4.6).
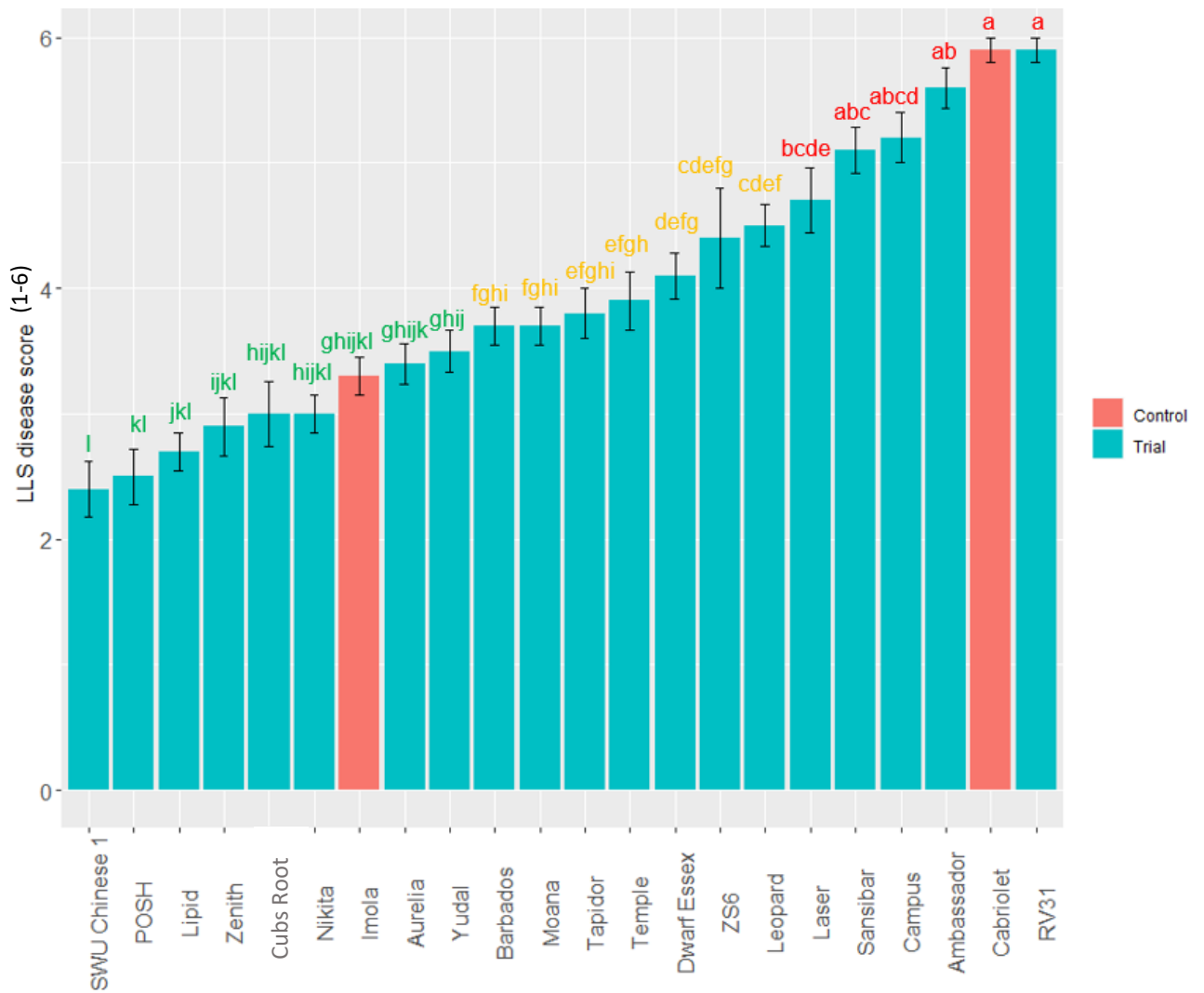
Figure 4.3: LLS disease score of commercial lines. Cultivars Cabriolet and Imola were used as controls. Green letters arbitrarily represent resistant, orange letters are intermediate and red represent susceptible cvs/lines. Barbados has a Recommended List (RL) score of 8 for *P. brassicae* and Ambassador has a RL score of 7. Nikita and Aurelia possess RL scores of 7 and 8, respectively. Error bars represent standard errors of five biological replicates each of two independent experiments combined (df 21).

.
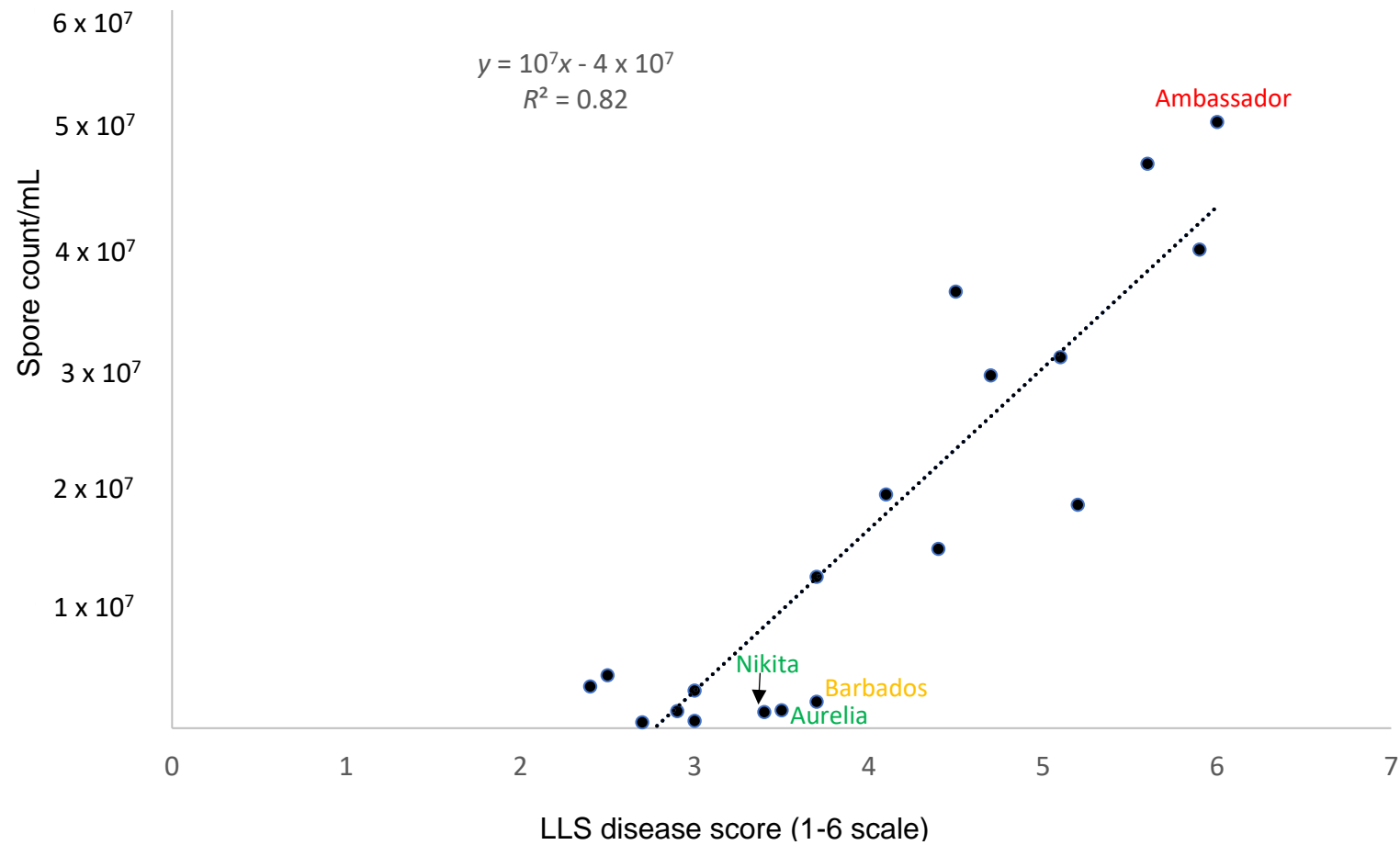
Figure 4.4: Correlation between disease score and *P. brassicae* spore numbers. Five biological replicates were used in each of two independent experiments. Cultivars Nikita, Aurelia, Barbados and Ambassador were AHDB RL lines.

.
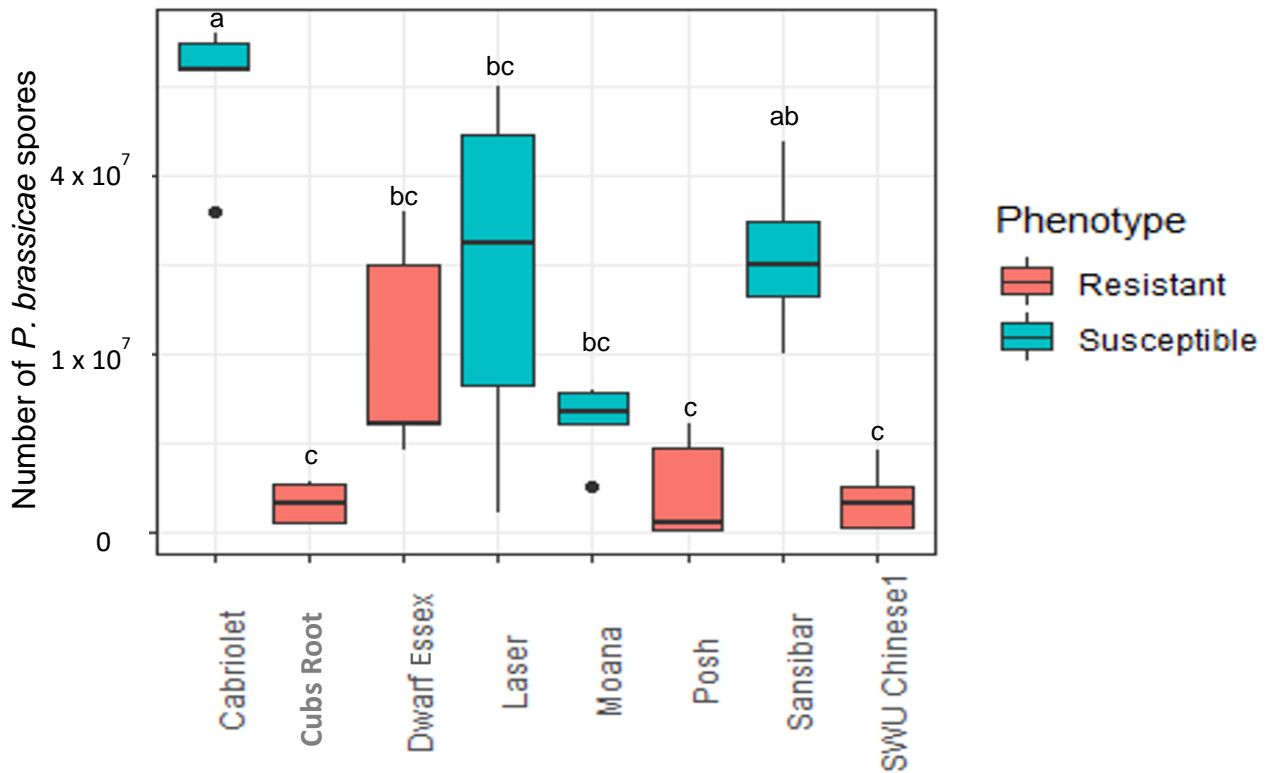
Figure 4.5: *P. brassicae* spore numbers on most resistant and most susceptible cvs/lines. Means from three biological replicates obtained from two independent glasshouse experiments (6 and 7). Significant differences ($P \le 0.05$) were calculated by one-way ANOVA with Tukey's HSD test and are indicated by different letters. Black dots represent outliers.
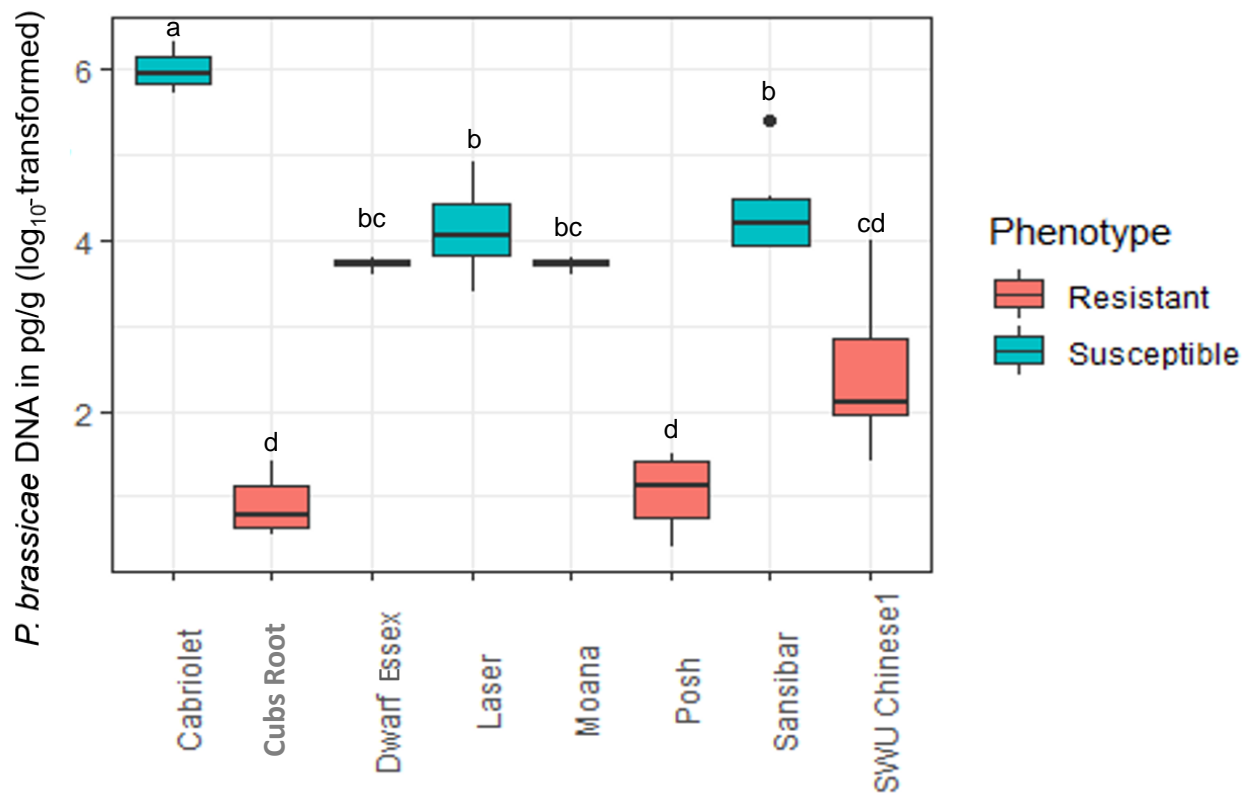
Figure 4.6: Amount *P. brassicae* DNA in cvs/lines in freeze dried samples as pg/g (log$_{10}$-transformed) from the most resistant and most susceptible cvs/lines; means of three biological replicates obtained from two independent glasshouse experiments (6 and 7). Significant differences ($P \leq 0.05$) were calculated by one-way ANOVA with Tukey's HSD test and are indicated by different letters; black dot represents the outlier.

Positive correlations were observed between LLS disease score and *P. brassicae* spore concentration (Figure 4.7), LLS disease score and quantity of *P. brassicae* DNA (Figure 4.8), and *P. brassicae* DNA and *P. brassicae* spore concentration (Figure 4.9). Cultivars Dwarf Essex and Moana were in the intermediate group in all these correlation graphs (Figures 4.7, 4.8, 4.9).

4.3.4 Visualisation of *P. brassicae* in infected *B. napus* leaves

To study if there are any differential interactions between *P. brassicae* and resistant (Cubs Root) or susceptible *B. napus* (Cabriolet) cvs during LLS disease progression, trypan blue staining was done. The results were used to decide the time points for further screening using scanning electron microscopy (SEM). Figure 4.10 shows the interaction of *P. brassicae* with the resistant cultivar Cubs Root and susceptible cultivar Cabriolet at various time points.

Trypan blue stained leaf discs had visible *P. brassicae* spores from 20 min post inoculation until 15 h after inoculation. The first signs of spore germination were observed at 1 dpi and at 2 dpi. *P. brassicae* penetrated the host cuticle at 2 dpi, hyphae started to branch at 4 dpi and subcuticular colonisation occurred at 8 dpi. During these initial stages, no sign of complete resistance was evident in resistant cvs/lines. However, at 4 dpi (Figure 4.10 g) and 8 dpi (Figure 4.10 i), resistant cv. Cubs Root showed more hyphal branching and colonisation on the surface of the leaves in contrast to the subcuticular growth in susceptible cv. Cabriolet (Figure 4.10 h, j). Furthermore, Cabriolet had extensive *P. brassicae* colonisation and more branching than Cubs Root.

4.3.5 Scanning electron microscopy (SEM)

SEM results were used to determine the time points for further qPCR analysis to assess the gene expression of GEMs identified from glasshouse experiment results combined with those from the GWAS project. An initial study using susceptible line Cabriolet was used to assess the pathogen-host interaction at early stages after inoculation. Furthermore, a resistant cv. Cubs Root and susceptible cv. Cabriolet were used to study any differential interactions.
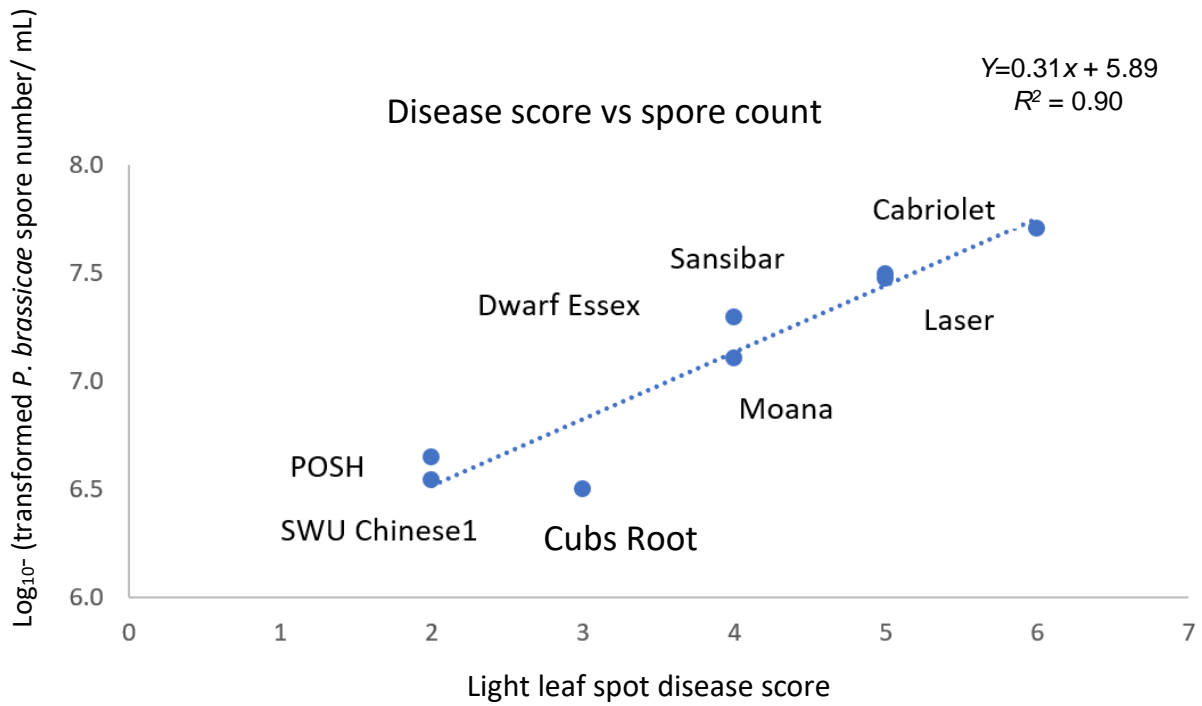
Figure 4.7: Correlation plot between LLS disease score (1-6 scale) and *P. brassicae* spore number ($\log_{10}$-transformed). 90% correlation was observed between LLS disease score and spore number.
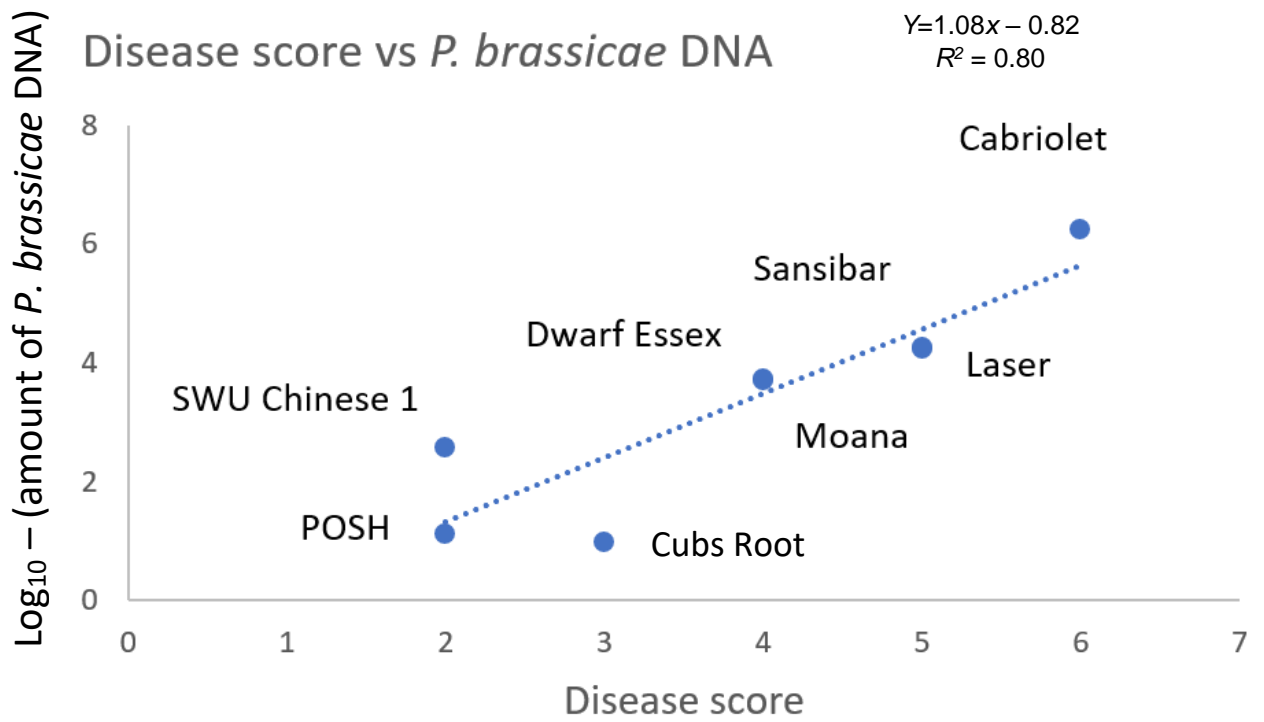
Figure 4.8: Correlation between LLS disease score and amount of *P. brassicae* DNA (log$_{10}$-transformed). A positive correlation was observed.

.
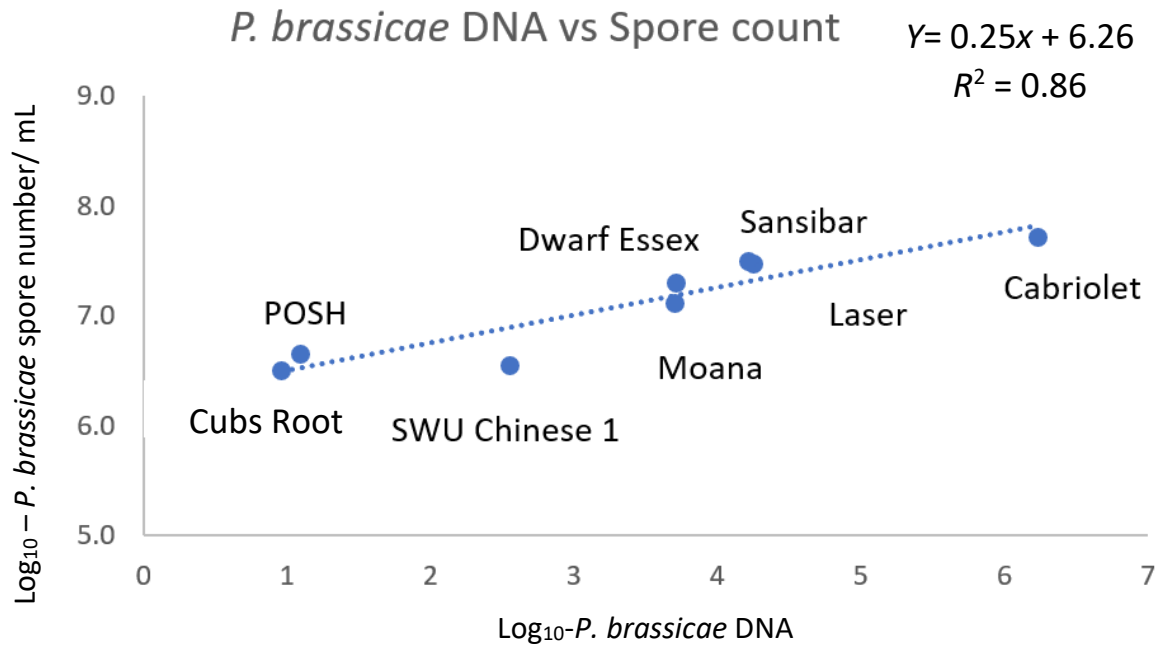
Figure 4.9: Correlation between amount of *P. brassicae* DNA (log$_{10}$-transformed) and number of *P. brassicae* spores (log$_{10}$-transformed). A positive correlation was observed.

.
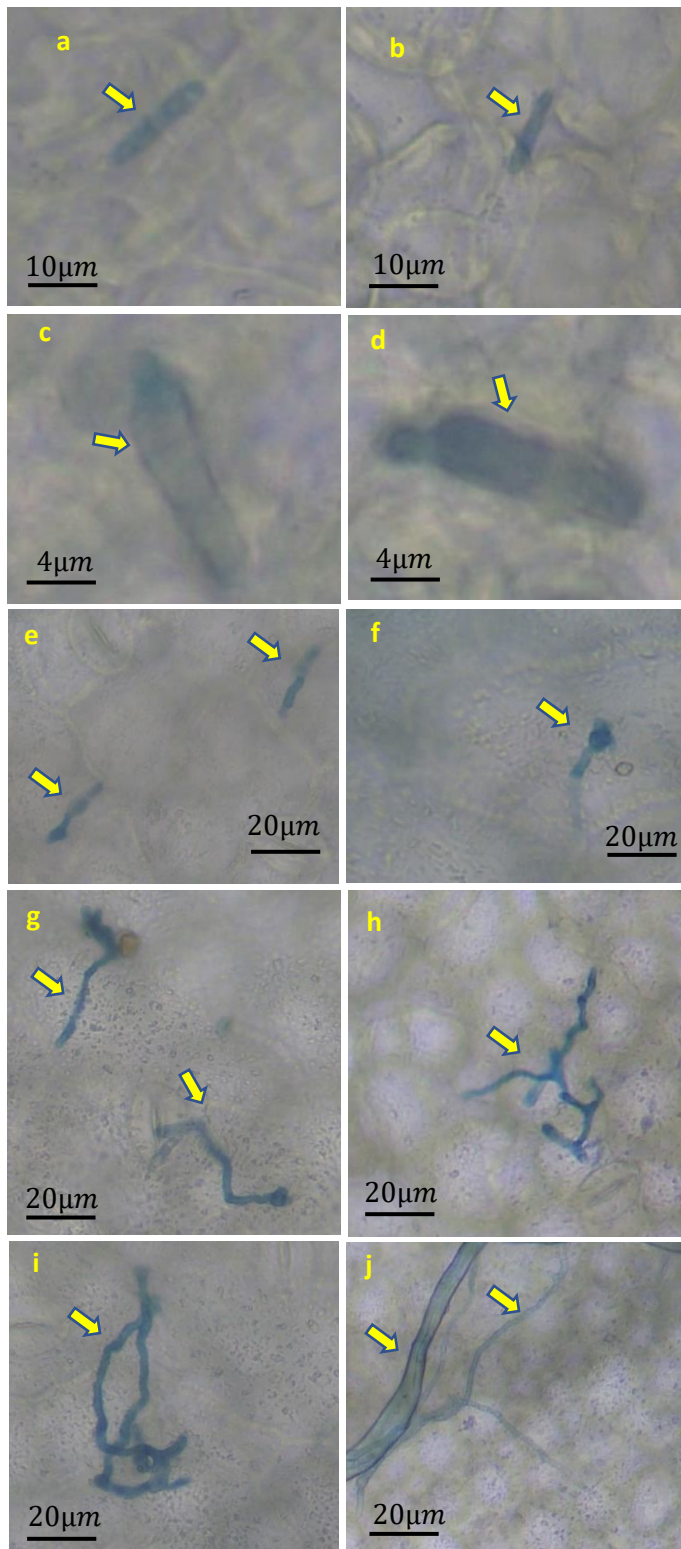
Figure 4.10: Trypan blue images during the *B. napus – P. brassicae* interaction on a resistant cultivar Cubs Root (a,c,e,g,i) and a susceptible cultivar Cabriolet (b,d,f,h,j) at 20 min after inoculation (a,b: visible spores), 1 dpi (c,d: starts to germinate), 2 dpi (e.f: penetration), 4 dpi (branching starts; (g): on the surface of leaves mostly and (h): in the subcuticular area) and 8 dpi (colonisation established: (i) on the leaf surface (j) in the subcuticular area). Arrows show the *P. brassicae* spore/colonisation.

4.3.5.1 SEM to study the *B. napus - P. brassicae* pathosystem

Figure 4.11 shows the initial interaction of *P. brassicae* spores with a susceptible cultivar Cabriolet. SEM images confirm that there was no germination until 1 dpi on susceptible cultivar Cabriolet. Spores were visible at 8, 10, 12, 16 and 20 h post inoculation. At 2 dpi, *P. brassicae* germ tubes started to penetrate, which indicates that there is no resistance operating at this stage to prevent *P. brassicae* entering the subcuticular space.

4.3.5.2 SEM using susceptible cv. Cabriolet and resistant cv. Cubs Root

P. brassicae had penetrated the cuticle of both susceptible and resistant cvs at 2 dpi. At 4 dpi, the hyphae started to branch and there was no significant difference observed between susceptible and resistant cvs. Furthermore, no differences between resistant and susceptible cvs were observed at 6 dpi. They both showed initial colonisation by *P. brassicae* in the subcuticular space. More extensive colonisation was seen in both resistant and susceptible cvs at 8dpi. Figure 4.12 shows the different interactions with *P. brassicae* between susceptible and resistant cvs.

Figure 4.13 summarises the major events in the interaction between *P. brassicae* and *B. napus.* Spore germination was initiated at 1 dpi; at 2 dpi, the hyphae penetrated the cuticle, at 4 dpi hyphal branching occurred and at 8 dpi colonisation by *P. brassicae* was visible. The subcuticular hyphae spread throughout the leaves as the pathogen progressed; colonisation was mainly adjacent to veins until 6 dpi and *P. brassicae* had spread perpendicularly into the leaf lamina as well as growing along the veins at 8 dpi.

Total length of hyphae quantified from the SE micrographs using ImageJ software showed a significant difference in total hyphal length between resistant cv. Cubs Root and susceptible cv. Cabriolet ($P = 0.010$) at 8 dpi. However, there was no significant difference between cvs at 4 dpi. Furthermore, in a susceptible cultivar, a significant difference in hyphal length between 4 dpi and 8 dpi was observed ($P = 0.0005$) (Figure 4.14).
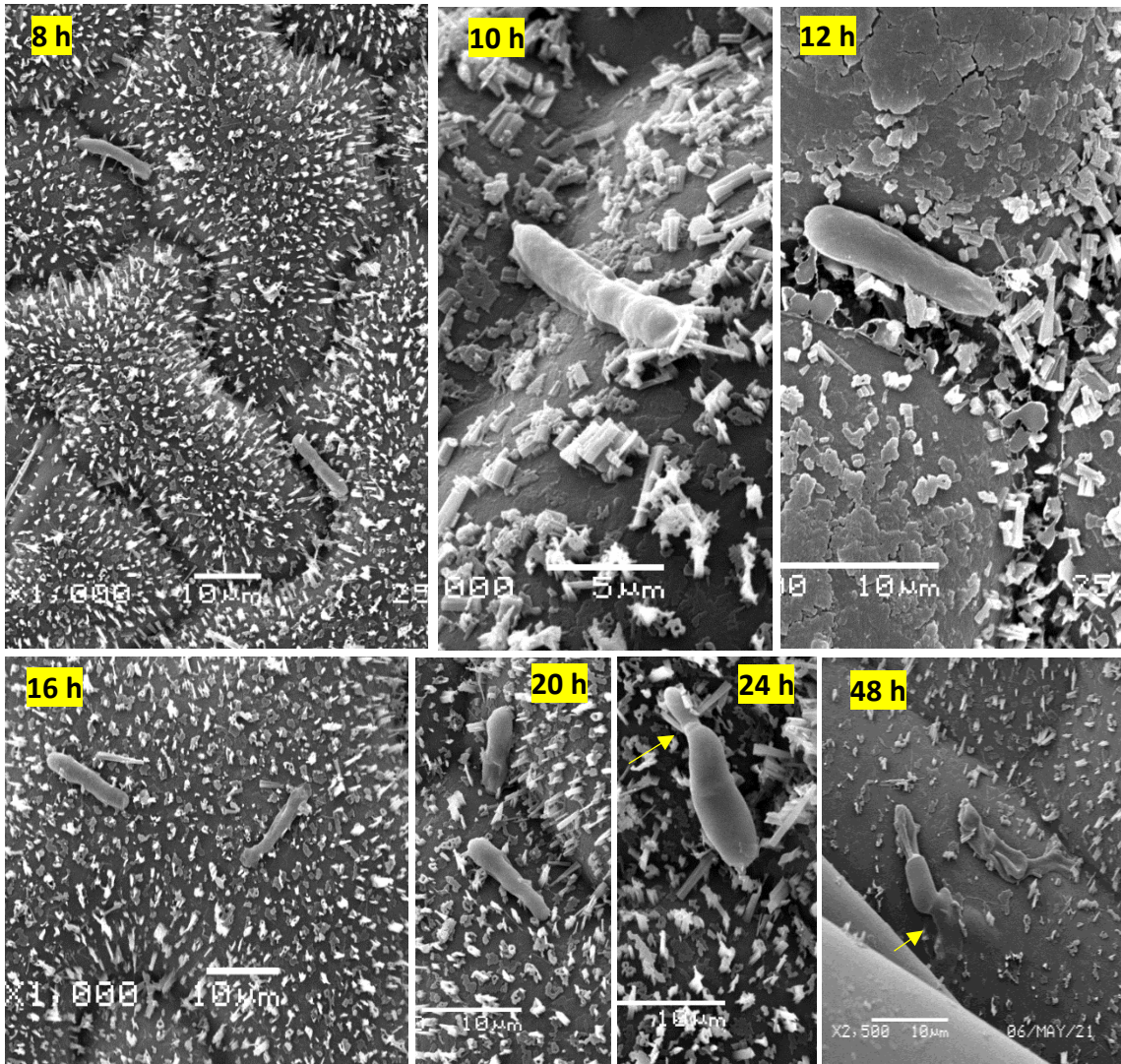
Figure 4.11: SEM images showing initial interactions between susceptible cultivar Cabriolet and *P. brassicae*. From 8 until 20 h pi spores are visible. At 24 h pi spores started to germinate and at 48 h pi penetration occurred.
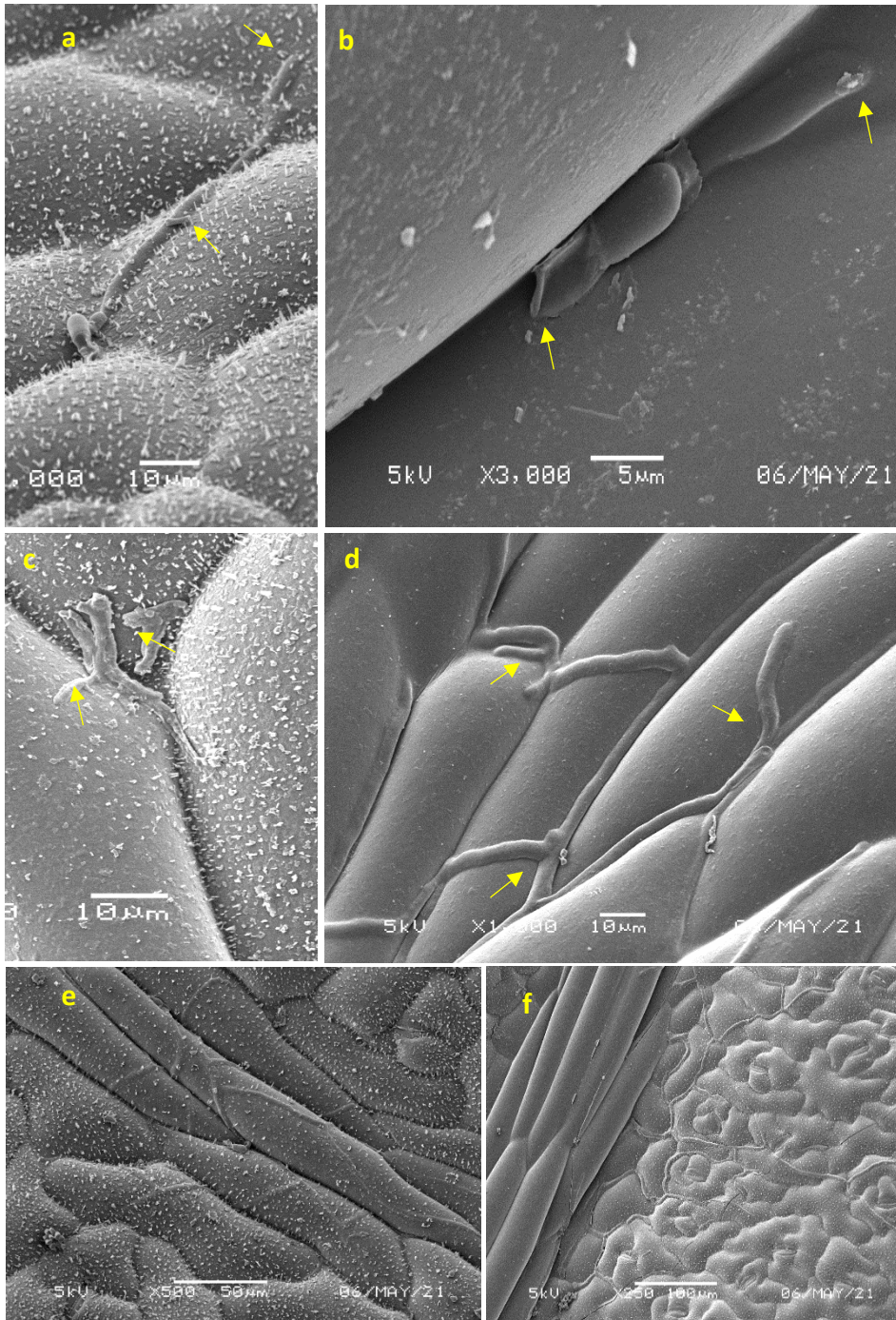
Figure 4.12: SEM images showing cuticular penetration by *P. brassicae* on resistant cv. Cubs Root (a: penetration at 2 dpi, c: branching at 4 dpi, e: colonisation at 8 dpi) and susceptible cv. Cabriolet (b: penetration at 2 dpi, d: branching at 4 dpi, f: colonisation at 8 dpi).

.
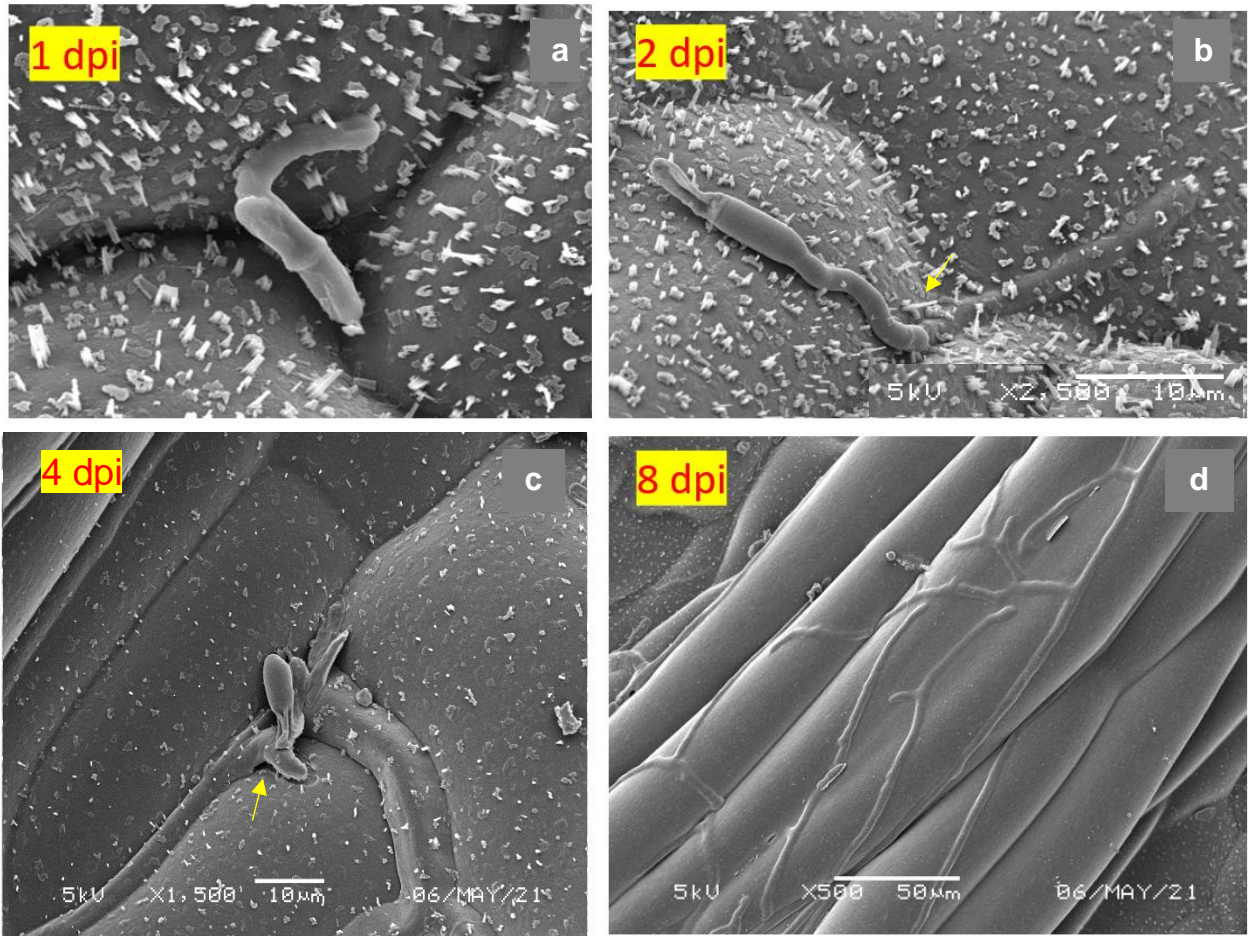
Figure 4.13: SEM images showing major stages of the pathogenicity of *P. brassicae* in the *B. napus* susceptible cv. Cabriolet. *P. brassicae* spores germinated at 1 dpi (a), penetrated the cuticle at 2 dpi (b), hyphal branching started at 4 dpi (c) and colonisation occurred at 8 dpi (d).

.
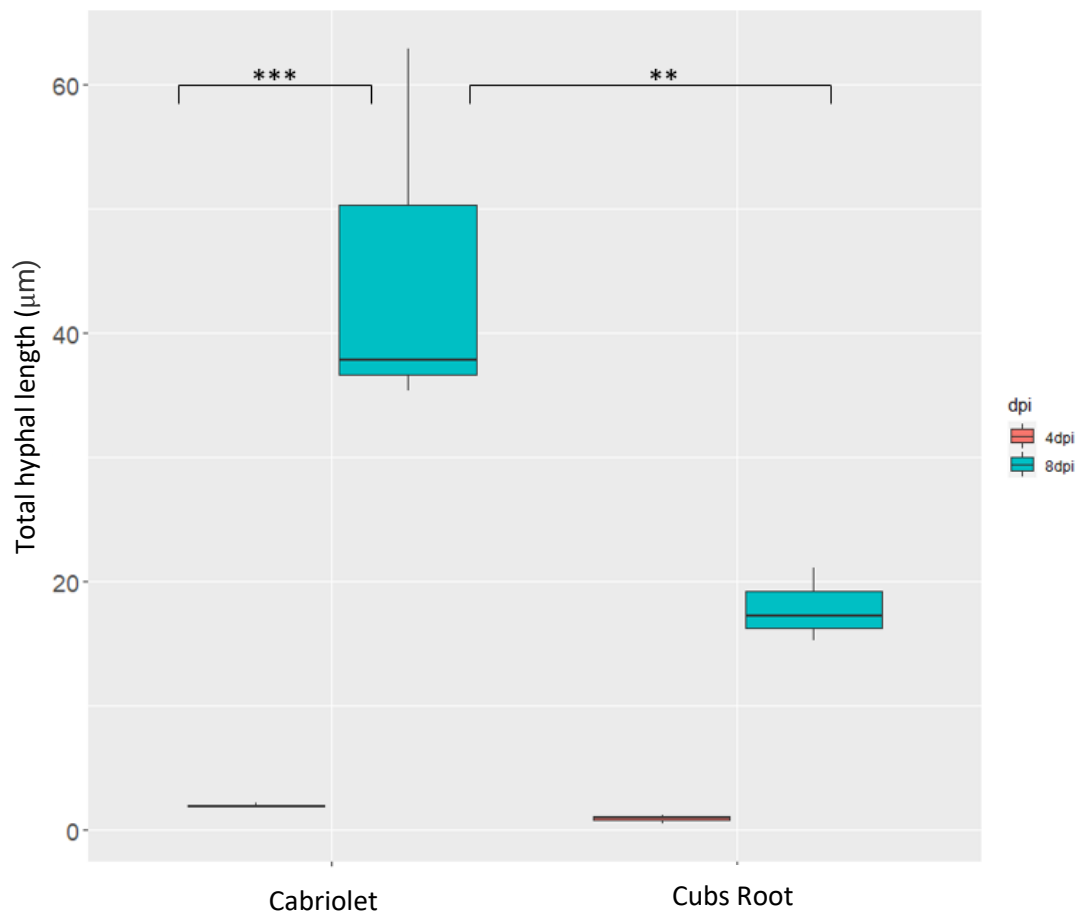
Figure 4.14: Quantification of *P. brassicae* hyphal length at 4 dpi and 8 dpi. Total lengths of *P. brassicae* hyphae were quantified from the scanning electron micrographs of *B. napus* susceptible cv. Cabriolet and resistant cv. Cubs Root using ImageJ software. Three micrographs each of 100 µm were used.

.

4.3.6 Gene expression profiling of GEMs

4.3.6.1 Identification of orthologous genes in *B. napus*

GEMs identified in *B. oleracea* and *B. rapa* from the associative transcriptomics study were used to identify the orthologous genes in *B. napus* (Fell *at al.*, 2023). Identification of BnaC04g14330D (*Cinnamate 4 hydroxylase*) in *B. napus* used the gene *Bo5g052100.1* in *B. oleracea*; this was used as an example to explain how the putative orthologous genes were identified. Figure 4.15 shows the Gene tree created for *Bo5g052100.1* in *B. oleracea* with orthologues in the *Brassicaceae* family and it has ten orthologues in *B. napus*. Figure 4.16 is the phylogeny tree of *Bo5g052100.1* and the putative orthologous gene (*BnaC04g14330D*) was identified in *B. napus* using the homoeologous gene list of Chalhoub *et al.* (2014). Table 4.3 summarises all the orthologous genes identified in *B. napus* using alignment and comparison.

4.3.6.2 Primer validation and optimisation

All nine primers show good efficiency and R^2 (RS)q values from the standard curve were plotted. In addition, melt curve analysis confirmed that all PCR products amplified were the same (Figure 4.17). The agarose gel electrophoresis image (Figure 4.18) shows that there was no amplification for *GAPDH* and *BnaA05g34100.* The *Polyadenylate-binding protein 1* agarose result appeared to have a double band but melting curve analysis showed that there was only one product amplified with a single curve. However, the amplification curve did not appear to be clear compared to other melt curves (Figure 4.17). Furthermore, expression of *BnaCo414330* and *BnaC07g27610* appeared limited. Single plex and duplex qPCR Ct values were nearly similar and acceptable. Figure 4.19 shows the amplification plots obtained for *Actin* and *PR1* from single plex qPCR and double plex qPCR, respectively. Ct values from single plex (*Actin* and *PR1* in separate wells) and duplex (*Actin* and *PR1* in the same well) qPCR were same. Appendices 5 and 6 show the amplification plot and standard curve of *Actin* using the serial dilution of the cDNA pool.
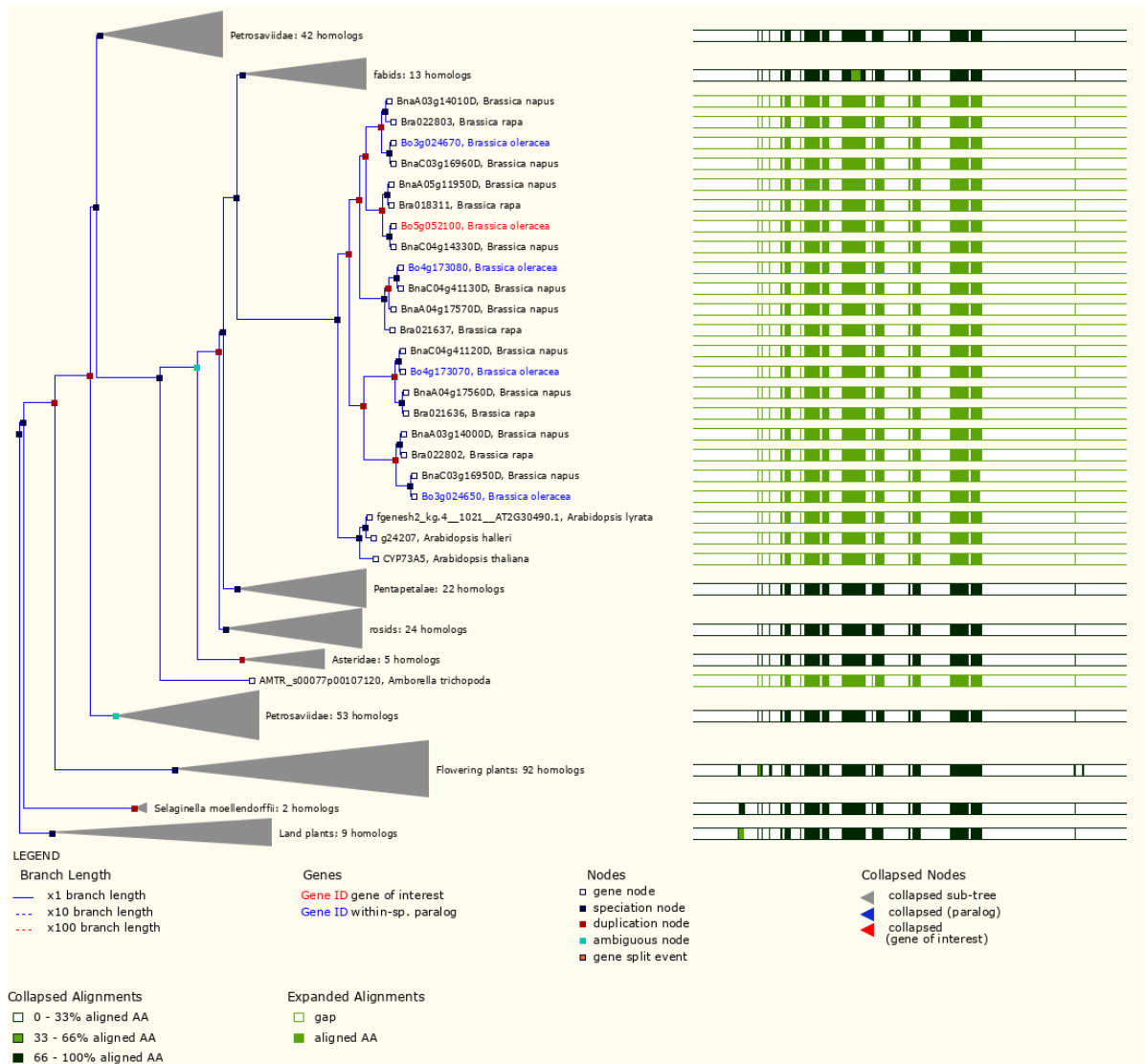
Figure 4.15: Phylogenetic comparison of candidate gene *Bo5g052100.1* of *B. oleracea* with paralogs in the *Brassicaceae* family. The gene of interest is shown in red and paralogs within *B. oleracea* species in blue. A single homolog of *A. thaliana* and ten homologs of *B. napus* were identified.
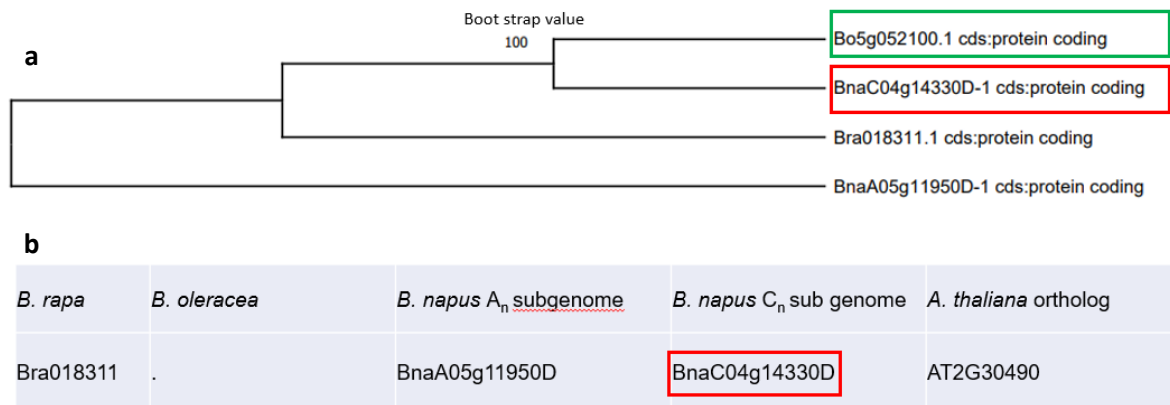
Figure 4.16: (a) Phylogenetic tree of *B. oleracea Bo5g052100.1* and the putative orthologous gene *BnaCO4g14330D* created with MEGA and (b) the homoeologous gene list from Chalhoub *et al.* (2014) confirming the same.

Table 4.3: Homolog genes identified in *Brassica napus* from *B. oleracea* and *B. rapa* using Chalhoub *et al.* (2014). Respective gene names in *Brassica* species are based on the protein encoded.

Genes in *B.oleracea* and *B. rapa*	Orthologous gene identified in *B. napus*	Gene description
Bo5g052100	*BnaC04g14330D*	Cinnamate-4-hydroxylase (*C4H*)
Bo2g028420	*BnaA02g07530D*	Phosphatidylinositol-specific phospholipase C4 (*PLC4)*
Bo7g093320	*BnaC07g27610D*	40s Ribosomal subunit protein S24e
Cab002134/ Bra019302	*BnaC07g38240D*	β-adaptin
Cab042707/ Bra035725	*BnaA10g05830D*	*Polyadenylate-binding protein 1*
Cab000575/ Bra007038	*BnaC08g24910D*	Universal stress protein
Cab046181/ Bra039146	*BnaA05g34100D*	*SNF1* kinase homolog 10 (KIN10)
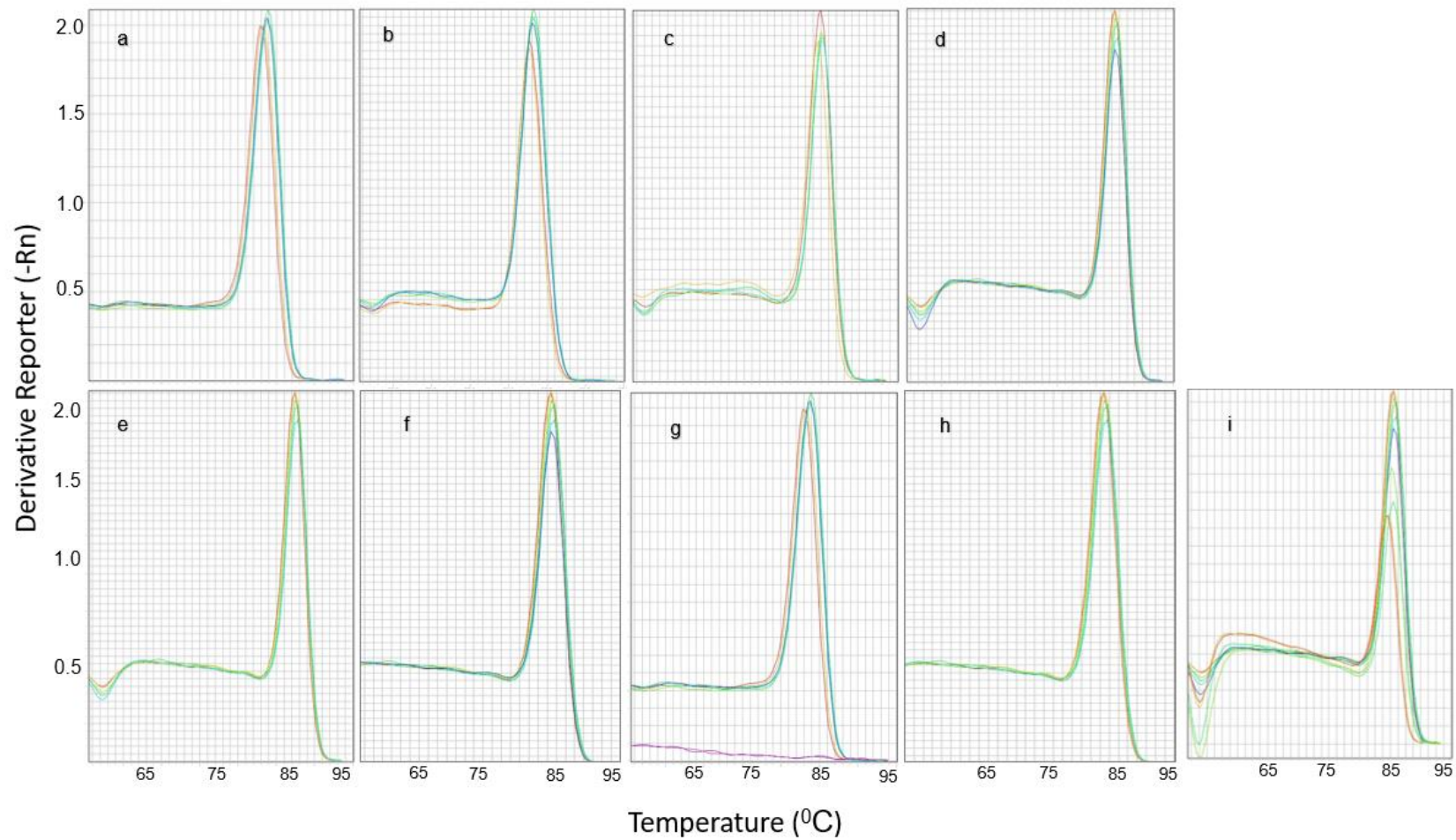
Figure 4.17: Melting curve analysis of qPCR obtained from GEM primers using a cDNA pool (control and inoculated leaf cDNA samples) as a template. Seven 10-fold dilutions were used. X axis represents the temperature in °C and Y axis represents the negative first derivative of the normalized fluorescence (Rn) generated by the reporter during PCR amplification. (a) *Actin* (b) *PR1* (c) *Acyl transferase* (d) *β-adaptin* (e) *PLC4* (f) *USP* (g) *C4H* (h) *40s Ribosomal subunit protein S24e* (i) *Polyadenylate-binding protein 1*

.
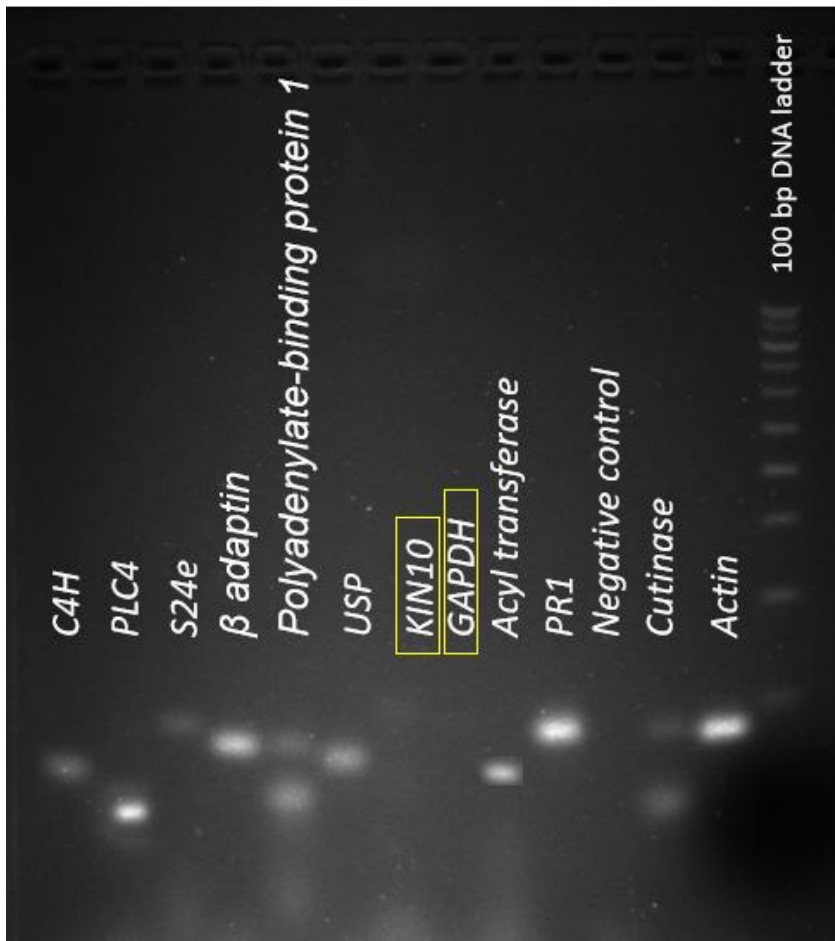
Figure 4.18: Agarose gel electrophoresis image of Taqman multiplex qPCR primers/assays. *C4H* and *40s ribosomal subunit protein S24e* showed relatively low expression. *KIN10* and *GAPDH* each primers/assays did not show any amplification. *Polyadenylate-binding protein 1* and *cutinase* showed two bands.

.
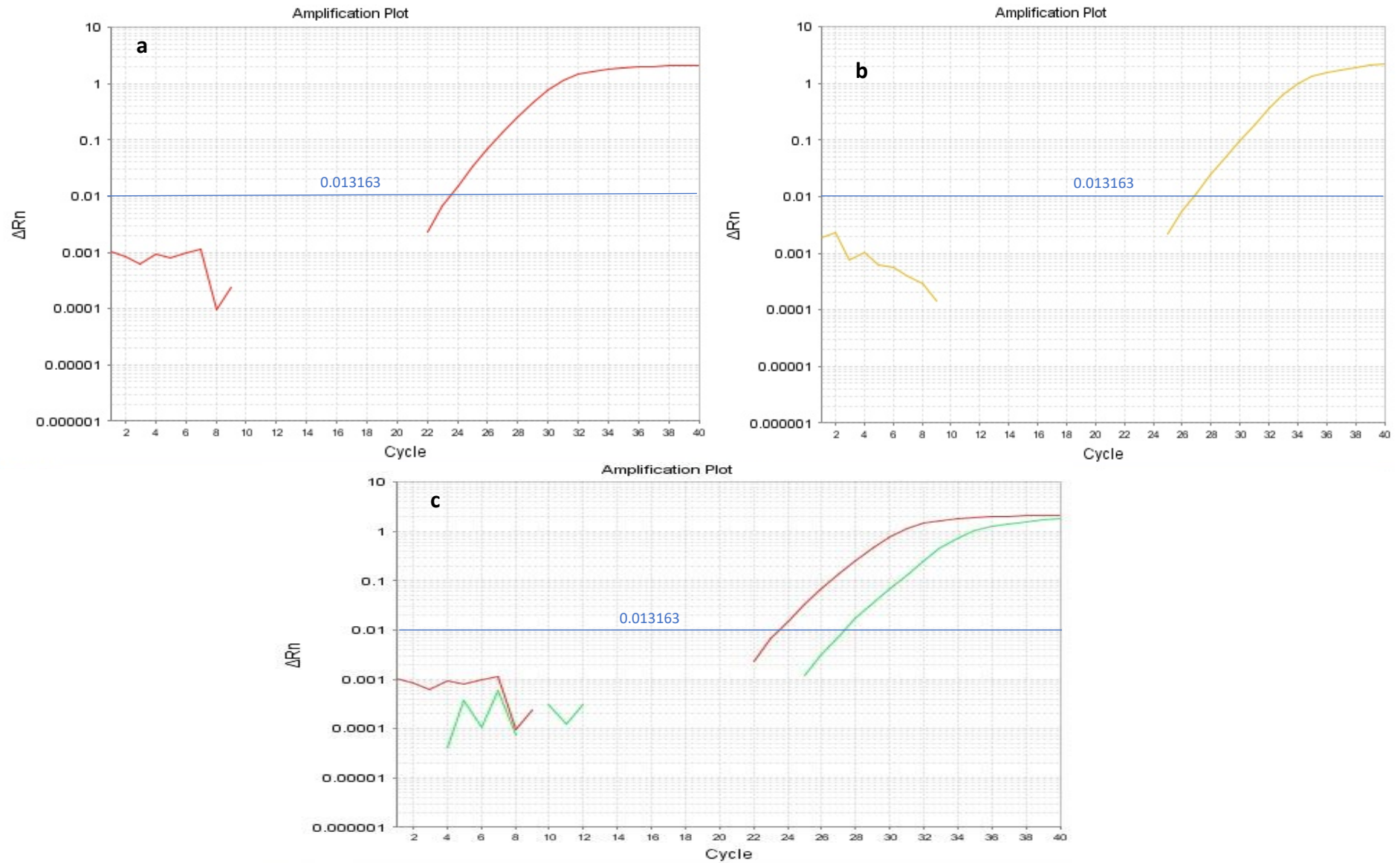
Figure 4.19: Amplification plots obtained for *Actin* (a) and *PR1* (b) from single plex and double plex (c) qPCR respectively. X axis: qPCR cycle number and Y axis: delta Rn/normalized fluorescence value subtracted by baseline. Ct values for *Actin* and *PR1* run separately (single plex) or together (duplex) were 24 and 27, respectively.

4.3.6.4 Normalisation of data

Table 4.4 shows the mean primer efficiency calculated for each Taqman multiplex assay using the LinRegPCR computer package.

4.3.6.5 Taqman multiplex qPCR to study GEMs

To better understand the genes involved in *B. napus* QDR against *P. brassicae* and to extend the information obtained about the GEMs from associative transcriptomic assessments (Fell *et al.*, 2023), qPCR was done. Significant variations between resistant/susceptible phenotypes and genotypes were studied using the NRQ AUGEC as the reference gene *Actin* expressed differentially in different genotypes.

Actin expression was considered as the co-variant, showed that there are significant variations between resistant phenotypes and genotypes (Figure 4.20). Significant differences were observed in *PR1* induction between resistant phenotypes and between genotypes (P = 0.0002, P 0.009), respectively. A significant difference in *BnaA04g20860* (*HXXXD- type acyl transferase*) induction was observed between resistant phenotypes (P = 9 x 10^{-5} and between genotypes (P = 6.78 x 10^{-6}). There was no significant difference noticed between phenotypes in contrast to genotypes (P = 0.001) for *BnaC04g14330* (*C4H*) expression. Greater significant differences between resistant/susceptible phenotypes (P = 1.91 x 10^{-4}) and genotypes (P = 1.38 x 10^{-7}) were observed in *PLC4* induction. Furthermore, a significant difference in induction of 40s ribosomal sub-unit protein S24e was observed between resistant phenotypes (P = 4.07 x 10^{-6}) and genotypes (P = 1.8 x 10^{-5}). Significant differences were noted between resistant phenotypes (P = 0.01891), genotypes (P = 1.8 x 10^{-5}) in the expression of *BnaC07g38240* (β-adaptin). There was no differential expression of *BnaA10g05830* (*Polyadenylate-binding protein 1*) observed between resistant/susceptible phenotypes and genotypes. In addition, a significant difference was observed between resistant phenotypes (P = 1.8 x 10^{-10}) and genotypes (P = 6.7 x 10^{-6}) of universal stress protein induction. GEMs that showed significant variations were analysed using TukeyHSD to compare pair wise significant variations (Appendix 7).

PR1 was differentially expressed between cvs/lines that were susceptible or resistant to *P. brassicae* (Figure 4.21). Within each resistant line, an increase in normalised

Table 4.4: Primer efficiency calculated using LinRegPCR for Taqman multiplex primers. Means were calculated from two technical replicates.

Assay name	Primer efficiency
BnaA02g07530	1.90
BnaA04g20860	1.83
BnaA10g05830	1.85
BnaC04g14330	1.83
BnaC07g27610	1.83
BnaC07g38240	1.91
BnaC08g24910	1.81
Actin	1.75
PR1	1.95
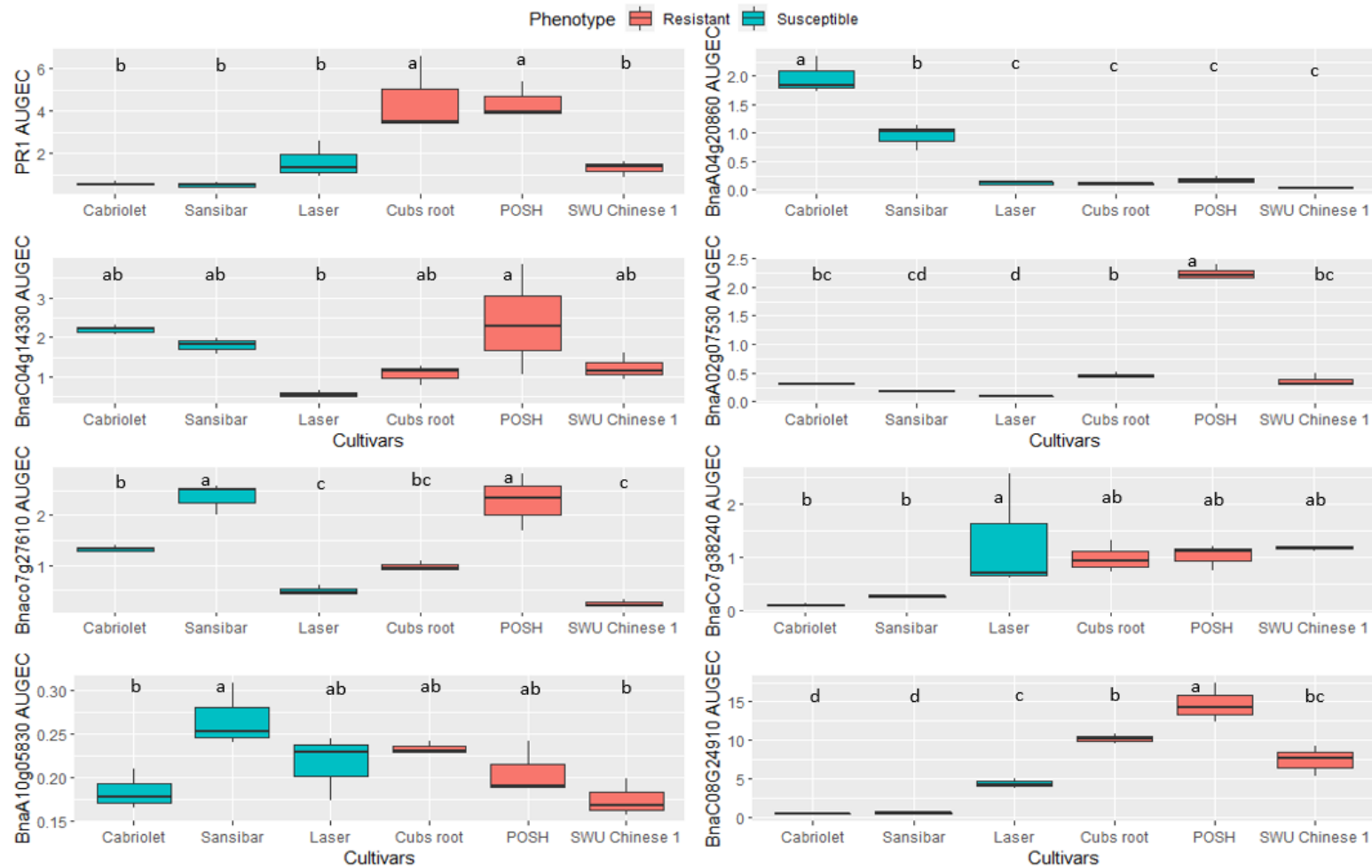
Figure 4.20: Normalised relative quantities (NRQ) of GEMs identified from associative transcriptomic analysis (Fell *et al.*, 2023). Susceptible (Cabriolet, Sansibar, Laser) and resistant (Cubs Root, POSH, SWU Chinese 1) cvs/lines inoculated with 10^5 conidia/ml of *P. brassicae*. At 0 dpi (mock inoculated control), 1 dpi, 2 dpi, 4 dpi and 8 dpi total RNA was extracted from inoculated leaves, cDNA synthesised and analysed using qPCR. NRQ was quantified with the Pfaffl method. Significant differences between resistant/susceptible phenotypes and genotypes in expression were assessed using total gene expression combined for all time points (AUGEC). Genotypes with the same letters did not differ significantly (ANOVA and Tukey HSD). Gene IDs corresponds to: *BnaAo4g20860* (*HXXXD-type acyl transferase*), *BnaCo4g1430* (*C4H*), *BnaA02g07530* (*PLC4*), *BnaC07g610* (*40s Ribosomal subunit protein S24e*), *BnaC07g38240* (*ß-adaptin*), *BnaA10g05830* (*Polyadenylate-binding protein 1*) and *BnaCo8g24910* (*Universal stress protein*).

89
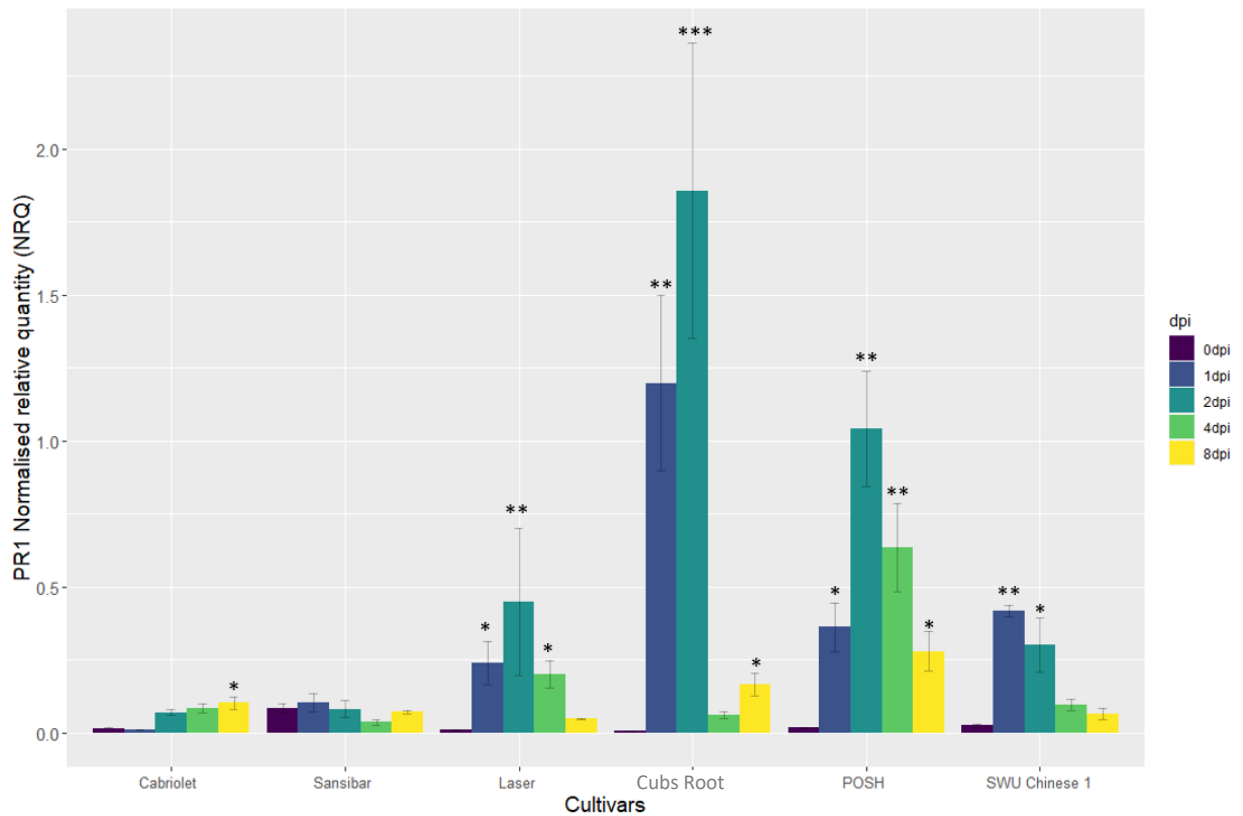
Figure 4.21: Normalised relative quantity (NRQ) of *PR1*. Susceptible (Cabriolet, Sansibar, Laser) and resistant (Cubs Root, POSH, SWU Chinese 1) cvs/lines inoculated with 10^5 conidia/ml of *P. brassicae*. At 0 dpi (mock inoculated control), 1 dpi, 2 dpi, 4 dpi and 8 dpi total RNA was extracted from inoculated leaves, cDNA synthesised and analysed using qPCR. NRQ was quantified with the Pfaffl method. Means and standard deviations (±) of three biological replicates and two technical replicates. Significant differences between mean values of control and time points within each genotype are indicated by asterisks using Dunnett's test result. ***P-value ≤ 0.001; ** P-value ≤ 0.01; * P-value ≤ 0.05

.

relative quantity (NRQ) of *PR1* was observed in comparison to the mock inoculated control (0 dpi). Cultivars/lines Cubs Root, POSH, Laser and SWU Chinese 1 showed as different to Sansibar. *PR1* was highly expressed at 1dpi and 2dpi in Cubs Root, whereas in POSH greatest expression was at 1, 2 and 4 dpi. An early induction (1 dpi) of *PR1* was observed in Laser and SWU Chinese 1, which indicates a potential host resistance response and a possible counter response mechanism by *P. brassicae*. The expression was greater in susceptible cvs/lines Cabriolet (2dpi, 4dpi), Sansibar (2dpi, 4dpi) and Laser (2dpi) for *BnaA04g20860* (*HXXXD-type acyl transferase*) (Figure 4.22). At 4 dpi, resistant lines Cubs Root and SWU Chinese 1 had an increase in *BnaC04g14330 (C4H)* expression (Figure 4.23). Susceptible cv. Laser appeared the same as the resistant cv. Cubs Root, except that the latter had enhanced expression at 4 dpi. Susceptible cvs Cabriolet and Sansibar generally expressed more *C4H* at 4dpi but there was no significant difference in contrast to 0dpi. However, resistant line POSH had an enhanced expression at 1, 2, 4 and 8dpi by contrast with 0dpi.

An increased induction of *PLC4* was observed in POSH at 1, 2, 4 and 8 dpi against the mock inoculated control at 0 dpi (Figure 4.24). Resistant cvs/lines Cubs Root and SWU Chinese 1 showed less expression of *BnaCo7g610* (*40s ribosomal sub-unit protein S24e*) in contrast to the mock-inoculated control but POSH showed a greater induction (Figure 4.25). Cultivars Cabriolet and Sansibar did not show significant difference in contrast to the control but generally appeared have a greater expression of *BnaCo7g610*. However, resistant line POSH had an enhanced expression at 1, 2, 4 and 8dpi by contrast with 0dpi.

An earlier induction (1 dpi) of β-adaptin was observed in resistant cvs/lines and in addition to the susceptible cv. Laser (Figure 4.26). There were no significant differences in *BnaA10g05830* (*Polyadenylate-binding protein 1*) expression within any genotype against mock-inoculated control (Figure 4.27). Greater expression of *BnaC08g24910* (*USP*) was noticed in resistant lines (Figure 4.28). *USP* showed a greater induction at 1 dpi in cvs/lines Cubs Root, POSH, SWU Chinese1 and Laser in comparison to *PR1*. These results suggest that cv. Laser is intermediate as opposed to the LLS disease scoring results where it was categorised as susceptible to *P. brassicae*.
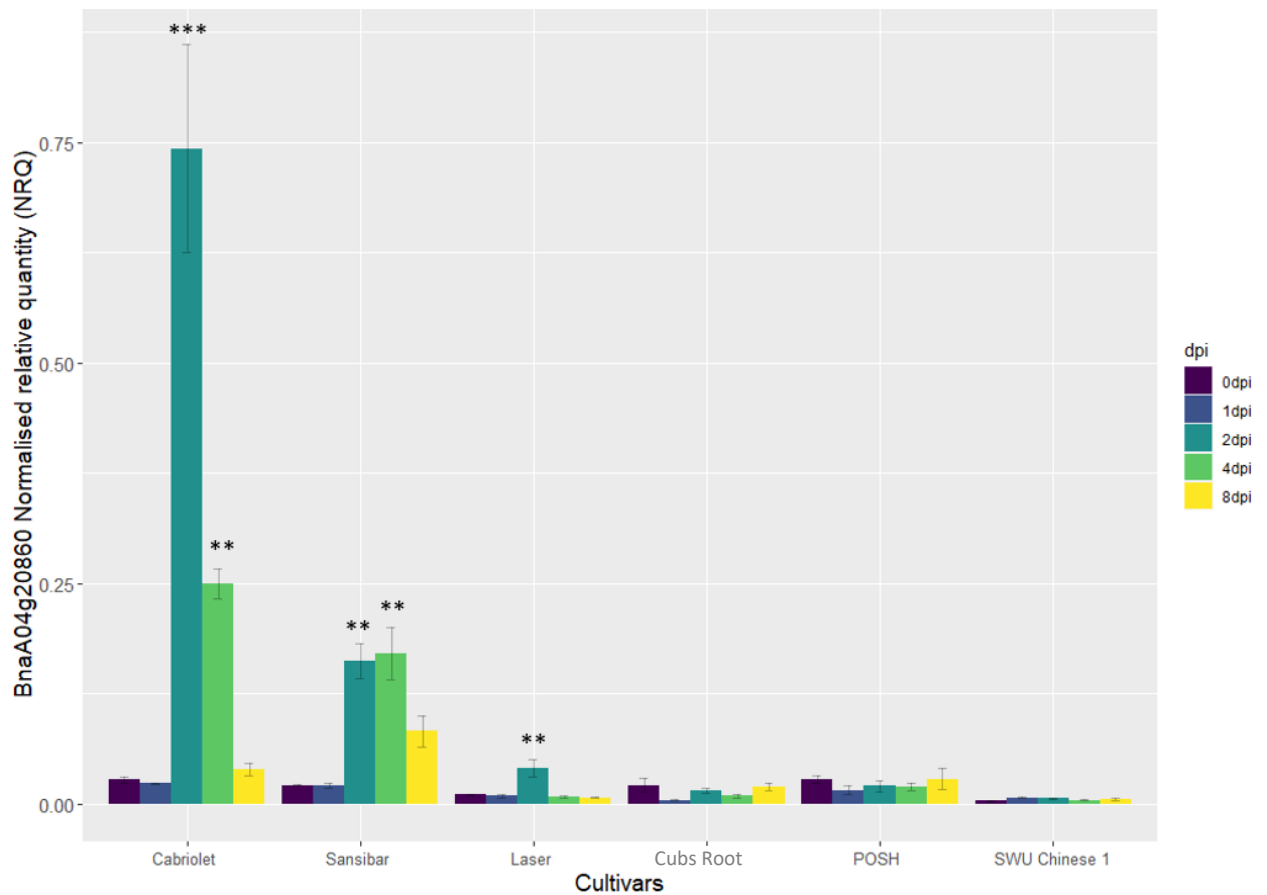
Figure 4.22: Normalised relative quantity of *BnaAo4g20860 (HXXXD-type acyl transferase).* Susceptible (Cabriolet, Sansibar, Laser) and resistant (Cubs Root, POSH, SWU Chinese 1) cvs/lines inoculated with 10^5 conidia/ml of *P. brassicae*. At 0 dpi (mock inoculated control), 1 dpi, 2 dpi, 4 dpi and 8 dpi total RNA was extracted from inoculated leaves, cDNA synthesised and analysed using qPCR. NRQ was quantified with the Pfaffl method. Significant variations between resistant/susceptible phenotypes and genotypes in expression were assessed using total gene expression combined for all time points (AUGEC). Means and standard deviations (±) of three biological replicates and two technical replicates. Significant differences between mean values of control and time points within each genotype are indicated by asterisks using Dunnett's test result. ***P-value ≤ 0.001; ** P-value ≤ 0.01; * P-value ≤ 0.05

Figure 4.23: Normalised relative quantity of *BnaCo4g1430 (C4H)*. Susceptible (Cabriolet, Sansibar, Laser) and resistant (Cubs Root, POSH, SWU Chinese 1) cvs/lines inoculated with 10^5 conida/ml of *P. brassicae*. At 0 dpi (mock inoculated control), 1 dpi, 2 dpi, 4 dpi and 8 dpi total RNA was extracted from inoculated leaves, cDNA synthesised and analysed using qPCR. NRQ was quantified with the Pfaffl method. Significant variations between resistant/susceptible phenotypes and genotypes in expression were assessed using total gene expression combined for all time points (AUGEC). Means and standard deviations (±) of three biological replicates and two technical replicates. Significant differences between mean values of control and time points within each genotype are indicated by asterisks using Dunnett's test result. ****P*-value ≤ 0.001; ** *P*-value ≤ 0.01; * *P*-value ≤ 0.05

Figure 4.24: Normalised relative quantity of *BnaA02g07530 (PLC4)*. Susceptible (Cabriolet, Sansibar, Laser) and resistant (Cubs Root, POSH, SWU Chinese 1) cvs/lines inoculated with 10^5 conidia/ml of *P. brassicae*. At 0 dpi (mock inoculated control), 1 dpi, 2 dpi, 4 dpi and 8 dpi total RNA was extracted from inoculated leaves, cDNA synthesised and analysed using qPCR. NRQ was quantified with the Pfaffl method. Significant variations between resistant/susceptible phenotypes and genotypes in expression were assessed using total gene expression combined for all time points (AUGEC). Means and standard deviations ($\pm$) of three biological replicates and two technical replicates. Significant differences between mean values of control and time points within each genotype are indicated by asterisks using Dunnett's test result. ***P-value ≤ 0.001; ** *P*-value ≤ 0.01; * *P*-value ≤ 0.05

.

Figure 4.25: Normalised relative quantity of *BnaC07g610* (*40s Ribosomal subunit protein S24e*). Susceptible (Cabriolet, Sansibar, Laser) and resistant (Cubs Root, POSH, SWU Chinese 1) cvs/lines inoculated with 10^5 conidia/ml of *P. brassicae*. At 0 dpi (mock inoculated control), 1 dpi, 2 dpi, 4 dpi and 8 dpi total RNA was extracted from inoculated leaves, cDNA synthesised and analysed using qPCR. NRQ was quantified with the Pfaffl method. Significant variations between resistant/susceptible phenotypes and genotypes in expression were assessed using total gene expression combined for all time points (AUGEC). Means and standard deviations ($\pm$) of three biological replicates and two technical replicates. Significant differences between mean values of control and time points within each genotype are indicated by asterisks using Dunnett's test result. ***P-value $\leq$ 0.001; ** P-value $\leq$ 0.01; * P-value $\leq$ 0.05.

Figure 4.26: Normalised relative quantity of *BnaC07g38240 (ß-adaptin).* Susceptible (Cabriolet, Sansibar, Laser) and resistant (Cubs Root, POSH, SWU Chinese 1) cvs/lines inoculated with 10^5 conidia/ml of *P. brassicae.* At 0 dpi (mock inoculated control), 1 dpi, 2 dpi, 4 dpi and 8 dpi total RNA was extracted from inoculated leaves, cDNA synthesised and analysed using qPCR. NRQ was quantified with the Pfaffl method. Significant variations between resistant/susceptible phenotypes and genotypes in expression were assessed using total gene expression combined for all time points (AUGEC). Means and standard deviations (±) of three biological replicates and two technical replicates. Significant differences between mean values of control and time points within each genotype are indicated by asterisks using Dunnett's test result. ***P-value ≤ 0.001; ** *P*-value ≤ 0.01; * *P*-value ≤ 0.05

Figure 4.27: Normalised relative quantity of *BnaA10g05830 (Polyadenylate-binding protein 1)*. Susceptible (Cabriolet, Sansibar, Laser) and resistant (Cubs Root, POSH, SWU Chinese 1) cvs/lines inoculated with 10^5 conidia/ml of *P. brassicae*. At 0 dpi (mock inoculated control), 1 dpi, 2 dpi, 4 dpi and 8 dpi total RNA was extracted from inoculated leaves, cDNA synthesised and analysed using qPCR. NRQ was quantified with the Pfaffl method. Significant differences between resistant/susceptible phenotypes and genotypes in expression were assessed using total gene expression combined for all time points (AUGEC). Means and standard deviations (±) of three biological replicates and two technical replicates. Significant differences between mean values of control and time points within each genotype are indicated by asterisks using Dunnett's test result. ***P-value ≤ 0.001; ** P-value ≤ 0.01; * P-value ≤ 0.05.

Figure 4.28: Normalised relative quantity of *BnaCo8g24910* (*Universal stress protein*). Susceptible (Cabriolet, Sansibar, Laser) and resistant (Cubs Root, POSH, SWU Chinese 1) cvs/lines inoculated with 10^5 conidia/ml of *P. brassicae*. At 0 dpi (mock inoculated control), 1 dpi, 2 dpi, 4 dpi and 8 dpi total RNA was extracted from inoculated leaves, cDNA synthesised and analysed using qPCR. NRQ was quantified with the Pfaffl method. Significant differences between resistant/susceptible phenotypes and genotypes in expression were assessed using total gene expression combined for all time points (AUGEC). Means and standard deviations (±) of three biological replicates and two technical replicates. Significant differences between mean values of control and time points within each genotype are indicated by asterisks using Dunnett's test result. ***P-value ≤ 0.001; ** P-value ≤ 0.01; * P-value ≤ 0.05.

4.3.7 Quantification of glucosinolates

Many studies report that GSLs are involved in the defence mechanisms against pathogens (Bennett *et al.*, 1994; Kliebenstein *et al.*, 2004; Rubel *et al.*, 2020). Furthermore, the orthologue in *B. napus* (*BnaC08g41550D*) for the GWA marker identified (*Bo8g108400*) by combining the results obtained from the glasshouse studies (Experiments 1 and 2) code flavin-containing monooxygenase. Genetic and biochemical characterization of flavin-containing monooxygenase showed that they are involved in GSL metabolism and defence responses against pathogens (Schlaich., 2007). The region also includes other flavin-containing monooxygenase coding genes such as *BnaC08g41500D*. This study helped in understanding the role of GSL and or the individual compound/s of GSL in resistance against *P. brassicae* in *B. napus*.

Susceptible cvs/lines except Moana showed less GSL than resistant cvs/lines (Figure 4.29). However, Moana appeared intermediate according to spore count and pathogen DNA content. All individual compounds, total aliphatic, total aromatic (2pe), total indolic and total GSL all showed significant differences between leaf number one and leaf number five. Younger leaves showed a greater GSL content than the older leaves. Figure 4.30 shows the total GSL contents in *B. napus* older and younger leaves. Furthermore, negative correlations were observed between total GSL, aliphatic, aromatic and indolic groups and LLS disease score (Figure 4.31).

Significant differences were observed between resistant and susceptible cvs/lines in aliphatic compounds (7-methyl sulfinyl heptyl: 7msh, 3-butenyl: 3but, 4-pentenyl: 4pent, 6-methyl sulfinyl hexyl: 6msh and 5 methylthiopropyl:5mtp); indolic compounds (4-methoxy-indolyl-3-methyl: 4moi3m, Indolyl-3-methyl: i3m) and aromatic compound: 2pe (Figure 4.32, Figure 4.33, Figure 4.34 respectively). Furthermore, 2pe and total aliphatic concentrations appeared different in susceptible cvs/lines and resistant cvs/lines (Figure 4.35). Similar patterns were shown in a correlation between aromatic 2pe vs total indolic concentration (Figure 4.36).

Resistant line POSH showed greater concentrations of aliphatic compounds, particularly 6msh and 7msh. In addition, the concentration of the aromatic compound 4moi3m was greater in POSH. Resistant cv. Dwarf Essex appeared to have greater aliphatic compound (7msh, 4pent) and aromatic i3m concentrations.
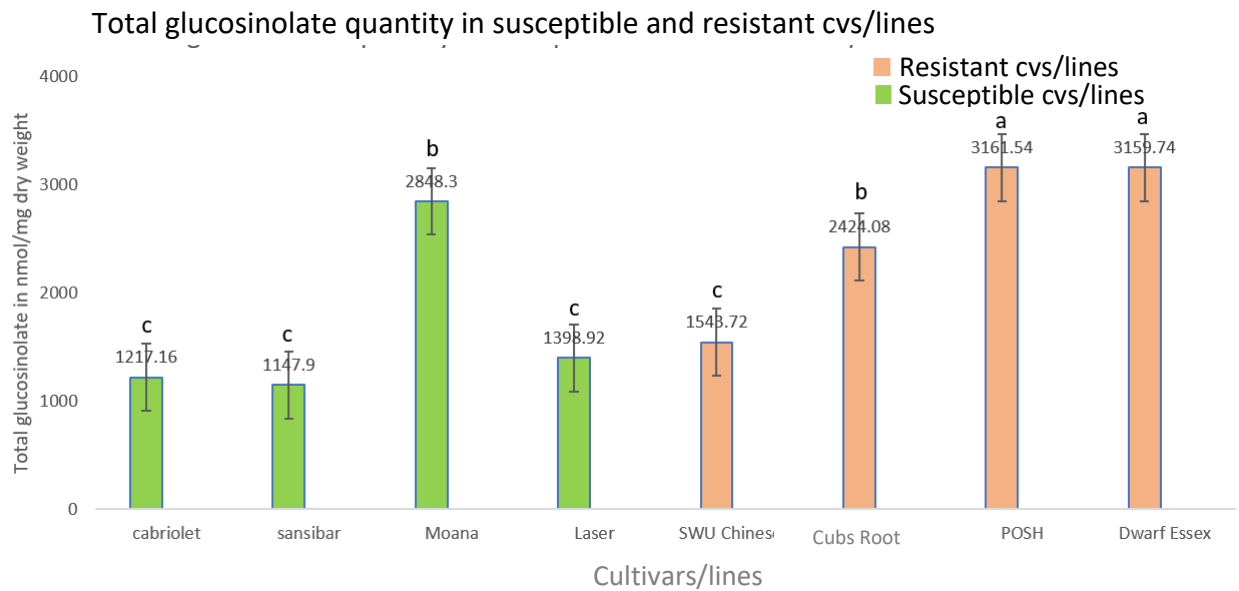
Figure 4.29: Total glucosinolates (GSL) quantified from susceptible (Cabriolet, Sansibar, Moana, Laser) and resistant lines/cvs (SWU Chinese 1, Cubs Root, POSH, Dwarf Essex) using HPLC (nmol/mg dry weight). All other susceptible cvs (Cabriolet, Sansibar and Laser) except Moana showed less GSL and all resistant lines/cvs Cubs Root, POSH and Dwarf Essex showed greater amounts of GSL except for SWU Chinese 1. Error bars represent standard errors of five biological replicates (df 7).
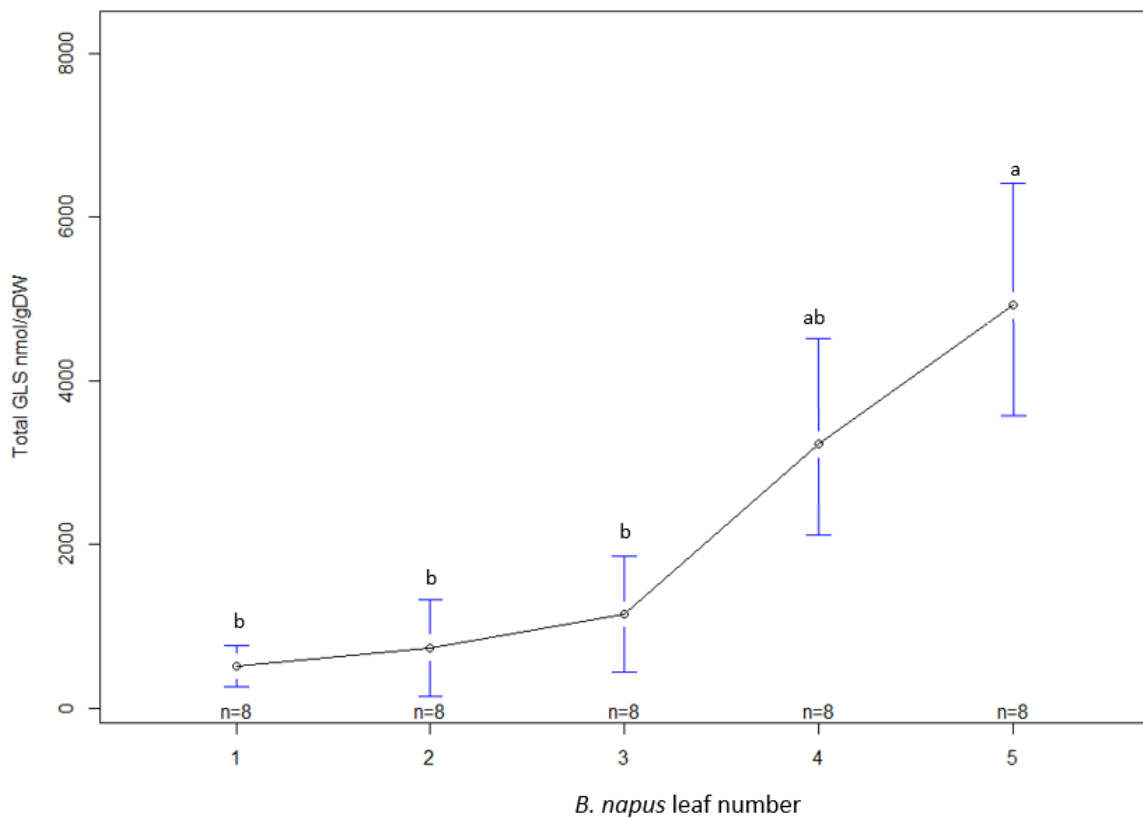
Figure 4.30: Glucosinolate concentration (nmol/g dry weight). in *B. napus* older and younger leaves (1 is the oldest and 5 is the youngest). Five replicates were used with average values and error bars represent standard errors of means. (df 4)
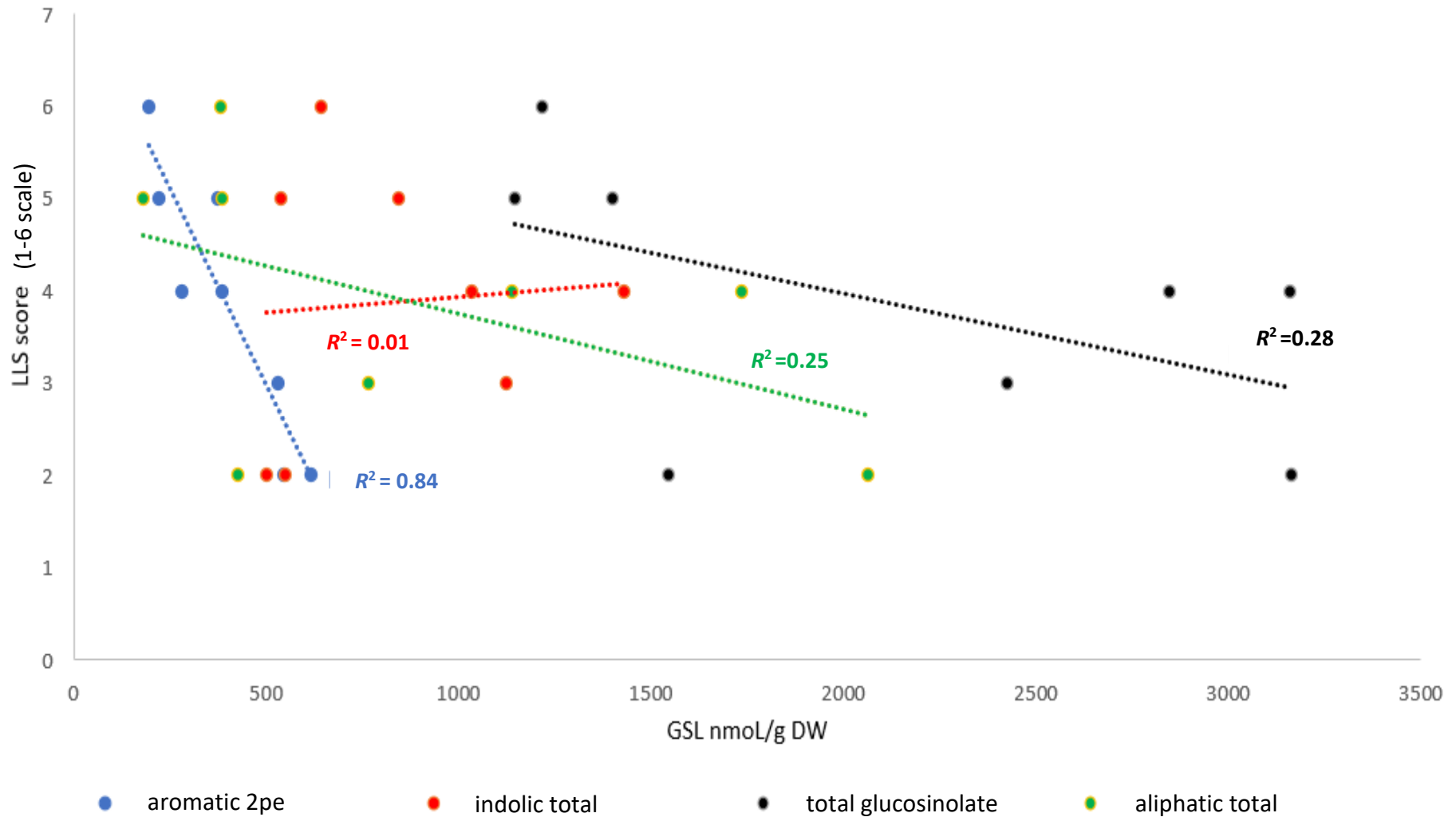
Figure 4.31: Correlation showing the associations between aliphatic, aromatic, indolic and total GSL (nmol/ g dry weight) against LLS disease score in *B. napus* cvs/lines. Correlation coefficient (R^2) 0.84 means 84% correlation and aromatic 2pe shows highest correlation with LLS score (1-6 scale).
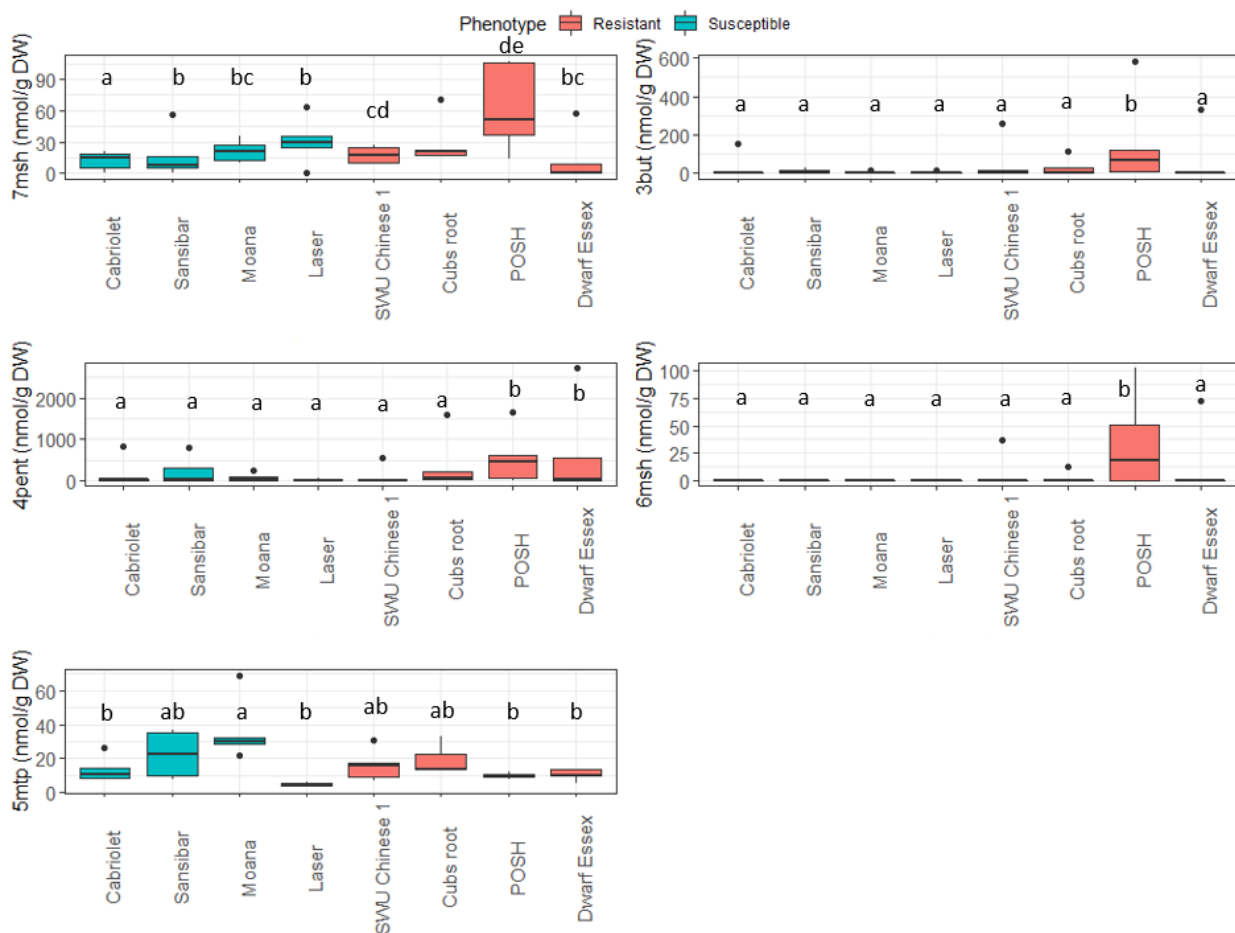
Figure 4.32: Aliphatic GSL compounds quantification. 7-methyl sulfinyl heptyl (7msh), 3-butenyl (3but), 4-pentenyl (4pent), 6-methyl sulfinyl hexyl (6msh) and 5 methylthiopropyl (5mtp) were quantified from susceptible (Cabriolet, Laser, Moana, Sansibar) and resistant (Cubs Root, Dwarf Essex, POSH, SWU Chinese 1) cvs/lines freeze dried leaf samples using HPLC (nmol/ g dry weight). Five biological replicates were used. Values with the same letters are not significantly different (Wilcoxon, Anova and TukeyHSD). Box plot middle line represents the median, whiskers show values outside the middle 50% and black dots are outliers.
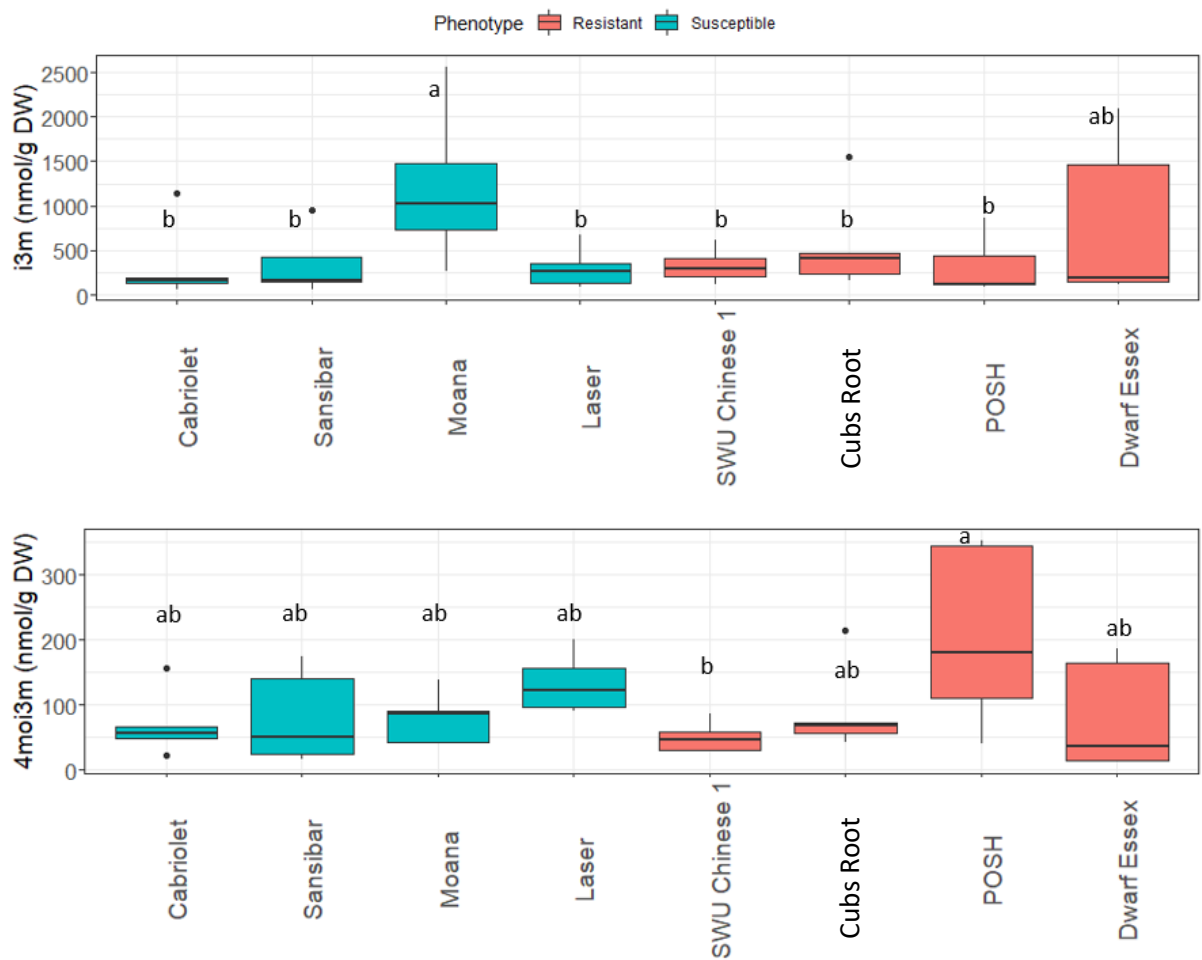
Figure 4.33: Indolic glucosinolate compounds quantification. Indolyl-3-methyl (i3m) and 4-methoxy-indolyl-3-methyl (4moi3m were quantified from susceptible (Cabriolet, Laser, Moana, Sansibar) and resistant (Cubs Root, Dwarf Essex, POSH, SWU Chinese 1) cvs/lines freeze dried leaf samples using HPLC (nmol/ g dry weight). Five biological replicates were used. Values with the same letters are not significantly different (Wilcoxon, Anova and TukeyHSD). Box plot middle line represents the median, whiskers show values outside the middle 50% and black dots are outliers.
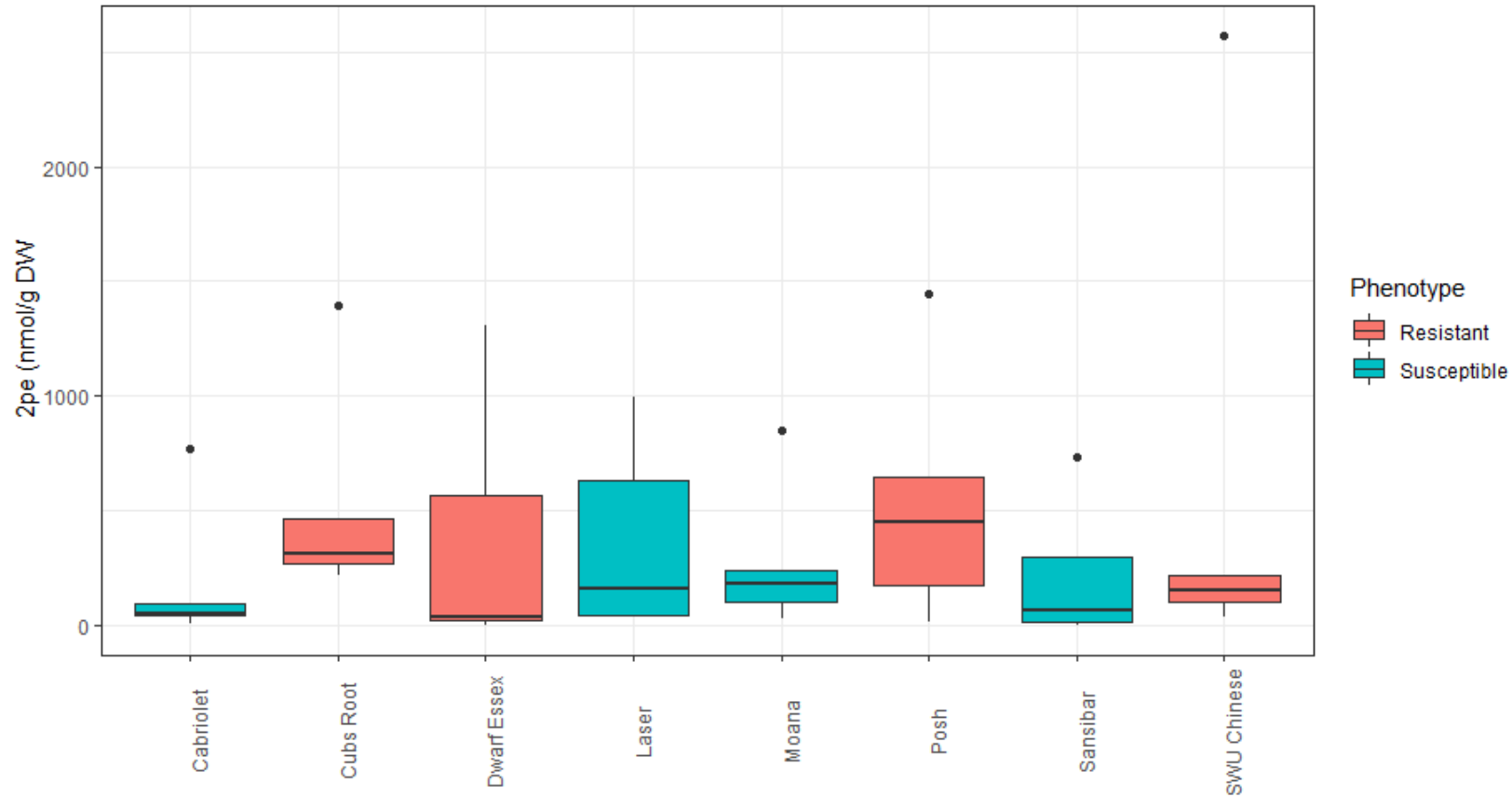
Figure 4.34: Aromatic GSL compound 2-phenylethyl (2pe) was quantified from susceptible (Cabriolet, Laser, Moana, Sansibar) and resistant (Cubs Root, Dwarf Essex, POSH, SWU Chinese 1) cvs/lines freeze dried leaf samples using HPLC (nmol/ g dry weight). Five biological replicates were used. Box plot middle line represents the median, whiskers show values outside the middle 50% and black dots are outliers.
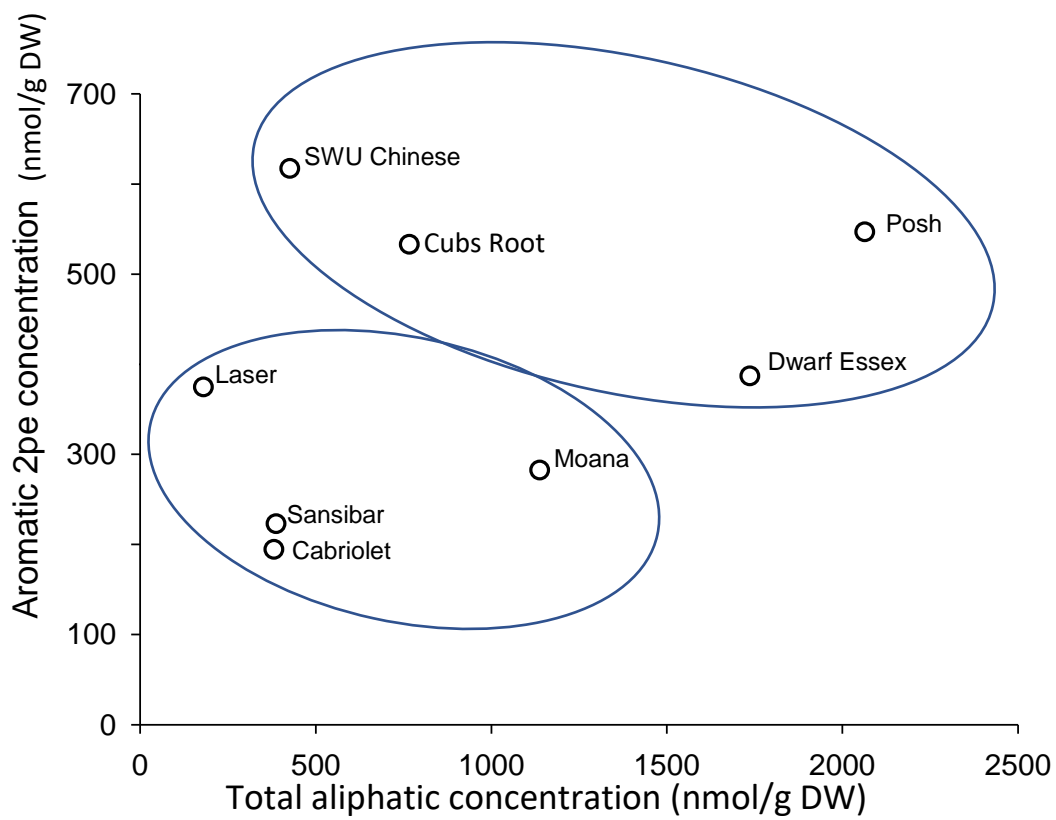
Figure 4.35: Total aromatic and aliphatic concentrations (nmol/g dry weight) in susceptible and resistant cvs/lines. The oval shapes show the arbitrary groups with highest and lowest aromatic and aliphatic contents.
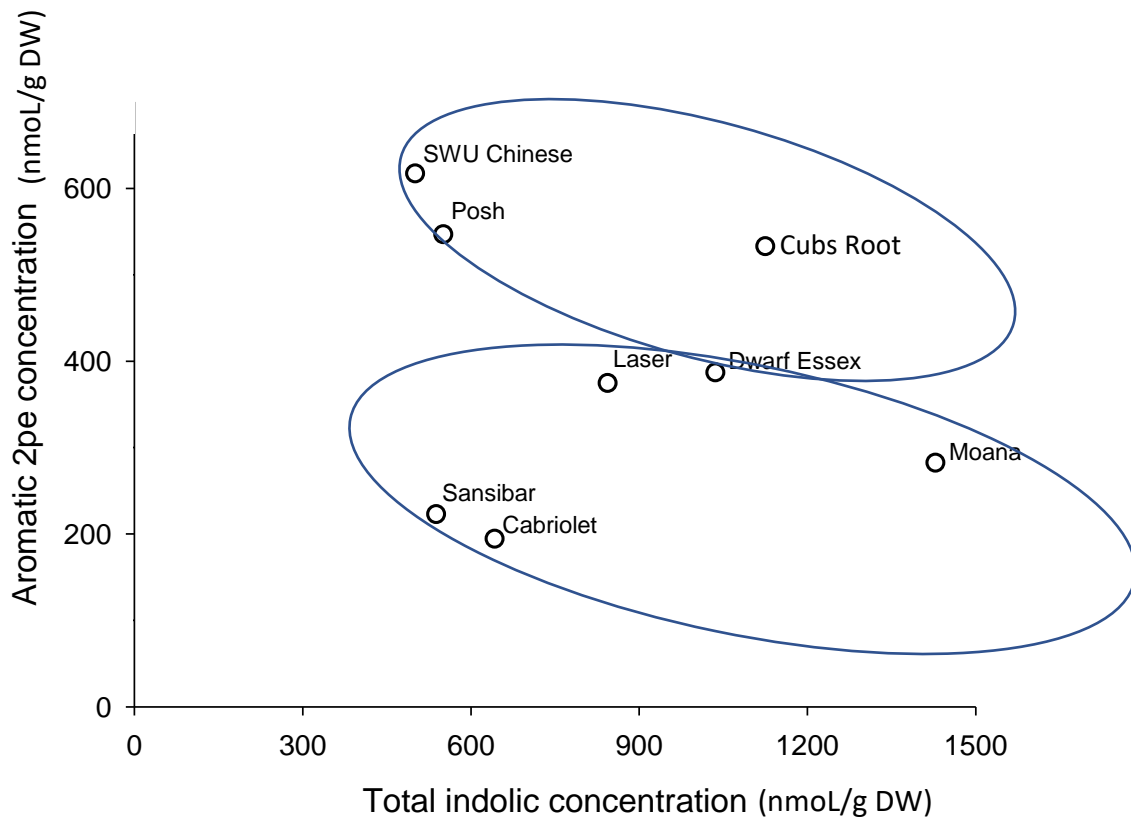
Figure 4.36: Total aromatic and indolic concentrations (nmol/g dry weight) in susceptible and resistant cvs/lines. The oval shapes show the arbitrary groups with highest and lowest aromatic 2pe and indoles contents.

4.4 Discussion

This study helped to complete the GWAS, where a total of 195 *B. napus* lines were screened under glasshouse conditions, and from the results four loci associated with QDR were identified. Furthermore, these results were used along with associative transcriptomics data to identify eight GEMs potentially involved in QDR or susceptibility against *P. brassicae* (Fell *et al.*, 2023). LLS disease scoring of commercial cvs/lines indicate a potential resistance issue for cultivars from the current Recommended List such as Ambassador which showed a greater susceptibility and Barbados (intermediate) despite having AHDB Recommended List resistance ratings of 7. However, under field conditions cv. Ambassador may perform well because it could out-grow early symptoms. This cultivar establishes very well. SEM studies added new knowledge about the initial stages of host-pathogen interactions in addition to the studies done at later stages by Karandeni Dewage *et al.* (2018a) and Boys *et al.* (2012). Moreover, the involvement of biochemical components in *B. napus* QDR against *P. brassicae* was examined for the first time by quantifying GSL in resistant and susceptible cvs/lines.

4.4.1 QDR is the predominant defence mechanism against *P. brassicae* in *B. napus*

LLS disease scoring was essential to find the GWA markers and GEMs involved in QDR against *P. brassicae*. Four QDR loci located at chromosomes A02, A09, C02, C08 and eight GEMs at A03, A04, A05, A09, A10, C02, C05, C07 were identified (Fell *et al.*, 2023). However, these markers are not on the same chromosomes as regions identified in previous studies (Table 1.1). This study revealed genes involved in host QDR against *P. brassicae* and possible molecular pathways. GWA marker genes identified include flavin-containing monooxygenase involved in GSL metabolism (Schlaich., 2007; Fell *et al.*, 2023) and a DEAD box ATP-dependent RNA helicase gene (Li *et al.*, 2008). Additionally, the GEMs identified are associated with resistance against *P. brassicae* in *B. napus*, except for *HXXXD-type acyl transferase* which promotes susceptibility (Fell *et al.*, 2023).

These results suggest that QDR is the predominant defence mechanism against *P. brassicae* in *B. napus.* For example, no complete resistance against *P. brassicae* was

observed in any of the resistant *B. napus* cvs/lines. There is evidence that ecotype-specific quantitative defence responses against *V. longisporum* in *A. thaliana* are mediated by salicylic acid, abscisic acid and jasmonic acid signalling pathways (Häffner *et al.*, 2014). Based on the genes identified and their putative functions (Fell *et al.*, 2023), it is apparent that the mode of defence against *P. brassicae* in *B. napus* is quantitative rather than the *R* gene-mediated resistance defence observed against *L. maculans* (Larkan *et al.*, 2020).

4.4.2 Genes involved in QDR or susceptibility against *P. brassicae* in *B. napus*

The present study has provided new insights into the molecular genetics by which *B. napus* resistant and susceptible cvs/lines respond to *P. brassicae* infection. Glasshouse experiments done during this project have improved understanding (GWAS) and helped to identify the most appropriate candidate resistance genes involved in the QTLs. GEMs identified included genes involved in vesicle trafficking (*β-adaptin*), lignification (*C4H*), Universal stress protein (*USP*) and others (Fell *et al.*, 2023).

Thordal-Christensen *et al.* (1997) showed that reactive oxygen species (ROS), namely hydrogen peroxide (H_2O_2) were produced as early as 6 hpi with barley powdery mildew and Chi *et al.* (2019) reported that *USPs* are involved in biotic stress tolerance. Furthermore, an enhanced ROS concentration was observed as a first line of defence against pathogens, and they can then activate further defence signalling genes including *PR1* and *C4H* (Sahu *et al.*, 2022). From the results obtained (Figure 4.37a), *USP* and *β-adaptin* were induced at 1 dpi in all resistant *B. napus* cvs/lines and susceptible cv. Laser. From the trypan blue staining and SEM assessment, *P. brassicae* conidia started to germinate at 1 dpi. This indicates that an early activation of *USP* in *B. napus* cvs/lines (Cubs Root, POSH, SWU Chinese 1 and Laser) at 1 dpi which may result in ROS production leading to downstream induction of *PR1* and *C4H*.

In addition, Feraru *et al.* (2010) showed that *β-adaptin* codes for adaptor proteins subunits AP1 and AP2. While AP1 is involved in bidirectional trafficking of proteins between trans-Golgi network and endosomal compartments, AP2 has a role in the trafficking of proteins from plasma membranes and endocytosis. They are both part of the clathrin and recognise cargos of the vesicles including those from the pathogens.

The endocytotic trafficking pathway can be modulated either by the host to activate defence response or by the pathogen to promote pathogenesis by delivering effector proteins (Gu *et al.*, 2017). This confirms the possibility of manipulating the endocytotic pathway by up-regulating β-adaptin in resistant *B. napus* cvs/lines at 1 dpi to trigger QDR.

PR1 was expressed greatly at 2 dpi (Figure 4.37a) in cvs/lines Laser, Cubs Root and POSH, suggesting the likelihood of its induction via ROS. Furthermore, expression of *40S ribosomal protein S24* and *C4H* was up-regulated at later time points in POSH (2, 4, 8 dpi). Resistant cvs/lines Cubs Root and SWU Chinese 1 have showed a greater induction of *C4H* at 4 dpi.

Therefore, the results indicate that *USP* and *β-adaptin* operate at 1 dpi to limit germination of the *P. brassicae* spores, while *PR1* and *C4H* potentially reduce *P. brassicae* penetration and branching, respectively (Figure 4.37a). Figure 4.37b shows a schematic representation of GEMs working at various stages of *P. brassicae* interaction with *B. napus*. This correlates with the findings from glasshouse experiments which showed decreases in LLS disease score, spore number and concentration of *P. brassicae* DNA in resistant *B. napus* cvs/lines by contrast with susceptible cvs/lines. The data also revealed that the potential resistance against *P. brassicae* mediated by *PLC4* and *40s ribosomal subunit s24e* were genotype-specific and POSH could be an ideal line to study them further. *USP*, *β-adaptin*, *PR1* and *C4H* were broader spectrum and showed a clear significant difference in expression between susceptible and resistant *B. napus* cvs/lines. Furthermore, these results indicate the promise of identifying GEMs by Rachel Wells from John Innes Centre, Norwich.

4.4.3 Qualitative and quantitative assessments of *P. brassicae*

AHDB Recommended List rating of LLS resistance is currently calculated using visual assessments. However, this method may be not reliable as *P. brassicae* has a long asymptomatic phase. Leaves need to be incubated for 7-10 days in polyethylene bags to promote sporulation (Karolewski *et al.*, 2006). This could be a reason why the commercial cv. Ambassador was rated resistant in terms of LLS resistance according to AHDB Recommended List but scored susceptible using visual assessments or
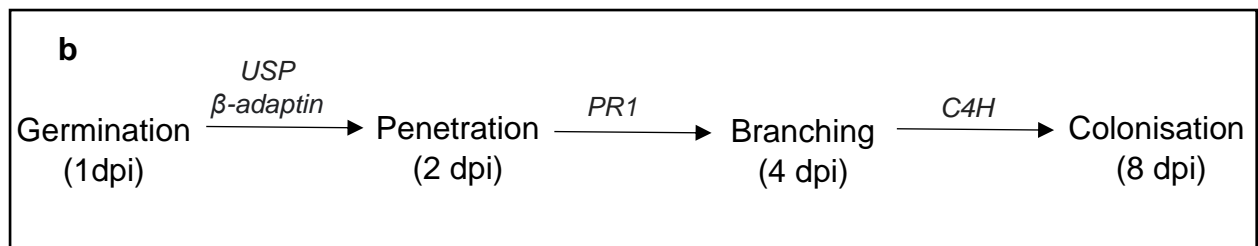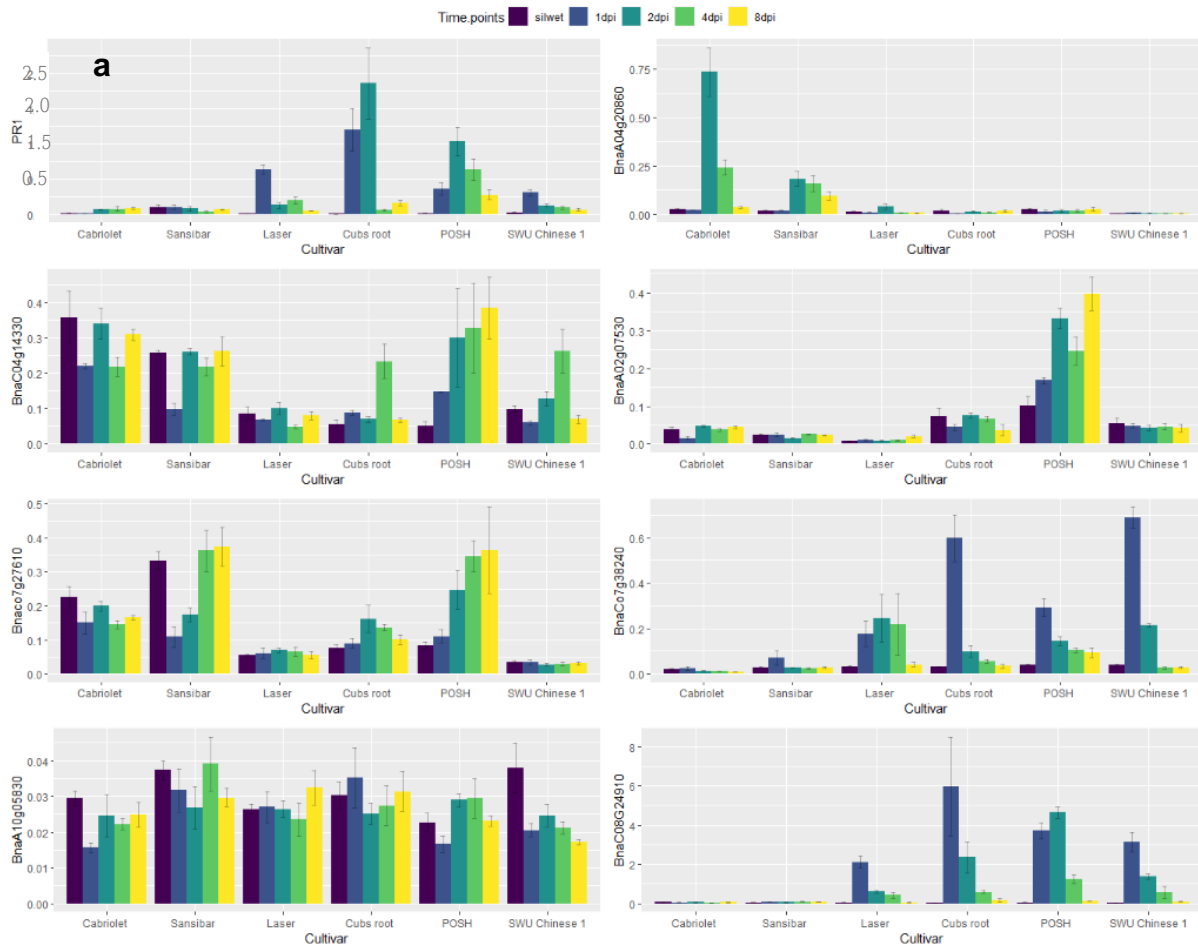
Figure 4.37: Normalised relative expression of GEMs. (a) *PR1, BnaAo4g20860* (*acyl transferase*)*, BnaCo4g1430* (*C4H*)*, BnaA02g07530* (*PLC4*)*, BnaCo7g610* (*40s ribosomal subunit s24e*)*, BnaCo7g38240 (ß-adaptin), BnaA10g05830* (*Polyadenylate-binding protein 1*)*, BnaCo8g24910* (*Universal stress protein*) at 0dpi (silwet), 1dpi, 2dpi, 4dpi and 8dpi in susceptible (Cabriolet, Sansibar, Laser) and resistant (Cubs Root, POSH, SWU Chinese 1) cvs/lines. Means and standard deviations (±) of three biological replicates and two technical replicates (df = 5). (b) Schematic representation of QDR genes operating at different stages of *P. brassicae* pathogenicity in *B. napus*.

spore counts. This study compared the visual assessment with *P. brassicae* spore count and DNA quantification using qPCR to assess *P. brassicae* pathogenicity in *B. napus*.

Figure 4.11 showed positive correlations (R^2 0.9) between LLS disease score and *P. brassicae* spore number at 21 dpi and after a further 5 days of incubation. Furthermore, a positive correlation (R^2 0.8) was observed between LLS score and amount *P. brassicae* DNA (Figure 4.12). Additionally, *P. brassicae* DNA and spore concentration showed a positive correlation with R^2 0.86 (Figure 4.13). Therefore, all these methods are acceptable as long as an extra incubation step at 4°C is added to increase humidity and *P. brassicae* sporulation. Furthermore, both qualitative and quantitative methods were used effectively without significant difference in characterising resistant/susceptible resistance characteristics in *B. napus* (Boys *et al.*, 2012; Karandeni Dewage *et al.*, 2022). However, it is more reliable to use the quantitative methods as this study showed that Moana was susceptible using visual assessment but intermediate using *P. brassicae* spore counts or DNA content.

4.4.4 Visualisation of *P. brassicae* – *B. napus* interactions

Trypan blue staining and SEM images indicated that *P. brassicae* was able to penetrate and colonise both susceptible and resistant *B. napus* cvs/lines. However, the total length of hyphae quantified using ImageJ software showed that the colonisation was significantly greater in susceptible cv. Cabriolet at 8 dpi. Furthermore, there was no significant change observed between 4 dpi and 8 dpi in resistant cv. Cubs Root, whereas an increase was observed in the susceptible cv. Cabriolet. These findings are in agreement with previous studies (Boys *et al.*, 2012; Karandeni Dewage *et al.*, 2022). Boys *et al.* (2012) showed that there was an increase in *P. brassicae* DNA in susceptible cv. Apex relative to resistant line Imola. In addition, extensive asexual sporulation and a 300-fold increase in *P. brassicae* DNA in susceptible cv. Apex was observed in contrast to resistant cv. Imola between 13 to 36 dpi. Likewise, the colonisation and sporulation of *P. brassicae* were reduced without eliminating the pathogen in a partially resistant line from a segregating DH population (Karandeni Dewage *et al.*, 2022). Boys *et al.* (2007) reported that the cvs Apex and Bristol were categorised as resistant against *P. brassicae* in the 1990s, after extensive commercial deployment resulted in the resistance breakdown in the early 2000s. The resistance

breakdown is mainly due to pathogen population (usually mutation/deletion of the pathogen effector gene that is recognised by a host resistance gene).

The present study increased knowledge of the *B. napus-P. brassicae* pathosystem because previous studies (Boys *et al.*, 2012, Karandeni Dewage *et al.*, 2022) did not consider initial stages of *P. brassicae* infection. This study established the sequence of germination, penetration, branching and colonisation by *P. brassicae* of *B. napus*. The significant difference in hyphal length between resistant and susceptible cvs indicates that QDR operates at 4 and 8 dpi to limit colonisation. As this study was based on single resistant and susceptible cvs, other cvs/lines should be observed to make more general conclusions.

4.4.5 GSL imparts resistance against *P. brassicae* in *B. napus*

GSL are an important source of phytoanticipins in *B. napus* and *A. thaliana*. Indolic and aliphatic GSL mutants were more susceptible to *S. sclerotiorum* in *A. thaliana* (Stotz *et al.*, 2011b). Furthermore, enhanced aliphatic and indolic glucosinolate concentrations were associated with seedling resistance of cabbage against *L. maculans* (Robin *et al.*, 2020). This PhD thesis showed a correlation between GSL concentration and resistance against *P. brassicae*. Five out of sixteen aliphatic GSL, two out of three indolic GSL and one aromatic GSL quantified showed a significant difference between resistant and susceptible *B. napus* cvs/lines. In addition, negative correlations were observed between aliphatic, aromatic and total GSL quantities and LLS disease score (Figure 4.31). Aromatic 2pe showed the greatest correlation, with R^2 0.84, and no correlation with LLS score was observed for indolic GSL.

Even though cv. Moana was categorised as susceptible based on LLS disease score, a greater GSL concentration was observed than in the other cvs/lines and resistant line SWU Chinese 1 showed a smaller GSL content than resistant cvs/lines (Cubs Root, POSH and Dwarf Essex). As expected, younger leaves showed a higher GSL content than older leaves (Figure 4.30) (Brown *et al.*, 2003).

Abuyusuf *et al.*, (2018) showed increased induction of aliphatic glucoiberverin (GIV) and indolic glucobrassicin (GBS) in white mould resistant cabbage lines. Furthermore, at 3 dpi aliphatic GSL biosynthetic genes (*ST5b-Bol026202* and *ST5c-Bol030757*) and indole biosynthetic genes (*ST5a-Bol026200* and *ST5a-Bol039395)* were induced after

infection with *Sclerotinia sclerotiorum* in resistant *B. oleracea*. For this PhD thesis, GSL contents were quantified in uninoculated *B. napus* leaves and it will be beneficial to study if there are significant changes when leaves are challenged with *P. brassicae* to better understand the role of GSL in *B. napus-P. brassicae* interactions.

4.4.6 Is *Actin* a good reference gene in *B. napus*?

Since Sun *et al.* (2010) determined that housekeeping genes *Actin* and *GAPDH* can be used as internal reference genes for *Clonorchis sinensis* qPCR analysis, researchers have been widely using these genes. Many studies validated the efficiency of *Actin* as a reference gene and showed stable expression across various treatments (Chandna *et al.*, 2012; Ma *et al.*, 2020; Wang *et al.*, 2017). However, these studies predominantly involved individual cvs/lines such as *Brassica juncea* cultivar Varuna (Chandna *et al.*, 2012), *Brassica rapa* winter rapeseed Longyou (Ma *et al.*, 2020) and *C*amellia *sinensis* cultivar Longjing-changyecha (Wang *et al.*, 2017).

For this PhD thesis, even though the expression of *Actin* across different cvs/lines (genotypes) looked similar by plotting Ct values (Figure 4.38), a significant difference was observed between genotypes (P = 2e-^{16}) using ANOVA. Similar differential expression in different genotypes was observed by Stotz *et al.* (2022). From these studies, it is evident that *Actin* is not an effective reference gene for studies across various genotypes. However, it is a good candidate to assess relative expression within a genotype and across time points.

The qPCR results can be interpreted as absolute quantification by applying a standard curve or as relative quantification using a reference gene. The reference gene must be steadily expressed across all cvs/lines and across all treatments. It is advisable to use at least three reference genes with steady expression to calculate normalised relative expression (Vandesompele *et al.*, 2002). *GAPDH* was included as a second reference gene to calculate NRQ, but the primer did not work.

To circumvent the differential expression of *Actin*, total expression of GEMs was calculated (AUGEC). Significant differences in AUGEC between resistant/susceptible phenotypes and between genotypes were assessed while considering *Actin* as a co-variate using an ANCOVA model. This study reports this issue for the first time and
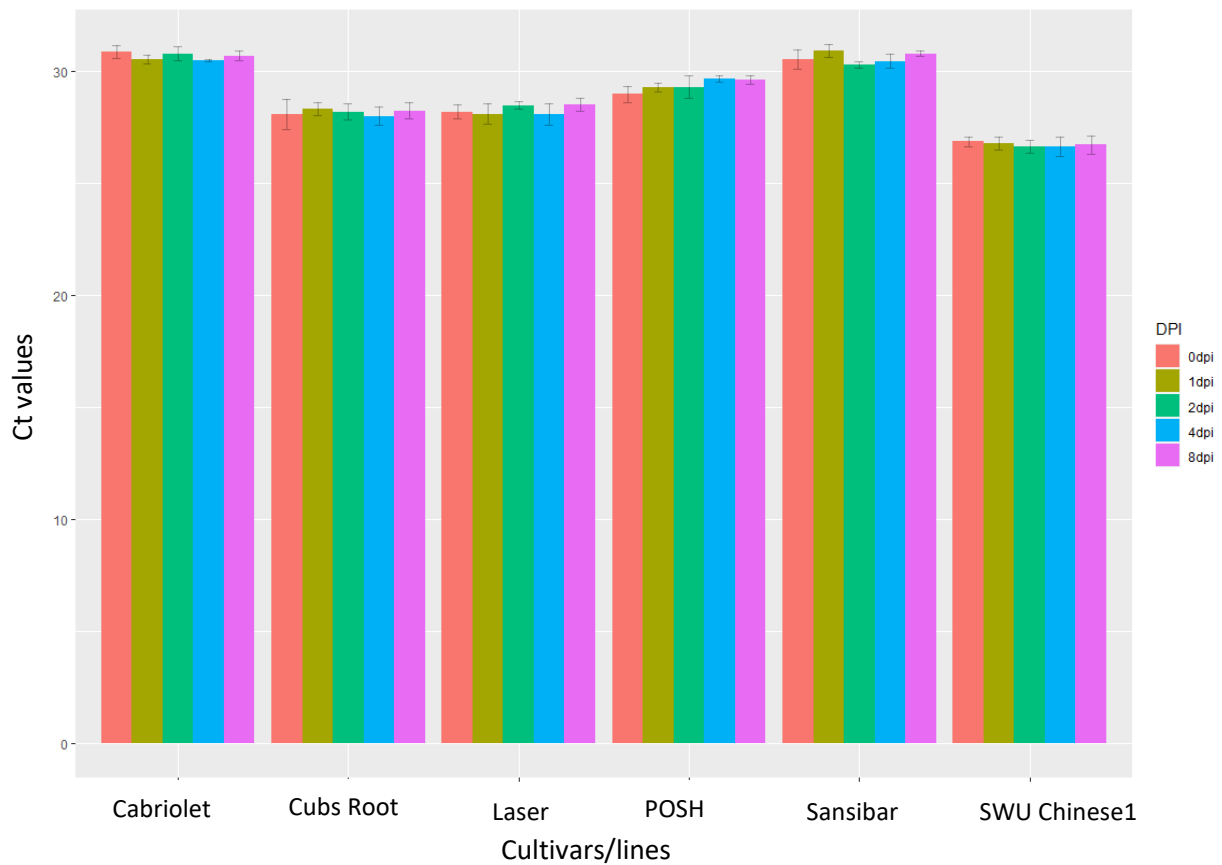
Figure 4.38: Bar plot showing *Actin* Ct values for *B. napus* cvs/lines (Cabriolet, Cubs Root, Laser, POSH, Sansibar, SWU Chinese 1). Error bars represent: *Y* min=mean-sd, *Y* max= mean+sd of three biological replicates each of two independent experiments combined. *Actin* expression remained the same across time points within each cultivar but there was a significant difference in expression between cvs/lines ($P = 2e^{-16}$).

the AUGEC calculation method can be benefit many researchers who face similar problems. Alternatively, other stable reference genes such as *GAPDH* can be used.

When each GEM is assessed within a genotype or across genotypes, measurements of the gene expression can take place at a single critical time point or at multiple time points after the host is challenged by a pathogenic isolate. For a candidate gene which was known to have a qualitative response (i.e., the gene had a switched on/off effect), measurement of the gene expression at a recognised critical time point can be valid and used for comparison above a triggering threshold expression value. However, for a candidate gene which showed a quantitative response (i.e., the gene had a dimmable effect), the gene expression can be measured at multiple time points within a defined growing window after infecting the host with a pathogenic isolate. The effect of this quantitative candidate gene expression at different time points can be integrated as the area under the gene expression curve (AUGEC) like the concept of the area under disease progress curve (AUDPC) used to assess development of a plant disease. The AUGEC was used to combine the multiple measurements of gene expression into a single value which acts as the total gene expression. So, the effect of gene expression at any specific time point was added into the total gene expression for the gene concerned. The larger the AUGEC, the stronger this gene should have expressed. The AUGEC values were used for analysis of variance to assess differences between resistant/susceptible phenotypes, and between genotypes with *Actin* as a co-variate. In the use of AUGEC, the effects of the candidate genes were implicitly assumed to be quantitative. It was felt that the expression of any candidate resistance genes should be measured at multiple time points after a pathogenic challenge to the host within a well-defined timeframe before it was known whether they have qualitative effects or quantitatively accumulative effect. Measurements of gene expression at different time points can reveal the temporal characteristics and/or patterns in gene expression. Then AUGEC can be calculated and compared between genotypes. The present results showed that the susceptible genotypes were more reactive by having more gene expression than the resistant genotypes. Overall, the lessons learned in this study were that research priorities should be focussed on finding (1) the critical stage to sample and measure the gene expression; (2) the gene expression threshold at which host response is triggered; and (3) the gene expression

duration during which the effect of gene response is accumulated and contributes to the targeted phenotype.

4.4.7 TaqMan Multiplex qPCR limitations

Multiplex qPCR assays are simple to use as they come in a single tube consisting of pairs of unlabelled primers and TaqMan probes with a dye label on the 5'-end and non-fluorescent quencher on the 3'-end. They are very sensitive and accurate to detect targets at small concentrations and minor-fold changes. Thermo Fisher Scientific recommend using these assays without either standard curve analysis or the gel electrophoretic analysis. In addition, up to four genes can be assessed at the same time and it is effective when evaluating multiple genes. However, due to proprietary issues, Thermofisher neither supply the primer or probe sequence details. They are pre-validated in the Thermofisher bioinformatics lab but not in a wet lab. Thus, it is not possible to trouble shoot (BLAST) using the primer sequences and custom assays are not cost-effective considering traditional primers. A traditional primer pair cost is less than £20 while the custom-made assay costs *c.* £300. Appendix 8 shows the amplicon context sequence details for each of the genes which were used for Taqman custom assays. Bustin *et al.* (2011) reported that if the primer or probe sequences cannot be disclosed, because they are commercially sensitive, then amplicon context sequence and an assay identification name must be provided by the vendor and assay validation must be supplied in order to publish the data. However, they recommended disclosure of the primer and probe sequences. Therefore, considering the cost, trouble shooting and ease of publication, it is ideal to opt for conventional SYBR green primers rather than multiplex qPCR assays.

4.4.8 Future work

4.4. 8.1 BnaA05g34100D (SNF1 kinase homolog 10) qPCR

Taqman primer did not work for *BnaA05g34100D (SNF1 kinase homolog 10/KIN10).* However, many studies indicate its involvement in resistance against various plant pathogens. Over-expression of *SnRK1* in barley plants resulted in increased resistance against *Blumeria graminis* (Han *et al.*, 2020). *SnRK1* provides wheat with resistance against *Fusarium graminearum* (Jiang *et al.*, 2020). In rice, *SnRK1* over-

expression resulted in broad spectrum resistance against *Xanthomonas oryzae* (Filipe *et al.*, 2018). Furthermore, *SnRK1* induced effective resistance against *Plasmodiophora brassicae* in *A. thaliana* (Chen *et al.*, 2021). Therefore, it will be beneficial to assess the expression of *KIN10* in future.

4.4.8.2 Kompetitive Allele Specific PCR (KASP) marker analysis to confirm the involvement of quantitative genes in resistance against *P. brassicae* in *B. napus*

Targeting Induced Local Lesions in Genomes (TILLING) mutants in *B. rapa* were generated by altering single nucleotides of the gene of interest to test the involvement of the genes in QDR assessed using qPCR. Appendix 9 shows the genes tested in *B. napus* using Taqman multiplex qPCR (*BnaC04g14330D, BnaC07g38240D, BnaA05g34100D)* and their corresponding homologs in *B. rapa* along with the TILLING mutant names. TILLING mutants for *C4H* (ji30317a, ji30819a), *β-adaptin* (ji30010b, ji320204a) and *KIN10 SNF1* (ji31647b) were ordered from the John Innes Centre, as were KASP marker primers ordered from LGC genomics UK. Appendix 10 shows the SNP details submitted to LGC for KASP primer synthesis. However, due to time limitations the experiment was not completed. It will be beneficial to assess the disease scores, spore numbers and to quantify *P. brassicae* DNA to determine the involvement of these genes in quantitative disease responses.

PhD student Laura Gimenez Molina has shown that the disease score and spore number were significantly reduced in TILLING mutants of *BnaA04g20860D (HXXXD-type acyltransferase)* in comparison to WT *B. napus*. This agrees with the suggestions from this study that acyl transferase may be involved in susceptibility to *P. brassicae* in *B. napus*.

4.4.8.3 Lignin staining

In this study, both the susceptible and resistant host plants did not show any lignin accumulation using Wiesner's reaction/phloroglucinol-HCl at 1, 2, 4 and 8 dpi. Only vascular bundles were stained at all time points and Appendix 11 shows staining at 8 dpi as an example. It will be therefore useful to repeat the experiment using Safranin O-fast green staining and a leaf embedding method where 5 µm thickness leaf sections are embedded in paraffin (Jia *et al.*, 2015).

4.5 Conclusion

In the UK, oilseed rape is the third most important arable crop and efficient LLS control will increase yield, which contributes to food security. Even though there has been immense progress in genetic linkage and physical mapping, information about the genes underlying quantitative resistance loci remains limited. This study helped to better understand the genetic basis of QDR loci in *B. napus* operating against *P. brassicae*.

Cultivar Laser was categorised as susceptible using qualitative and quantitative assessments after inoculation with *P. brassicae*. However, qPCR analysis of GEMs showed induction of GEM expression in Laser. Therefore, it can be concluded that Laser can be used as a potential resource to breed for resistance against *P. brassicae*. In addition, susceptible cv. Moana showed a substantial GSL content and therefore it can be a potential candidate to exploit GSL content mediated resistance against *P. brassicae*. However, the line that showed significant induction of GEM as well as GSL content was POSH and it is much better for breeding programmes.

LLS disease scoring results from this and the previous studies (Fell *et al*., 2023) under different glasshouse conditions, locations and in different years show that the resistance response of specific cvs/lines were similar or did not show significant variation. Furthermore, populations of *P. brassicae* similar to natural inoculum were used. Therefore, specific resistant lines can be used to breed an effective line resistant against *P. brassicae*. However, extensive cultivation of a specific cultivar can result in resistance breakdown due to *P. brassicae* pathogenicity gene/s mutations as we have seen with cv. Apex (Boys *et al*., 2007).

This study will enable breeders to utilize the new information about genes associated with quantitative resistance and to produce genetically improved lines. Furthermore, it will help others to better understand other closely related apoplastic fungal pathosystems such as barley/*Rhynchosporium commune* and apple/*Venturia inaequalis*.

Chapter 5: Role of the cuticle in resistance against *P. brassicae*

5.1 Introduction

It is a great challenge for breeders to enhance the diversity of the *B. napus* gene pool available to face the challenges associated with climatic change while maintaining yield and broader resistance to pathogens. One of the main factors contributing to genetic bottlenecks in *B. napus* is the continuous selection of various traits such as low seed erucic acid and low glucosinolate contents (Snowdon *et al.*, 2012). Furthermore, the domestication of *B. napus* as an oilseed crop was done 400-500 years ago and therefore, the germplasm is narrower than that of *B. rapa* and *B. oleracea* (Mei *et al.*, 2011). However, it is possible to introgress resistance to *P. brassicae* from related species such as *B. rapa* into *B. napus* and increase the diversity of germplasm available for breeding.

The host cuticle plays a central role as a barrier against water loss as well as against pathogens in almost all crops. Therefore, identifying new allelic variants of already known or novel genes involved in cuticle-associated traits, such as resistance against *P. brassicae,* in available genetic resources will be beneficial for crop improvement. This is achievable with many methods such as phenotyping (visually or by scanning electron microscopy etc.), analysing the cuticular wax and cutin using gas chromatography mass spectrometry (GC-MS) and staining techniques such as toluidine blue (Tanaka *et al.*, 2004; Petit *et al.*, 2017).

The cutinase enzyme secreted by fungal pathogen species has an important role in overcoming the cuticle barrier by hydrolysing the ester linkages between cutin monomers. Cutinases are involved in aiding spore adhesion to the cuticle, germination on the cuticle, spore germ tube elongation, formation of penetrating structures, penetration of cuticle and colonisation inside the tissue (Arya *et al.*, 2022). Therefore, cutinase expression was assessed in this study to better understand the role of the cuticle in resistance against *P. brassicae* in *B. napus* and *B. rapa.*

5.1.1 Structure and function of the cuticle

The cuticle is an extracellular hydrophobic barrier which covers the epidermal cell layer to protect the plant against water loss and against pathogens. Plant cuticle microscopic structure has two main layers based on histochemical staining and chemical composition. The cuticular layer is closely linked to the epidermal cell walls. It consists of intra-cuticular waxes, cutin made up of lipid polymers (fatty acids and fatty alcohols) and polysaccharides. On top of the cuticular layer lies the cuticle itself, which is a cutin-rich domain partly covered and interspersed with waxes. These waxes are either accumulated on the cutin surface as epicuticular wax crystals or films, or deposited within the cutin matrix as intracuticular wax (Yeats & Rose, 2013; Serrano *et al.*, 2014).

5.1.2 Role of the cuticle in fungal pathogenesis

During pathogenesis, cutin monomers and chemical components of cuticular wax facilitate spore germination and initial fungal growth (Ahmed *et al.,* 2003). Woloshuk and Kolattukudy (1986) showed that addition of cutin to a spore suspension induced cutinase production by *Fusarium solani* spores. They proposed that cuticle penetrating fungi sense cutin monomers on plant surfaces and produce cutinase. Initially, small amounts of cutin monomers are released from the host cuticle by fungi and detecting this then induces greater concentrations of cutinase needed for penetration.

Podila *et al.* (1993) showed that the avocado fruit surface wax triggered *Colletotrichum gloeosporioides* spore germination and appressorium formation. Chromatography revealed that the fatty alcohol fraction with C24 and longer-chain alcohol was the appressorium-inducing factor. Analysis of avocado wax by gas-liquid chromatography or mass spectrometry assay showed large amounts of very long aliphatic compounds. A typical component of surface wax, very long chain aldehydes, induces spore germination in the barley powdery mildew fungus *Blumeria graminis* (Hansjakob *et al.*, 2012).

5.1.3 Cuticle components, structural variations and plant resistance

Many studies indicate that cutin monomers not only facilitate disease progression but also induce resistance in plants. A reduced systemic acquired resistance was

observed in *A. thaliana* mutants *acp4* (*acyl carrier protein*) and *gl1* (*GLABRA1*) with cuticular lipid defects (Bernard *et al.*, 2013). Addition of active cutin monomers into potato cell suspension culture activates production of the hormone ethylene and expression of defence related genes (Schweizer *et al.*, 1996a). Spray application of two cutin monomers from the C18 family protected a highly susceptible barley cultivar against *Blumeria graminis* and was also effective in rice against *Magnaporthe grisea* (Schweizer *et al.*, 1994, 1996b).

Li *et al.* (2007) showed that the *A. thaliana* double mutant (*gpat4/gpat8*) of two acyl transferases involved in cutin biosynthesis resulted in significant reduction in cutin and was less resistant against *Alternaria brassicicola*. Furthermore, an enhanced permeability was observed in these mutants, confirming that cutin is important as a water barrier. However, the over-expressor of *A. thaliana* (*CYP86A1*) had an 80% increase in cutin monomers and impaired water permeability but showed normal resistance against *Alternaria brassicicola.*

Numerous publications report that *Arabidopsis thaliana* mutants with increased cuticular permeability had improved resistance signalling and responses. Table 5.1 summarises various studies done on *A. thaliana* mutants with increased cuticular permeability due to impaired cutin or cuticular wax biosynthesis that showed an enhanced resistance against *Botrytis cinerea.* Nyadanu *et al.,* (2012) showed an increased resistance against *Phytophthora palmivora* and *Phytophthora megakarya* in cocoa leaves and pods with wax by contrast with those leaves where wax was removed by washing with chloroform for 30 sec. In addition, cutin mutants of *A. thaliana* (*att1* and *lacs2*) were more susceptible to *Pseudomonas syringae* while many mutants including *lacs2* showed enhanced resistance against *B. cinerea* (Bernard *et al.*, 2013)*.*

A greater resistance against *P. syringae* was observed in *A. thaliana* mutant *cer1* with a smaller alkane content. On the other hand*,* over-expression of *CER1* in *A. thaliana* with higher cuticular alkane content delayed the defence response against *P. syringae* and increased susceptibility to *Sclerotinia sclerotiorum* (Bernard *et al.*, 2013)*.* The *CER1* gene promotes biosynthesis of very long chain alkane cuticular wax and thus it indicates that a larger amount of wax increases the hydrophobicity and reduces cuticle

Table 5.1: Summary of studies illustrating that impaired cutin or cuticular wax results in greater cuticle permeability and enhanced resistance against *Botrytis cinerea* in *A. thaliana*.

Mutation	Function of gene	Result of mutation	Reference
lacs2 (Long-chain acyl-CoA synthetase)	Synthesis of cutin or cuticular waxes	- Thinner cuticle - Increased cuticular permeability - Reduced dicarboxylic acid monomers in the cutin polyester - Amplified resistance against *B. cinerea*	Schnurr *et al.,* 2004
bre1 (*Botrytis*-resistant 1)	Synthesis of cutin or cuticular waxes	- Thinner cuticle - Increased cuticular permeability - Amplified resistance against *B. cinerea*	Bessire *et al.,* 2007
myb96 (MYB transcription factor)	Transcriptional activator of genes coding very long chain fatty acid condensing enzymes involved in cuticular wax biosynthesis	- Increased cuticle permeability - Reduced ABA dependent cuticular wax production - Resistance to *Botrytis cinerea*	Seo *et al.,* 2011

permeability, thus aiding disease progression. This also indicates that the individual compound alkane can affect the resistance against pathogens. In addition, less cuticle permeability might reduce perception of fungal effectors by the host and therefore delay defence responses (Bourdenx *et al.*, 2011).

A modification of *A. thaliana* and *B. oleracea* wax composition was observed as an indirect defence response when a large cabbage white butterfly *Pieris brassicae* deposited its egg, which led to the arrest of the parasitoid *Trichogramma brassicae* (Blenn *et al.*, 2012). Thus, published data indicated that both higher and lower cuticular wax and cutin or variation in their composition are involved in resistance against various pathogens in different plant species. Therefore, it will be beneficial to enhance our current knowledge about variation in cuticular wax, cutin content and composition in *B. napus* and *B. rapa* and their potential correlation with *P. brassicae* pathogenicity to guide breeding for resistant lines. Availability of wax mutants in *B. rapa* makes it a better candidate to study the role of wax in resistance against *P. brassicae* as precise mutation in allotetraploid *B. napus* is difficult.

5.1.4 Resistance against *P. brassicae* in *B. rapa*

Allotetraploid oilseed rape (*B. napus*) is a hybrid between *B. rapa* and *B. oleracea* with A and C genomes, one from each parent, respectively. A simple sequence repeat marker that assisted introgression from *B. rapa* was used to broaden the diversity of germplasm in *B. napus* (Mei *et al.*, 2011). Four QTLs involved in resistance against *P. brassicae* were identified in DH lines derived from a secondary gene pool (*B. oleracea* X *B. rapa*) crossed with *B. napus* cv. Tapidor (Karandeni Dewage et al., 2022). Moreover, an associative transcriptomics platform was applied to identify eight gene expression markers (GEMs) and additional genome wide association marker loci in *B. rapa* and *B. oleracea* associated with resistance against *P. brassicae* (Fell *et al.*, 2023). Orthologous genes of those GEMs identified showed a differential expression pattern in susceptible and resistant *B. napus* lines/cvs when challenged with *P. brassicae* (Chapter 4).

5.1.5 Chemical composition of cuticular wax and cutin

It is possible to quantify and define the chemical composition of cuticular wax and cutin accurately, which can help to better understand the differential interaction between

host-plant and pathogens because of varying wax and cutin contents. Variations in the total quantity and composition in different species (*B. napus* and *B. rapa*) and different genotypes within the species can have a potential role in mediating resistance to pathogens. Surface wax extracted with organic solvents is composed of very long chain fatty acids (VLCFAs) and their derivates, namely alkanes, fatty alcohols, fatty aldehydes, ketones and wax esters (Jin et al., 2020).

Cuticular waxes are mainly generated by the alcohol forming pathway, which produces primary alcohols, branched alcohols and esters, and the alkane forming pathway, which produces alkanes, aldehydes, secondary alcohols and ketones (Bernard *et al.*, 2013). Synthesis of wax components starts in the plasmid with C_{16}-C_{18} fatty acid formation. Further elongation happens at the endoplasmic reticulum and transport to the plasma membrane by an unknown mechanism. ABC transporters mediate the transfer of these components into the extracellular space across the plasma membrane and the trafficking into the cuticle is suggested to be via lipid transfer like proteins such as *CER (Eceriferum), LACS1* etc. (Bernard *et al.*, 2013). Figure 5.1 shows a schematic representation of synthesis of wax components through alcohol and alkane forming pathways and their export into the cuticle.

Cutin is an insoluble polyester mainly composed of C_{16} and C_{18} aliphatic monomers derived from fatty acids and found in the surface of the outer cell wall of epidermal cells (Bonaventure *et al.*, 2004). The most abundant C16 monomers are 16-hydroxyhexadecanoate (omega-hydroxy fatty acid) and 1,16-hexadecanedioic acid (alpha,omega-dicarboxylic fatty acid). The common C18 monomers are 18:1 and 18:2 alpha,omega-dicarboxylic fatty acids (Li-Beisson *et al.*, 2013).

5.1.6 Aims and objectives

From the published data, it is evident that the cuticle components, such as cuticular wax/cutin monomers, their quantity and composition affect the resistance against pathogens. Therefore, the main aim of this study was to understand if these factors affect the resistance against *P. brassicae* in *B. napus* and *B. rapa*. *B. rapa* wax mutants were used to assess the involvement of wax load as well the structural variation in resistance against *P. brasssicae.* Glossy mutants used in this study have a reduction

in wax load (up to 80%) and the non-glaucous mutants have a structural variation with the same wax load as that of WT R-0-18.

Hypothesis

- Variation in cutin/wax content and composition contribute to the resistance against *P. brassicae* in *B. napus* and *B. rapa.*

Aim:

- To analyse effects of variation in cuticular wax/cutin and their chemical composition on the compatibility or incompatibility with *P. brassicae* using *B. rapa* wax mutants and *B. napus* (resistant and susceptible) lines/cvs.

Objectives:

- To assess *P. brassicae* disease progression using LLS disease scoring, *P. brassicae* spore numbers and DNA quantification with *B. rapa* wax mutants to better understand any correlation with cuticular wax and cutin or their components.
- To compare the LLS disease score and *P. brassicae* spore numbers in *B. rapa* wax mutants with *B. napus* (resistant and susceptible) cvs/lines.
- To quantify the cutinase expression of *P. brassicae* in *B. rapa* wax mutants and *B. napus* (resistant and susceptible) cvs/lines using qPCR.
- To quantify cuticular wax and cutin components of *B. rapa* wax mutants and *B. napus* (resistant and susceptible) cvs/lines before and after infection by *P. brassicae.*

5.2 Materials and methods

B. rapa wax glossy mutants (GL1: 795) and GL2: 1864) and non-glaucous mutants (NG1: 1914 and NG2: 2051) as well as R-0-18 seeds were supplied by Dr Frederic Beaudoin, Rothamsted Research, Harpenden, UK. GL1 and GL2 mutants have a severely reduced wax load (up to 80%) whereas NG1 and NG2 mutants have a change in wax structure (smooth epicuticular wax instead of crystals) but nearly normal or WT-like wax load.
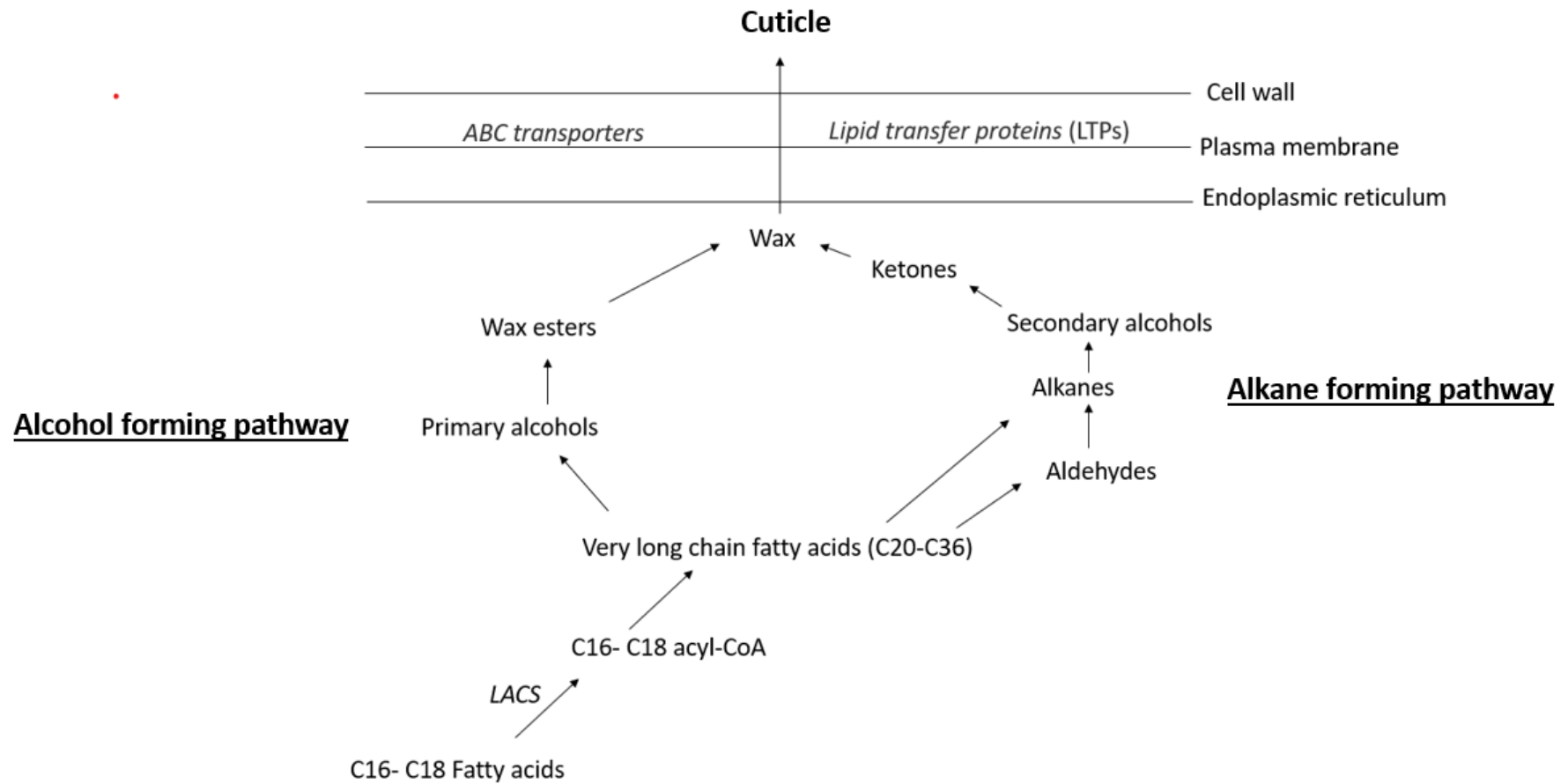
Figure 5.1: Schematic representation of alcohol and alkane forming pathways. C16 and C18 fatty acids are elongated into very long chain fatty acids (VLCFAs). The alcohol-forming pathway and the alkane-forming pathway modify VLCFAs into wax components and are mobilized from endoplasmic reticulum through the plasma membrane to the outside of the cell wall by ABC transporters and lipid transfer proteins (LTPs). Adapted from Ma *et al.* (2015).

5.2.1 Assessing the function of wax in resistance against *P. brassicae* by using *B.rapa* wax mutants

B. rapa wax mutants were used to study if there was any association between resistance against *P. brassicae* and the wax by using quantitative category measurement (LLS disease scoring) and quantitative continuous scoring (*P. brassicae* spore numbers and DNA quantification) methods. Glossy mutants with less wax (GL1, GL2) and non-glaucous mutants with structural variation (NG1, NG2) and the wild type (WT) R-0-18 (control) were grown under glasshouse conditions (experiments 8, 9) as explained in section 2.2 for spray inoculation with *P. brassicae* spore suspension (section 2.4). Lines were arranged in a randomised replicated α-design (Appendix 12) and Appendix 13 shows the environmental conditions during glasshouse experiments. Five biological replicates were used for disease scoring and three replicates each were collected for spore counting and *P. brassicae* DNA quantification, respectively. The whole experiment was repeated twice. A disease scoring scale of 1-6 was used and assessed with the assistance of a light microscope (Fell *et al*., 2023) and the spore counting was done in the same way as in section 2.5.

DNA was extracted from spray inoculated leaf samples (section 2.9) and *P. brassicae* DNA was quantified (section 2.10). For a negative control, sterile distilled water was used and the positive control was 1ng of *P. brassicae* DNA as template. Two repeats of qPCR were done with non-template control, positive control, five calibration standards and plant DNA.

5.2.2 Comparison of wax-mediated resistance against *P. brassicae* in *B. rapa* and *B. napus*

The four most susceptible and four most resistant cvs/lines of *B. napus* identified from glasshouse experiments 1-5 (chapter 4) (susceptible cvs: Cabriolet, Sansibar, Moana, Laser and resistant lines/cvs: Cubs Root, Dwarf Essex, POSH, SWU Chinese 1) were grown along with *B. rapa* wax mutants (section 5.2.1) under glasshouse conditions (experiments 8, 9). Disease scores and spore counts were compared to assess the resistance characteristics of *B. napus* and *B. rapa* against *P. brassicae*.

5.2.3 Cutinase expression in *B. rapa* and *B. napus*

To investigate the expression patterns of the cutinase gene during disease progression, *B. rapa* (wax mutants and WT R-0-18) and *B. napus* cvs/lines (susceptible cvs: Cabriolet, Sansibar, Moana, Laser and resistant cvs/lines: Cubs Root, Dwarf Essex POSH, SWU Chinese 1) were grown under controlled environment conditions (16 °C for 12 h in daylight and 14 °C for 12 h) and spot inoculated with *P. brassicae* (section 2.6) (CE experiment 11). RNA extracted and cDNA synthesised (section 2.12) from spot inoculated leaf discs were collected at 1dpi, 2dpi, 4dpi and 8dpi. Silwet treated leaf discs were used as a negative control. Three biological replicates and two technical replicates were included in this experiment. The RT-qPCR was done using ABI 7700 real time PCR System with the following cycling parameters: 95 °C for 2 min, followed by 45 cycles of 95 °C for 15 s and 60 °C for 1 min. A melting curve stage was included, with 95 °C for 15 s, 60 °C for 30 s, 95 °C for 15 s and a final step of 60 °C for 15 s.

Primer sequences for internal reference (*GAPDH*) and cutinase (*Pbc1*) were:

GAPDH
F- CAT CGT CGA GGG TCT CAT GAC 21 bases Tm 63.2
R- CGC CAA TCC TTA GCA GAT GGG 21 bases Tm 63.2
Pbc1
F-CTC TCA CAG GTT TCG GAC AGG 21 bases Tm 63.2
R-TGC CAG GTT CGG ATG TTC CTC 21 bases Tm 63.2

A 20 µL qPCR reaction mixture was prepared by adding 12.5 µL SYBR® Green jumpstart Taq Ready Mix with $MgCl_2$ in buffer (Sigma Aldrich), 0.025 µL SYBR® Green reference, 0.5 µl 10 µM *Pbc1*F, 0.5 µL 10 µM *Pbc1*R, 5.475 µL sterile nuclease-free water and 1 µL 20 ng/µL template DNA. Sterile nuclease-free water was added into no-template controls instead of template DNA. Five standards were used to quantify the amount of target DNA from the standard curve plotted. Primer efficiencies were calculated using the LinRegPCR software package. The basal or constitutive expression level of cutinase was determined by comparing the fold changes with

respect to a stable reference gene (*GAPDH*) by using the Pfaffl method (Pfaffl., 2001) and the equation used was:

$$\text{Pfaffl fold changes to control} = \frac{(E_{target})^{CT\ target\ (control-sample)}}{(E_{reference})^{CT\ reference\ (control-sample)}}$$

E = primer efficiency

Area under gene expression curve (AUGEC) was calculated from the induction at different time points to study the total cutinase expressed during infection progression between genotypes. In addition, cutinase expression at different time points was assessed.

5.2.4 Quantification of cuticular wax and biochemical composition characterisation

5.2.4.1 Wax extraction

B. rapa (wax mutants and WT R-0-18) and *B. napus* cvs/lines (susceptible cvs: Cabriolet, Sansibar, Moana, Laser and resistant cvs/lines: Cubs Root, Dwarf Essex POSH, SWU Chinese 1) were grown under glasshouse conditions (glasshouse experiment 8) until growth stages 1,4 and 1,5 and spray inoculated with 10^5 spores/mL *P. brassicae* conidial suspension. Accessions were arranged in a randomised replicated α-design with three biological replicates (Appendix 12) and Appendix 13 shows the environmental conditions for the experiment. Untreated, water treated and mock (with water and silwet) inoculated accessions were used as controls. Leaf discs of 5 cm^2 area were cut out using a razor blade at 28 dpi and rolled into Pyrex tubes gently with the adaxial side inside without disturbing the wax crystals. 10 mL chloroform stock solution with internal standards were added into each tube. Chloroform stock solution was prepared by adding internal standards C20 fatty alcohol and C24 alkane (360 µL of 20 µM each) into 900mL chloroform. After adding the stock solution, the tube was rocked gently back and forth for 60 s to cover the leaf in solvent. The chloroform wash with dissolved wax was transferred into fresh tubes and evaporated under nitrogen at 50°C. The leaf samples were left at -20°C for cutin

extraction. External standards were prepared by adding 10mL of stock solution with internal standards and dried under a stream of nitrogen.

5.2.4.2 Derivatisation of wax

Dried wax residue was dissolved in 200 µl BSTFA/TMCS (99% trimethylsilyl 2,2,2-trifluoro-N- (trimethylsilyl)acetimidate and 1% chlorotrimethylsilane) and heated for 1 h 30 min at 85º C in a heated block for gas chromatography-mass spectrometry (GC-MS) analysis. 400 µL of heptane was added before transferring into GC-MS vials.

5.2.4.3 Identification and quantification of wax compounds

Wax samples were heated at 50º C for 5 min and diluted 1:5 (20 µL sample + 80 µL heptane). One µL diluted wax sample was injected into the GC-MS for identification and GC-FID (gas chromatography flame ionization detector) for quantification. In addition, C26-C30 aldehydes, C32-C40 esters, C44-C48 esters, C24-C30 fatty acids, C26-C28 alcohols and n-alkanes of 0.5nmol/ µL each were used as external standards to identify the corresponding maxima.

Agilent 6890N GC system with Hewlett Packard HP1-MS UI capillary column (30 m, 0.25 mm, 0.25 µm) and the carrier gas helium at 1.5 mL/min flow rate were used for both identification and quantification. The inlet and transfer line temperatures were set to 325°C with pressure 17.61 psi and the oven temperature cycle was: 70°C for 1 min, 50°C per 1 min ramp until 325°C, and 325°C hold for 25min.

5.2.4.3 Normalisation of data

The largest maximum area obtained for internal standard (C24 alkane) was considered to have 100% extraction/recovery efficiency and therefore its area was divided by that of each standard area to obtain a correction factor. In each sample, the maximum area for each compound obtained from GC-FID was corrected/normalised by multiplying by the internal standard-based correction factor. Because molecular standards are not available for all wax compounds detected, precise response factors cannot be calculated. So, the numbers of carbons were considered to correct the biased GC-FID data. Correction factors were calculated by dividing carbon number of internal standard with carbon number of each compound. For example, to the response of C27 alkane using internal standard C24 alkane, the correction factor was

24/27. Furthermore, the quantity of each compound was expressed in ng/ μL injected by multiplying each corrected value by a response factor of 0.0707. Calculation to obtain response factor was as follows:

Each sample contained 1 nmole of C24 internal standard per μL

Molecular weight of internal standard C24 alkane= 338.66 g/mol

For 1nmol: 1e-9 x 338.99 =0.000000338.99 g = 338.99 ng/mol

Each sample was diluted 5 times before injecting and therefore,

338.99/5 = 67.8 ng/mol were injected on the GC column.

958.7 was the largest maximum area for the internal standard

Therefore, response factor was 67.8/958 = 0.0707 ng/unit area

Each compound quantity in ng was calculated by multiplying corrected maximum areas by this response factor.

5.2.5 Cutin monomer compositions in *B. rapa* and *B. napus* leaves

5.2.5.1 Delipidation

Leaf samples stored at $-20^{\circ C}$ were thawed and excess chloroform removed using a vacuum tube. Inside a fume hood, 10mL of chloroform: methanol (2:1) was added and samples were shaken at 30 mot/rpm for 24 h using a IKA HS 260 basic shaking machine. After 24 h, the solvent wash was removed and the step repeated using 1:1 chloroform: methanol, followed by 1:2 chloroform: methanol wash for 24 h and finally using 100% methanol. Subsequently, delipidated leaf samples after discarding methanol wash were freeze-dried for 48 h.

5.2.5.2 Depolymerization of residue

Freeze dried leaves were pushed down using a glass rod, then 2 mL of depolymerisation/transmethylation solution was added and the mix was heated at $85^{\circ C}$ for 2 h in a heat block. Depolymerisation solution was prepared in a fume hood by mixing methanol (66 mL), toluene (28 mL), 2,2-dimethoxypropane (4 mL) and sulphuric acid (2mL) to make up 100 mL stock solution. Into the mix, internal standards

of 50mM each of ω-hydroxypentadecanoate (ωOH-C15:0), 2-hydroxydodecanoate (C12:0), 8-pentadecanone (C15 ketone) were added. After cooling down to 20°C, 2 mL 1% w/v sodium chloride in Tris 100 mM pH 8.0 were added to improve phase separation and clear samples from polar contaminants. Finally, 2 mL dichloromethane was added to solubilise released and derivatised cutin monomers. Tubes were shaken and centrifuged for 2 min at 1500 g. The lower organic phase (first extract) was collected into a new tube. 2mL dichloromethane was added into the sample again. Samples were vortexed, centrifuged as before and the lower organic phase (second extract) was collected and pooled with the first extract. The combined organic phases were dried at 50^0 C under nitrogen. 100 μL of heptane was added before injecting 3 μL in the GC-MS column. GC-MS specifications and oven cycles were the same as for wax (section 5.2.4.3), except that the final hold stage at 325°C was for 12 min. Cutin compound identification was done by GC-MS but quantification was done using a GC-FID with the same experimental set-up as that for wax (section 5.2.4.2).

5.2.6 Statistical analysis

Bartlett's test and Shapiro's-tests were done to check the homogeneity of variance and normal distribution, respectively. A non-parametrical Wilcoxon signed rank test was applied to non-homogenously distributed data with heterogenous variances. For normally distributed data with homogenous variances, ANOVA was used. Significant variances within or between groups were tested by using Tukey HSD (normally distributed data) or Wilcoxon mean comparisons (non-normally distributed data).

5.3 Results

An assessment was necessary to determine whether there were differences in disease severity between wax mutants because of potential differences caused by the cuticular wax, cutin contents or by their compositions.

5.3.1 Assessing the function of wax in resistance against *P. brassicae* by using *B.rapa* wax mutants.

Significant differences in LLS score (Figure 5.2a), *P. brassicae* spore count (Figure 5.2b) and *P. brassicae* DNA content (Figure 5.2c) were observed between *B. rapa* wild type control (WT, R-0-18) and wax mutants. Non-glaucous mutants (structurally
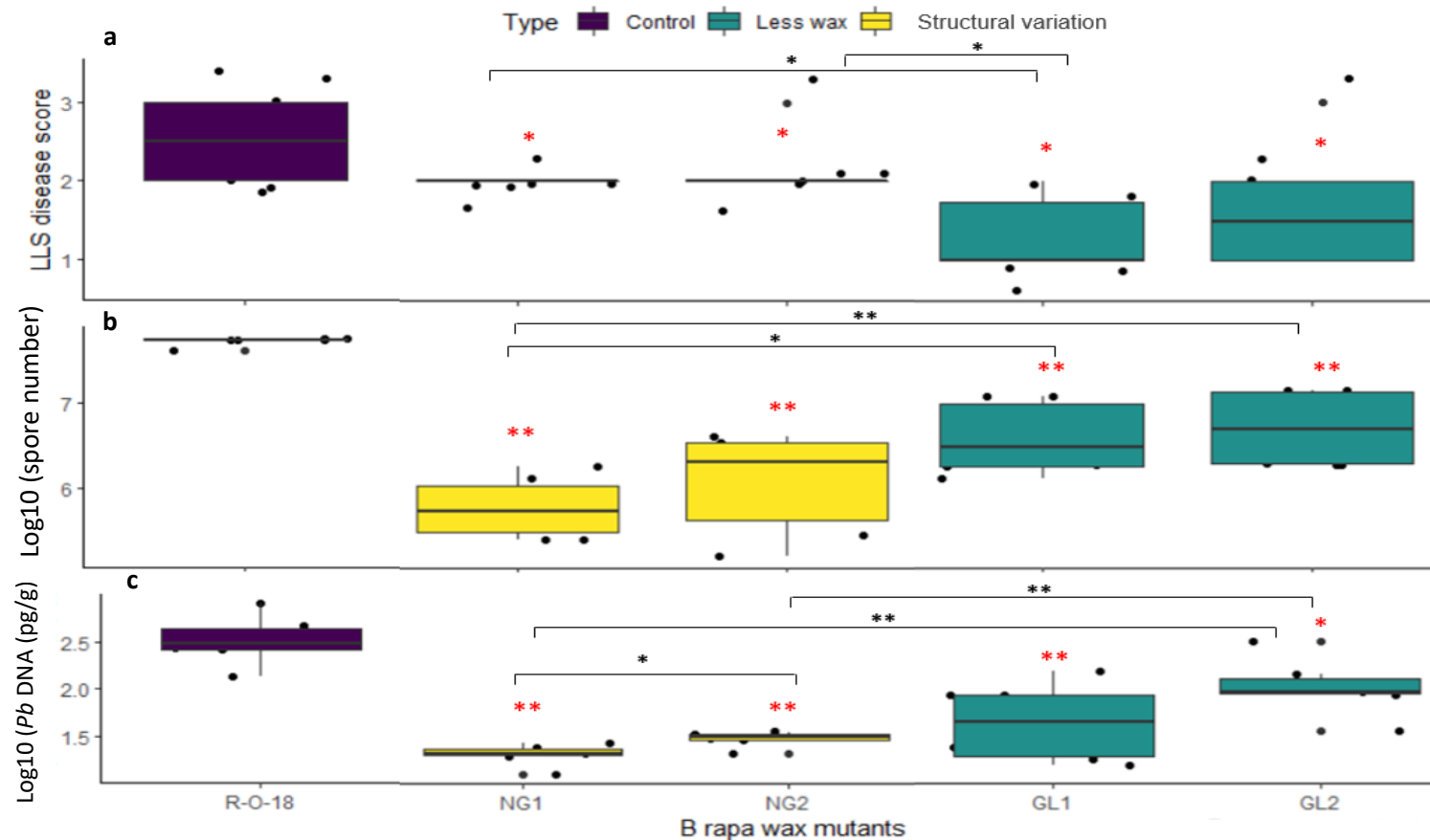
Figure 5.2: Spray inoculated *B. rapa* wax mutants and WT were grown under glasshouse conditions. 21 dpi leaf samples collected and incubated for 5 days, then scored for LLS disease (1-6 scale), spore numbers from washed leaves and amount of *P. brassicae* DNA quantified using qPCR. (a) LLS disease score in *B. rapa* wax mutants, (b) *P. brassicae* spore count after being washed off from *B. rapa* wax mutant leaves and log$_{10}$ transformed, (c) Amount *P. brassicae* DNA in pg/g (log$_{10}$-transformed) quantified from spray inoculated *B. rapa* wax mutant leaves. Glossy mutants (GL1, GL2) with less wax and non-glaucous mutants (NG1, NG2) with different wax structure in comparison to the WT control R-0-18. Red asterix shows individual significant differences against R-0-18 and black asterixes show differences between mutants using a Wilcoxon test. From two independent experiments, five biological replicates were included for LLS disease scoring and there were three replicates for both spore concentration and *P. brassicae* DNA quantification. Box plot middle line represents the median, whiskers show values outside the middle 50% and black dots are outliers.

different surface wax) appeared more susceptible to *P. brassicae* according to the LLS score but had less *P. brassicae* DNA and produced fewer spores, by contrast to the glossy mutants (less wax), which had larger amounts of DNA and more spores but showed a resistant phenotype. GL1 showed a significant difference in LLS score from NG1 and NG2. There was no significant difference in LLS score between two glossy mutants (GL1, GL2) or between two non-glaucous mutants (NG1, NG2). Both categorical quantitative (LLS disease score) and continuous quantitative assessments (spore count and DNA content) showed a significant difference between all mutants and the WT.

5.3.2 Comparison of wax-mediated resistance against *P. brassicae* in *B. rapa* and *B. napus*

There was a significant difference in LLS score between the species ($P = 1.4 \times 10^{-4}$) (Figure 5.3a). WT R-0-18 showed different scores from susceptible *B. napus* cvs/lines and showed similar resistance characteristics to *B. napus* resistant cvs/lines. NG2 and resistant *B. napus* lines (POSH and SWU Chinese 1) appeared not significantly different according to LLS disease score.

No significant difference in *P. brassicae* spore count was observed between *B. rapa* and *B. napus* species (Figure 5.3 b) as the glossy wax mutants and the WT *B. rapa* showed similar resistance characteristics to *B. napus* resistant cv. Cubs Root. However, between genotypes a significant difference was observed. NG1 and NG2 (with smooth wax/ crystalline wax absent) showed the greatest resistance against *P. brassicae* with the smallest number of spores and showed a significant difference from *B. napus* cvs/lines.

5.3.3 Cutinase expression in *B. rapa* and *B. napus*

Analysis of cutinase expression in *B. rapa* and *B. napus* was done to better understand the interaction of *P. brassicae* with the host cuticle. Li *et al*. (2003) showed that the cutinase gene (*Pbc1*) is involved in pathogenicity of *P. brassicae* on oilseed rape. Therefore, analysis of cutinase expression during pathogenesis will help to understand if there are differences during disease progression in *B. rapa* lines and *B. napus* cvs/lines.
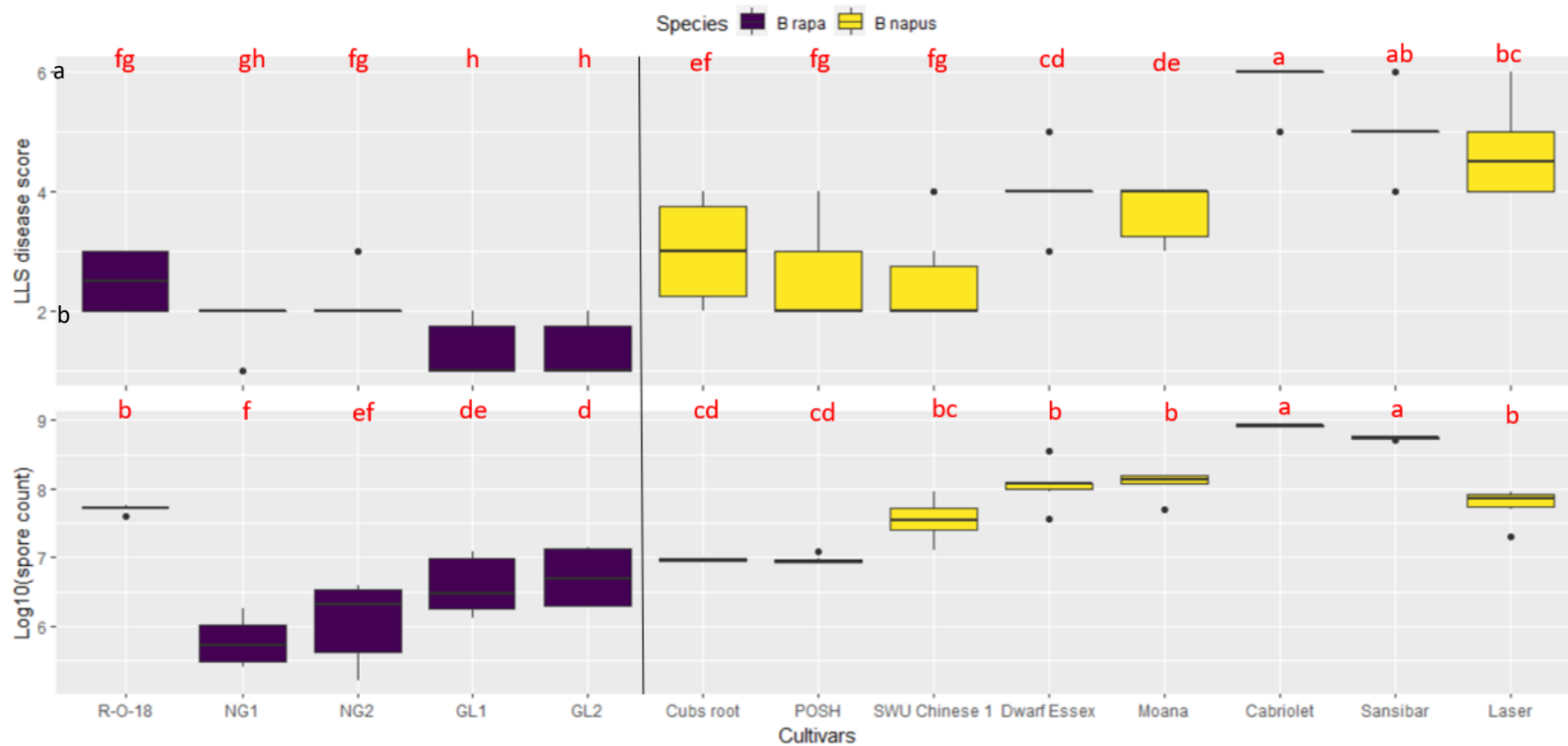
Figure 5.3: LLS disease score (a) and spore numbers, (b) after washing off of spray inoculated leaves of *B. rapa* and *B. napus* genotypes. Bars with similar letters did not show any significant difference (Wilcoxon, Anova and Tukey HSD). From two independent experiments, five biological replicates were included for LLS disease score and three replicates for spore number. The box plot middle line represents the median, whiskers show 50% outside the middle and black dots are outliers.

A significant difference in cutinase expression was seen between wax mutants and WT at all time points (Figure 5.4). A significant reduction in cutinase expression was observed at 8 dpi in NG1, NG2 and GL2 in comparison to the WT. Glossy mutants showed significantly greater cutinase induction at 4 dpi compared to the WT and non-glaucous mutants. The resistant *B. napus* cultivar/line (Cubs Root and POSH) showed significantly less induction of cutinase than the susceptible cvs Laser and Cabriolet (Figure 5.5). As well as differences in cutinase expression between time points in susceptible/resistant phenotypes, some significant differences within each time point between genotypes were observed. Cultivars Cubs Root and Cabriolet showed a difference at 2dpi ($P = 0.018$), 4dpi ($P = 0.039$) and 8dpi ($P = 0.045$). Laser showed a significant difference in cutinase induction from POSH at 1dpi (P 0.025) and from Cubs Root at 4dpi (P 0.00003).

Both *B. rapa* and *B. napus* showed a strong difference in expression between time points ($P = 2 \times 10^{-16}$ each in both species). Wax mutants (GL2, NG1, NG2) showed less expression at 8dpi in comparison to the control *B. rapa* (R-0-18) and conversely *B. napus* cvs/lines showed an increase in expression from 1dpi until 8dpi (Appendix 14).

Glossy mutants induced significantly greater cutinase in comparison to the WT and the non-glaucous wax mutants (Figure 5.6). A significant difference in AUGEC was observed between genotypes in *B. napus* ($P = 4.83 \times 10^{-5}$). Cutinase was expressed significantly less in resistant cvs/lines Cubs Root and POSH than in cvs Cabriolet and Laser (Figure 5.7). Sansibar showed a similar expression pattern to that of resistant lines and SWU Chinese 1 showed greater induction than susceptible cvs Cabriolet and Laser.

5.3.4 Quantification of cuticular wax, content and composition

Total cuticular wax and individual components of main wax molecular species (primary alcohols and wax esters of alcohol forming pathways and alkanes, secondary alcohols, aldehydes, fatty acids, esters, ketones and diosl of alkane forming pathways) were quantified to determine their involvement in quantitative resistance against *P. brassicae*. Wax mutants of *B. rapa* and *B. napus* resistant and susceptible cvs/lines were analysed to study if there was any significant difference between uninoculated and inoculated plants as well as differences between genotypes within each species
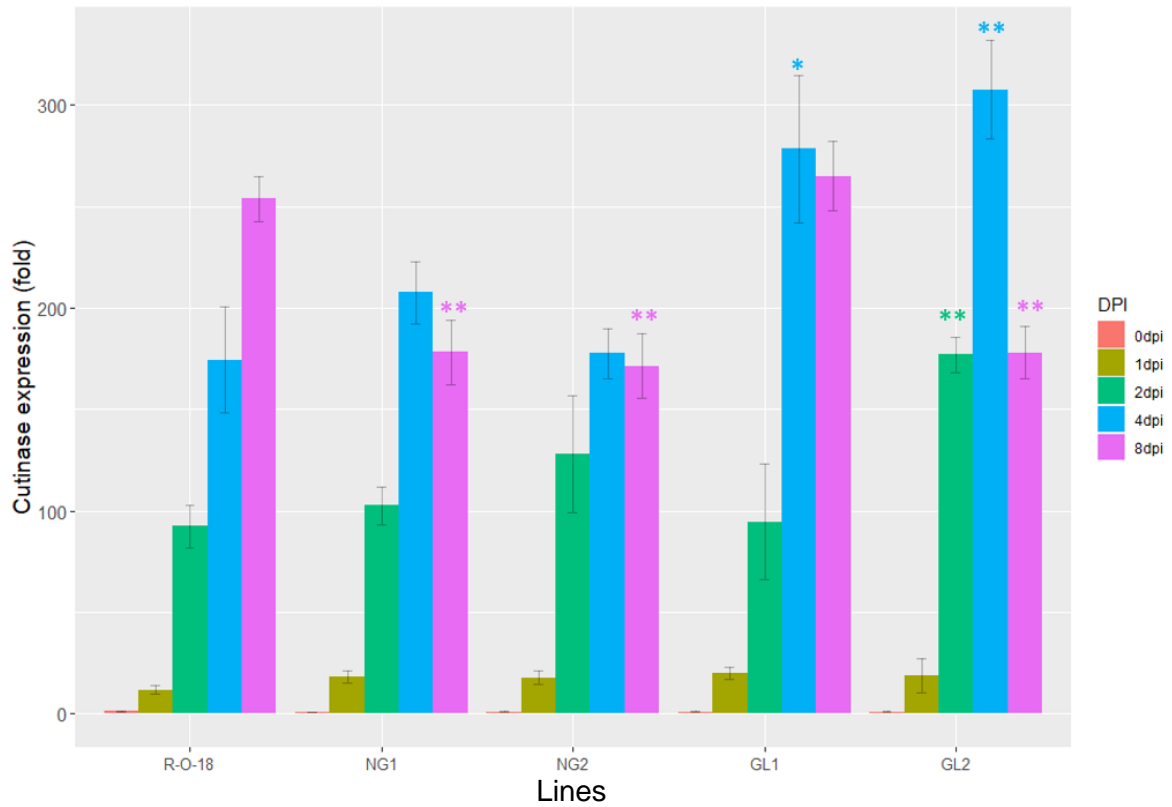
Figure 5.4: Cutinase expression in *B. rapa* wax mutants (at 0dpi (control), 1dpi, 2dpi, 4dpi and 8dpi). A significant difference in expression from that of the control was observed at all time points. Asterixes indicate the significant variation within each time point (green= 2dpi, blue= 4dpi, pink= 8dpi) in comparison to WT control (R-0-18) based on the results from ANOVA and TukeyHSD. Error bars represent standard deviation of three replicates from two independent experiments. *** *P*-value ≤ 0.001; ** *P*-value ≤ 0.01; * *P*-value ≤ 0.05
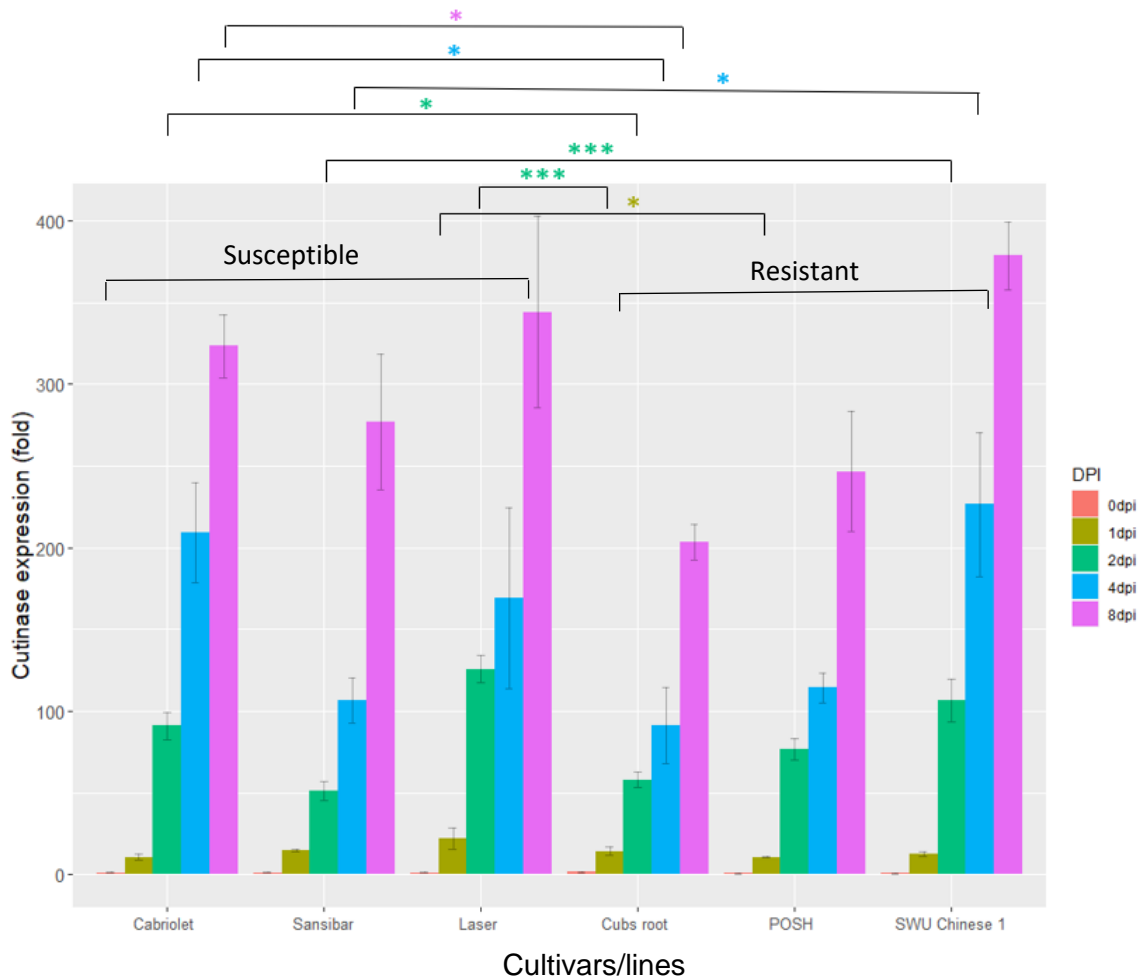
Figure 5.5: Cutinase expression in *B. napus* cvs/lines (susceptible: Cabriolet, Sansibar, Laser and resistant: Cubs Root, POSH, SWU Chinese1) at 0dpi (control), 1dpi, 2dpi, 4dpi and 8dpi. A significant difference in expression from that of the control was observed at all time points. Asterixes indicate the significant difference within each time point between genotypes (brown= 1dpi, green= 2dpi, blue= 4dpi, pink= 8dpi) based on the results from ANOVA and TukeyHSD. Error bars represent sd of three replicates from two independent experiments. *** *P*-value ≤ 0.001; ** *P*-value ≤ 0.01; * *P*-value ≤ 0.05
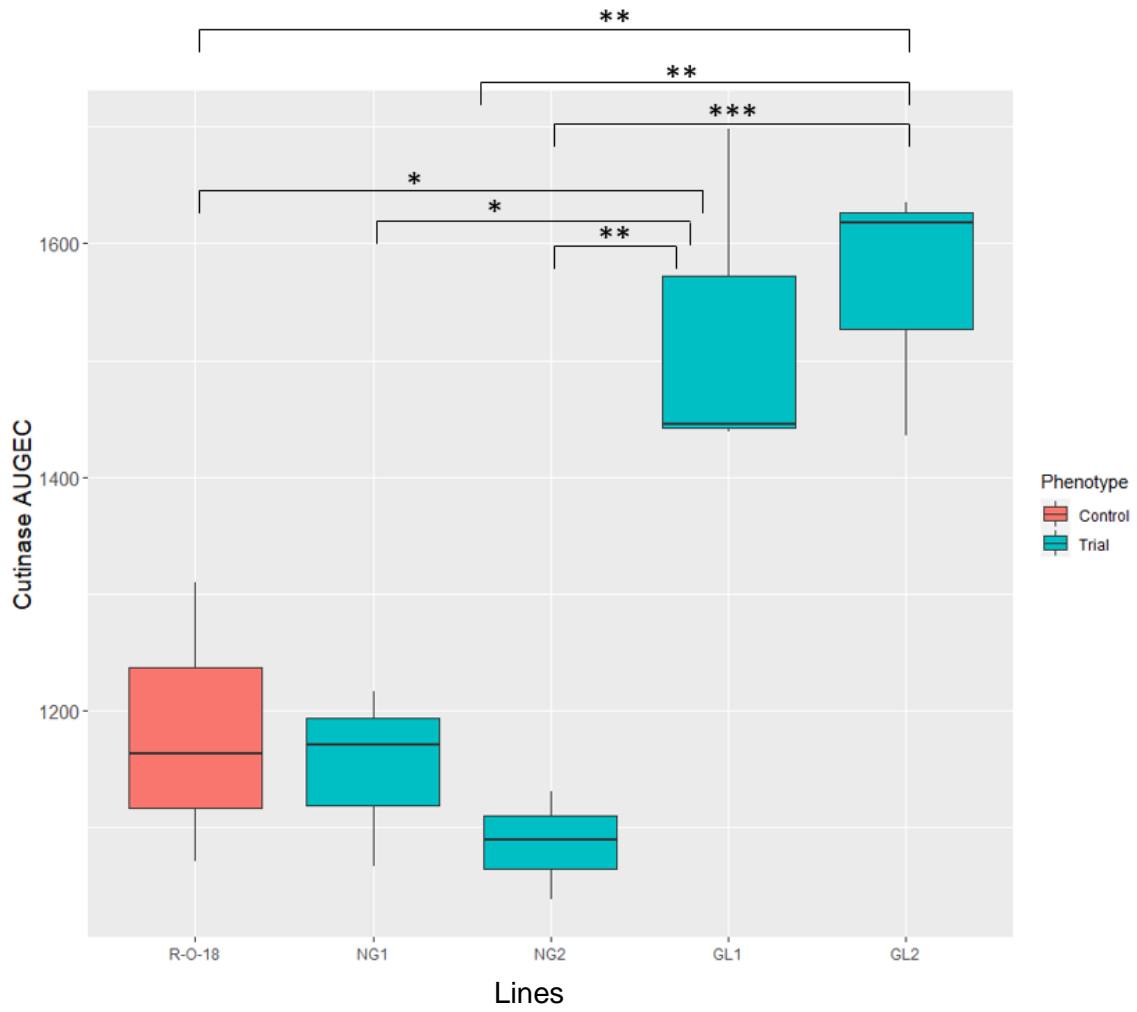
Figure 5.6: Cutinase area under gene expression curve (AUGEC) in *B. rapa* wax mutants (NG1, NG2: more wax, GL1, GL2: less wax) and WT R-0-18 at 0dpi (control), 1dpi, 2dpi, 4dpi and 8dpi. Asterixes indicate the significant differences between genotypes. *** *P*-value ≤ 0.001; ** *P*-value ≤ 0.01; * *P*-value ≤ 0.05
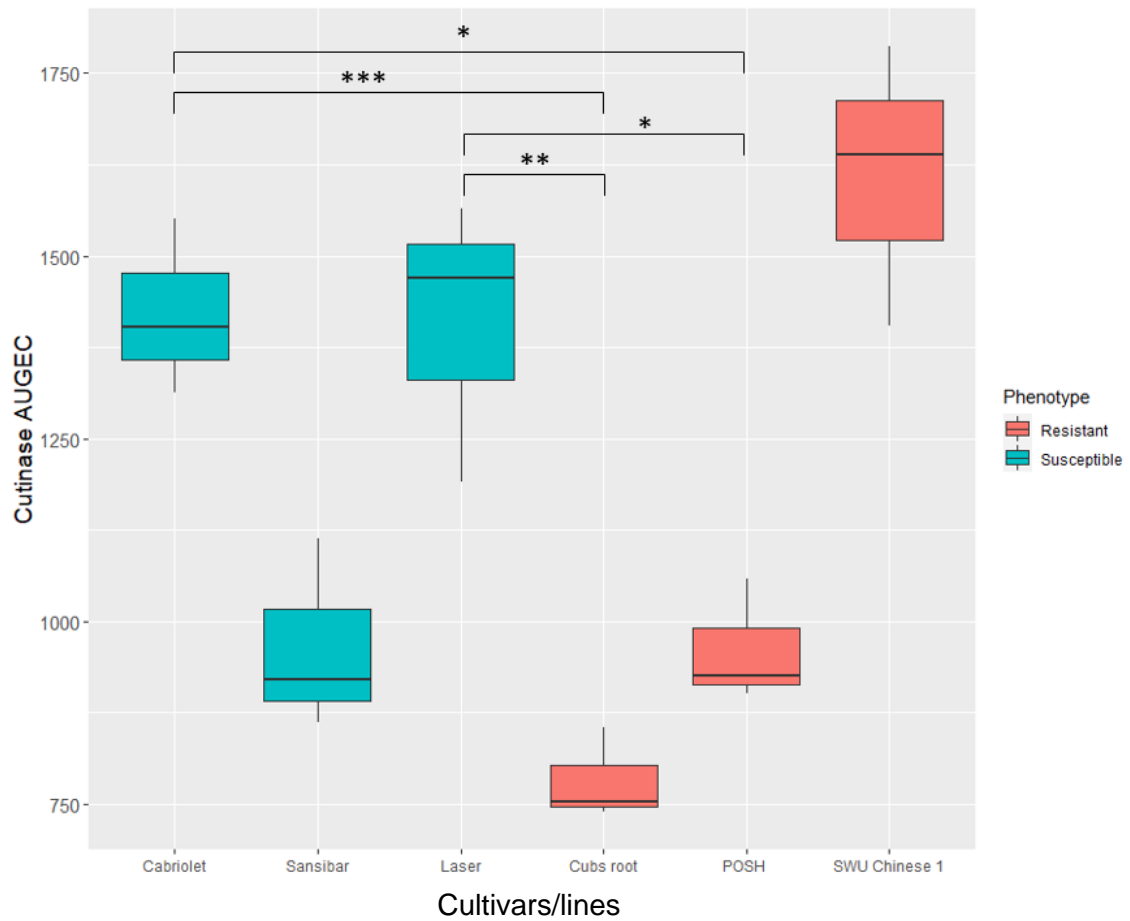
Figure 5.7: Cutinase area under gene expression curve (AUGEC) in *B. napus* cvs/lines at 0dpi (control), 1dpi, 2dpi, 4dpi and 8dpi. Asterixes indicate the significant differences between genotypes. *** *P*-value ≤ 0.001; ** *P*-value ≤ 0.01; * *P*-value ≤ 0.05

Water or mock (including silwet) treated samples were used as additional negative controls. However, there were no significant differences in total wax concentration between three negative controls (uninoculated, water or mock inoculations) in *B. napus* ($P = 0.894$) or *B. rapa* ($P = 0.995$). Therefore, further comparative analysis was done between the uninoculated negative control and inoculated samples. The leaf epicuticular waxes of both *B. rapa* and *B. napus* were rich in alkanes, alcohols, fatty acids, aldehydes, esters, ketones and diols. The most common and abundant component was alkanes, and it did account for 55% of total wax in *B. napus* and 65% in *B. rapa* WT R-0-18, respectively.

5.3.4.1 Cuticular wax; content and components in *B. rapa* mutants

Uninoculated glossy mutants as expected showed significant reduction in wax load than WT and non-glaucous mutants (Figure 5.8). Non-glaucous mutants expected to have similar wax load as that of WT. However, NG2 showed an increased wax load than WT and it may be due to glasshouse conditions. A significant reduction in wax load was observed in *B. rapa* wax mutants and WT after inoculation with *P. brassicae*. Alkanes, diols and ketones were significantly greater in uninoculated NG2 in comparison to other lines. 1^0 alcohols, branched alcohols, aldehydes and wax esters were significantly greater in uninoculated glossy mutants but alkanes, 2^0 alcohols and ketones were significantly less. After inoculating with *P. brassicae*, 1^0 alcohols remained unaffected in WT and non-glaucous mutants, but glossy mutants showed a significant reduction.

Significant decreases in individual alkanes (Figure 5.9) and fatty acids (Figure 5.10) were observed, which corresponds to the overall decrease in total wax load after treatment. C27, C29, C30 and C31 alkanes were significantly increased in uninoculated NG2. C30 branched and C30 linear alkanes were greater in NG1. Most of the individual alkanes were significantly less in glossy mutants. Both the glossy and non-glaucous mutants showed a lower C30 FA content in comparison to the WT.

The reduction in fatty acid content confirms the reason for decreased concentration of other products such as 2^0 alcohols in the alkane forming pathways (Appendix 15). Furthermore, 1^0 alcohol (Appendix 16) and wax esters (Appendix 17) showed a similar pattern of lowered concentration after treatment. Aldehydes, especially C30 aldehyde
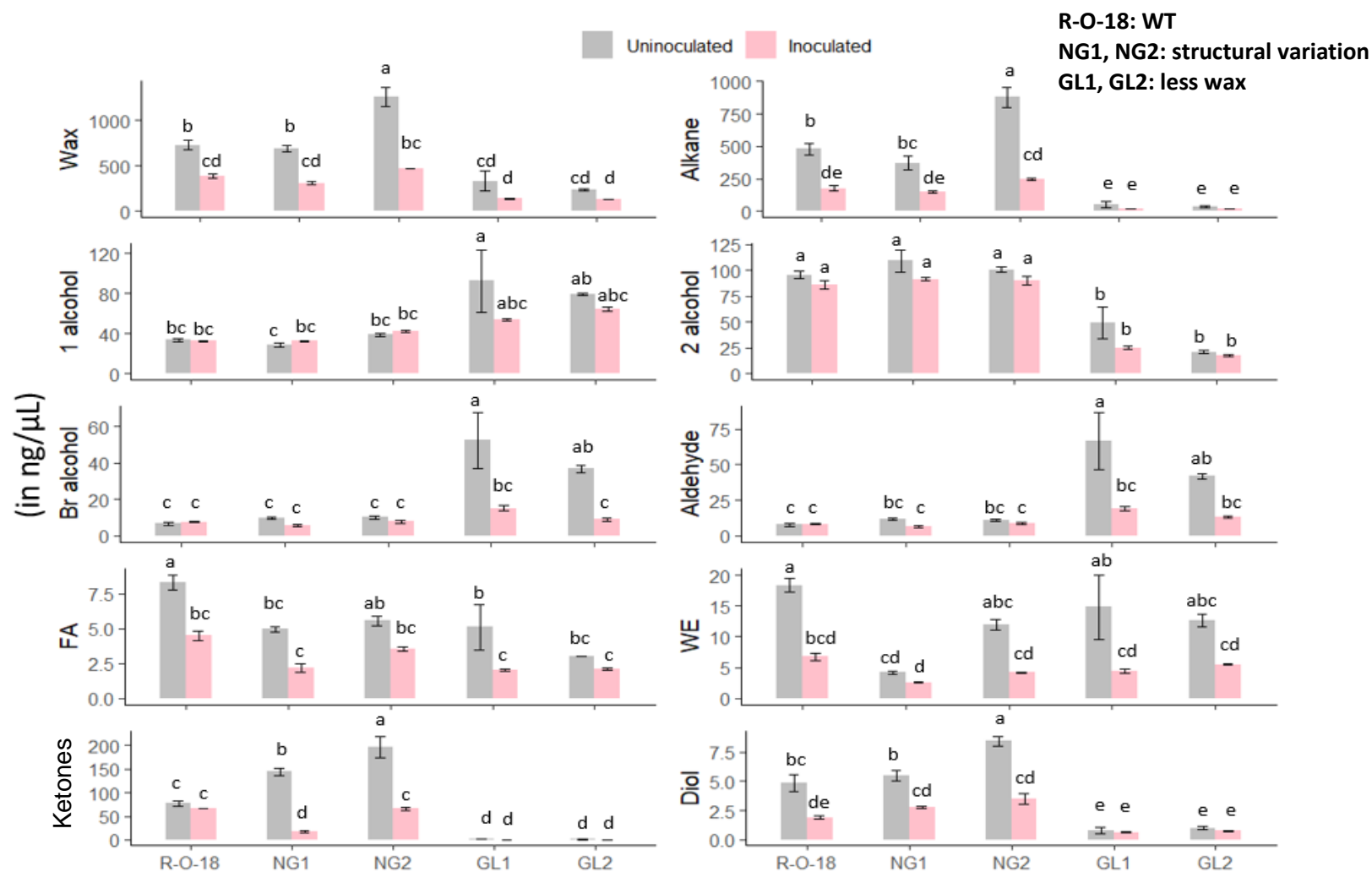
Figure 5.8: Total wax and major molecular species (alkanes, 1^0 alcohol, 2^0 alcohol, branched (Br) alcohol, aldehyde, fatty acid (FA), wax ester (WE), ketones and Diol) quantified from *B. rapa* wax mutants spray inoculated with *P. brassicae* (28 dpi) using GCMS. Ketones refer to C29 ketones as that was the only ketone identified. Error bars represent standard deviations of three biological replicates. Values with the same letters are not significantly different (Wilcoxon, Anova and TukeyHSD, df 4).
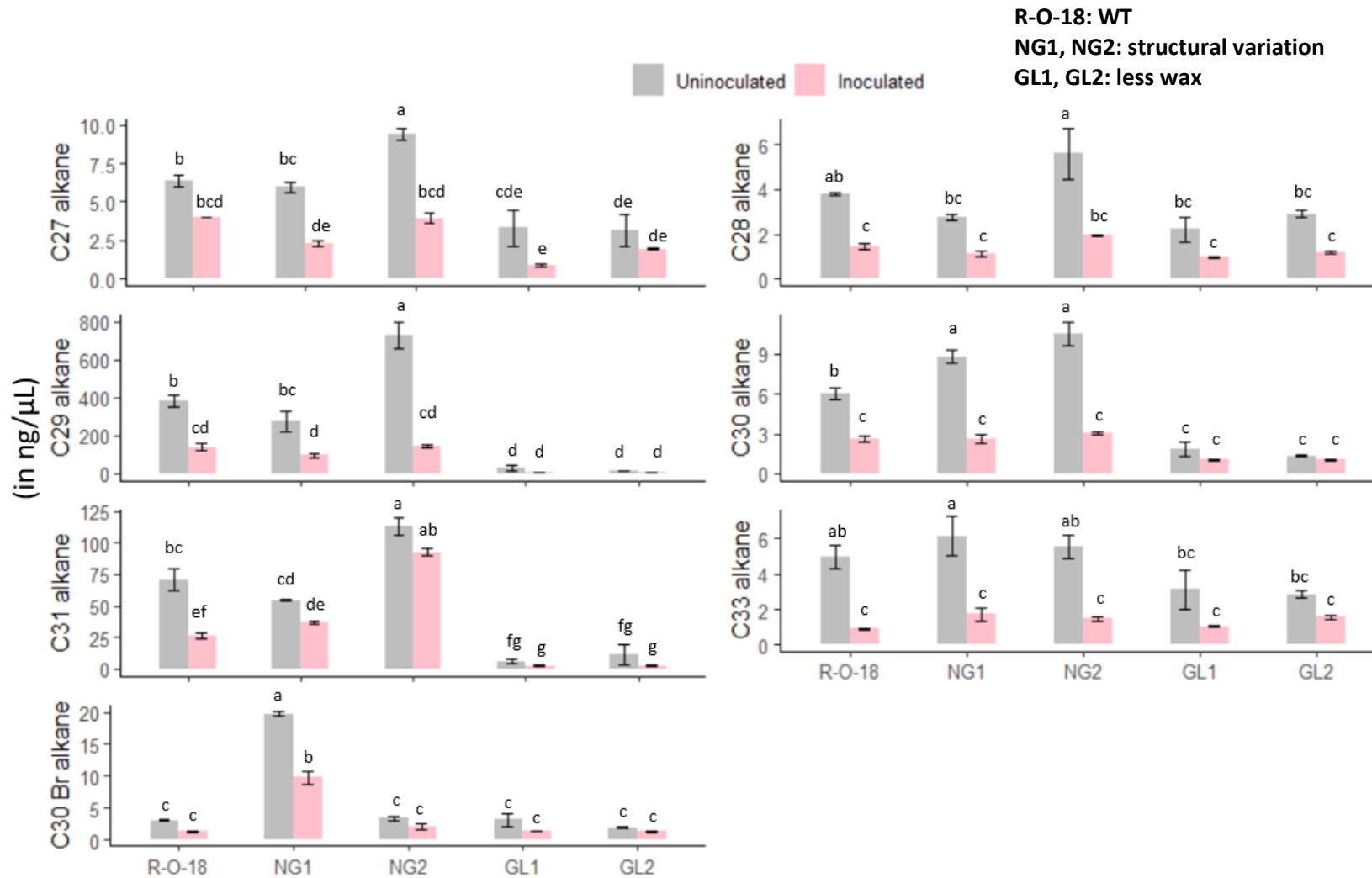
Figure 5.9: Individual compounds of alkane identified and quantified from *B. rapa* wax mutants spray inoculated with *P. brassicae* (28 dpi) using GCMS. Error bars represent standard deviations of three biological replicates. Values with the same letters are not significantly different (Wilcoxon, Anova and TukeyHSD, df 4).
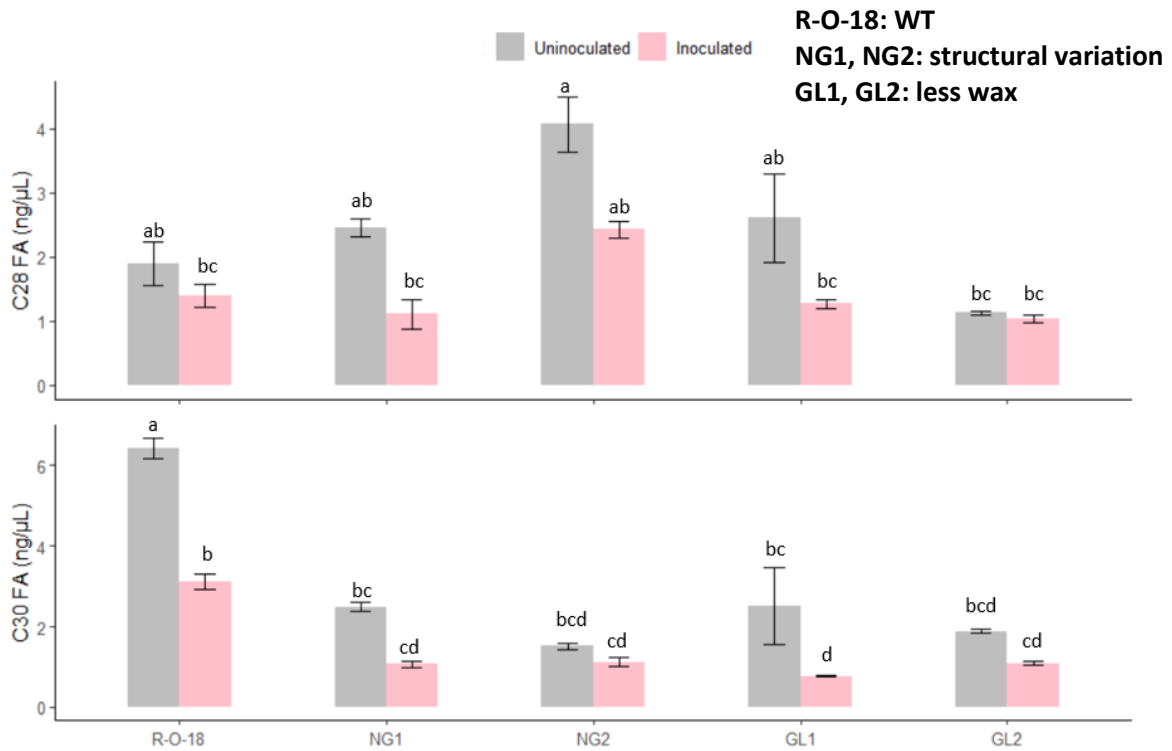
Figure 5.10: Individual compounds of fatty acid (FA) identified and quantified from *B. rapa* wax mutants spray inoculated with *P. brassicae* (28 dpi) using gas chromatography-mass spectrometry (GCMS). Error bars represent standard deviations of three biological replicates. Values with the same letters are not significantly different (Wilcoxon, Anova and TukeyHSD, df 4).

were significantly less after treatment (Figure 5.11). Furthermore, glossy mutants showed significantly greater content of aldehyde compounds than WT and non-glaucous mutants. Glossy mutants showed an enhanced C27 Br alcohol in comparison to WT and non-glaucous mutants (Figure 5.12).

5.3.4.2 Comparison of cuticular wax, content and composition in susceptible and resistant *B. napus* cultivars/lines

Uninoculated *B. napus* resistant cvs/lines showed significantly greater wax load than susceptible cvs/lines (P 1.03 x 10^{-4}) except for cv. Moana (Figure 5.13). However, both categorical quantitative and continuous quantitative LLS disease quantification showed that Moana is intermediate rather than a susceptible cultivar (Figure 4.5 and Figure 4.6). Inoculated resistant *B. napus* cvs/lines showed a significant reduction in total wax and most abundant individual wax compounds compared to susceptible cvs (Figure 5.13).

In addition, uninoculated resistant *B. napus* cvs/lines had greater loads of alkanes than susceptible cvs/lines. As observed in *B. rapa* WT and non-glaucous mutants, 1^0 alcohols did not alter much in resistant *B. napus* cvs/lines after treatment. In contrast, *B. napus* susceptible cvs/lines showed increased 1^0 alcohols after inoculation. Furthermore, aldehydes and fatty acids were significantly reduced after treatment in *B. napus* resistant cvs/lines in comparison to susceptible cvs/lines. A significantly greater amount of most of the individual alkanes including C30 alkane was observed in uninoculated *B. napus* resistant cvs/lines (Figure 5.14). Except C33 alkanes, most components of alkanes showed a reduced concentration after treatment. C24, C28 and C30 1^0 alcohols were significantly higher in uninoculated susceptible cvs Cabriolet and Sansibar than most of the resistant cvs/lines (Figure 5.15). Most of the individual 1^0 alcohol components were increased (C26 1^0 alcohol) or mostly remained same after treatment in *B. napus* cvs/lines. Long chain aldehydes (C32 aldehyde) were not affected after treatment in resistant *B. napus* cvs/lines but C30 and C28 were reduced significantly in *B. napus* resistant cvs/lines except for SWU Chinese 1 with C28 aldehyde (Figure 5.16). Susceptible cv. Laser appeared different to others with enhanced wax load and increased amounts of most of the individual components after treatment. Branched alcohol, 2^0 alcohol, fatty acid and wax esters were reduced
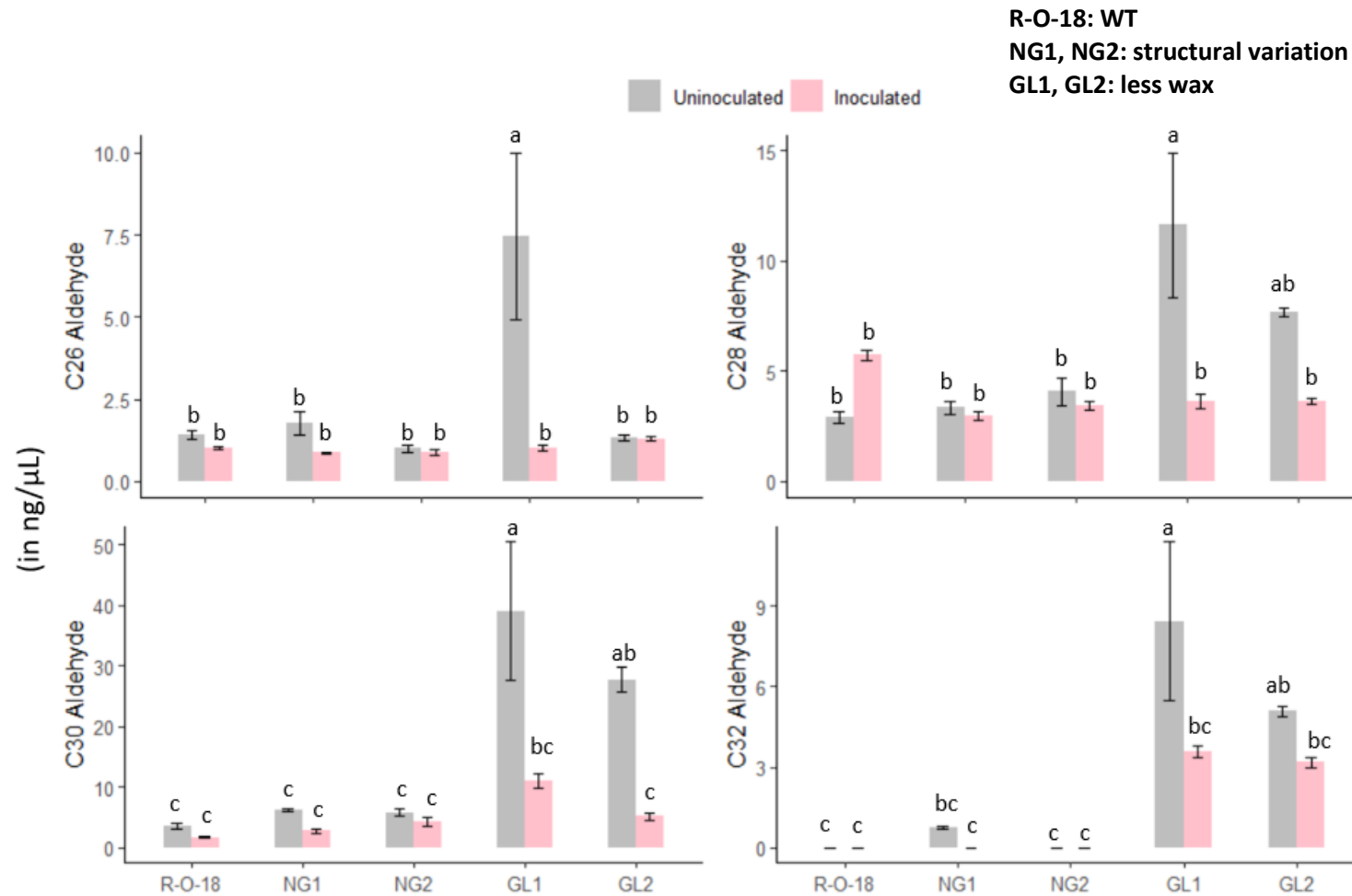
Figure 5.11: Individual compounds of aldehyde identified and quantified from *B. rapa* wax mutants spray inoculated with *P. brassicae* (28 dpi) using GCMS. Error bars represent standard deviations of three biological replicates. Values with the same letters are not significantly different (Wilcoxon, Anova and TukeyHSD, df 4).
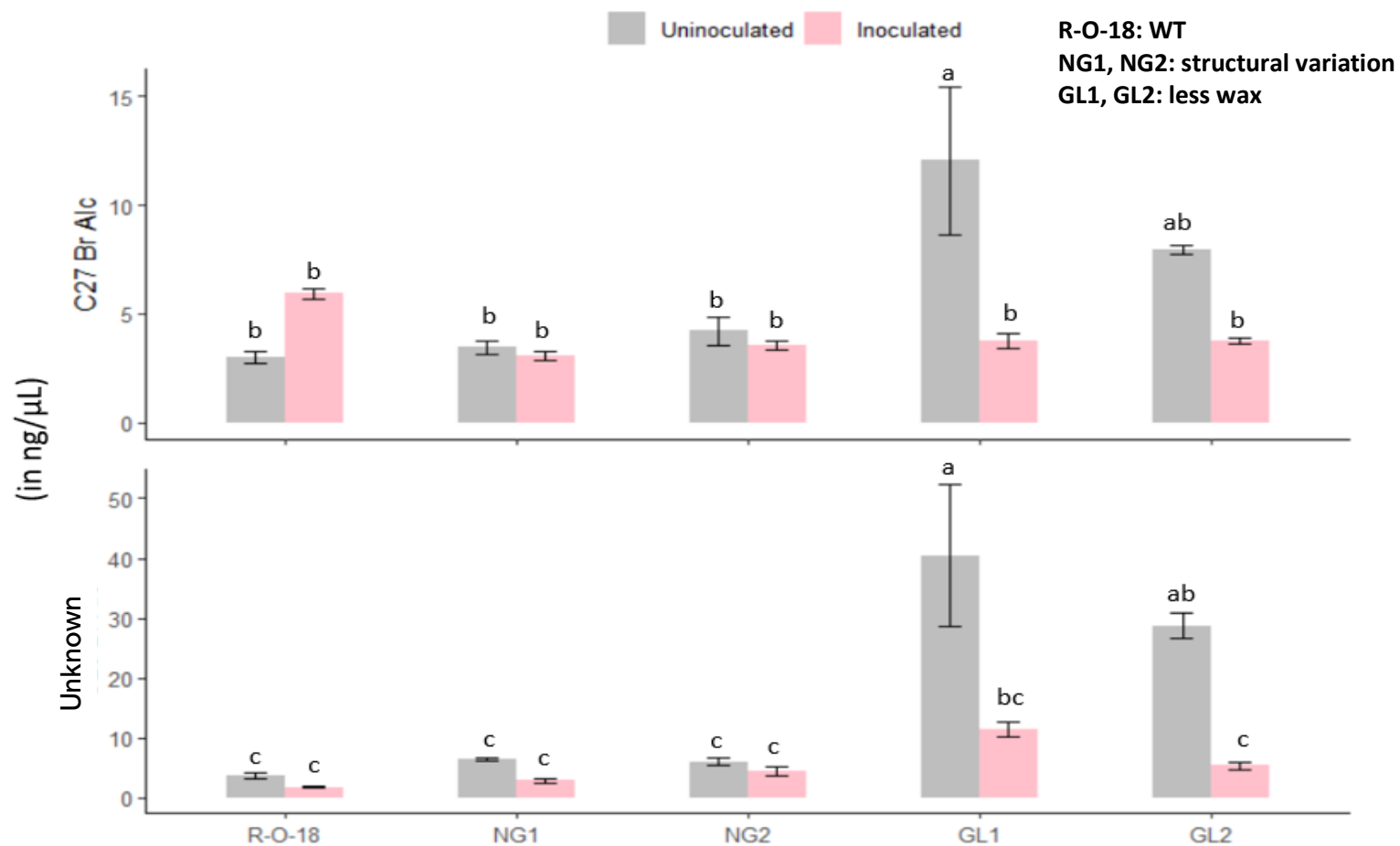
Figure 5.12: C27 branched alcohol and an unknown compound identified and quantified from *B. rapa* wax mutants spray inoculated with *P. brassicae* (28 dpi) using GCMS. Error bars represent standard deviations of three biological replicates. Values with the same letters are not significantly different (Wilcoxon, Anova and TukeyHSD, df 4).
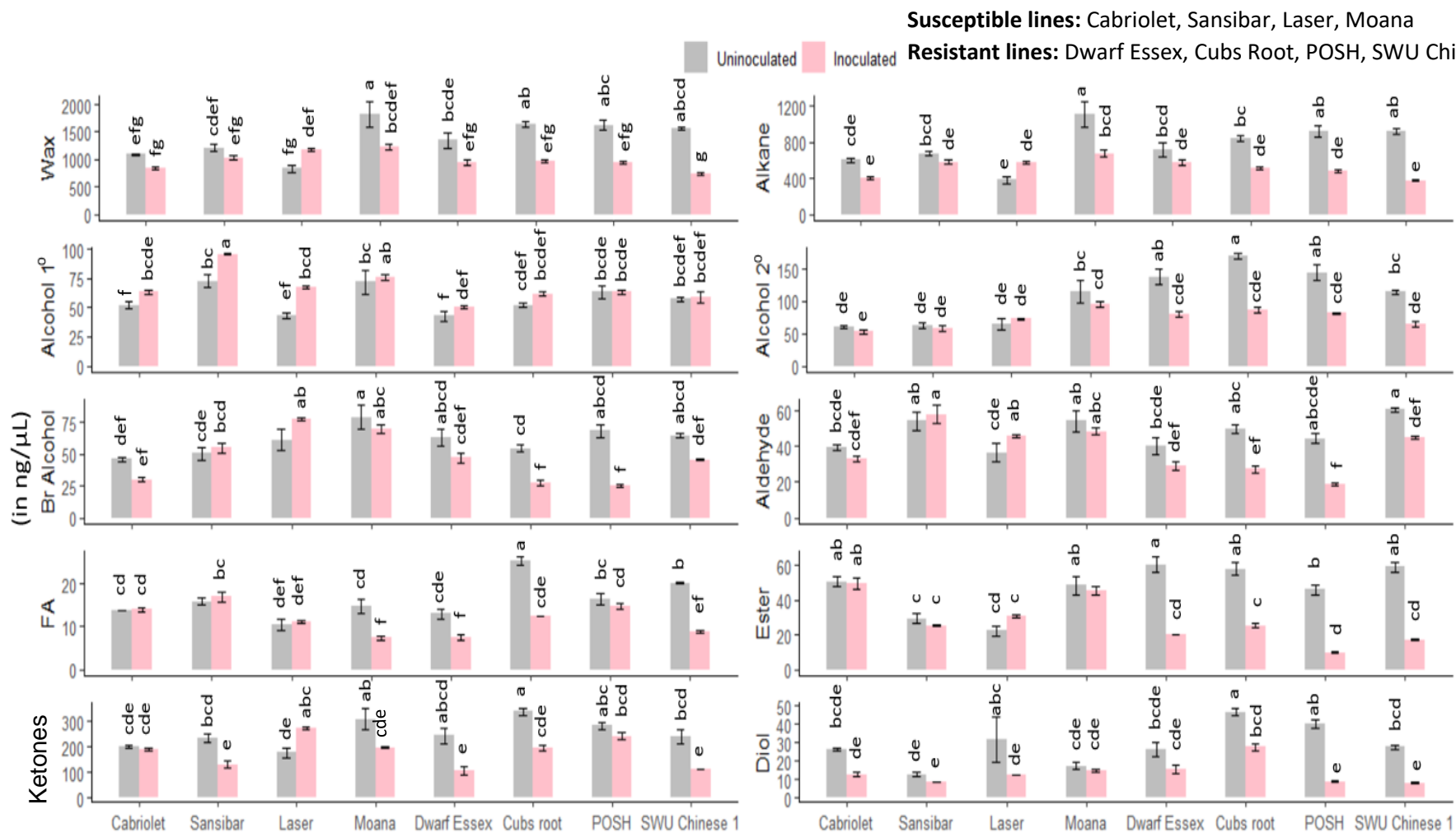
Figure 5.13: Total wax and major molecular species (alkanes, 1^0 alcohol, 2^0 alcohol, branched (Br) alcohol, aldehyde, fatty acid (FA), wax ester (WE), ketones and Diol) quantified from *B. napus* lines spray inoculated with *P. brassicae* (28 dpi) using GCMS. Ketones represent C29 ketone as other ketones were not identified. Error bars represent standard deviations of three biological replicates. Values with the same letters are not significantly different (Wilcoxon, Anova and TukeyHSD, df 4).
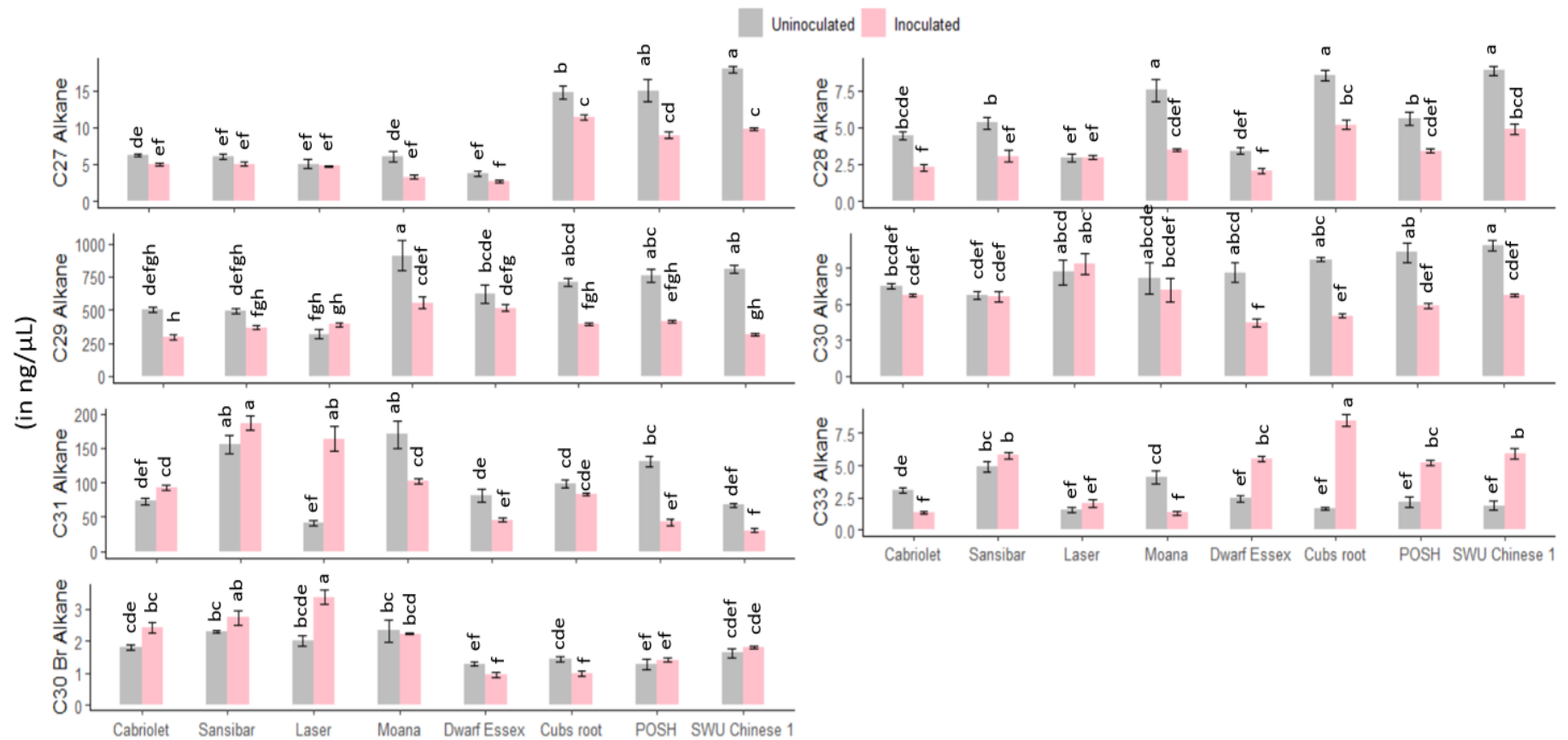
Figure 5.14: Individual compounds of alkanes identified and quantified from *B. napus* cvs/lines spray inoculated with *P. brassicae* (28 dpi) using GCMS. Error bars represent standard deviations of three replicates. Values with the same letters are not significantly different (Wilcoxon, Anova and TukeyHSD, df 7).
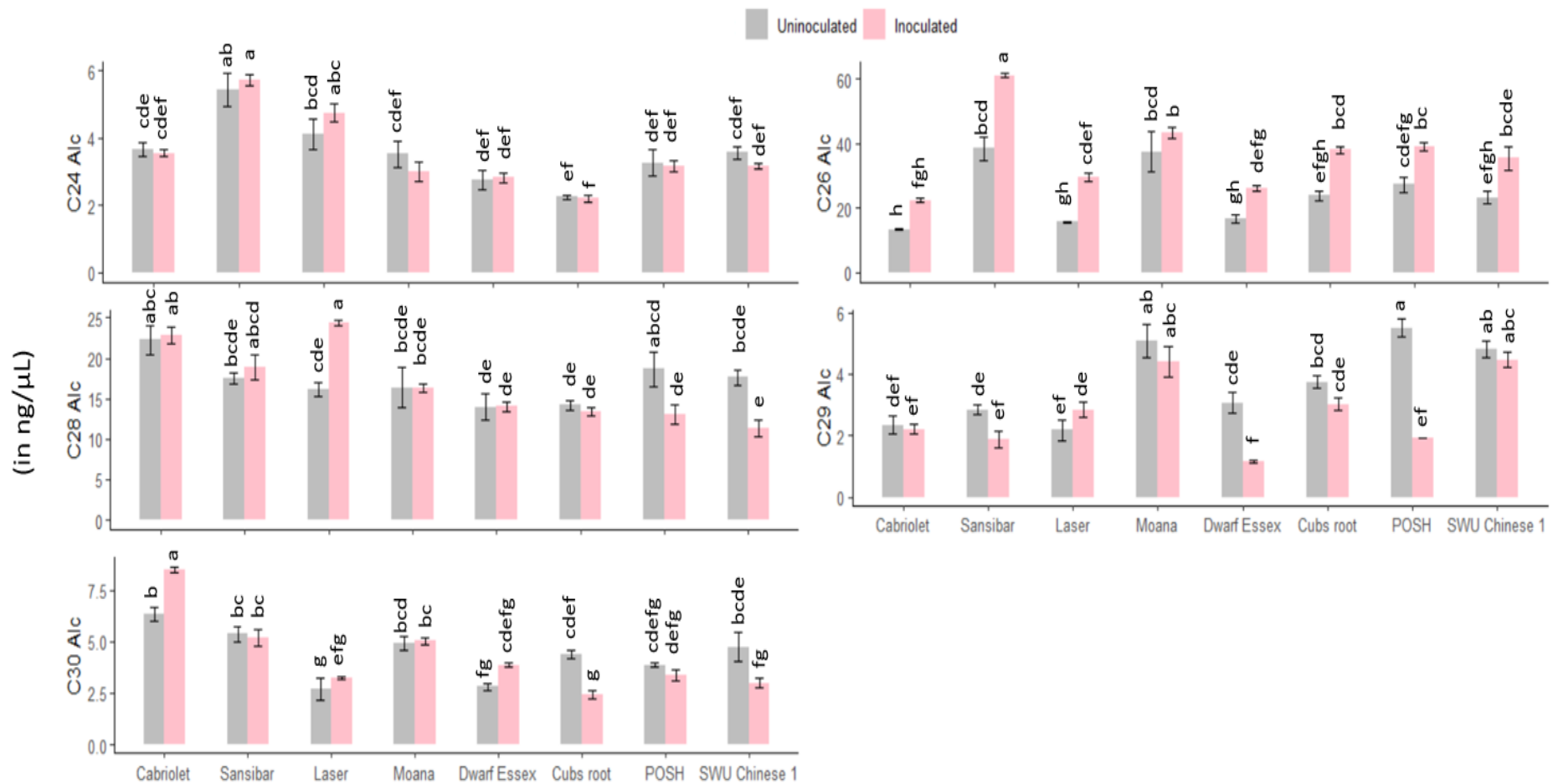
Figure 5.15: Individual compounds of 1^0 alcohol identified and quantified from *B. napus* cvs/lines spray inoculated with *P. brassicae* (28 dpi) using GCMS. Error bars represent standard deviations of three replicates. Values with the same letters are not significantly different (Wilcoxon, Anova and TukeyHSD, df 7).
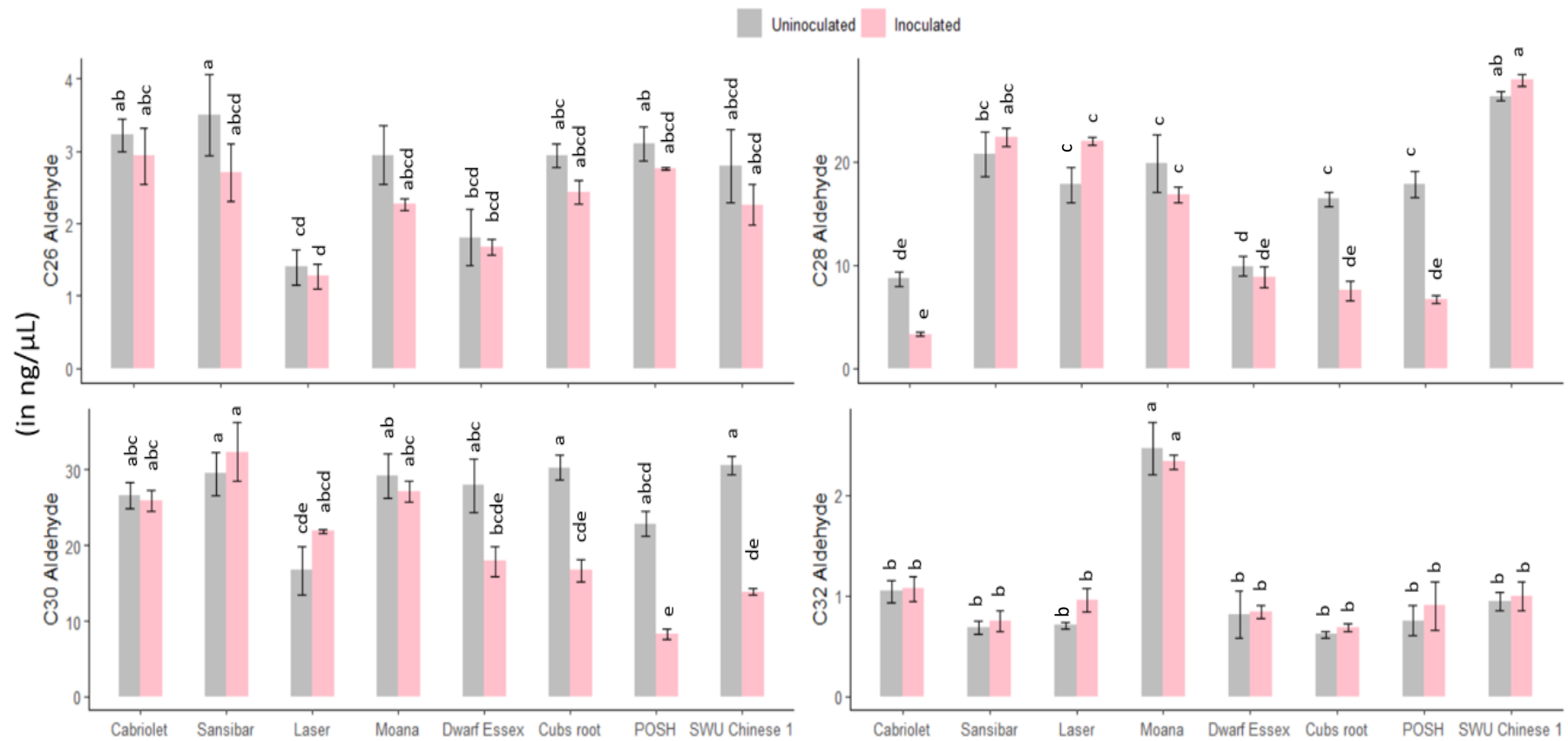
Figure 5.16: Individual compounds of aldehyde identified and quantified from *B. napus* cvs/lines spray inoculated with *P. brassicae* (28 dpi) using GCMS. Error bars represent standard deviations of three replicates. Values with the same letters are not significantly different (Wilcoxon, Anova and TukeyHSD, df 7).

significantly after treatment in *B. napus* resistant cvs/lines, as was the total wax profile (Appendices 15, 16, 17 and 18, respectively).

5.3.5 Cutin monomer compositions in *B. rapa* and *B. napus* leaves

The main aim of studying cutin monomer composition was to enhance the current knowledge about the differences in the content between resistant and susceptible *B. napus* cvs/lines as well as *B. rapa* wax mutants. This is the first time the difference in composition between resistant and susceptible cvs/lines before and after treatment with *P. brassicae* has been studied. Of the compounds identified, the most abundant was C18:2 dicarboxylic acid (DCA) and C16:0 DCA in *B. napus*. Similar compounds were found in *B. rapa* but with a greater percentage of C18:2 DCA and less C16:0 DCA. The internal standards were degraded and therefore the results obtained from this study are qualitative rather than quantitative. The average of each individual component was calculated from the total wax extracted.

5.3.5.1 Biochemical composition of cutin in *B. rapa*

C16:0 DCA were down-regulated in NG2 but WT, glossy mutants and NG1 showed greater induction (Figure 5.17). C16:1 DCA were expressed in WT and NG2 only after inoculation and increased significantly after inoculation in GL2. In glossy mutants, C18:2 DCA were significantly increased after inoculation but WT and non-glaucous mutants showed decreased amounts after inoculation. C18:0 DCA were greater only in NG2 after inoculation in contrast to the reduction in WT. Mixtures of C22 alcohol and C24 fatty acid, C24 alcohol and C26 fatty acid and 2Keto C29 were increased in WT and NG2 after inoculation while NG1 showed an increase only in 2Keto C29 (Figure 5.18). However, glossy mutants showed a decrease (Figure 5.18).

5.3.5.2 Biochemical composition of cutin in *B. napus*

A significant decrease in C16:0 DCA was found in susceptible cvs/lines after inoculation while an increase was observed in Cubs Root and SWU Chinese 1 (Figure 5.19). All susceptible cvs/lines except Moana showed significant increase in C16:1 DCA. Laser also showed an increase in C18:2 DCA after inoculation but Sansibar Cubs Root had a significant decrease. A significant increase in C18:0 was observed
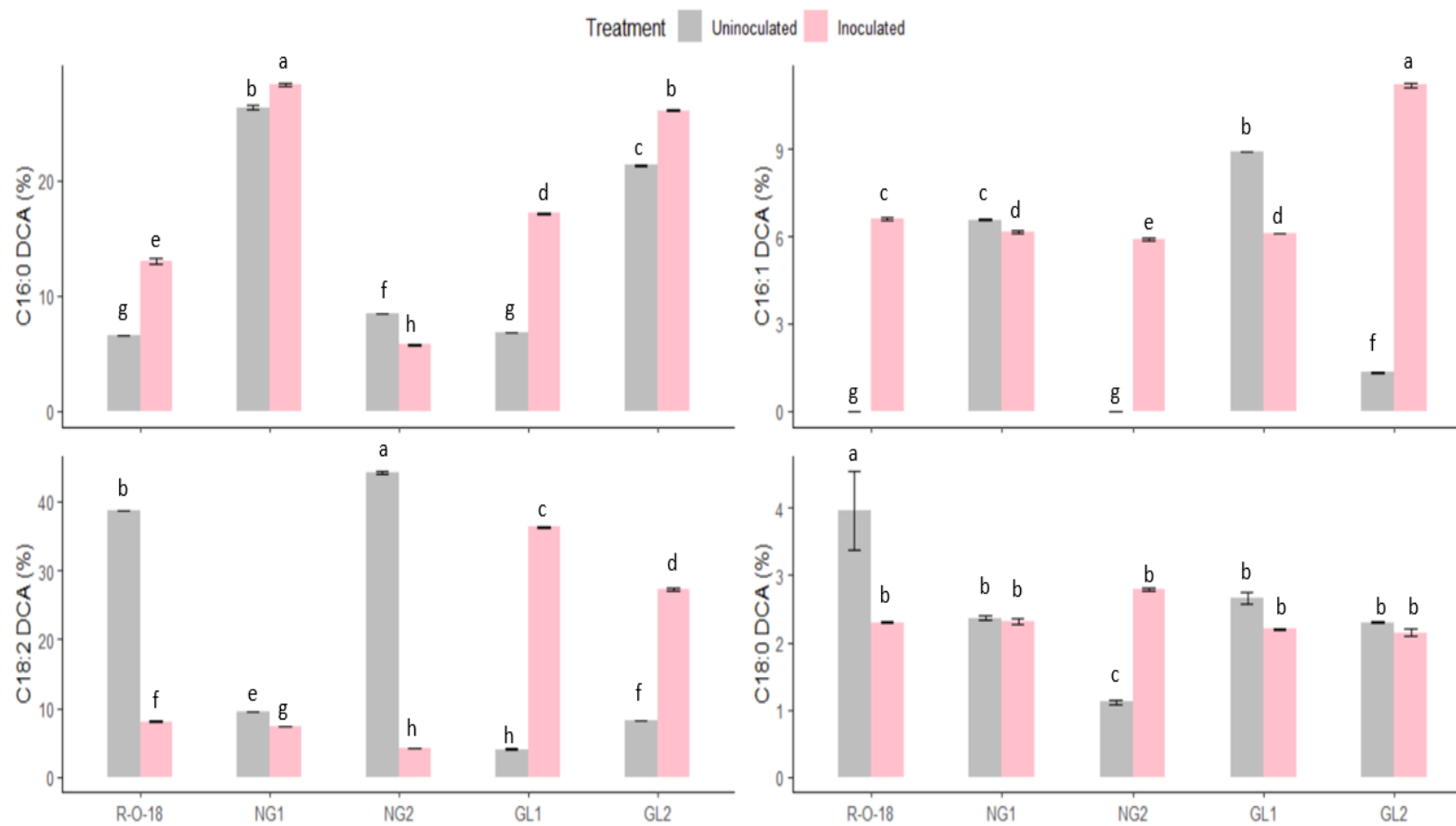
Figure 5.17: Percentage of individual compounds of dicarboxylic acids (DCAs) out of total cutin extracted from *B. rapa* wax mutants spray inoculated with *P. brassicae* (28 dpi) using GCMS. Error bars represent standard deviations of three replicates. Values with the same letters are not significantly different (Wilcoxon, Anova and TukeyHSD, df 4).
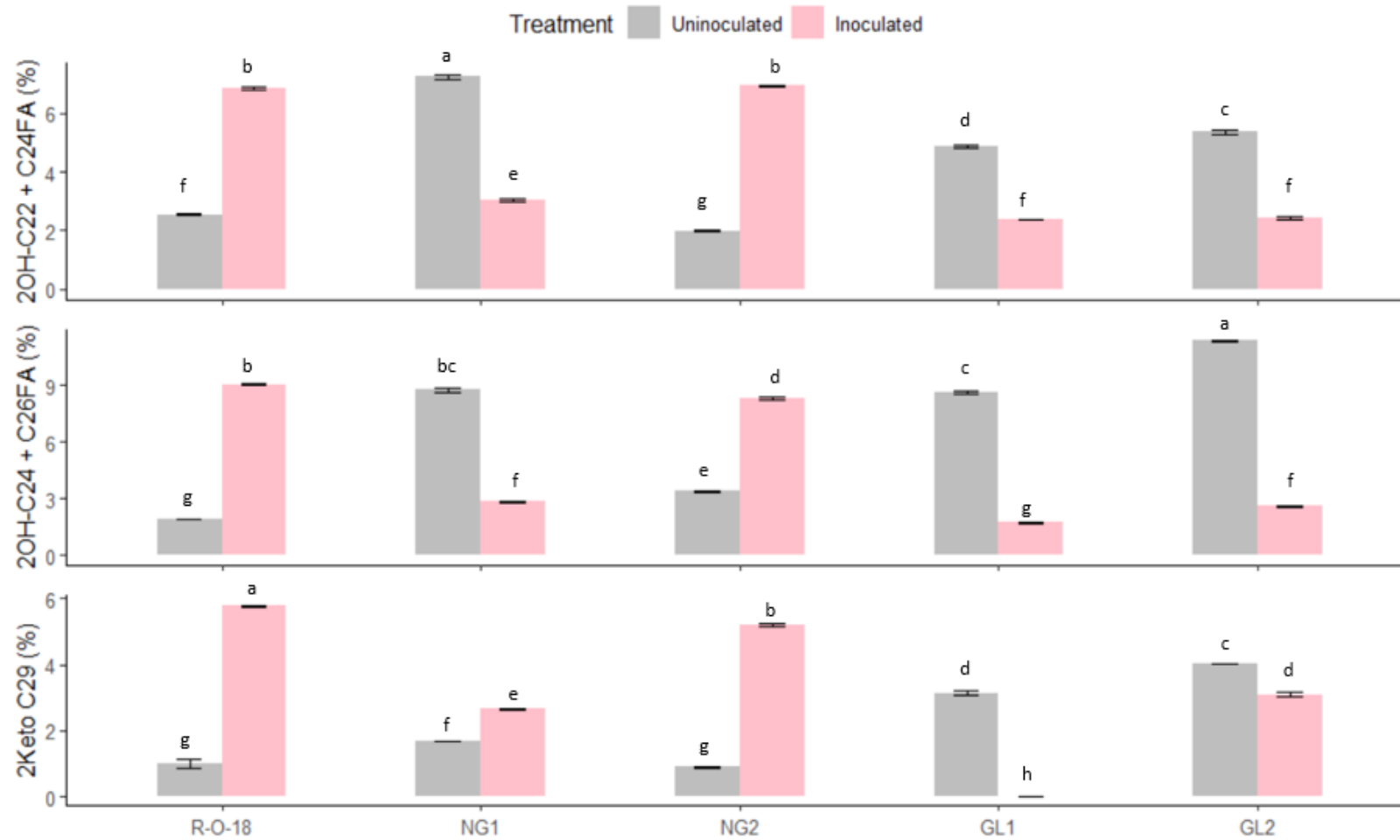
Figure 5.18: Percentage of individual compounds of alcohol and fatty acid mixture as well as ketone out of total cutin extracted from *B. rapa* wax mutants spray inoculated with *P. brassicae* (28 dpi) using GCMS. Error bars represent standard deviations of three replicates. Values with the same letters are not significantly different (Wilcoxon, Anova and TukeyHSD, df 4).
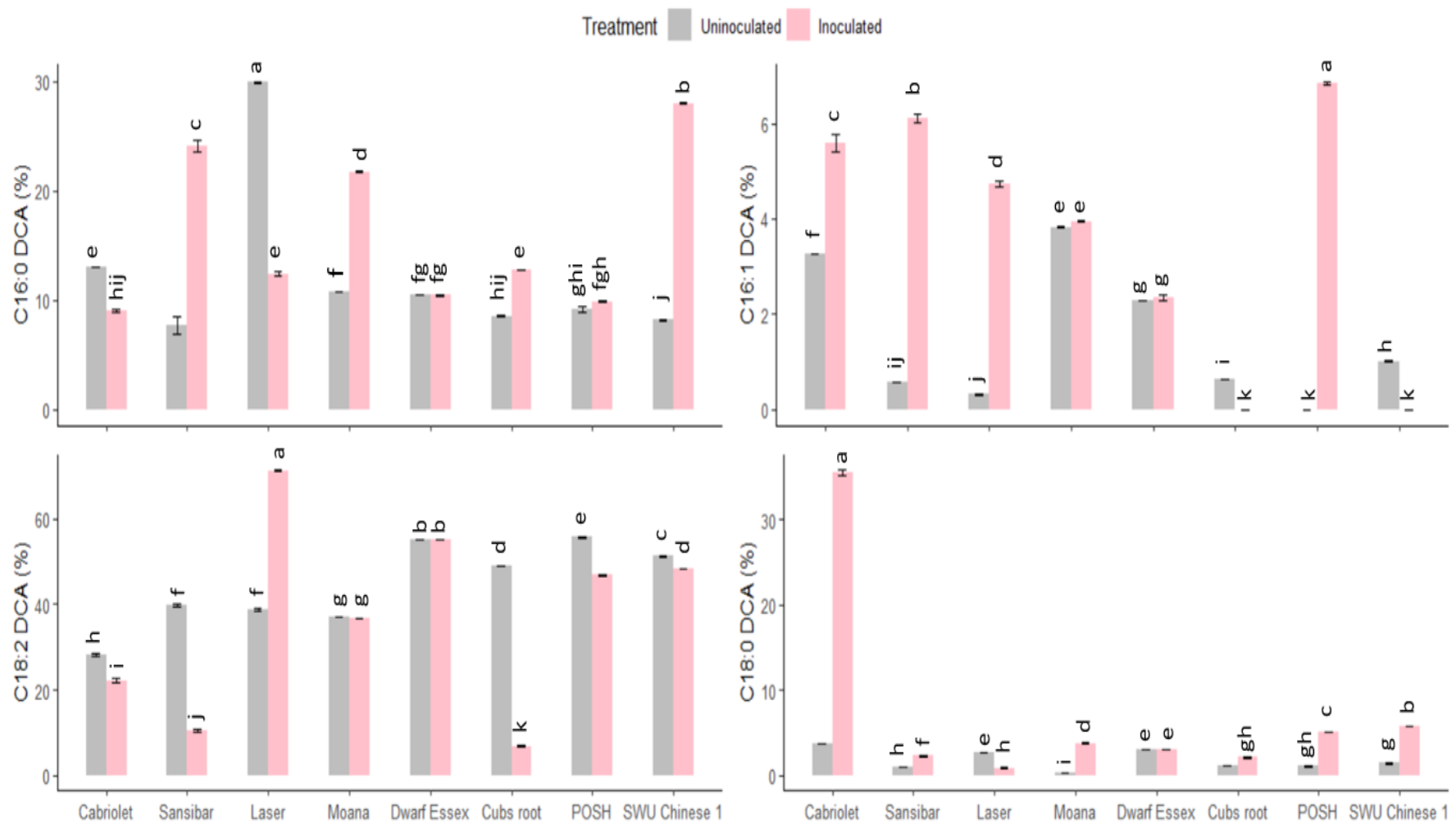
Figure 5.19: Percentage of individual dicarboxylic acids (DCAs) out of total cutin extracted from *B. napus* leaves spray inoculated with *P. brassicae* (28 dpi) using GCMS. Error bars represent standard deviations of three replicates. Values with the same letters are not significantly different (Wilcoxon, Anova and TukeyHSD, df 7).

in susceptible cvs Cabriolet, Sansibar and Moana after inoculation, as with lines POSH and SWU Chinese 1.

Discussion

5.4.1 *B. rapa* is a good source of resistance against *P. brassicae*

Results from this study show that disease severity was less in *B. rapa* than *B. napus,* thus indicating the resistance mechanism/s operating in *B. rapa*. The occurrence of loci for resistance against *P. brassicae* in *B. rapa* was reported and the resistance was successfully transferred into agronomically acceptable breeding lines (cv. Imola and DH lines) (Bradburne *et al.*, 1999). Furthermore, Karandeni Dewage *et al.* (2022) identified QTL operating against *P. brassicae* in *B. rapa*. All these results indicate that the brassica species *B. rapa* is a better source of resistance against *P. brassicae* than *B. napus*. Further studies can be done to dissect the molecular and biochemical components involved in resistance against *P. brassicae.*

5.4.2 Down-regulation/degradation of cuticular wax and alkane components limit *P. brassicae* pathogenesis

It was hypothesised that the host defence system down-regulates certain components of wax re-synthesis after inoculation (28 dpi) or degrades the wax load, which reduces the pathogenicity of *P. brassicae*. From the results obtained, there was an overall reduction in total wax and wax components after inoculation of *B. rapa* or *B. napus*. Both *B. napus* resistant cvs/lines and *B. rapa* showed 40% decrease in the total wax load after treatment while susceptible cvs/lines showed less reduction (an average of 18%) with the exception of cv. Laser, which showed an increase of 40% (Table 5.2). Of the major molecular species of epicuticular wax, alkanes were significantly reduced after treatment in *B. rapa* and *B. napus* resistant cvs/lines (Figure 5.8 and 5.13, respectively).

However, the reduction in amounts of wax and alkane could also be due to the enzymes produced by *P. brassicae* to promote pathogenicity or due to cutinase expression. The involvement of *cytochrome P450* as a pathogenicity factor in fungi has been reported in many studies and they are associated with alkane degradation

Table 5.2: Average percentage of total wax reduction at 28 dpi with *P. brassicae.* Colour formatted with green, yellow and red ranges (from lower to higher) for each molecular species and total wax. Cultivar Laser featured an increase in wax content.

Cultivar	Resistant/Susceptible	Species	% Reduction
Cabriolet			21.75
Sansibar	Susceptible		15.14
Laser			-41.15
Moana		*B napus*	32.27
Dwarf Essex			30.55
Cubs root	Resistant		40.55
POSH			41.90
SWU Chinese 1			52.96
R-O-18			46.51
NG1			55.00
NG2		*B rapa*	62.42
GL1			58.57
GL2			42.71

(Chen *et al.*, 2014; Karlsson et al., 2008; Shin *et al.*, 2017; Yamada-Onodera *et al.*, 2002). Therefore, it is possible that *cytochrome P450* or similar alkane/hydrocarbon degrading enzymes are secreted by *P. brassicae*. However, a potential defence signalling pathway is activated as a result in resistant *B. napus* lines and *B. rapa* to limit pathogen asexual sporulation at *c.* 28 dpi (Figure 5.3). Therefore, the wax regeneration load was decreased by down-regulating the alkanes and lowering the wax load as a defence response in *B. napus* resistant cvs/lines and *B. rapa*. As the susceptible *B.napus* cvs/lines did not show a significant reduction observed in resistant cvs/lines (Figure 5.13), the down-regulation hypothesis seems to be the mechanism rather than the degradation by the fungus. Alternatively, the reduction in wax load and alkanes may be a result of both pathogen enzyme degradation and down-regulation as a result of host defence responses. It can be hypothesised that the wax load/alkane reduction is to favour the pathogenesis of *P. brassicae* as *c.* 28 dpi the asexual sporulation occurs and lower wax load aids the cuticle penetration of germinated spores. However, the results showed that the cutinase expression was not higher in all susceptible cvs/lines such as cv. Sansibar. Therefore, the reduction in wax load indicates the host defence mechanism than promoting susceptibility. Furthermore, the glossy mutants with lower wax correlates with higher resistance against *P. brassicae*.

Many studies indicate the positive correlation of certain wax components with the LLS disease progression. Namely, C24 1^0 alcohol on the avocado fruit surface stimulate spore germination as well as appressorium differentiation in *Colletotrichum gloeosporioides* (Podila *et al.*, 1993) and major decrease in C29 and C31 alkanes in cucumber fruit which impaired the pathogenicity of *B. cinerea* (Wang *et al.*, 2015). Therefore, down-regulation of certain wax components results in overall reduction in wax concentration. Many studies indicate that less cuticular wax enhances the cuticular permeability and improves the resistance signalling pathways (Table 5.1). Thus, down-regulating the wax content may be a defence mechanism to limit *P. brassicae* pathogenesis by enhancing cuticular structure/permeability. Characterising the expression patterns of genes involved in wax synthesis in lines that are resistant or susceptible against *P. brassicae* can add to current knowledge. In addition, the cutinase expression at 28 dpi can enhance the knowledge about the susceptibility hypothesis.

5.4.3 Aldehyde promotes the pathogenicity of *P. brassicae*

The results showed that the minor component aldehydes were significantly decreased after treatment in *B. rapa* and resistant *B. napus* cvs/lines (Figure 5.11 and 5.16, respectively). Furthermore, aldehydes were constitutively increased in glossy mutants and baseline increase was observed in resistant *B. napus* lines. The greatest baseline levels were observed in C30 aldehyde. Reisige *et al.* (2006) reported that C28 aldehyde promotes spore germination of *Puccinia graminis* in wheat and C26 aldehyde is essential for germination and appressorial formation of *Blumeria graminis* in maize (Hansjakob *et al.*, 2010). The current study was focussed on 28 dpi and therefore, down-regulation of aldehyde might be related to the reduced *P. brassicae* DNA (reduced colonisation) and decreased spore number (limited asexual sporulation) in resistant *B. napus* cvs/ines and *B. rapa.*

5.4.4 Cuticular wax load and/or branched fatty alcohols (structural variation) regulate cutinase expression in *P. brassicae*

Both glossy (with up to 80% wax reduction) and non-glaucous (structural variation - reduced or absence of branched C27 and C29 fatty alcohols) mutants showed greater resistance against *P. brassicae* than WT. This indicates the involvement of both wax load and structural variation in resistance against *P. brassicae*. Furthermore, the cutinase expression was reduced significantly in both wax mutants at 8 dpi. Furthermore, resistant *B. napus* cvs/lines showed a significant reduction in C27 branched alcohol (Dwarf Essex, Cubs Root and POSH) (Appendix 18) after inoculation. Susceptible cvs/lines showed an enhanced branched alcohol after inoculation except for cv. Cabriolet which showed a decrease in C27 branched alcohol after inoculation. Liu *et al.*, (2021) reported that mutation in fatty acyl-coenzyme A reductases coding genes (*BnA1.CER4* and *BnC1.CER4*) results in enhanced cuticular permeability and resistance against *Sclerotinia sclerotiorum* in *B. napus*. This suggests that the down-regulation of C27 branched fatty alcohol (structural variation) is a potential defence mechanism against *P. brassicae* in *B. napus* resistant lines. In addition, the lower wax load enhances permeability and increased resistance against *P. brassicae*. Appendix 25 shows the total wax content and composition in *B. napus* and *B. rapa* tested in this study. Percentage compositions of each molecular species

of epicuticular wax identified from *B. napus* and *B. rapa* before and after inoculation with *P. brassicae* are shown in Table 5.3.

5.4.5 Visual LLS assessment did not correlate with *P. brassicae* spore count and pathogen DNA in *B. rapa*

Glossy mutants were more resistant but had greater *P. brassicae* spore numbers and greater amounts *P. brassicae* DNA and an opposite result was observed in non-galucous mutants (Figure 5.2). No correlations of LLS score with either *P. brassicae* spore number or amount *P. brassicae* DNA were observed in wax mutants (Figure 5.20). However, a positive correlation was observed between *P. brassicae* spore number and amount *P. brassicae* DNA (Figure 5.21). In addition, LLS scoring of *B. rapa* by eye was difficult and a light microscope was used to achieve efficient results. However, in *B. napus* the conidia were visible and it was possible to score LLS without a microscope.

5.4.6 Cutin monomers impart resistance against *P. brassicae*

A review by Ziv *et al*. (2018) indicates the involvement of cutin monomers in providing resistance against pathogens in plants. From the results obtained, fatty acids mixtures (2OH-C22 + C24 FA and 2OH-C24 + C26 FA) and C28 fatty acid appeared to have been up-regulated significantly in *B. rapa* (WT and non-glaucous mutants) and in resistant *B. napus* cv. Cubs Root when challenged with *P. brassicae* (Figure 5.18, Appendix 22, Appendix 23 and Appendix 24, respectively). These monomers are also abundant in suberin which is present inside the primary cell wall and the suberin is associated with pathogen invasion (Harman-Ware *et al*., 2021). The current study showed that C16:0 DCA was significantly increased in uninoculated Laser and C18:2 DCA was upregulated significantly in Laser after inoculation (Figure 5.19). Furthermore, susceptible cvs Cabriolet showed a significant decrease with C16:0 DCA after inoculation but resistant cvs/lines showed an increase. In addition, C18:0 DCA was significantly increased after inoculation in susceptible cv Cabriolet. C9 DCA was found as a signalling molecule involved in systemic defence responses (Javvadi *et al*., 2018). Conversely, the same study reported C9 DCA as a pathogenic factor secreted by *P. syringae*. Intriguingly, C18:0 DCA was up-regulated significantly in

Table 5.3: Percentage composition of each molecular species in the cuticular wax before and after inoculation (28 dpi) with *P. brassicae*.

Cultivar	Species	Treatment	Alkane	Alcohol 1	Alcohol 2	Br Alcohol	Aldehyde	Fatty acid	Keto	Diol	Wax ester
Cabriolet		Uninoculated	55.00	4.78	5.58	4.23	3.63	1.27	18.47	2.41	4.63
Cabriolet		Inoculated	47.82	7.47	6.20	3.55	3.89	1.64	22.11	1.52	5.81
Sansibar		Uninoculated	56.12	5.99	5.10	4.17	4.48	1.31	19.34	1.06	2.42
Sansibar		Inoculated	56.20	9.36	5.69	5.37	5.68	1.65	12.73	0.86	2.47
Laser		Uninoculated	45.78	5.25	7.85	7.33	4.37	1.25	21.41	4.09	2.66
Laser		Inoculated	49.22	5.80	6.23	6.65	3.95	0.95	23.50	1.08	2.62
Moana		Uninoculated	60.93	3.93	6.30	4.37	3.01	0.82	16.93	1.03	2.68
Moana	*B napus*	Inoculated	54.78	6.18	7.76	5.68	3.94	0.60	16.15	1.23	3.68
Dwarf Essex		Uninoculated	53.30	3.19	10.25	4.68	2.99	0.97	18.01	2.07	4.53
Dwarf Essex		Inoculated	61.70	5.38	8.66	5.03	3.13	0.80	11.45	1.69	2.17
Cubs Root		Uninoculated	51.50	3.18	10.36	3.33	3.07	1.55	20.61	2.87	3.54
Cubs Root		Inoculated	52.35	6.36	8.91	2.81	2.80	1.28	20.05	2.86	2.58
POSH		Uninoculated	56.64	3.89	8.85	4.19	2.73	1.01	17.36	2.50	2.82
POSH		Inoculated	50.88	6.73	8.65	2.67	1.97	1.56	25.56	0.95	1.03
SWU Chinese 1		Uninoculated	58.75	3.67	7.34	4.13	3.89	1.29	15.35	1.78	3.80
SWU Chinese 1		Inoculated	50.90	8.06	8.90	6.24	6.13	1.20	15.15	1.12	2.30
R-0-18		Uninoculated	65.39	4.63	13.11	0.91	1.07	1.14	10.56	0.67	2.52
R-0-18		Inoculated	44.85	8.38	22.09	1.99	2.17	1.15	17.15	0.50	1.72
NG1		Uninoculated	53.44	4.22	15.96	1.45	1.77	0.72	21.04	0.79	0.62
NG1		Inoculated	47.90	10.43	29.43	1.92	2.13	0.70	5.74	0.90	0.83
NG2	*B rapa*	Uninoculated	69.54	3.10	8.05	0.82	0.87	0.44	15.55	0.68	0.96
NG2		Inoculated	52.28	8.97	18.91	1.70	1.83	0.75	13.93	0.73	0.89
GL1		Uninoculated	14.00	27.79	14.89	16.16	20.36	1.55	0.53	0.33	4.38
GL1		Inoculated	11.98	39.34	18.10	10.96	13.91	1.49	0.60	0.47	3.15
GL2		Uninoculated	15.51	34.13	8.97	15.77	18.00	1.30	0.48	0.43	5.41
GL2		Inoculated	14.46	48.59	13.13	6.83	9.96	1.58	0.72	0.57	4.13
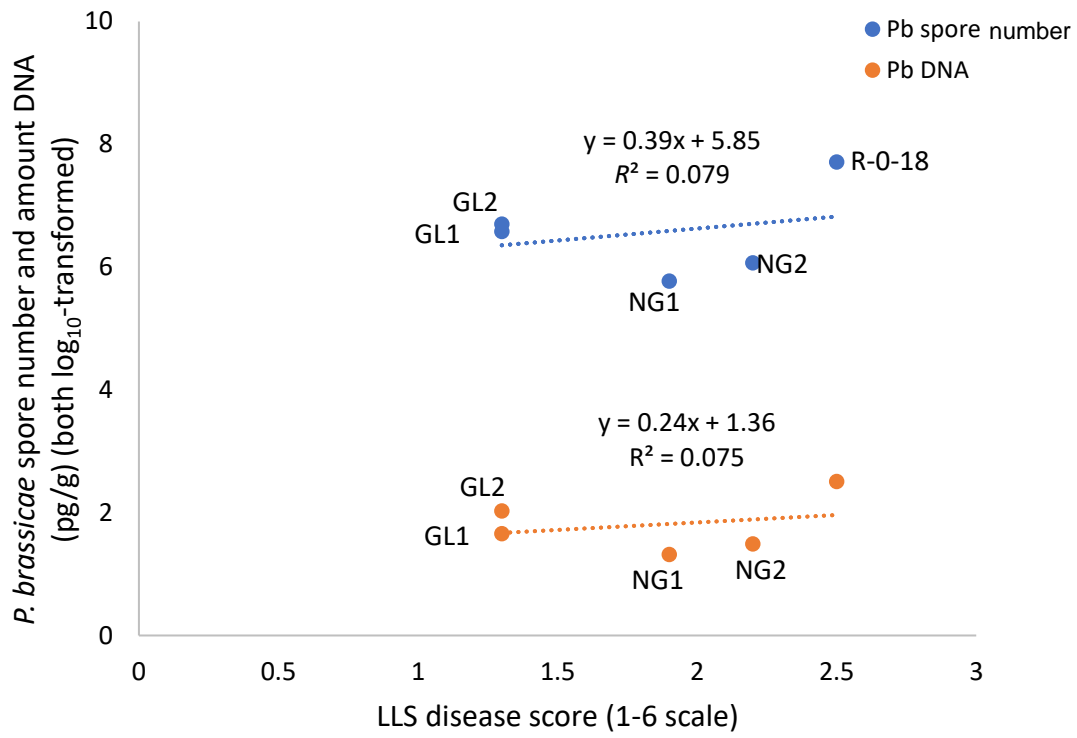
Figure 5.20: Correlation graphs of LLS score against *P. brassicae* spore number ($\log_{10}$-transformed) and amount *P. brassicae* DNA ($\log_{10}$-transformed), respectively.
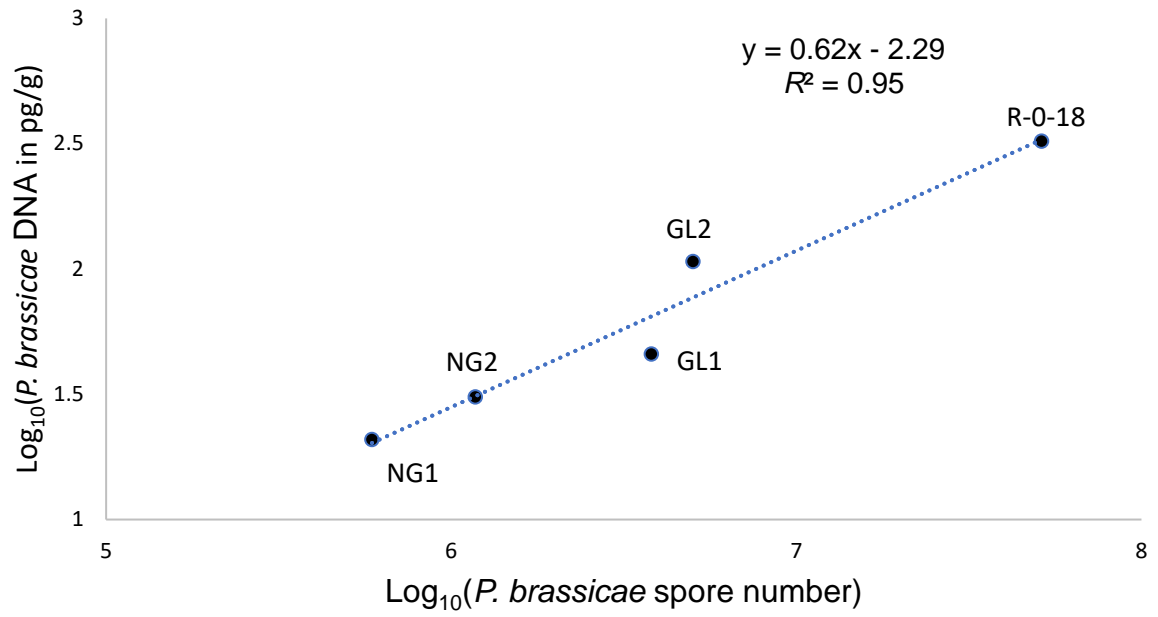
Figure 5.21: Correlation graph between *P. brassicae* spore number and amount DNA (both log$_{10}$-transformed).

susceptible cv. Cabriolet after inoculation by comparison with other cvs/lines and it may be a potential immune hijacking mechanism by *P. brassicae*.

5.4.7 Future work

5.4.7.1 Screening for resistance against *P. brassicae* in *Arabidopsis thaliana*

B. napus and *Arabidopsis thaliana* both belong to the family *Brassicaceae* (Yamamoto & Nishio., 2014). *Arabidopsis* and *Brassica* genera were separated evolutionarily *c.* 15 million years ago. Since their separation, whole genome duplication has occurred in *Brassica* and not in *Arabidopsis*. The gene in *Arabidopsis* may have several ortholog genes in *B. napus* (Town *et al.*, 2006). *Arabidopsis* genome structure is closely related to the complex genome of *B. napus*. In addition, *Arabidopsis* has a small incidence of repeated sequences and a small genome size. Whole genome sequence information is available for *Arabidopsis* (The Arabidopsis Genome Initiative, 2000) and *B. napus, B. rapa, B. oleracea, B. juncea* etc. (Chalhoub *et al.*, 2014; Wang *et al.*, 2011; Liu *et al.*, 2014; Yang *et al.*, 2016). Hybridisation is a valuable tool to transfer desirable genes from wild species into arable crops (Kuckuck *et al.*, 1991). Asymmetric hybrids between *B. napus* and *A. thaliana* have been produced in the past (Forsberg *et al.*, 1998; Yamagishi *et al.*, 2002*)*. Previously, *A. thaliana*-derived resistance against *Leptospaeria maculans* has been successfully transferred into *B. napus* (Bohman *et al.*, 2002).

During this research, an attempt has been made to study the interaction between *A. thaliana* and *P. brassicae* using trypan blue staining (Appendix 26). The main aim was to identify at least one ecotype of *A. thaliana* susceptible and one resistant against *P. brassicae,* so that further molecular genetic dissection can be done. *A. thaliana* ecotypes (Ws-0, Nd-1 and Col-0) did not show any penetration by *P. brassicae* under a microscope at 7 dpi. Some hyphal growth was visible at 18 dpi in Nd-1 leaves. However, it was not substantial, and hyphae did not branch (Appendix 26: a, b). Further analysis at 25 dpi showed minimal colonisation in Nd-1 (Appendix 26: c, d) and Ws-0 (Appendix 26: l), yet there was no extensive growth, and the lack of branching was also evident. Furthermore, ecotypes N22651, N22652, N22653, N22654, N22655, N22656 and N22658 showed no growth until 25 dpi (Appendix 26: e, f, g, h, i, j, k respectively). However, no ecotype showed high susceptibility to *P.*

brassicae with extensive branching and colonisation, neither at early stages nor at late stages of pathogenesis. This indicates a potential involvement of cuticular wax and/ or cutin components to reduce initial penetration in *A. thaliana*. Therefore, it will be beneficial to screen a large number of ecotypes to identify a susceptible and resistant *A. thaliana* ecotype to understand the resistance mechanism against *P. brassicae* and to potentially introgress the resistance into *B. napus*.

5.4.7.2 Association of cuticular permeability with resistance against *P. brassicae*

L'Haridon *et al.* (2011) showed an association of increased cuticular permeability with ROS production and resistance against *B. cinerea* in *A. thaliana* mutants such as bodyguard (*bdg*), *lacs2.3*, *aba2* and *aba3.* Furthermore, enhanced cuticle permeability is usually associated with increased diffusion of signalling molecules and thus with ROS generation and triggering innate immunity (L'Haridon *et al.*, 2011; Ziv *et al.*,2018). Since there was no indication of hypersensitive response related lesions that usually result due to ROS production, it will be interesting to determine the underlying mechanisms of resistance against cuticle penetration in relation to cuticular wax content and/or composition. Conversely, increased cuticular wax content and hydrophobic wax components, such as alkanes and or ketones, can lead to decreased cuticular permeability and *A. thaliana* mutants with diminished cuticular permeability showed increased resistance to *B. cinerea* (L'Haridon *et al.*, 2014; Ziv *et al.*,2018). The current study indicates the latter possibility as the resistant *B. napus* lines showed increased wax load and increased alkane and ketone contents by comparison with susceptible cvs/lines. Furthermore, non-glaucous mutants which showed the greater resistance against *P. brassicae* had similar profiles of wax and hydrophobic components.

Toluidine staining to assess cuticular permeability during pathogenesis of *P. brassicae* in *B. rapa* was done during this study. However, no significant variations were observed (Appendix 27). Therefore, it will be beneficial to do further permeability assays with improved toluidine staining with greater concentrations or to quantify permeability using chlorophyll leaching or using electron microscopy.

5.5 Conclusion

Many studies indicate the involvement of cuticle and epicuticular wax in resistance against pathogens. Cuticular wax repels water drops containing fungal spores (Wagner *et al.,* 2003). It also acts as a hydrophobic barrier, which repels water and thus prevents the pathogen surviving and gaining entry into the host (Koch., 2004). *B. napus* has inadequate levels of resistance against *P. brassicae* and this study demonstrates the potential resistance mechanisms present in other species, namely *B. rapa* and *A. thaliana*. An association of cuticular wax, cutin and their components with resistance against *P. brassicae* was observed during this project as well as from previous published data. The current study confirms the multifaceted role of epicuticular and intra-cuticular wax quantity and their components in both host defence and promoting pathogenesis of *P. brassicae*. Furthermore, the results showed that these interactions are far more complex and regulated by many components from both the host plant and *P. brassicae*. Multiple factors could have influenced this host-pathogen interaction, namely biochemical, structural variations and permeability of the cuticle. The wax mutant approach was challenging as changes in one group of cuticular components or structural change (decrease to no branched alcohols in non-glaucous mutants) does affect other biochemical group/s of cuticular wax (increased alkanes in non-glaucous mutants). Therefore, it is difficult to make final conclusions about which components are the main influential factor. However, gene expression profiling of wax biosynthesis genes in question can enhance current knowledge and aid in breeding cvs/lines that are resistant against *P. brassicae*. Previous studies suggested various potential mechanisms of cuticle defence, such as production of ROS, accumulation of fungitoxic compounds on cuticle surfaces, transcriptional defence responses and changes to cuticle permeability to limit pathogen infection (Arya *et al.,* 2021). Thus, the interaction of cuticle components and the pathogenicity factors from *P. brassicae* and other pathogens requires considerable research to better understand the role of the cuticle in limiting infection.

This study helped to identify certain components of epicuticular wax (alkanes, primary alcohols, branched fatty alcohols and aldehydes) and cutin monomers (fatty acids and DCAs) involved in resistance or susceptibility against *P. brassicae*. This new knowledge will facilitate breeding of cvs/lines with improved cuticle function and

therefore improved resistance to *P. brassicae* and increased yield. However, some wax mutants showed resistance to *B. cinerea* and susceptibility *to P. syringae* at the same time. Therefore, further research and careful consideration need to be given while breeding for resistance by optimising cutin monomers and wax components. Furthermore, plant cuticles contain terpenoids and flavonoids which have antifungal activities. Thus, the cuticular study is incomplete without taking into account the involvement of these components in resistance against *P. brassicae*.

Chapter 6: General discussion

The main aim of this research was to better understand the resistance of *Brassica napus* (oilseed rape) against *Pyrenopeziza brassicae* (light leaf spot) by analysing GWAS mapping, gene expresssion and biochemical components (glucosinolates, cuticular wax and cutin). In addition, differences in pathogenicity *of P. brassicae* populations and isolates from Aberdeenshire, Scotland and Hertfordshire, England were studied. Table 6.1 summarises the overall results obtained during this PhD study including LLS scoring, *P. brassicae* spore counting, *P. brassicae* DNA count, total glucosinolate content, area under gene expression curve (AUGEC) of cutinase, total wax from uninocuted cvs/lines and percentage decrease in total wax after inoculation with *P. brassicae* in *B. napus* and *B. rapa*.

6.1 Variations in pathogenicity of *P. brassicae* in oilseed rape

This study showed that there is a regional variation in the LLS disease severity. Karandeni Dewage *et al*. (2021) showed an isolate-specific resistance interaction of *B. napus* cvs/lines (Imola, Yudal, and the DH line Q83) with isolates from Herefordshire, Cambridgeshire and Norfolk. Furthermore, significant differences in LLS score were observed between most genotypes and between most *P. brassicae* isolates, and there were genotype x isolate interactions. This PhD thesis reports a significant difference in pathogenicity between two isolates of *P. brassicae* (A1 from Aberdeen and R3 from Rothamsted) on *B. napus*. However, the variation between single spore isolate does not necessarily represent the entire geographical population. Therefore, further dissection of molecular genetics of these isolates can broaden current knowledge about the pathogenicity factors in *P. brassicae*. Boys *et al*. (2012) showed a complete absence of asexual sporulation on cv. Imola inoculated with a *P. brassicae* population whereas Karandeni Dewage *et al*. (2021) observed reduced sporulation on cv. Imola. This indicates a potential novel pathogenicity factor in *P. brassicae* operating to overcome the complete resistance (*R*-gene mediated) in resistant cv. Imola. The new information about significant difference/s in interactions between isolates and genotypes obtained in this study can be investigated further using advanced techniques such as sequencing and micro-arrays to improve insights about this host and pathogen interactions.

Table 6.1: Summary of the overall results obtained during this PhD study including LLS scoring, *P. brassicae* spore counting (Pb spore), *P. brassicae* DNA count (Pb DNA), total glucosinolate (GLS) content, area under gene expression curve (AUGEC) of cutinase, total wax from uninocuted cvs/lines and percentage decrease in total wax after inoculation with *P. brassicae* in *B. napus* and *B. rapa*. Colour formatted with green, yellow and red ranges (from lower to higher).

Cultivar	Resistant/Susceptible	Species	LLS score	Pb spore	Pb DNA	Total GLS	Cutinase AUGEC	Total wax uninoculated	% decrease wax after treatment
Cabriolet	Susceptible	*B. napus*	5.9	7.7	6.24	1217.16	1422.25	1087.703665	21.75
Sansibar			5.1	7.48	4.22	1147.9	964.94	1207.532616	15.14
Laser			4.7	7.3	4.26	1398.92	1408.00	828.3522982	-41.15
Moana	Resistant		3.7	7.07	3.71	2848.3		1817.271902	32.27
Dwarf Essex			4.1	7.16	3.72	3159.74		1345.495334	30.55
Cubs Root			3	6.34	1.1	2424.08	782.86	1637.256433	40.55
POSH			2.5	6.1	0.97	3161.54	961.73	1627.619263	41.90
SWU Chinese 1			2.4	6.21	2.56	1543.72	1609.88	1560.845971	52.96
R-O-18		*B rapa*	2.5	7.71	2.51		1181.46	730.8801758	46.51
NG1			1.3	6.58	1.66		1151.50	690.3186969	55.00
NG2			1.3	6.7	2.03		1086.22	1260.429999	62.42
GL1			1.9	5.77	1.32		1527.63	333.2948126	58.57
GL2			2.2	6.07	1.49		1562.88	233.0440513	42.71

6.2 Defence response genes involved in resistance against *P. brassicae*

This is the first-time potential GEMs associated with QDR against *P. brassicae* in *B. napus* have been quantified and compared. Cubs Root, SWU Chinese 1, POSH and Laser showed significantly less susceptibility to *P. brassicae* than other cvs/lines and showed induction of certain genes involved in defence responses. Induction of defence genes upon challenging with *P. brassicae* appeared mostly genotype-dependent, even though most resistant cvs/lines showed similar responses. The interesting genes were *universal stress protein*, *β-adaptin*, *PR1*, *cinnamate 4 hydroxylase* and *phosphatidylinositol-specific phospholipase C4*. They were expressed in all resistant cvs/lines and even susceptible cv. Laser behaved mostly like a resistant cultivar/line with higher expression of quantitative defence related genes. All these cvs/lines can be used as potential resistance sources for breeding resistance against *P. brassicae.* This novel information about these defence genes can be beneficial to reduce the yield loss by employing genome editing methods, namely clustered regularly interspaced short palindromic repeats and the CRISPR associated protein 9 (CRISPR-Cas9) system to create genome-edited oilseed rape crops resistant against *P. brassicae.* Furthermore, the same system can be used to remove any undesired gene or any gene promoting susceptibility such as acyl transferase in *B. napus.*

6.3 Role of glucosinolates, cuticular wax and cutin in resistance against *P. brassicae*

Results from this study showed that *B. napus* resistant cvs Cubs Root, POSH, Dwarf Essex as well as susceptible cv. Moana possess significantly greater concentrations of glucosinolates (GSL) than susceptible cvs Cabriolet, Sansibar and Laser. A negative correlation was observed between LLS disease score and subgroups of GSL (aliphatic, aromatic and indolic). Therefore, it can be concluded that there is an association of GSL with resistance against *P. brassicae* in *B. napus*. Resistant line POSH showed significantly greater amounts of total GSL as well as the individual bio-compounds of it. Thus, it can be an ideal candidate to study the GSL content and individual compounds, especially after challenging with *P. brassicae*.

This study showed the possibility of exploiting the cuticle composition and structure to limit *P. brassicae* pathogenesis. Most alkane forming pathway products (aldehydes, alkanes, ketones and secondary alcohols) were decreased and an increase in alcohol forming pathway components (primary alcohols, branched alcohols and wax esters) with pathogenesis of *P. brassicae* (28 dpi) as observed. This indicates a potential mechanism of down-regulating the alkane forming pathway as a defence response mechanism to limit the colonisation and asexual reproduction in *B. napus* resistant cvs/lines and *B. rapa*. In addition, negative correlations between many cutin monomers and LLS disease score were observed. Furthermore, *B. rapa* wax mutants showed greater resistance to *P. brassicae* than *B. rapa* wild type and *B. napus*, confirming the association of epicuticular wax load, composition, structural variation and cutin in resistance against *P. brassicae*. Thus, *B. napus* cvs/lines (Cubs Root, POSH, SWU Chinese 1, Laser, Moana and Dwarf Essex) which showed significantly different epicuticular wax components and cutin monomers can be utilised to produce lines with better resistance against *P. brassicae* by optimising these biochemical components.

6.4 Laser and Moana: need to re-categorise as intermediately resistant lines against *P. brassicae*

Cultivars Moana and Laser were classified as susceptible to *P. brassicae* based on initial visual assessment. However, Moana showed increased GSL content and expression of defence genes against *P. brassicae* in Laser appeared like that of resistant lines. Furthermore, they both appeared intermediate in spore counting and *P. brassicae* DNA quantification. Therefore, lines Moana and Laser should be re-categorised as intermediate instead of susceptible to *P. brassicae*.

B. napus susceptible cv Laser showed an enhanced cuticular wax production as well as majority of the components after the inoculation. Furthermore, Laser and Moana showed significantly different composition in many cutin monomers before and after inoculation with *P. brassicae* than other lines. C18:1 fatty acid content in uninoculated Laser and Moana were significantly greater than other lines/cvs. 2OH-C22 and C24 FA mixture and 2Keto C29 content were increased after inoculation in both Laser and Moana. Ahuja *et al*. (2016) reported a close association between chemical defence system involving metabolites such as glucosinolates and physical defence barriers

namely cuticle. Thus, it indicates an association of the higher GSL content and cutin monomers in Moana with increased resistance to *P. brassicae*.

6.5 Conclusion

Preliminary observations showed an initial resistance which limits *P. brassicae* penetration through the cuticle in *Arabidopsis thaliana*. Furthermore, *B. rapa* appeared to have more resistance against *P. brassicae* than *B. napus* according to qualitative and quantitative LLS disease scoring methods. As there is a lack of complete resistance against *P. brassicae* in *B. napus*, an alternative approach would be to transfer resistance from the non-host *Arabidopsis* or ancestor *B. rapa* into oilseed rape. Furthermore, this study showed the potential breakdown of the resistance in commercial cv. Ambassador, which is on the current AHDB Recommended List and therefore, there is a great need to exploit the resistance against *P. brassicae* available in other species.

This study enabled identification of many sources of resistance against *P. brassicae* in *B. napus* and other related species. In addition, it aided identification of many genes and bio-chemical compounds operating to limit the pathogenesis of *P. brassicae*. However, it is necessary to understand how these molecular components work against other pathogens as well in a crop of oilseed rape. Therefore, more comprehensive phenotyping of the resources identified in this research for complex traits operating in several environments will be a key to utilise these diverse germplasms to breed efficient *B. napus* cultivars with improved and stable yield under fluctuating biotic and abiotic stresses.

Bibliography

Abuyusuf, M., Robin, A., Lee, J. H., Jung, H. J., Kim, H. T., Park, J. I., & Nou, I. S. (2018). Glucosinolate profiling and expression analysis of glucosinolate biosynthesis genes differentiate white mold resistant and susceptible cabbage lines. *International Journal of Molecular Sciences*, *19*, 4037. https://doi.org/10.3390/ijms19124037

AHDB Cereals & Oilseeds. (2016). AHDB Recommended Lists for Cereals and Oilseeds (2016/17). Agriculture and Horticulture Development Board. Available at: https://cereals.ahdb.org.uk/varieties/ahdb-recommended-lists/rl-archive-2019-20. aspx (accessed 19 July 2019).

AHDB Fungicide performance in cereals and oilseed rape. (2022). Fungicide performance for oilseed rape. https://ahdb.org.uk/knowledge-library/fungicide-performance-in-cereals-and-oilseed-rape (accessed 13 May 2023).

Ahmed, A., Crawford, T., Gould, S., Ha, Y. S., Hollrah, M., Noor-E-Ain, F., *et al*. (2003). Synthesis of (R)- and (S)-10,16-dihydroxyhexadecanoic acid: cutin stereochemistry and fungal activation. *Phytochemistry* 63, 47–52. doi: 10.1016/S0031-9422(03)00003-7.

Arabidopsis Genome Initiative. (2000). Analysis of the genome sequence of the flowering plant *Arabidopsis thaliana*. *Nature, 408*, 796-815. https://doi.org/10.1038/35048692

Arya, G. C., Sarkar, S., Manasherova, E., Aharoni, A., & Cohen, H. (2021). The plant cuticle: an ancient guardian barrier set against long-standing rivals. *Frontiers in Plant Science*, *12*, 663165. https://doi.org/10.3389/fpls.2021.663165

Arya, G. C., & Cohen, H. (2022). The multifaceted roles of fungal cutinases during infection. *Journal of Fungi (Basel, Switzerland)*, *8*, 199. https://doi.org/10.3390/jof8020199

Ashby, A. M. (1997). A molecular view through the looking glass: The *Pyrenopeziza brassicae-Brassica* interaction. *Advances in Botanical Research*, 24, 31-70.

Ashby, A. M. (2000). Biotrophy and the cytokinin conundrum. *Physiological and Molecular Plant Pathology*, *57*, 147–158. https://doi.org/10.1006/PMPP.2000.0294

Batish, S., Hunter, A., Ashby, A. M., & Johnstone, K. (2003). Purification and biochemical characterisation of Psp1, an extracellular protease produced by the oilseed rape pathogen *Pyrenopeziza brassicae*. *Physiological and Molecular Plant Pathology*, 62, 13-20.

Barrett, L. G., Thrall, P. H., Burdon, J. J., & Linde, C. C. (2008). Life history determines genetic structure and evolutionary potential of host-parasite interactions. *Trends in Ecology & Evolution*, *23*, 678–685. https://doi.org/10.1016/j.tree.2008.06.017.

Becker, M. G., Zhang, X., Walker, P. L., Wan, J. C., Millar, J. L., *et al.* (2017) Transcriptome analysis of the *Brassica napus–Leptosphaeria maculans* pathosystem identifies receptor, signaling and structural genes underlying plant resistance. *Plant Journal,* 9, 573–586. https://doi.org/10.1111/tpj.13514

Bernard, A., & Joubès, J. (2013). *Arabidopsis* cuticular waxes: advances in synthesis, export and regulation. *Progress in Lipid Research*, *52*, 110–129. https://doi.org/10.1016/j.plipres.2012.10.002

Bessire, M., Chassot, C., Jacquat, A.-C., Humphry, M., Borel, S., Petétot, J. M.-C., Nawrath, C., *et al.* (2007). A permeable cuticle in *Arabidopsis* leads to a strong resistance to *Botrytis cinerea*. *The EMBO Journal*, *26*, 2158–2168. https://doi.org/10.1038/sj.emboj.7601658.

Bennett, R. N., & Wallsgrove, R. M. (1994). Secondary metabolites in plant defence mechanisms. *New Phytologist*, *127*, 617-633. https://doi.org/10.1111/j.1469-8137.1994.tb02968.x

Blenn, B., Bandoly, M., Küffner, A., Otte, T., Geiselhardt, S., Fatouros, N. E., & Hilker, M. (2012). Insect egg deposition induces indirect defense and epicuticular wax changes in *Arabidopsis thaliana*. *Journal of Chemical Ecology*, *38*, 882–892. https://doi.org/10.1007/s10886-012-0132-8

Bohman, S., Wang, M., & Dixelius, C. (2002). *Arabidopsis thaliana*-derived resistance against *Leptosphaeria maculans* in a *Brassica napus* genomic background. *Theoretical and Applied Genetics*, *105*, 498–504. https://doi.org/10.1007/s00122-002-0885-5.

Bonaventure, G., Beisson, F., Ohlrogge, J., & Pollard, M. (2004). Analysis of the aliphatic monomer composition of polyesters associated with *Arabidopsis* epidermis: occurrence of octadeca-cis-6, cis-9-diene-1,18-dioate as the major component. *The Plant Journal*, *40*, 920–930. https://doi.org/10.1111/j.1365-313X.2004.02258.x

Bourdenx B., Bernard A., Domergue F., Pascal S., Léger A., Roby D., Pervent M., Vile D., Haslam R.P., Napier J.A., Lessire R., Joubès J. (2011). Over expression of *Arabidopsis ECERIFERUM1* promotes wax very-long-chain alkane biosynthesis and influences plant response to biotic and abiotic stresses. *Plant Physiology*. 156, 29–45. https://doi.org/10.1104/pp.111.172320

Boyd, L. A., Ridout, C., O'Sullivan, D. M., Leach, J. E., & Leung, H. (2013). Plant–pathogen interactions: disease resistance in modern agriculture. *Trends in Genetics, 29, 233-240.* https://doi.org/10.1016/j.tig.2012.10.011

Boys, E. F., Roques, S. E., Ashby, A. M., Evans, N., Latunde-Dada, A. O., Thomas, J. E., west, J.S. & Fitt, B. D. L. (2007). Resistance to infection by stealth: *Brassica napus* (winter oilseed rape) and *Pyrenopeziza brassicae* (light leaf spot). *European Journal of Plant Pathology*, 118, 307-321. https://doi. org/10. 1007/s 10658-007-9141-9

Boys, E. F., Roques, S. E., West, J. S., Werner, C. P., King, G. J., Dyer, P. S., & Fitt, B. D. L. (2012).   Effects of *R* gene-mediated resistance in *Brassica napus* (oilseed rape) on asexual and sexual sporulation of *Pyrenopeziza brassicae* (light leaf spot). *Plant Pathology*, 61, 543-554. https://doi.org/10.1111/j.1365- 3059 .20 11.02529.x

Brader G, Mikkelsen MD, Halkier BA, Palva ET. 2006. Altering glucosinolate profiles modulates disease resistance in plants. *The Plant Journal*, 46, 758 –767. http://dx.doi.org/10.1111/j.1365-313X.2006.02743.x

Bradburne, R., Majer, D., Magrath, R., Werner, C. P., Lewis, B., & Mithen,R. (1999). Winter oilseed rape with high levels of resistance to *Pyrenopeziza brassicae* derived from wild *Brassica* species. *Plant Pathology*, 48, 550–558. https://doi.org/10.1046/j.1365-3059.1999.00373.x

Brown, P. D., Tokuhisa, J. G., Reichelt, M., Gershenzon, J. (2003). Variation of glucosinolate accumulation among different organs and developmental stages of *Arabidopsis thaliana*. *Phytochemistry,* 62, 471-481. https://doi.org/10.1016/ S0031-9422(02)00549-6

Bustin, S. A., Benes, V., Garson, J. A., Hellemans, J., Huggett, J., Kubista, M., Mueller, R., Nolan, T., Pfaffl, M. W., Shipley, G. L., Vandesompele, J., & Wittwer, C. T. (2011). Primer sequence disclosure: a clarification of the MIQE guidelines. *Clinical Chemistry*, *57*, 919–921. https://doi.org/10.1373/ clinchem.2011.162958

Calenge F., Drouet D., Denance C., Van de Weg W. E., Brisset M. N., Paulin J. P., et al. (2005). Identification of a major QTL together with several minor additive or epistatic QTLs for resistance to fire blight in apple in two related progenies. *Theoretical Applied Genetics, 111,* 128–135. https://doi.org/10.1007/s00122-005-2002-z

Carmody, S. M., King, K. M., Ocamb, C. M., Fraaije, B. A., West, J. S., & du Toit, L. J. (2020). A phylogenetically distinct lineage of *Pyrenopeziza brassicae* associated with chlorotic leaf spot of *Brassicaceae* in North America. *Plant Pathology*, *69*, 518–537. https://doi.org/10.1111/ppa.13137

Carter, H. E., Cools, H. J., West, J. S., Shaw, M. W., & Fraaije, B. A. (2013). Detection and molecular characterisation of *Pyrenopeziza brassicae* isolates resistant to methyl benzimidazole carbamates. *Pest Management Science*, *69*, 1040–1048. https://doi.org/10.1002/ps.3585.

Carter, H. E., Fraaije, B. A., West, J. S., Kelly, S. L., Mehl, A., Shaw, M. W., & Cools, H. J. (2014). Alterations in the predicted regulatory and coding regions of the sterol 14α-demethylase gene (*CYP51*) confer decreased azole sensitivity in the oilseed rape pathogen *Pyrenopeziza brassicae*. *Molecular Plant Pathology*, *15*, 513–522. https://doi.org/10.1111/mpp.12106.

Chalhoub, B., Denoeud, F., Liu, S., Parkin, I. A. P., Tang, H., Wang, X., Wincker, P., *et al*. (2014). Early allopolyploid evolution in the post-neolithic *Brassica napus* oilseed genome. *Science*, 345, 950-953. https://doi.org/10.1126/science.1253435

Chandna, R., Augustine, R., & Bisht, N. C. (2012). Evaluation of candidate reference genes for gene expression normalization in *Brassica juncea* using real time quantitative RT-PCR. *PloS One*, *7*, e36918. https://doi.org/10.1371/journal.pone.0036918

Cheah, L. H., Hartill, W. F. T. & Corbin, J. B. (1980). First report of the natural occurrence of *Pyrenopeziza brassicae* Sutton et Rawlinson, the apothecial state of *Cylindrosporium concentricum Greville*, in brassica crops in New Zealand. *New Zealand Journal of Botany*, 18, 197-202. https://doi.org/10.1080/0028825X.1980.10426917

Chen, W., Lee, M. K., Jefcoate, C., Kim, S. C., Chen, F., & Yu, J. H. (2014). Fungal cytochrome p450 monooxygenases: their distribution, structure, functions, family expansion, and evolutionary origin. *Genome Biology and Evolution*, *6*, 1620–1634. https://doi.org/10.1093/gbe/evu132

Chen, W., Li, Y., Yan, R., Ren, L., Liu, F., Zeng, L., Sun, S., Yang, H., Chen, K., Xu, L., Liu, L., Fang, X., & Liu, S. (2021). *SnRK1.1*-mediated resistance of *Arabidopsis thaliana* to clubroot disease is inhibited by the novel *Plasmodiophora brassicae* effector PBZF1. *Molecular Plant Pathology*, *22*, 1057–1069.

Chi, Y. H., Koo, S. S., Oh, H. T., Lee, E. S., Park, J. H., Phan, K., Wi, S. D., Bae, S. B., Paeng, S. K., Chae, H. B., Kang, C. H., Kim, M. G., Kim, W. Y., Yun, D. J., & Lee, S. Y. (2019). The physiological functions of universal stress proteins and their molecular mechanism to protect plants from environmental stresses. *Frontiers in Plant Science*, *10*, 750. https://doi.org/10.3389/fpls.2019.00750

Corwin, J. A., & Kliebenstein, D. J. (2017). Quantitative resistance: more than just perception of a pathogen. *The Plant Cell*, *29*, 655–665. https://doi.org/10.1105/tpc.16.00915

Cowger C, Brown JKM (2019) Durability of quantitative resistance in crops: greater than we know? *Annual Review of Phytopathology,* 57, 253-277. https://doi.org/10.1146/annurev-phyto-082718-100016

Crocoll, C., Halkier, B. A., & Burow, M. (2016). Analysis and quantification of glucosinolates. *Current Protocols in Plant Biology*, 1, 385-409, https://doi.org/10.1002/cppb.20027

CropMonitor. (2019). Survey of commercially grown winter oilseed rape. Department for Environment, Food, and Rural Affairs. Available at: www.cropmonitor.co.uk/wosr/surveys/wosr.cfm (accessed 1 February 2019)

Evans, N., Butterworth, MH., Baierl, A., Semenov, MA., West, JS., Barnes, AP., Moran, D., & Fitt, BDL. (2010). The impact of climate change on disease constraints on production of oilseed rape. *Food Security*, *2*, 143 - 156.

Evans, N., Ritchie, F., West, J., Havis, N., Matthewman, C., & Maguire, K. (2017). *Investigating components of the oilseed rape light leaf spot epidemic responsible for increased yield loss to the UK Arable Industry*. Retrieved from https://ahdb.org.uk/investigating-components-of-the-oilseed-rape-light-leaf-spot-epidemic-responsible-for-increased-yield-loss-to-the-uk-arable-industry.

FAOSTAT. (2019). Food and agriculture organization corporate statistical database. Food and Agriculture Organisation of the United Nations. Available at http://faostat3.fao.org/home/E (accessed 15 April 2019).

Fell, H., Ali, A.M., Wells, R., Mitrousia, G.K., Woolfenden, H., Schoonbeek, H., Fitt, B. D. L., Ridout, C.J., Stotz, H. U. (2023). Novel gene loci associated with susceptibility or cryptic quantitative resistance to *Pyrenopeziza brassicae* in *Brassica napus. Theoretical and Applied Genetics.* DOI: 10.21203/rs.3.rs-1327286/v1

Feraru, E., Paciorek, T., Feraru, M. I., Zwiewka, M., De Groodt, R., De Rycke, R., Kleine-Vehn, J., & Friml, J. (2010). The AP-3 *β-adaptin* mediates the biogenesis and function of lytic vacuoles in *Arabidopsis. The Plant Cell*, *22*, 2812–2824. https://doi.org/10.1105/tpc.110.075424

Figueroa, L., Fitt, B. D. L., Welham, S. J., Shaw, M. W., McCartney, H. A. (1995). Early development of light leaf spot (*Pyrenopeziza brassicae*) on winter oilseed rape (*Brassica napus*) in relation to temperature and leaf wetness. *Plant Pathology*, 44, 641–654. https://doi.org/10.1111/j.1365-3059.1995.tb01688.x

Filipe, O., De Vleesschauwer, D., Haeck, A., Demeestere, K., & Höfte, M. (2018). The energy sensor *OsSnRK1a* confers broad-spectrum disease resistance in rice. *Scientific Reports*, *8*, 3864. https://doi.org/10.1038/s41598-018-22101-6

Fitt, B. D. L., Doughty, K. J., Gilles, T., Gladders, P., Steed, J. M., Su, H., & Sutherland, K. G. (1998a). Methods for assessment of light leaf spot (*Pyrenopeziza brassicae*) on winter oilseed rape (*Brassica napus*) in the UK. *Annals of Applied Biology*, 133, 329-341. https://doi.org/10.1111/j.1744-7348.1998.tb05834.x

Fitt, B. D. L., Doughty, K. J., Gladders, P., Steed, J. M., & Sutherland, K. G. (1998b). Diagnosis of light leaf spot (*Pyrenopeziza brassicae*) on winter oilseed rape (*Brassica napus*) in the UK. *Annals of Applied Biology,* 133, 155-166. https://doi.org/10.1111/j.1744-7348.1998.tb05816.x

Fitt, B. D. L., Brun, H., Barbetti, M. J., & Rimmer, S. R. (2006). World-wide importance of phoma stem canker (*Leptosphaeria maculans* and *L. biglobosa*) on oilseed rape (*Brassica napus*). *European Journal of Plant Pathology*, *114*, 3–15. https://doi.org/10.1007/s10658-005-2233-5

Forsberg, J., Lagercrantz, U., & Glimelius, K. (1998). Comparison of UV light, X-ray and restriction enzyme treatment as tools in production of asymmetric somatic hybrids between *Brassica napus* and *Arabidopsis thaliana*. *Theoretical and Applied Genetics*, *96*, 1178–1185. https://doi.org/10.1007/s001220050854

Foster, S. J., Ashby, A. M. & Fitt, B. D. L. (2002). Improved PCR-based assays for pre-symptomatic diagnosis of light leaf spot and determination of mating type of *Pyrenopeziza brassicae* on winter oilseed rape. *European Journal of Plant Pathology,* 108, 379–383. https://doi.org/10.1023/A:1015659527542

Giamoustaris A, Mithen R. 1997. Glucosinolates and disease resistance in oilseed rape (*Brassica napus* ssp. *oleifera*). *Plant Pathology,* 46, 271–275. https://doi.org/10.1046/j.1365-3059.1997.d01-222.x

Gilles, T., Evans, N., Fitt, B. D. L., & Jeger, M. J. (2000). Epidemiology in relation to methods for forecasting light leaf spot (*Pyrenopeziza brassicae*) severity on winter oilseed rape (*Brassica napus*) in the UK. *European Journal of Plant Pathology*, 106, 593-605. https://doi.org/10.1023/A:1008701302853

Gilles, T., Ashby, A. M., Fitt, B. D. L. and Cole, T. (2001). Development of *Pyrenopeziza brassicae* apothecia on oilseed rape debris and agar. *Mycological Research*, 105, 705-714. https://doi.org/10.1017/S0953756201003902

Gu, Y., Zavaliev, R., & Dong, X. (2017). Membrane trafficking in plant immunity. *Molecular Plant*, *10*, 1026–1034. https://doi. org/10.1016 /j.molp. 2017. 07.001

Häffner, E., Karlovsky, P., Splivallo, R., *et al.* (2014) ERECTA, salicylic acid, abscisic acid, and jasmonic acid modulate quantitative disease resistance of *Arabidopsis thaliana* to *Verticillium longisporum*. *BMC Plant Biology* 14, 85. https:// doi.org/ 10.1186/1471-2229-14-85

Han, X., Zhang, L., Zhao, L., Xue, P., Qi, T., Zhang, C., Yuan, H., Zhou, L., Wang, D., Qiu, J., & Shen, Q. H. (2020). SnRK1 phosphorylates and destabilizes *WRKY3* to enhance barley immunity to powdery mildew. *Plant Communications*, *1*, 100083. https://doi.org/10.1016/j.xplc.2020.100083

Hansjakob, A., Bischof, S., Bringmann, G., Riederer, M.A., & Hildebrandt, U. (2010). Very-long-chain aldehydes promote in vitro prepenetration processes of *Blumeria graminis* in a dose- and chain length-dependent manner. *New Phytologist, 188*, 1039-54. https://doi.org/10.1111/j.1469-8137.2010.03419.x

Hansjakob, A., Riederer, M., and Hildebrandt, U. (2012). Appressorium morphogenesis and cell cycle progression are linked in the grass powdery mildew fungus *Blumeria graminis*. *Fungal Biology,* 116, 890–901. doi: 10.1016 / j.funbio. 2012.05.006.

Harman-Ware, A. E., Sparks, S., Addison, B., & Kalluri, U. C. (2021). Importance of suberin biopolymer in plant function, contributions to soil organic carbon and in the production of bio-derived energy and materials. *Biotechnology for Biofuels*, *14*, 75. https://doi.org/10.1186/s13068-021-01892-3

Harper, A. L., Trick, M., Higgins, J., Fraser, F., Clissold, L., Wells, R., Bancroft, I., *et al.* (2012). Associative transcriptomics of traits in the polyploid crop species *Brassica napus*. *Nature Biotechnology*, *30*, 798–802. https:// doi.org/ 10.1038 /nbt.2302.

Hubbard, A., Lewis, C. M., Yoshida, K., Ramirez-Gonzalez, R. H., de Vallavieille-Pope, C., Thomas, J., Saunders, D., *et al.* (2015). Field pathogenomics reveals the emergence of a diverse wheat yellow rust population. *Genome Biology*, *16*, 23. https://doi.org/10.1186/s13059-015-0590-8.

Ichino, T., & Yazaki, K. (2022). Modes of secretion of plant lipophilic metabolites via ABCG transporter-dependent transport and vesicle-mediated trafficking. *Current Opinion in Plant Biology*, *66*, 102184. https://doi.org/10.1016/j.pbi.2022.102184

Jameson, P. E. (2000). Cytokinins and auxins in plant-pathogen interactions - An overview. *Plant Growth Regulation,* 32, 369–380. doi: 10.1023/a: 10107 3361 754 3.

Javvadi, S. G., Cescutti, P., Rizzo, R., Lonzarich, V., Navarini, L., Licastro, D., Guarnaccia, C., & Venturi, V. (2018). The spent culture supernatant of *Pseudomonas syringae* contains azelaic acid. *BMC Microbiology*, *18*, 199. https://doi.org/10.1186/s12866-018-1352-z

Jeger, M., Viljanen-Rollinson, S. (2001). The use of the area under the disease-progress curve (AUDPC) to assess quantitative disease resistance in crop lines. *Theoretical and Applied Genetics* 102, 32–40. https://doi.org/10. 1007/s001 220051615

Jensen, L. M., Jepsen, H. S., Halkier, B. A., Kliebenstein, D. J., & Burow, M. (2015). Natural variation in cross-talk between glucosinolates and onset of flowering in *Arabidopsis. Frontiers in Plant Science*, *6*, 697. https://doi.org/10.3389/fpls.2015.00697

Jia, X. L., Wang, G. L., Xiong, F., Yu, X. R., Xu, Z. S., Wang, F., & Xiong, A. S. (2015). *De novo* assembly, transcriptome characterization, lignin accumulation, and anatomic characteristics: novel insights into lignin biosynthesis during celery leaf development. *Scientific Reports*, *5*, 8259. https://doi.org/10.1038/srep08259

Jiang, C., Hei, R., Yang, Y., Zhang, S., Wang, Q., Wang, W., Zhang, Q., Yan, M., Zhu, G., Huang, P., Liu, H., & Xu, J. R. (2020). An orphan protein of *Fusarium graminearum* modulates host immunity by mediating proteasomal degradation of *TaSnRK1α*. *Nature Communications*, *11*, 4382. https://doi.org/10.1038/s41467-020-18240-y

Jin, S., Zhang, S., Liu, Y., *et al.* (2020). A combination of genome-wide association study and transcriptome analysis in leaf epidermis identifies candidate genes involved in cuticular wax biosynthesis in *Brassica napus*. *BMC Plant Biology* 20, 458. https://doi.org/10.1186/s12870-020-02675-y

Kaiser, S. J., Mutters, N. T., Blessing, B., & Günther, F. (2017). Natural isothiocyanates express antimicrobial activity against developing and mature biofilms of *Pseudomonas aeruginosa*. *Fitoterapia*, *119*, 57–63. https://doi.org /10. 1016/J.FITOTE.2017.04.006.

Karandeni Dewage, C. S., Klöppel, C. A., Stotz, H. U., & Fitt, B. D. L. (2018a). Host-pathogen interactions in relation to management of light leaf spot disease (caused by *Pyrenopeziza brassicae*) on *Brassica species*. *Crop and Pasture Science*, *69*, 9–19. https://doi.org/10.1071/CP16445.

Karandeni Dewage, C. S. (2018b). Resistance against *Pyrenopeziza brassicae* for control of light leaf spot, PhD thesis, University of Hertfordshire, Hatfield, UK.

Karandeni Dewage, C. S., Qi, A., Stotz, H. U., Huang, Y. J., Fitt, B. D. L. (2021). Interactions in the *Brassica napus–Pyrenopeziza brassicae* pathosystem and sources of resistance to *P. brassicae* (light leaf spot). *Plant Pathology,* 70, 2104–2114. doi: 10.1111/ppa.13455

Karandeni Dewage, C. S., Cools, K., Stotz, H. U., Qi, A., Huang, Y. J., Wells, R., & Fitt, B. D. L. (2022). Quantitative trait locus mapping for resistance against *Pyrenopeziza brassicae* derived from a *Brassica napus* secondary gene pool. *Frontiers in Plant Science*, *13*, 786189. https://doi.org/1 0.3389 /fpls. 2022. 786189

Karlsson, M., Elfstrand, M., Stenlid, J., & Olson, A. (2008). A fungal cytochrome P450 is expressed during the interaction between the fungal pathogen *Heterobasidion annosum sensu lato* and conifer trees. *DNA sequence: the Journal of DNA Sequencing and Mapping, 19*, 115–120. https://doi.org/10. 1080/10425 170701 447473

Karolewski, Z., Fitt, B. D. L., Latunde-Dada, A. O., Foster, S. J., Todd, A. D., Downes, K., & Evans, N. (2006). Visual and PCR assessment of light leaf spot (*Pyrenopeziza brassicae*) on winter oilseed rape (*Brassica napus*) lines. *Plant Pathology*, 55, 387-400. https://doi.org/10.1111/j.1365-3059.2006.01383.x

Kim, J. I., Dolan, W. L., Anderson, N. A., & Chapple, C. (2015). Indole glucosinolate biosynthesis limits phenylpropanoid accumulation in *Arabidopsis thaliana*. *The Plant Cell*, *27*, 1529–1546. https://doi.org/10.1105/tpc.15.00127

Kim, J. I., Zhang, X., Pascuzzi, P. E., Liu, C. J., & Chapple, C. (2020). Glucosinolate and phenylpropanoid biosynthesis are linked by proteasome-dependent degradation of PAL. *New Phytologist*, *225*, 154–168. https://doi.org/10. 1111/nph. 16108

Kirkegaard, J. A., & Sarwar, M. (1998). Biofumigation potential of brassicas. *Plant and Soil*, *201*, 71–89. https://doi.org/10.1023/A:1004381129991

Kliebenstein, D. J. (2004). Secondary metabolites and plant/environment interactions: a view through *Arabidopsis thaliana* tinged glasses. *Plant, Cell & Environment*, *27*, 675-684. https://doi.org/10.1111/j.1365-3040.2004.01180.x

Koch, K. (2004). Self assembly of epicuticular waxes on living plant surfaces imaged by atomic force microscopy (AFM). *Journal of Experimental Botany*, *55*, 711–718. https://doi.org/10.1093/jxb/erh077.

Kuckuck, H., Kobabe, G. & Wenzel, G. 1991 *Fundamentals of Plant Breeding*. Berlin: Springer Verlag. https://doi.org/10.1515/9783112321331

Kump, K. L., Bradbury, P. J., Wisser, R. J., Buckler, E. S., Belcher, A. R., Oropeza-Rosas, M. A., Holland, J. B., *et al.* (2011). Genome-wide association study of quantitative resistance to southern leaf blight in the maize nested association mapping population. *Nature Genetics*, *43*, 163–168. https://doi.org /10.1038 /ng. 747.

Larkan, N. J., Ma, L., Haddadi, P., Buchwaldt, M., Parkin, I., Djavaheri, M., & Borhan, M. H. (2020). The *Brassica napus* wall-associated kinase-like (WAKL) gene *Rlm9* provides race-specific blackleg resistance. *Plant Journal*, *104*, 892–900. https://doi.org/10.1111/tpj.14966

Lee, S., Kaminaga, Y., Cooper, B., Pichersky, E., Dudareva, N., & Chapple, C. (2012). Benzoylation and sinapoylation of glucosinolate R-groups in *Arabidopsis*. *Plant Journal*, *72*, 411–422. https://doi.org /10.1111/j.1365-313X.2012.05096.x

L'Haridon F., Besson-Bard A., Binda M., Serrano M., Abou-Mansour E., Balet F., *et al.* (2011). A permeable cuticle is associated with the release of reactive oxygen species and induction of innate immunity. *PLoS Pathogens.* 7:e1002148. 10.1371/journal.ppat.1002148. https://doi.org/10.1371/journal.ppat.1002148

Li-Beisson, Y., Shorrosh, B., Beisson, F., Andersson, M. X., Arondel, V., Bates, P. D., Baud, S., Bird, D., Debono, A., Durrett, T. P., Franke, R. B., Graham, I. A., Katayama, K., Kelly, A. A., Larson, T., Markham, J. E., Miquel, M., Molina, I., Nishida, I., Rowland, O., Ohlrogge, J., *et al.* (2013). Acyl-lipid metabolism. *The Arabidopsis Book*, *11*, e0161. https://doi.org/10.1199/tab.0161

Li, C. H., Cervantes, M., Springer, D. J., Boekhout, T., Ruiz-Vazquez, R. M., Torres-Martinez, S. R., Heitman, J., & Lee, S. C. (2011). Sporangiospore size dimorphism is linked to virulence of *Mucor circinelloides*. *PLoS Pathogens*, *7*, e1002086. https://doi.org/10.1371/journal.ppat.1002086

Li, D., Ashby, A. M., & Johnstone, K. (2003) Molecular evidence that the extracellular cutinase *Pbc1* is required for pathogenicity of *Pyrenopeziza brassicae* on oilseed rape. *Molecular Plant-Microbe Interactions*, 16, 545–552. https://doi.org/10. 1094/ MPMI.2003.16.6.545

Li, D., Liu, H., Zhang, H., Wang, X., & Song, F. (2008). *OsBIRH1*, a DEAD-box RNA helicase with functions in modulating defence responses against pathogen infection and oxidative stress. *Journal of Experimental Botany*, *59*, 2133–2146. https://doi.org/10.1093/jxb/ern072

Li, Y., Beisson, F., Koo, A. J., Molina, I., Pollard, M., & Ohlrogge, J. (2007). Identification of acyltransferases required for cutin biosynthesis and production of cutin with suberin-like monomers. *Proceedings of the National Academy of Sciences of the United States of America*, *104*, 18339–18344. https://doi.org/10.1073/pnas.0706984104

Liu, S., Liu, Y., Yang, X., Tong, C., Edwards, D., Parkin, I. A., Zhao, M., Ma, J., Yu, J., Huang, S., Wang, X., Wang, J., Lu, K., Fang, Z., Bancroft, I., Yang, T. J., Hu, Q., Wang, X., Yue, Z., Li, H., … Paterson, A. H. *et al.* (2014). The *Brassica oleracea* genome reveals the asymmetrical evolution of polyploid genomes. *Nature Communications*, *5*, 3930. https://doi.org/10.1038/ncomms4930

Liu, J., Zhu, L., Wang, B., Wang, H., Khan, I., Zhang, S., Wen, J., Ma, C., Dai, C., Tu, J., Shen, J., Yi, B., & Fu, T. (2021). *BnA1.CER4* and *BnC1.CER4* are redundantly involved in branched primary alcohols in the cuticle wax of *Brassica napus. Theoretical and Applied Genetics, 134*, 3051–3067. https://doi.org/ 10.1007/s 001 22-021-03879-y

Lu, G. U., Harper, A. N. L., Trick, M. A., Morgan, C. O., Fraser, F. I., Neill, C. A. O., & Bancroft, I. A. N. (2014). Associative transcriptomics study dissects the genetic architecture of seed glucosinolate content in *Brassica napus. DNA Research*, *21*, 613-625. https://doi.org/10.1093/dnares/dsu024

Lyons, R., Iwase, A., Gänsewig, T., *et al.* (2013). The RNA-binding protein FPA regulates *flg22*-triggered defense responses and transcription factor activity by alternative polyadenylation. *Scientific Reports* 3, 2866. https://doi.org/ 10.1038 /s rep02866.

Ma, L., Wu, J., Qi, W., Coulter, J. A., Fang, Y., Li, X., Liu, L., Jin, J., Niu, Z., Yue, J., & Sun, W. (2020). Screening and verification of reference genes for analysis of gene expression in winter rapeseed (*Brassica rapa* L.) under abiotic stress. *PloS One*, *15*, e0236577. https://doi.org/10.1371/journal.pone.0236577

Ma, X., Wang, P., Zhou, S., Sun, Y., Liu, N., Li, X., & Hou, Y. (2015). *De novo* transcriptome sequencing and comprehensive analysis of the drought-responsive genes in the desert plant *Cynanchum komarovii. BMC Genomics*, *16*, 753. https://doi.org/10.1186/s12864-015-1873-x

Majer, D., Lewis, B. G., & Mithen, R. (1998). Genetic variation among field isolates of *Pyrenopeziza brassicae*. *Plant Pathology*, *47*, 22–28. https://doi.org/10.1046/j.1365-3059.1998.00204.x

McDonald, B. A., & Linde, C. (2002a). The population genetics of plant pathogens and breeding strategies for durable resistance. *Euphytica*, 124, 163–180.

McDonald B.A., Linde C. (2002b): Pathogen population genetics, evolutionary potential, and durable resistance. *Annual Review of Phytopathology*, 40, 349–379

Mei, J., Y. Fu, L. Qian, X. Xu, J. Li, and W. Qian, 2011: Effectively widening the gene pool of oilseed rape (*Brassica napus* L.) by using Chinese *B. rapa* in a 'virtual allopolyploid' approach. *Plant Breeding* 130, 333— 337. https://doi. org/10. 1111 /j.1439-0523.2011.01850.x

Moore, D., Robson, G., & Trinci, T. (2011). *21st Century Guidebook to Fungi. Cambridge University Press,* Cambridge. https://doi.org/ 10.1017/CB O97805 119 77022

Niks, R. E., Qi, X., & Marcel, T. C. (2015). Quantitative resistance to biotrophic filamentous plant pathogens: concepts, misconceptions, and mechanisms. *Annual Review of Phytopathology*, *53*, 445–470. https://doi.org/10.1146/annurev-phyto-080614-115928.

Norton, R., Kirkegaard, J., Angus, J., & Potter, T. (1999). Canola in rotations. *Regional Institute of Online Publishing*, 1–7. http://www.regional.org.au/au/gcirc/canola/p-06.htm

Nyadanu, D., Akromah, R., Adomako, B., Kwoseh, C., Dzahini-Ob, H., Lowor, S. T., Assuah, M. K., *et al.* (2012). Host plant resistance to phytophthora pod rot in cacao (*Theobroma cacao* L.): The role of epicuticular wax on pod and leaf surfaces. *International Journal of Botany*, 8, 13–21. https://scialert. net/abstract/ ?doi=ijb.2012.13.21

Onaga, G., Wydra, K., Koopmann, B., Séré, Y., & von Tiedemann, A. (2015). Population structure, pathogenicity and aating type distribution of *Magnaporthe oryzae* Isolates from east Africa. *Phytopathology*, *105*, 1137–1145. https://doi. org/10.1094/PHYTO-10-14-0281-R

Papastamati, K., Bosch, F. V., Welham, S. J., Fitt, B. D. L., Evans, N. N., Steed, J. M. (2002). Modelling the daily progress of light leaf spot epidemics on winter oilseed rape (*Brassica napus*), in relation to *Pyrenopeziza brassicae* inoculum concentrations and weather factors. *Ecological Modelling* – 148. 169-189. https://doi.org /10.1016 /S0 304-3800(01)00419-7

Penselin, D., Münsterkötter, M., Kirsten, S., Felder, M., Taudien, S., Platzer, M., Knogge, W., *et al.* (2016). Comparative genomics to explore phylogenetic relationship, cryptic sexual potential and host specificity of *Rhynchosporium* species on grasses. *BMC Genomics*, *17*, 1–32. https://doi.org/10.1186/s12864-016-3299-5

Petit, J., Bres, C., Mauxion, J. P., Bakan, B., & Rothan, C. (2017). Breeding for cuticle-associated traits in crop species: traits, targets, and strategies. *Journal of Experimental Botany*, *68*, 5369–5387. https://doi.org/10.1093/jxb/erx341

Pfaffl, M. W. (2001). A new mathematical model for relative quantification in real-time RT-PCR. *Nucleic Acids Research,* 29, e45. doi: 10.1093/nar/29.9.e45.

Pilet, M. L., Delourme, R., Foisset, N., & Renard, M. (1998). Identification of QTL involved in field resistance to light leaf spot (*Pyrenopeziza brassicae*) and blackleg resistance (*Leptosphaeria maculans*) in winter rapeseed (*Brassica napus* L.). *Theoretical and Applied Genetics*, 97, 398-406. https://doi.org/10.1007/s001220050909

Pilet-Nayel, M. L., Moury, B., Caffier, V., Montarry, J., Kerlan, M. C., Fournet, S., Delourme, R., *et al*. (2017). Quantitative resistance to plant pathogens in pyramiding strategies for durable crop protection. *Frontiers in Plant Science*, *8*, 1838. https://doi.org/10.3389/fpls.2017.01838

Plissonneau, C., Benevenuto, J., Mohd-Assaad, N., Fouché, S., Hartmann, F. E., & Croll, D. (2017). Using population and comparative genomics to understand the genetic basis of effector-driven fungal pathogen evolution. *Frontiers in Plant Science*, *8*, 119. https://doi.org/10.3389/fpls.2017.00119.

Podila, G. K., Rogers, L. M., and Kolattukudy, P. E. (1993). Chemical signals from avocado surface wax trigger germination and appressorium formation in *Colletotrichum gloeosporioides. Plant Physiology,* 103, 267–272. https:// doi. org/10.1104/pp.103.1.267

Pu, Y., Gao, J., Guo, Y. *et al.* (2013). A novel dominant glossy mutation causes suppression of wax biosynthesis pathway and deficiency of cuticular wax in *Brassica napus. BMC Plant Biology,* 13, 215. https://doi.org/10.1186/1471-2229-13-215

Rahmanpour, S., Backhouse, D., Nonhebel, H. M. (2009). Induced tolerance of *Sclerotinia sclerotiorum* to isothiocyanates and toxic volatiles from *Brassica* species. *Plant Pathology*, 58, 479 –486. http://dx.doi.org/10.1111/j.1365 -3059.2008.02015.x.

Ramakers, C., Ruijter, J.M., Lekanne-Deprez, R.H., Moorman, A.F.M. (2003). Assumption-free analysis of quantitative real-time polymerase chain reaction (PCR) data. *Neuroscience Letters,* 339, 62-66. https://doi.org/10.1016/s0304-3940(02)01423-4

Rawlinson, C. J., Muthyalu, G., & Turner, R. H. (1978). Effect of herbicides on epicuticular wax of winter oilseed rape (*Brassica napus*) and infection by *Pyrenopeziza brassicae. Transactions of the British Mycological Society*, 71, 441-451. https://doi.org/10.1016/S0007-1536(78)80071-0

Reed, E., Nunez, S., Kulp, D., Qian, J., Reilly, M. P., & Foulkes, A. S. (2015). A guide to genome-wide association analysis and post-analytic interrogation. *Statistics in Medicine*, *34*, 3769–3792. https://doi.org/10.1002/sim.6605.

Reisige, K., Gorzelanny, C., Daniels, U., Moerschbacher, B. M. (2006). The C28 aldehyde octacosanal is a morphogenetically active component involved in host plant recognition and infection structure differentiation in the wheat stem rust fungus. *Physiological and Molecular Plant Pathology,* 68, 33–40. doi: 10.101 6/j. pmpp.2006.05.006

Rieu, I., Powers, S. J. (2009) Real-time quantitative RT-PCR: design, calculations and statistics. *Plant Cell* 21:1031-1033. https://doi.org/10.1105/tpc.109.066001

Robin, A., Laila, R., Abuyusuf, M., Park, J. I., & Nou, I. S. (2020). *Leptosphaeria maculans* alters glucosinolate accumulation and expression of aliphatic and indolic glucosinolate biosynthesis genes in blackleg disease-resistant and -susceptible cabbage lines at the seedling stage. *Frontiers in Plant Science*, *11*, 1134. https://doi.org/10.3389/fpls.2020.01134

Rubel, M. H., Abuyusuf, M., Nath, U. K., Robin, A. H. K., Jung, H. J., Kim, H. T., Park, J. I., & Nou, I. S. (2020). Glucosinolate profile and glucosinolate biosynthesis and breakdown gene expression manifested by black rot disease infection in cabbage. *Plants (Basel, Switzerland)*, *9*, 1121. https:// doi.org /10.3390 /plants 9091121

Sahu, P. K., Jayalakshmi, K., Tilgam, J., Gupta, A., Nagaraju, Y., Kumar, A., Hamid, S., Singh, H. V., Minkina, T., Rajput, V. D., & Rajawat, M. V. S. (2022). ROS generated from biotic stress: Effects on plants and alleviation by endophytic microbes. *Frontiers in Plant Science*, *13*, 1042936. https://doi.org /10.3389 /fpls. 2022.1042936

Schlaich N. L. (2007). Flavin-containing monooxygenases in plants: looking beyond detox. *Trends in Plant Science, 12*, 412–418. https://doi.org/10.1016/j.tplants. 2007.08.009

Schnurr, J., Shockey, J., Browse, J. (2004) The acyl-CoA synthetase encoded by *LACS2* is essential for normal cuticle development in *Arabidopsis. Plant Cell*, 16, 629–642. https://doi.org/10.1105/tpc.017608

Schoch, G. A., Nikov, G. N., Alworth, W. L., & Werck-Reichhart, D. (2002). Chemical inactivation of the cinnamate 4-hydroxylase allows for the accumulation of salicylic acid in elicited cells. *Plant Physiology*, *130*, 1022–1031. https:// doi.org/ 10.1104/pp.004309

Schweizer, P., Jeanguénat, A., Métraux, J. P., Mösinger, E. (1994). "Plant protection by free cutin monomers in two cereal pathosystems," in *Advances Molecular Genetics Plant-Microbe Interactions*, eds M. J. Daniels, J. A. Downie, and A. E. Osbourn (Dordrecht: Kluwer), 371–374. doi: 10.1007/978-94-011-0177-6_55

Schweizer, P., Felix, G., Buchala, A., Muller, C., and Métraux, J. P. (1996a). Perception of free cutin monomers by plant cells. *Plant Journal,* 10, 331–341. doi: 10.1046/j.1365-313X.1996.10020331.x

Schweizer, P., Jeanguenat, A., Whitacre, D., Métraux, J. P., Mosinger, E. (1996b). Induction of resistance in barley against *Erysiphe graminis* f. sp. *hordei* by free cutin monomers. *Physiological and Molecular Plant Pathology,* 49, 103–120. doi: 10.1006/pmpp.1996.0043.

Second world seed conference. (2009). Responding to the challenges of a changing world: The role of new plant varieties and high quality seed in agriculture. 292. Retrieved from http://www.fao.org/docrep/014/am490e/am490e.pdf.

Seo P. J., Lee S. B., Suh M. C., Park M. J., Go Y. S., & Park C. M. (2011). The *MYB96* transcription factor regulates cuticular wax biosynthesis under drought conditions in *Arabidopsis. Plant Cell* 23, 1138–1152. https://doi.org/10.1105/tpc.111.083485

Serrano, M., Coluccia, F., Torres, M., Métraux, J.-P., Lionetti, V., Singh, P., & Juan Reina-Pinto, J. (2014). The cuticle and plant defense to pathogens. *Frontiers in Plant Science*, *5*, 274. https://doi.org/10.3389/fpls.2014.00274.

Shin, J. Y., Bui, D. C., Lee, Y., Nam, H., Jung, S., Fang, M., Kim, J. C., Lee, T., Kim, H., Choi, G. J., Son, H., & Lee, Y. W. (2017). Functional characterization of cytochrome P450 monooxygenases in the cereal head blight fungus *Fusarium graminearum. Environmental Microbiology*, *19*, 2053–2067. https://doi.org/ 10.11 11/1462-2920.13730

Singh, G., & Ashby, A. M. (1998). Cloning of the mating type loci from *Pyrenopeziza brassicae* reveals the presence of a novel mating type gene within a discomycete *MAT 1-2* locus encoding a putative metallothionein-like protein. *Molecular Microbiology*, *30*, 799–806. https://doi.org/10.1046/j.1365-2958.1998.01112.x

Snowdon, R. J., & Iniguez Luy, F. L. (2012). Potential to improve oilseed rape and canola breeding in the genomics era. *Plant Breeding, 131*, 351–360. doi: 10.1111/j.1439-0523.2012.01976.x

Solano de la Cruz, M.T., Adame-García, J., Gregorio-Jorge, J., Jiménez-Jacinto, V., Vega-Alvarado, L., Iglesias-Andreu, L.G., Escobar-Hernández, E.E., & Luna-Rodríguez, M. (2019). Increase in ribosomal proteins activity: Translational reprogramming in *Vanilla planifolia* Jacks. against *Fusarium* infection. *BioRxiv.* DOI: 10.1101/660860

Sork, V. L. (2016). Gene flow and natural selection shape spatial patterns of genes in tree populations: implications for evolutionary processes and applications. *Evolutionary Applications*, *9*, 291–310. https://doi.org/10.1111/eva.12316.

Sotelo, T., Lema, M., Soengas, P., Cartea, M. E., & Velasco, P. (2015). *In vitro* activity of glucosinolates and their degradation products against *Brassica. Pathogenic Bacteria and Fungi*. *81*, 432-440. https://doi.org/10.1128/AEM.03142-14

Stotz, H. U., Jikumaru, Y., Shimada, Y., Sasaki, E., Stingl, N., Mueller, M. J., & Kamiya, Y. (2011a). Jasmonate-dependent and COI1-independent defense responses against *Sclerotinia sclerotiorum* in *Arabidopsis thaliana*: auxin is part of COI1-independent defense signaling. *Plant & Cell Physiology*, *52*, 1941–1956. https://doi.org/10.1093/pcp/pcr127

Stotz, H. U., Sawada, Y., Shimada, Y., Hirai, M. Y., Sasaki, E., Krischke, M., Brown, P. D., Saito, K., & Kamiya, Y. (2011b). Role of camalexin, indole glucosinolates, and side chain modification of glucosinolate-derived isothiocyanates in defense of *Arabidopsis* against *Sclerotinia sclerotiorum*. *Plant Journal*, *67*, 81–93. https://doi.org/10.1111/j.1365-313X.2011.04578.x

Stotz, H. U., Mitrousia, G. K., de Wit, P. J. G. M., & Fitt, B. D. L. (2014). Effector-triggered defence against apoplastic fungal pathogens. *Trends in Plant Science*, 19, 491-500. https://doi.org/10.1016/j.tplants.2014.04.009

Sun, M., Wang, Y., Yang, D., Wei, C., Gao, L., Xia, T., *et al.* (2010). Reference genes for real- time fluorescence quantitative PCR in *Camellia sinensis*. *Chinese Bulletin Botany*, 45, 579–587. DOI: 10.3969/j.issn.1674-3466.2010.05.007

Sylvester-Bradley, R., Makepeace, R. & Broad, H. (1984). A code for stages of development in oilseed rape (*Brassica napus* L.). *Aspects of Applied Biology*, 6, 399-419.
Sylvester -Bradley R. (1985). A revised code for stages of development in oilseed rape (*Brassica napus* L.). Field trials methods and data handling. *Aspects of Applied Biology*, 10, 395–400.

Tanaka, T., Tanaka, H., Machida, C., Watanabe, M., & Machida, Y. (2004). A new method for rapid visualization of defects in leaf cuticle reveals five intrinsic patterns of surface defects in Arabidopsis. *Plant Journal*, *37*, 139–146. https://doi.org/10.1046/j.1365-313x.2003.01946.x

The Economist Group. (2018). Global Food Security Index 2018: Build resilience in the face of rising food-security risks. *The Economist Group*. Retrieved April 12, 2021, from http://foodsecurityindex.eiu.com/Country/Details#Germany.

The Daily Telegraph (2017). *Goodbye, olive oil: why we have all fallen in love with rapeseed*. Retrieved June 22, 2017, from *rapeseed*. Retrieved June 22, 2017, from http://www.telegraph.co.uk/foodanddrink/11710297/Goodbye olive oil, why we have all fallen in love with rapeseed.html.http://www.telegraph.co.uk /foodanddrink/11710297/Goodbye olive oil, why we have all fallen in love with rapeseed.html.

Thordal-Christensen, H., Zhang, Z., Wei, Y. and Collinge, B.D. (1997) Subcellular localization of H_2O_2 in plants. H_2O_2 accumulation in papillae and hypersensitive response during the barley-powdery mildew interaction. *Plant Journal*, 11, 1187-1194. https://doi.org/10.1046/j.1365-313X.1997.11061187.x

Town, C.D., Cheung, F., Maiti, R., *et al*. (2006). Comparative genomics of *Brassica oleracea* and *Arabidopsis thaliana* reveal gene loss, fragmentation, and dispersal after polyploidy. *Plant Cell* 18, 1348–1359. https://doi.org/10.1 105/tpc. 106.04 1665

Urbancsok, J., Bones, A. M., & Kissen, R. (2017). Glucosinolate-derived isothiocyanates inhibit *Arabidopsis* growth and the potency depends on their side chain structure. *International Journal of Molecular Sciences*, *18* (11). https://doi.org/10.3390/ijms18112372

Vandesompele, J., De Preter, K., Pattyn, F., Poppe, B., Van Roy, N., De Paepe, A. and Speleman, F. (2002) Accurate normalisation of real-time quantitative RT-PCR data by geometric averaging of multiple internal control genes. *Genome Biology,* 3. https://doi.org/10.1186/gb-2002-3-7-research0034

Vossen, J. H., Abd-El-Haliem, A., Fradin, E. F., van den Berg, G. C., Ekengren, S. K., Meijer, H. J., Seifi, A., Bai, Y., ten Have, A., Munnik, T., Thomma, B. P., & Joosten, M. H. (2010). Identification of tomato phosphatidylinositol-specific phospholipase-C (PI-PLC) family members and the role of *PLC4* and *PLC6* in HR and disease resistance. *Plant Journal*, *62*, 224–239. https://doi.org/10.1111/j.1365-313X.2010 .04136.x

Wagner, P., Furstner, R., Barthlott, Neinhuis, C., (2003). Quantitative assessment to the structural basis of water repellency in natural and technical surfaces. J*ournal of Experimental Botany* 54, 1295–1303. https://doi.org/10.1093/jxb/erg127

Wang, X., Wang, H., Wang, J., Sun, R., Wu, J., Liu, S., Bai, Y., Mun, J. H., Bancroft, I., Cheng, F., Huang, S., Li, X., Hua, W., Wang, J., Wang, X., Freeling, M., Pires, J. C., Paterson, A. H., Chalhoub, B., Wang, B., *et al*. (2011). *Brassica rapa* Genome Sequencing Project Consortium. The genome of the mesopolyploid crop species *Brassica rapa*. *Nature Genetics*, *43*, 1035–1039.

Wang, W., Liu, X., Gai, X., Ren, J., Liu, X., Cai, Y., *et al*. (2015). *Cucumis sativus* L. WAX2 plays a pivotal role in wax biosynthesis, influencing pollen fertility and plant biotic and abiotic stress responses. *Plant Cell Physiology,* 56, 1339–1354. https://doi.org/10.1371/journal.pone.0175863

Wang, M. L., Li, Q. H., Xin, H. H., Chen, X., Zhu, X. J., & Li, X. H. (2017). Reliable reference genes for normalization of gene expression data in tea plants (*Camellia sinensis*) exposed to metal stresses. *PloS One*, *12*, e0175863. https://doi.org/ 10. 1371/journal.pone.0175863

West, J. S., Kharbanda, P. D., Barbetti, M. J., & Fitt, B. D. L. (2001). Epidemiology and management of *Leptosphaeria maculans* (phoma stem canker) in Australia, Canada and Europe. *Plant Pathology*, *50*, 10–27. https://doi.org/10.1046/j.1365-3059.2001.00546.x

West, J.S. (2021). AHDB porject report no: 632. Provision of oilseed rape decision support systems to the UK Arable Industry (Phoma and light leaf spot forecasts) Agriculture and horticulture development board. 12pp.

Woloshen, V., Huang, S., & Li, X. (2011). RNA-binding proteins in plant immunity. *Journal of Pathogens*, *2011*, 278697. https://doi.org/10.4061/2011/278697

Woloshuk, C. P., and Kolattukudy, P. E. (1986). Mechanism by which contact with plant cuticle triggers cutinase gene-expression in the spores of *Fusarium solani* f.s*p.pisi. Proceedings of National Academy of Science. U.S.A.* 83, 1704–1708. doi:10.1073/pnas.83.6.1704.

Yamada-Onodera, K., Mukumoto, H., Katsuyama, Y., & Tani, Y. (2002). Degradation of long-chain alkanes by a polyethylene-degrading fungus, *Penicillium simplicissimum* YK. *Enzyme and Microbial Technology, 30*, 828-831. https:// doi. org /10.1016/S0141-0229(02)00065-0

Yamagishi, H., Landgren, M., Forsberg, J., & Glimelius, K. (2002). Production of asymmetric hybrids between *Arabidopsis thaliana* and *Brassica napus* utilizing an efficient protoplast culture system. *Theoretical and Applied Genetics*, *104*, 959–964. https://doi.org/10.1007/s00122-002-0881-9

Yamamoto, M., & Nishio, T. (2014). Commonalities and differences between *Brassica* and *Arabidopsis* self-incompatibility. *Horticulture Research*, *1*, 14054. https:// doi. org/10.1038/hortres.2014.54

Yan, Q., Si, J., Cui, X. *et al.* (2019). The soybean cinnamate 4-hydroxylase gene *GmC4H1* contributes positively to plant defense via increasing lignin content. *Plant Growth Regul*ation, 88, 139–149. https://doi.org/10.1007/s10725-019-00494-2

Yang, J., Liu, D., Wang, X., Ji, C., Cheng, F., Liu, B., Hu, Z., Chen, S., Pental, D., Ju, Y., Yao, P., Li, X., Xie, K., Zhang, J., Wang, J., Liu, F., Ma, W., Shopan, J., Zheng, H., Mackenzie, S.A., Zhang, M., *et al*. (2016). The genome sequence of allopolyploid *Brassica juncea* and analysis of differential homoeolog gene expression influencing selection. *Nature Genetics, 48*, 1225-1232. https://doi.org/10.1038/ng.3657

Yeats, T. H., & Rose, J. K. C. (2013). Topical review on cuticle synthesis and function, the formation and function of plant cuticles 1. *Plant Physiology*, *163*, 5–20. https://doi.org/10.1104/pp.113.222737.

Yong, M., Yu, J., Pan, X., Yu, M., Cao, H., Song, T., Qi, Z., Du, Y., Zhang, R., Yin, X., Liu, W., & Liu, Y. (2020). Two mating-type genes MAT1-1-1 and MAT1-1-2 with significant functions in conidiation, stress response, sexual development, and pathogenicity of rice false smut fungus Villosiclava virens. *Current Genetics*, *66*, 989–1002. https://doi.org/10.1007/s00294-020-01085-9

Zheng, Z., Qualley, A., Fan, B., Dudareva, N., & Chen, Z. (2009). An important role of a BAHD acyl transferase-like protein in plant innate immunity. *Plant Journal*, *57*, 1040–1053. https://doi.org/10.1111/j.1365-313X.2008.03747.x

Ziv, C., Zhao, Z., Gao, Y. G., & Xia, Y. (2018). Multifunctional roles of plant cuticle during plant-pathogen interactions. *Frontiers in Plant Science*, *9*, 1088. https://doi.org/10.3389/fpls.2018.01088

Appendices

Appendix 1: Key stages of oilseed rape growth (Sylvester-Bradley et al. 1984; Sylvester-Bradley, 1985).

Developmental stages in plant	Growth stage expressed in decimals	Description
Germination and emergence	0,0	Dry seed
Leaf production	1,0	Both cotyledons unfolded and green
	1,1	First true leaf emerged
	1,2	Second true leaf emerged
	1,3 etc.	Third true leaf emerged
Stem extension	2,0	No internodes (rosette)
	2,5	About five internodes
Flower bud development	3,0	Only leaf buds present
	3,1	Flower buds present but enclosed by leaves
	3,3	Flower buds visible from above ('green bud')
	3,5	Flower buds raised above leaves
	3,6	First flower stalks extending
	3,7	First flower buds yellow ('yellow bud')
Flowering	4,0	First flower opened
	4,1	10% all buds opened
	4,3	30% all buds opened
	4,5	50% all buds opened
Pod development	5,3	30% potential pods
	5,5	50% potential pods
	5,7	70% potential pods
	5,9	All potential pods
Seed development	6,1	Seeds expanding
	6,2	Most seeds translucent but full size
	6,3	Most seed green.
	6,4	Most seed green-brown mottled
	6,5	Most seeds brown
	6,6	Most seed dark brown
	6,7	Most seed black but soft
	6,8	Most seed black and hard
	6,9	All seeds black and hard
Leaf senescence	7,0	
Stem senescence	8,1	Most stem green
	8,5	Half stem green
	8,9	Little stem green
Pod senescence	9,1	Most pods green
	9,5	Half pods green
	9,9	Few pods green

Appendix 2: Glasshouse experiments with randomised replicated α-design. Experiments 1, 2 and 3.

These experiments were done to score LLS severity on *B. napus* cvs/lines to complete the screening of 195 cvs/lines for quantitative disease resistance (QDR) to *Pyrenopeziza brassicae*. Results are published in Fell *et al.*, (2023). (Chapter 4). Cultivars Cabriolet, Imola, Tapidor and Temple were used as reference cultivars.

Randomized Layout

REPLICATION 1			
Block 1	5	15	20
Block 2	19	14	4
Block 3	23	8	10
Block 4	7	9	22
Block 5	17	2	12
Block 6	6	16	21
Block 7	11	1	24
Block 8	18	3	13

REPLICATION 2			
Block 1	3	11	19
Block 2	24	8	16
Block 3	23	15	7
Block 4	4	20	12
Block 5	9	1	17
Block 6	22	6	14
Block 7	21	13	5
Block 8	10	18	2

REPLICATION 3			
Block 1	22	1	13
Block 2	3	15	24
Block 3	6	10	19
Block 4	5	18	9
Block 5	23	2	14
Block 6	20	7	11
Block 7	21	12	8
Block 8	4	17	16

REPLICATION 4			
Block 1	1	14	18
Block 2	7	24	12
Block 3	13	17	8
Block 4	19	15	2
Block 5	4	21	9
Block 6	6	23	11
Block 7	3	20	16
Block 8	5	10	22

REPLICATION 5			
Block 1	11	21	2
Block 2	1	10	20
Block 3	12	3	22
Block 4	24	5	14
Block 5	6	17	15
Block 6	16	7	18
Block 7	4	13	23
Block 8	9	19	8

	Experiment 1		Experiment 2		Experiment 3
1	**Cabriolet**	1	**Cabriolet**	1	**Cabriolet**
2	**Imola**	2	**Imola**	2	**Imola**
3	Moana	3	Norde	3	Moana
4	Mohican	4	OASE	4	Ragged Jack
5	Musette	5	Orlando	5	Smart
6	Mytnickij	6	Pacific	6	Sobotkowski
7	Nemerschanskij 1	7	Panter	7	Sollux
8	NK Bravour	8	Phil	8	SWGospel
9	Odin	9	Pirola	9	SWU Chinese 1
10	Omega	10	Pollen	10	SWU Chinese 2
11	Pobeda	11	Prince	11	SWU Chinese 3
12	Ragged Jack	12	Rapid	12	SWU Chinese 5
13	Rucabo	13	Remy	13	SWU Chinese 8
14	SURPASS400-024DH	14	RESYN-H048	14	SWU Chinese 9
15	Svalsfos Gulle	15	Rodeo	15	**Tapidor**
16	TANTAL	16	Roxet	16	**Temple**
17	**Tapidor**	17	Sansibar	17	V8
18	**Temple**	18	Sarepta	18	Vige DH
19	Tribune	19	Savannah	19	Viking
20	Tribute	20	SLAPSKA, SLAPY	20	Vinnickij 15/59
21	VIGE DH1	21	SLM 0413	21	WILD ACCESSION
22	WEIHENSTEPHANER	22	SLM 0512	22	Zenith
23	Willi	23	**Tapidor**	23	Zephir
24	Zairai Chousenshu	24	**Temple**	24	Pollen

Appendix 3: Glasshouse experiment 1 with randomised replicated α-design done at Rothamsted Research, Harpenden, UK (Chapter 4).

Glass house experiment 1 done at Rothamsted Research (a) randomised replicated α-design 1 x 5 replicates ready to be inoculated, (b) Spray inoculated cultivar Surpass 400, (c) Inoculated *B. napus* cvs/lines covered with polyethylene sheet to increase humidity, (d) Inoculated *B. napus* plants ready for sampling.

Appendix 4: Glasshouse experiments with randomised replicated α-design. Experiments 4 and 5

Randomized layout

Cultivars/lines of *B. napus* and *B. rapa*

REPLICATION 1			
Block 1	5	14	19
Block 2	18	13	4
Block 3	22	8	17
Block 4	7	9	11
Block 5	16	2	21
Block 6	20	6	15
Block 7	10	1	12
Block 8	23	3	

REPLICATION 2			
Block 1	3	21	19
Block 2	20	8	16
Block 3	7	1	23
Block 4	4	2	12
Block 5	9	15	17
Block 6	22	11	14
Block 7	5	13	6
Block 8		18	10

REPLICATION 3			
Block 1	23	1	
Block 2	3	15	10
Block 3	6	21	19
Block 4	5	18	9
Block 5	13	2	14
Block 6	16	7	20
Block 7	21	12	8
Block 8	4	17	22

REPLICATION 4			
Block 1		14	21
Block 2	7	23	12
Block 3	2	17	8
Block 4	19	15	22
Block 5	4	18	9
Block 6	6	13	11
Block 7	3	20	16
Block 8	5	10	1

REPLICATION 5			
Block 1	11	21	2
Block 2	1	10	5
Block 3	12	3	22
Block 4	20		14
Block 5	6	17	15
Block 6	16	7	18
Block 7	4	13	23
Block 8	9	19	8

#	Cultivar/line
1	Cabriolet
2	Sansibar
3	Moana
4	Laser
5	Ambassador
6	Aurelia
7	Nikita
8	Barbados
9	Lipid
10	Leopard
11	RV31
12	Yudal
13	Zenith
14	R-O-18
15	SWU Chinese 1
16	Cubs Root
17	Posh
18	Dwarf Essex
19	Glossy 1-795
20	Glossy 2-1864
21	Nonglaucous 1-2051
22	Nonglaucous 2-1914
23	WT-R-O-18

Appendix 5: Amplification curve generated for *Actin* TaqMan multiplex primer using cDNA serial dilutions of 10-fold as template.
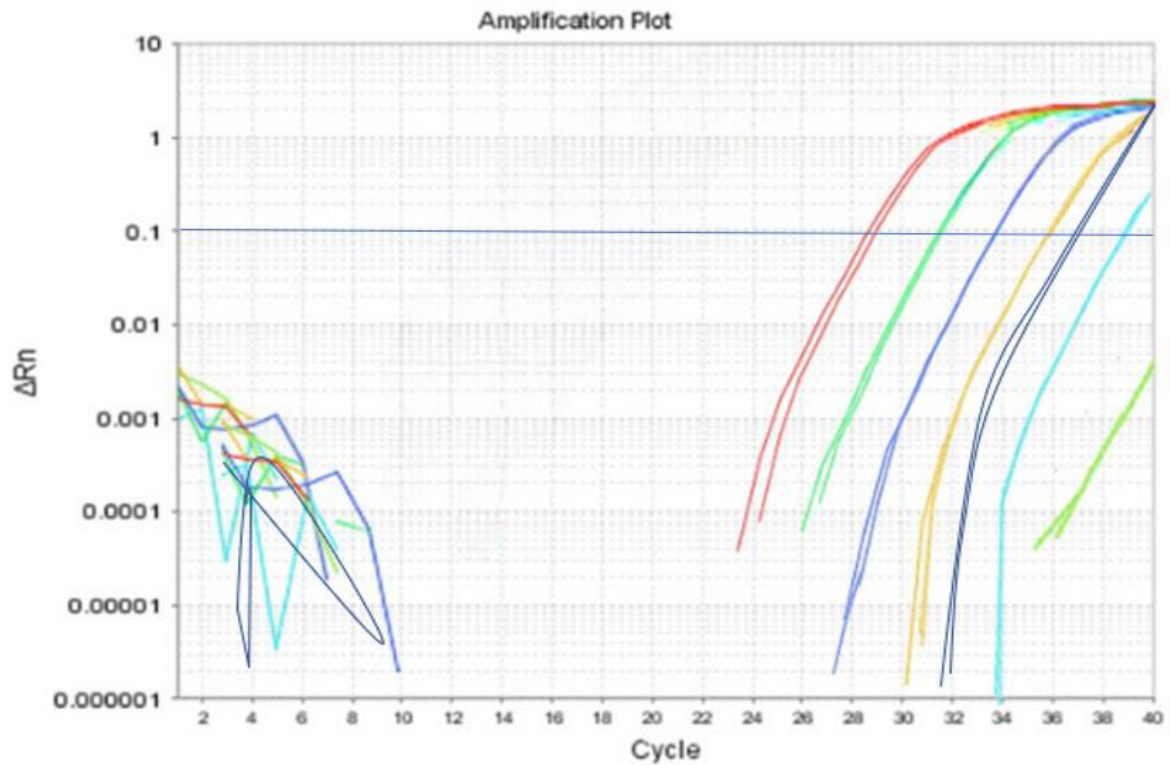
Amplification plots of qPCR generated with Applied Biosystems 7500 real time PCR systems, UK for *Actin* using a cDNA pool (control and inoculated leaf cDNA samples) as a template. Seven 10-fold dilutions were used. X axis: qPCR cycle number and Y axis: delta Rn/normalized fluorescence value subtracted by baseline.

.

Appendix 6: Standard curve generated for reference gene *Actin* TaqMan primer assay

Standard Curve

Slope = -3.11

$R^2 = 0.999$

E = 101.9%
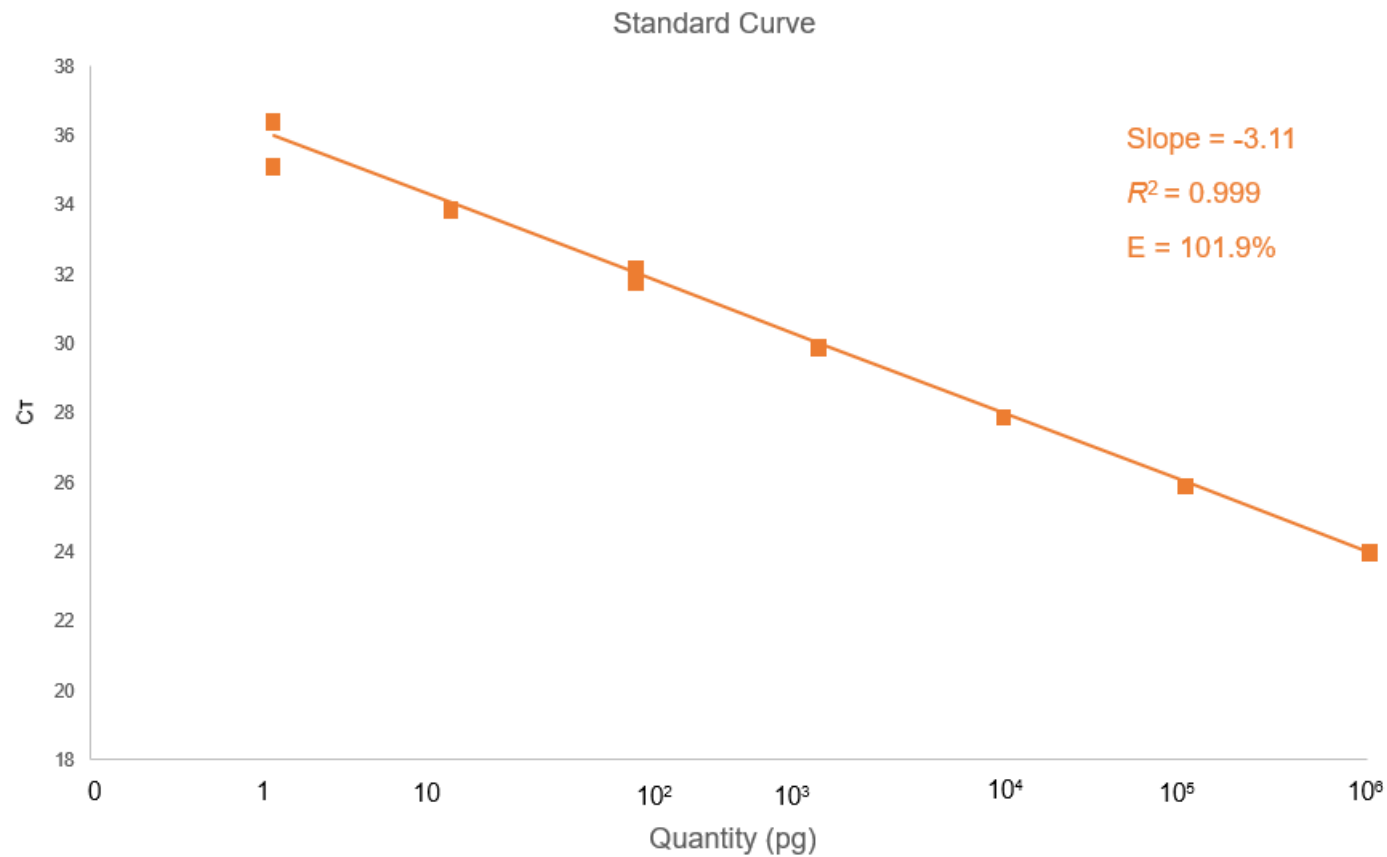
Standard curve of *Actin* using a cDNA pool (control and inoculated leaf cDNA samples) as a template. Seven 10-fold dilutions were used. Graph shows threshold cycle (Ct) on the y-axis and quantity of cDNA on the x-axis. Slope, correlation coefficient value (R^2) and efficiency (E) are used to provide information about the performance of the reaction.

Appendix 7: Gene expression markers (GEMs) area under gene expression curve (AUGEC) Tukey HSD result

Tukey HSD pair-wise comparison to assess the significant variation in expression of GEMs between genotypes using an AUGEC linear model considering *Actin* AUGEC as co-variant. *** *P*-value ≤ 0.001; ** *P*-value ≤ 0.01; * *P*-value ≤ 0.05

GEM	Significant cultivar pairs		*P* value
PR1	Cubs Root-Cabriolet		0.002028
	POSH-Cabriolet		0.002569
	Laser-Cubs Root		0.019999
	Sansibar-Cubs Root		0.001786
	POSH-Laser		0.025719
	Sansibar-POSH		0.002260
HXXXD- type acyl transferase	Cubs Root- Cabriolet		0.000011
	Laser-Cabriolet		0.000011
	POSH-Cabriolet		0.000014
	SWU Chinese 1-Cabriolet		0.000009
	Sansibar-Cubs Root		0.001270
	Sansibar-Laser		0.001338
	Sansibar-POSH		0.002008
	SWU Chinese 1-Sansibar		0.000834
Cinnamate-4-hydroxylase	Laser-Cabriolet		0.055819
	POSH-Laser		0.028967
PLC4	POSH-Cabriolet		0.000000
	Laser-Cubs Root		0.004218
	POSH-Cubs Root		0.000000
	Sansibar-Cubs Root		0.017607
	POSH-Laser		0.000000
	SWU Chinese 1-Laser		0.021096
	Sansibar-POSH		0.000000
	SWU Chinese 1-POSH		0.000000
40s ribosomal sub-unit protein S24e	Laser-Cabriolet		0.007288
	POSH-Cabriolet		0.003292
	Sansibar-Cabriolet		0.002156
	SWU Chinese 1-Cabriolet		0.001731
	Laser-Cubs Root		0.084164
	Sansibar-Cubs Root		0.000444
	POSH-Laser		0.000104
	Sansibar-Laser		0.000081
	SWU Chinese 1-Sansibar		0.000037
β-adaptin	Laser-Cabriolet		0.045445
	SWU Chinese 1-Cabriolet		0.072123
Universal stress protein	Cubs Root-Cabriolet		0.000090
	Laser-Cabriolet		0.012656
	POSH-Cabriolet		0.000008
	SWU Chinese 1-Cabriolet		0.000592
	Laser-Cubs Root		0.001661
	Sansibar-Cubs Root		0.000101
	POSH-Laser		0.000063
	Sansibar-Laser		0.015898
	SWU Chinese 1-Laser		0.039870
	Sansibar-POSH		0.000008
	SWU Chinese 1-Sansibar		0.000686

Appendix 8: Taqman multiplex qPCR assays names and amplicon context sequences. Details supplied by Thermo Fisher Scientific, UK. Four separate dyes (ABY, VIC, JUN, FAM) were given to assays aimed to do fourplex.

Vendor assay name	Gene name Ensembl Plants	Gene description	Amplicon context sequence	Assay number	Dye
BnaA04g20860D	BnaA04g20860D	Acyl transferase	CGATTGCGGTTCGAGGCGGA	66176946_7706976 #2	JUN
BnaC04g14330D	BnaC04g14330D	Cinnamate 4 hydroxylase (*C4H*)	AGCTTGCTTTGGATCTCAGG	66176946_7706976 #7	FAM
BnaA02g07530D	BnaA02g07530D	Phosphatidylinositol-specific phospholipase C4 (*PLC4)*	TCAGAGTCACCGAGCCAGAT	66176946_7706976 #4	ABY
BnaC07g27610D	BnaC07g27610D	40S ribosomal protein S24	AGCTTATTAGGTTAAGCTGT	66176946_7706976 #4	VIC
BnaC07g38240D	BnaC07g38240D	*β-adaptin*	GCAGTGGAGGACCTGACGGA	66176946_7706976 #1	JUN
BnaA10g05830D	BnaA10g05830D	*Polyadenylate-binding protein 1*	ACGTAGGAGAAGAAGGCGCT	66176946_7706976 #8	FAM
BnaC08g24910D	BnaC08g24910D	Universal stress protein (*USP*)	GGAATCGCCATGGACTTCTC	66176946_7706976 #5	ABY
PR1_*B. napus*	BnaC03g45470D	*PR1*	TATAACCACGATTCGAACAC	66176946_7706976 #6	ABY

Appendix 9: *Brassica napus* candidate genes for quantitative resistance against *Pyrenopeziza brassicae* and their corresponding homologs in *B. rapa* along with the TILLING mutant names.

Candidate gene in *B. napus*	Gene description	Homolog in *B. rapa*	TILLING mutant
BnaC04g14330D	Cinnamate hydroxylase (*C4H*)	*Bra018311*	ji30317a
BnaC04g14330D	Cinnamate hydroxylase (*C4H*)	*Bra018311*	ji30819a
BnaC07g38240D	Beta adaptin	*Bra019302*	ji30010b
BnaC07g38240D	Beta adaptin	*Bra019302*	ji320204a
BnaA05g34100D	AKIN10 SNF1 kinase homolog 10	*Bra039146*	ji31647b

Appendix 10: Single nucleotide polymorphisms (SNP) details submitted for Kompetitive Allele Specific PCR (KASP) primer design to LGC Genomics UK.

Section (A) shows the mutation details and gene ID obtained from John Innes Centre, Norwich, UK. Using the Ensemble Plant BLAST, the sequences were assessed and BLAST forward sequences were done for those genes on reverse strand. 52 bp upstream and downstream were chosen from the single nucleotide polymorphism (SNP). Homologous gene sequences were obtained from gene tree and aligned using MEGA. Finally, the anchoring was done using the KASP anchoring guideline from LGC. Section (B) shows the SNP details submitted to LGC, UK for KASP primer synthesis.

(A)

Mutation Request

Species:	Brassica rapa R-0-18 (RS)
Gene:	Bra018311
Gene Mutation:	stop_gained:Caa/Taa:p.Gln263*/c.787C>T
Plant Line:	ji30317-a
Is Heterozygous:	Yes
WT	AGAAATTAAAACAGG T AAATCGCGAGTTGGA

Mutation Request

Species:	Brassica rapa R-0-18 (RS)
Gene:	Bra018311
Gene Mutation:	stop_gained:tgG/tgA:p.Trp46*/c.138G>A
Plant Line:	ji30819-a
Is Heterozygous:	Yes
WT	AATCTTCGGAAACTG A CTCCAAGTCGGAGAC

Mutation Request

Species:	Brassica rapa R-0-18 (RS)
Gene:	Bra019302
Gene Mutation:	stop_gained:tgG/tgA:p.Trp438*/c.1314G>A
Plant Line:	ji30010-b
Is Heterozygous:	Yes
WT	TCGCTTCTGGTTCAT T CAATGTGTCTAGACT

Mutation Request

Species:	Brassica rapa R-0-18 (RS)
Gene:	Bra039146
Gene Mutation:	stop_gained:Cag/Tag:p.Gln395*/c.1183C>T
Plant Line:	ji31647-b
Is Heterozygous:	Yes
WT	AAGGGATCAAGACCT A AAGTCCAAGAGCCCA

Mutation Request

Species:	Brassica rapa R-0-18 (RS)
Gene:	Bra019302
Gene Mutation:	stop_gained:Caa/Taa:p.Gln310*/c.928C>T
Plant Line:	ji32024-a
Is Heterozygous:	Yes
WT	TAGTGGGCCTTTTTT A GACAATAAGGTTAAT

(B)

1. Bra018311 (ji30317-a):
GAGTTTGTATTATTCTTGTTTCTTGAAACTGACATTGAGAAATTAAAACAGG[T/C]
AAATCGCGAGTTCGAAGCCTACAGGAAGCGAAGGATTGAAATGCGCAATTGA

Amino acid C in wild type is replaced with T in mutant

2. Bra018311 (ji30819-a):
AGAAGCTGAAGCTCCCTCCCGGTCCTATGCCGATTCCAATCTTCGGAAACTG[A/G]
CTCCAAGTCGGAGACGATCTAAACCACCGTAACCTCGTCGACTACGCTAAGA

3. Bra019302 (ji30010-b):
GTGCAGGTATGAGTCCATAATTGCAACACTCTGTGAGAGTCTAGACACATTG[A/G]
ATGAACCAGAAGCGAAGGTAATAAAATTTGTTTATT
TGCTGGTGTAAAATAG

4. Bra039146 (ji31647-b):
AGTTGGCTTGAGATCTCAGTACCCTGTTGAGAGAAAATGGGCTCTTGGACTT[T/C]
AGGTCTTGATCCCCTTTTGTTCTCTCTTAATTTATACTTTATAATGATATCA

5. Bra019302 (ji32024-a):
TGCAGAACCTGAGATCCAATATGTTGCACTTCGTAACATTAACCTTATTGTC[T/C]
AAAAAAGGCCCACTATTCTTGCCCATGAAATCAAGGTAGTTTGGTTCTGTTT

Appendix 11: Wiesner's reaction/phloroglucinol-HCl
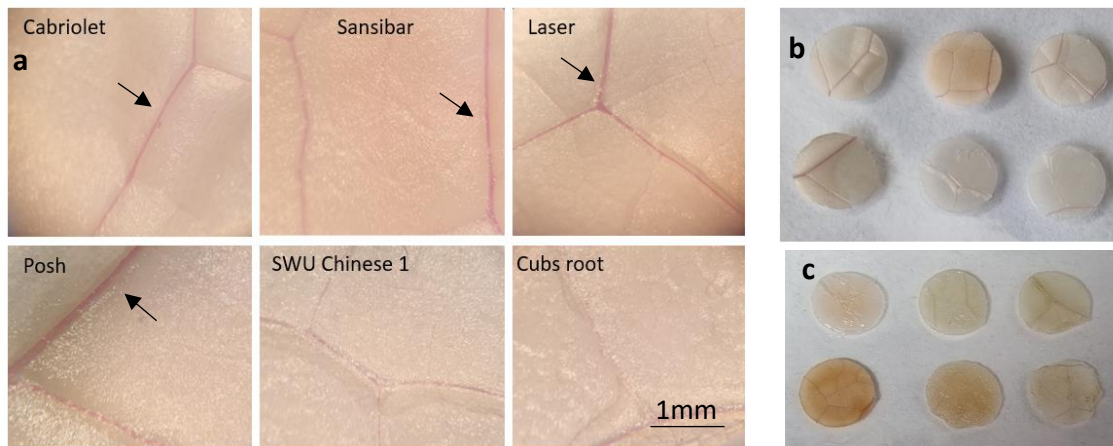
Wiesner's reaction/phloroglucinol-HCl: Spot inoculated *B. napus* leaf discs were immersed in a mixture of 10% phloroglucinol and 95% ethanol for 5 min. Leaf discs were then dipped in pure HCl, washed off, mounted in a droplet of 70% glycerol and visualised under a 3x GXM-XTC3A1 stereo microscope (Becker *et al.*, 2017; Mitra & Loqué, 2014). No variation in lignification staining was observed between mock inoculated (0 dpi) and 8dpi *Brassica napus* susceptible cultivars (Cabriolet, Sansibar, Laser) and resistant cvs/lines (POSH, SWU Chinese 1, Cubs Root) with *P. brassicae*. Arrows shows the vascular bundles stained. (a): stained leaf sections under light microscope. (b): mock control and (c): 8dpi *B. napus* leaf discs where top from left are Cabriolet, Sansibar, Laser and bottom are POSH, SWU Chinese 1, Cubs Root.

Appendix 12: Glasshouse experiments 8 and 9 randomised replicated α-designs to screen *Brassica rapa* and *Brassica napus* for resistance against *Pyrenopeziza brassicae* and cuticle study (Chapter 5)

Randomized layout

REPLICATION 1			
Block 1	6	9	5
Block 2	1		7
Block 3	11	4	12
Block 4		13	2
Block 5	3	10	8

REPLICATION 2			
Block 1	8	5	2
Block 2	12	1	11
Block 3	6	7	
Block 4	10	3	13
Block 5		9	4

REPLICATION 3			
Block 1	4	11	3
Block 2	13	8	5
Block 3	9		12
Block 4	6	1	
Block 5	2	10	7

REPLICATION 4			
Block 1	4	13	
Block 2	6	3	11
Block 3	8	1	
Block 4	12	10	9
Block 5	2	7	5

REPLICATION 5			
Block 1	2	10	6
Block 2	9	5	
Block 3	7	13	1
Block 4	11	3	8
Block 5	4	12	

REPLICATION 6			
Block 1	7	5	
Block 2	9	2	8
Block 3	1	12	3
Block 4	13		10
Block 5	11	4	6

1	Cabriolet
2	Sansibar
3	Moana
4	Laser
5	WT R-0-18
6	SWU Chinese 1
7	Cubs Root
8	POSH
9	Dwarf Essex
10	Glossy 1-795
11	Glossy 2-1864
12	Nonglaucous 1-2051
13	Nonglaucous 2-1914

Appendix 13: Weather information (temperature[2]) during two glasshouse experiments (8 and 9) to screen *Brassica rapa* and *Brassica napus* for resistance against *Pyrenopeziza brassicae* and to quantify cuticular wax and cutin. Information was obtained from https://www.worldweatheronline.com/luton-weather-history/bedfordshire/gb.aspx.

Environmental conditions during glasshouse experiments for susceptibililty of *Brassica rapa and B. napus* to *Pyrenopeziza brassicae*.

Location	Experiment	Germination[1]			Transplanting[1]			Inoculation[1]			Sampling[1]		
Rothamsted	8	29th December 2020			2nd January 2021			24th January 2021			17th February 2021		
		Max °C	Avg °C	Min °C	Max °C	Avg °C	Min °C	Max °C	Avg °C	Min °C	Max °C	Avg °C	Min °C
		4	2	1	2	1	0	3	1	0	9	6	2
Rothamsted	9	2nd January 2021			7th January 2021			28th January 2021			21st February 2021		
		Max °C	Avg °C	Min °C	Max °C	Avg °C	Min °C	Max °C	Avg °C	Min °C	Max °C	Avg °C	Min °C
		2	1	0	2	0	-4	11	7.3	6	12	10.5	9

[1] Germination, transplanting, inoculation and sampling refers to the *B. rapa* and *B. napus* seedlings.

[2] Information about temperature was obtained from United Kingdom Weather History in Luton, England

51.88 °N, **0.36** °W

Appendix 14: Cutinase gene expression in *B. rapa* and *B. napus* cultivars/lines at different time points
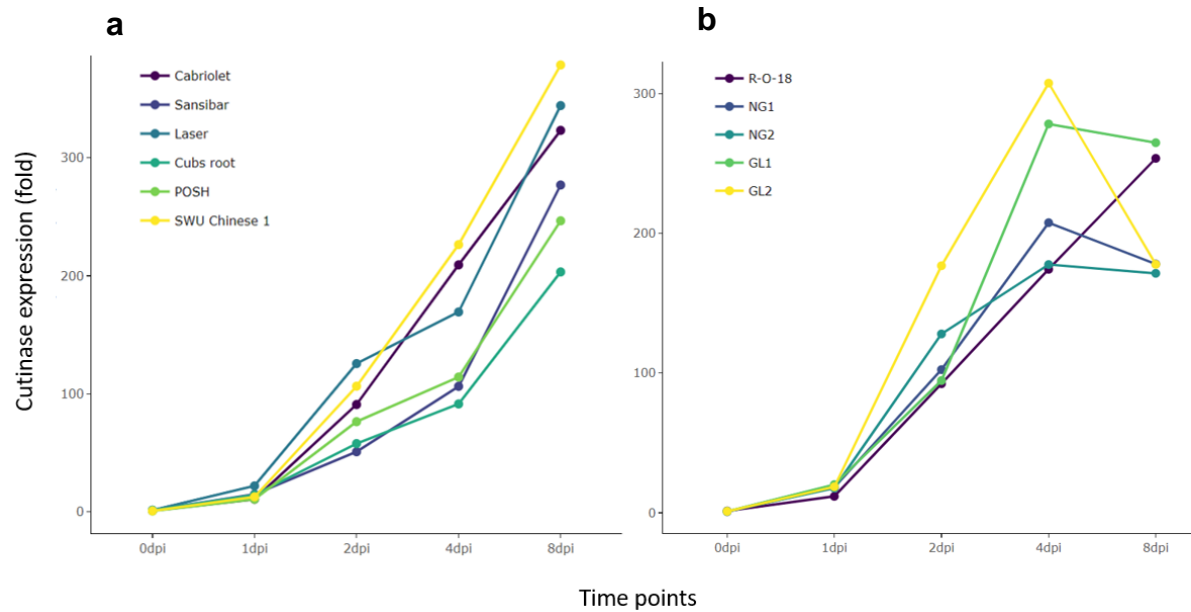
Cutinase expression in *B. napus* cvs/lines (a) and *B. rapa* (b) at 0dpi (control), 1dpi, 2dpi, 4dpi and 8dpi.

Appendix 15: Individual secondary (2^0) alcohol compounds identified and quantified from *Brassica rapa* wax mutants spray inoculated with *Pyrenopeziza rassicae* (28 dpi) using GCMS.
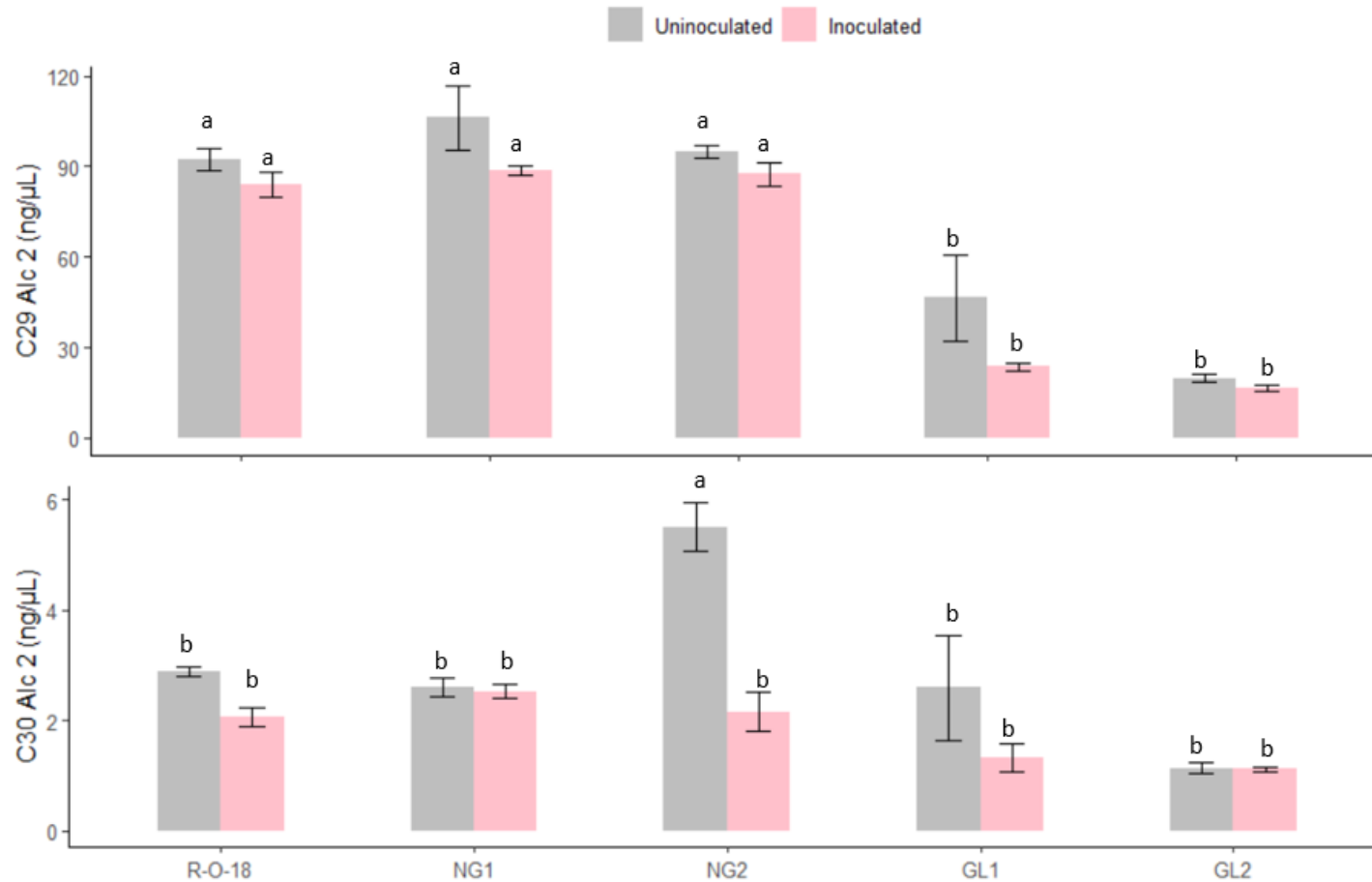
Individual compounds of 2^0 alcohol identified and quantified from *Brassica rapa* wax mutants spray inoculated with *Pyrenopeziza brassicae* (28 dpi) using GCMS. Error bars represent standard deviations of three replicates. Columns with the same letters are not significantly different (Wilcoxon, Anova and TukeyHSD).

Appendix 16: Individual primary alcohol (1⁰) compounds identified and quantified from *Brassica rapa* wax mutants spray inoculated with *Pyrenopeziza brassicae* (28 dpi) using GCMS.
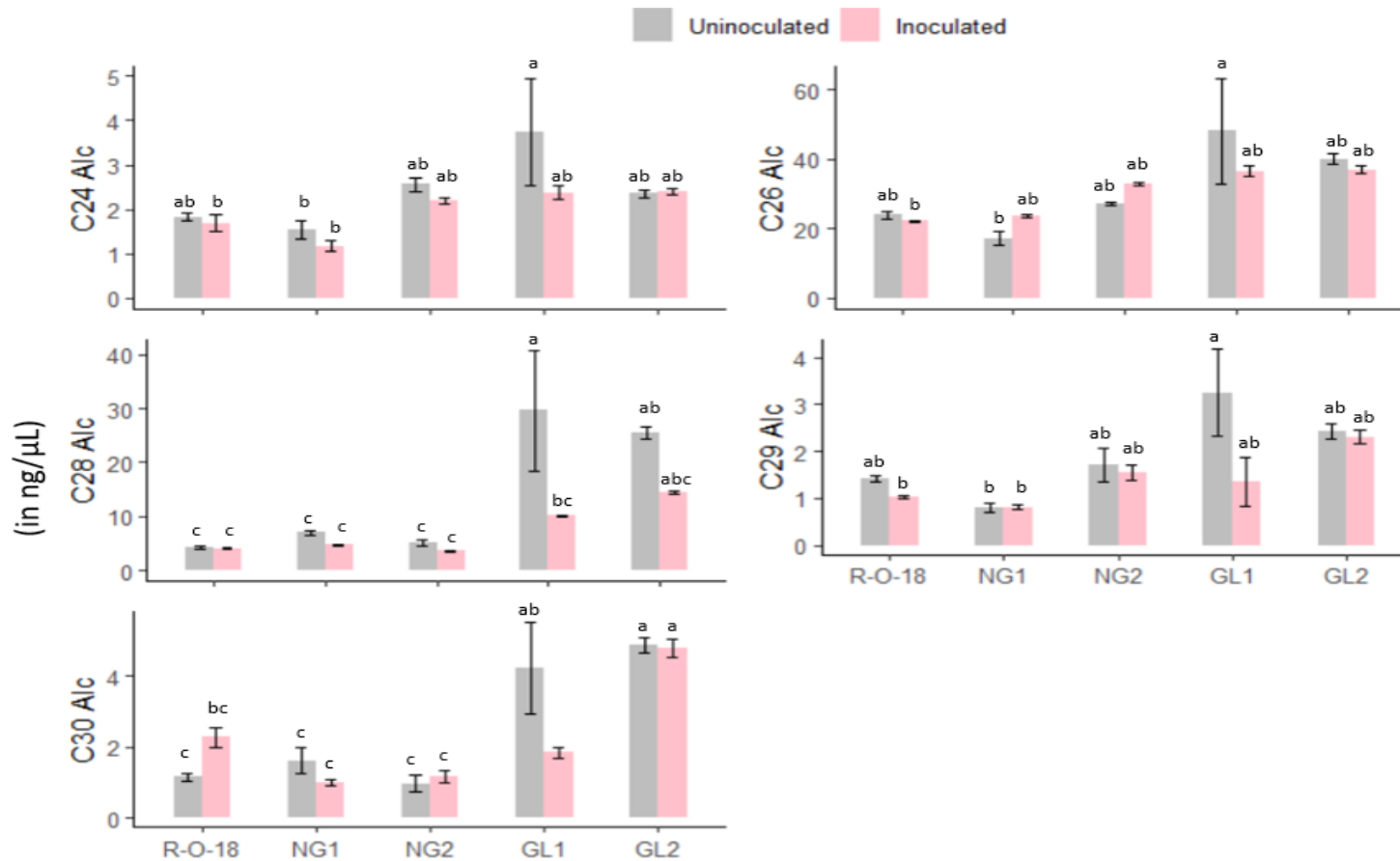
Individual compounds of 10 alcohol identified and quantified from *Brassica rapa* wax mutants spray inoculated with *Pyrenopeziza brassicae* (28 dpi) using GCMS. Error bars represent standard deviations of three replicates. Columns with the same letters are not significantly different (Wilcoxon, Anova and TukeyHSD).

Appendix 17: Individual wax ester compounds identified and quantified from *B. rapa* wax mutants spray inoculated with *Pyrenopeziza brassicae* (28 dpi) using GCMS.
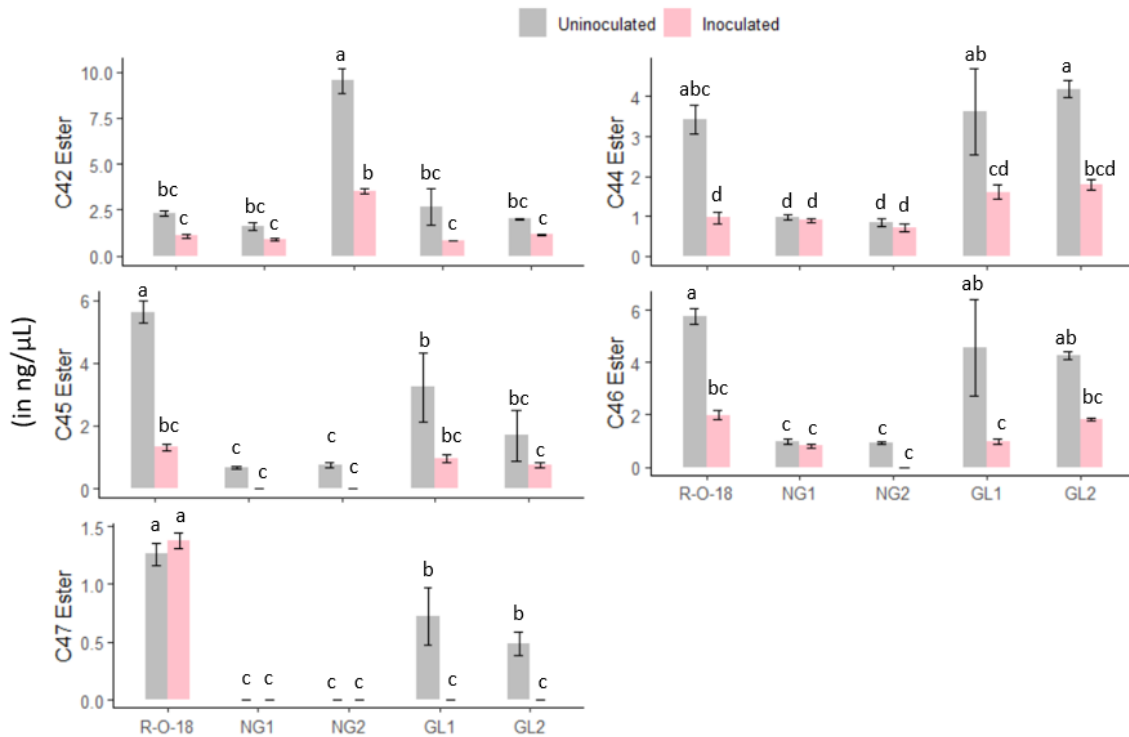
Individual compounds of wax ester identified and quantified from *Brassica rapa* wax mutants spray inoculated with *Pyrenopeziza brassicae* (28 dpi) using GCMS. Error bars represent standard deviations of three replicates. Columns with the same letters are not significantly different (Wilcoxon, Anova and TukeyHSD).

Appendix 18: Branched C27 alcohol and an unknown compound quantified from *Brassica napus* lines/cvs spray inoculated with *Pyrenopeziza brassicae* (28 dpi) using GCMS.
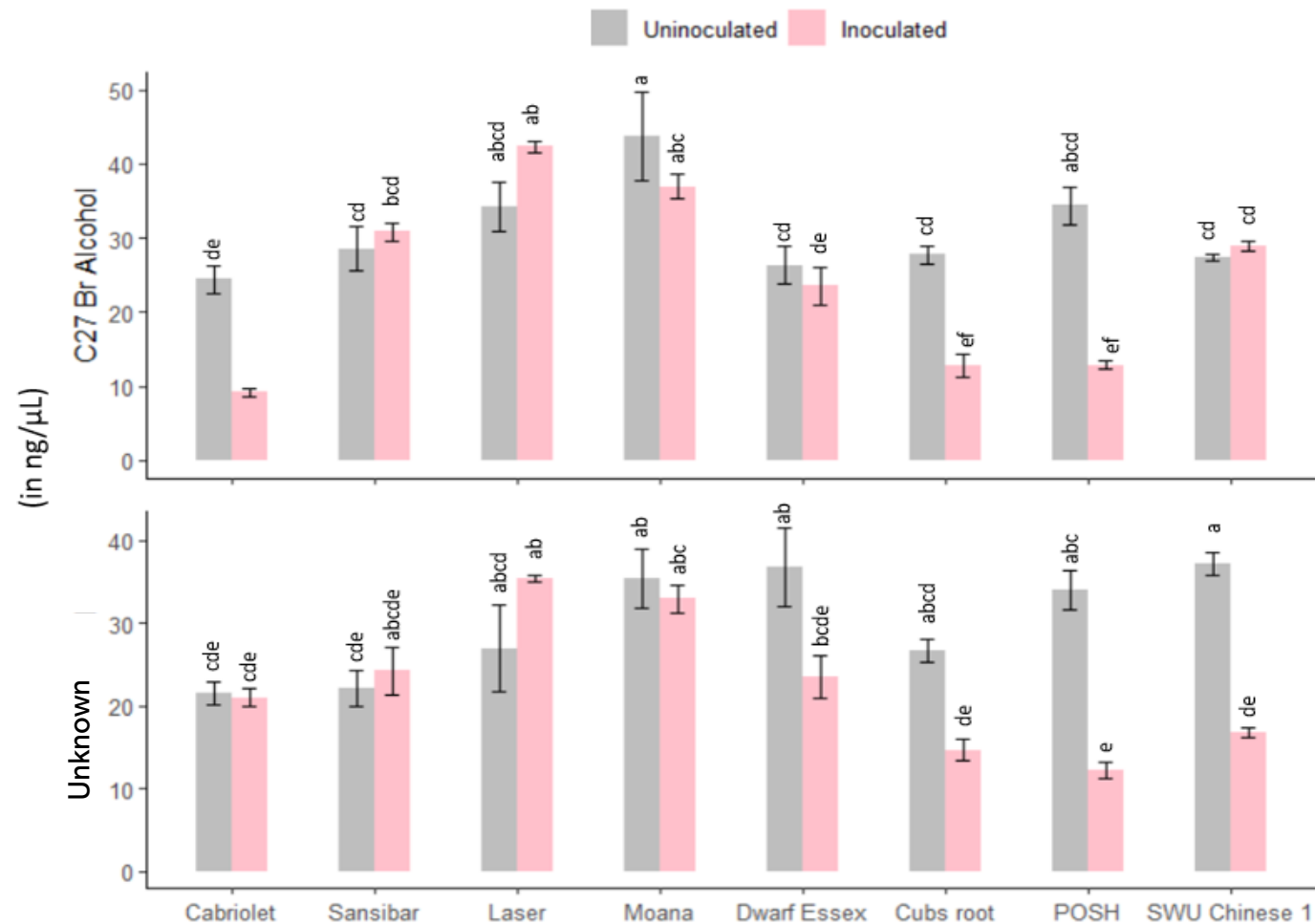
Individual compounds of branched (Br) alcohol identified and quantified from *Brassica napus* lines spray inoculated with *Pyrenopeziza brassicae* (28 dpi) using GCMS. Error bars represent standard deviations of three replicates. Columns with the same letters are not significantly different (Wilcoxon, Anova and TukeyHSD) (df 7).

Appendix 19: Individual compounds of secondary (2^0) alcohol quantified from *Brassica napus* lines/cvs spray inoculated with *Pyrenopeziza brassicae* (28 dpi) using GCMS.
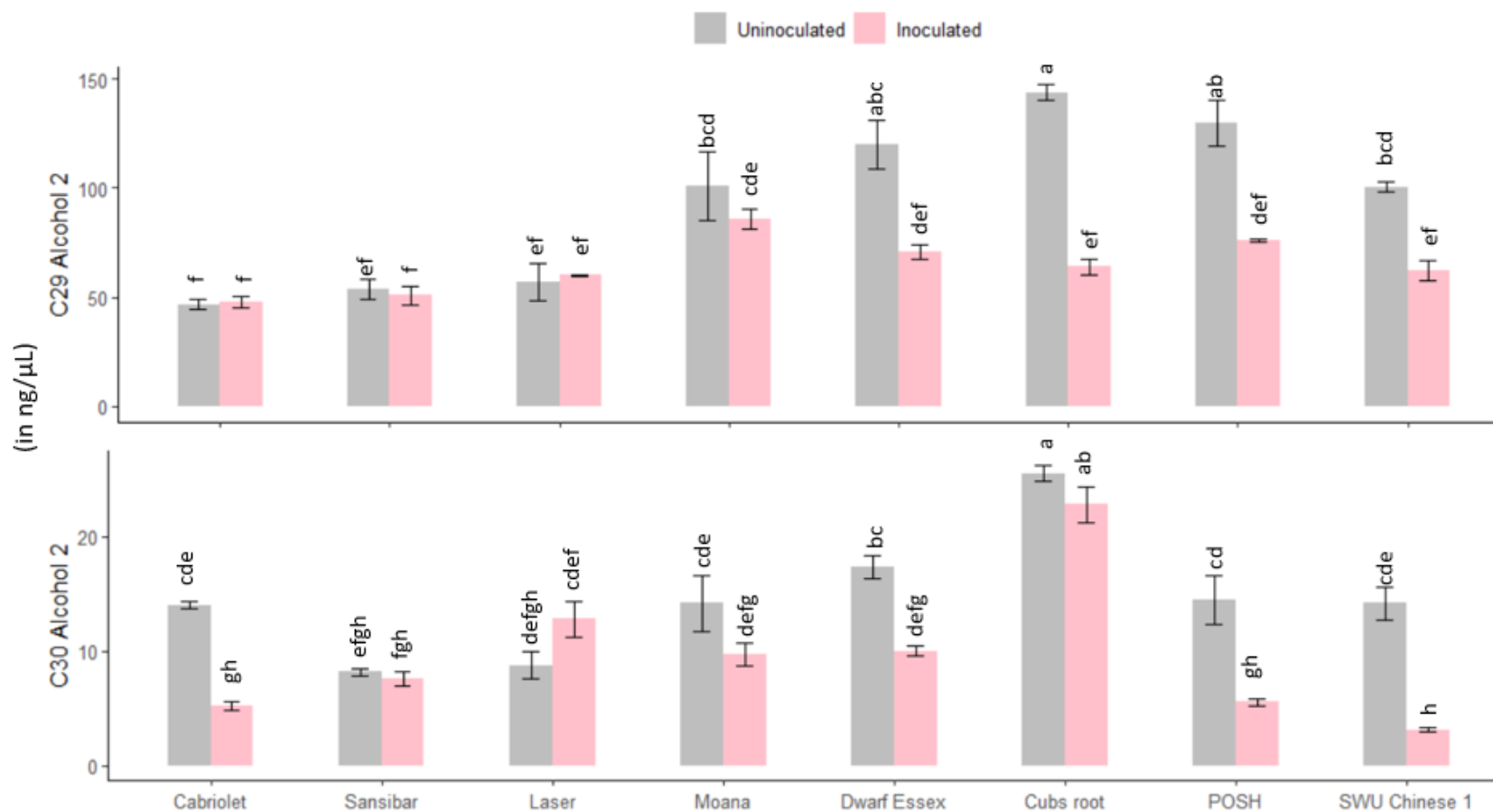
Individual compounds of 2^0 alcohol identified and quantified from *Brassica napus* lines spray inoculated with *Pyrenopeziza brassicae* (28 dpi) using GCMS. Error bars represent standard deviations of three replicates. Columns with the same letters are not significantly different (Wilcoxon, Anova and TukeyHSD) (df 7).

Appendix 20: Individual compounds of fatty acid quantified from *Brassica napus* lines/cvs spray inoculated with *Pyrenopeziza brassicae* (28 dpi) using GCMS.
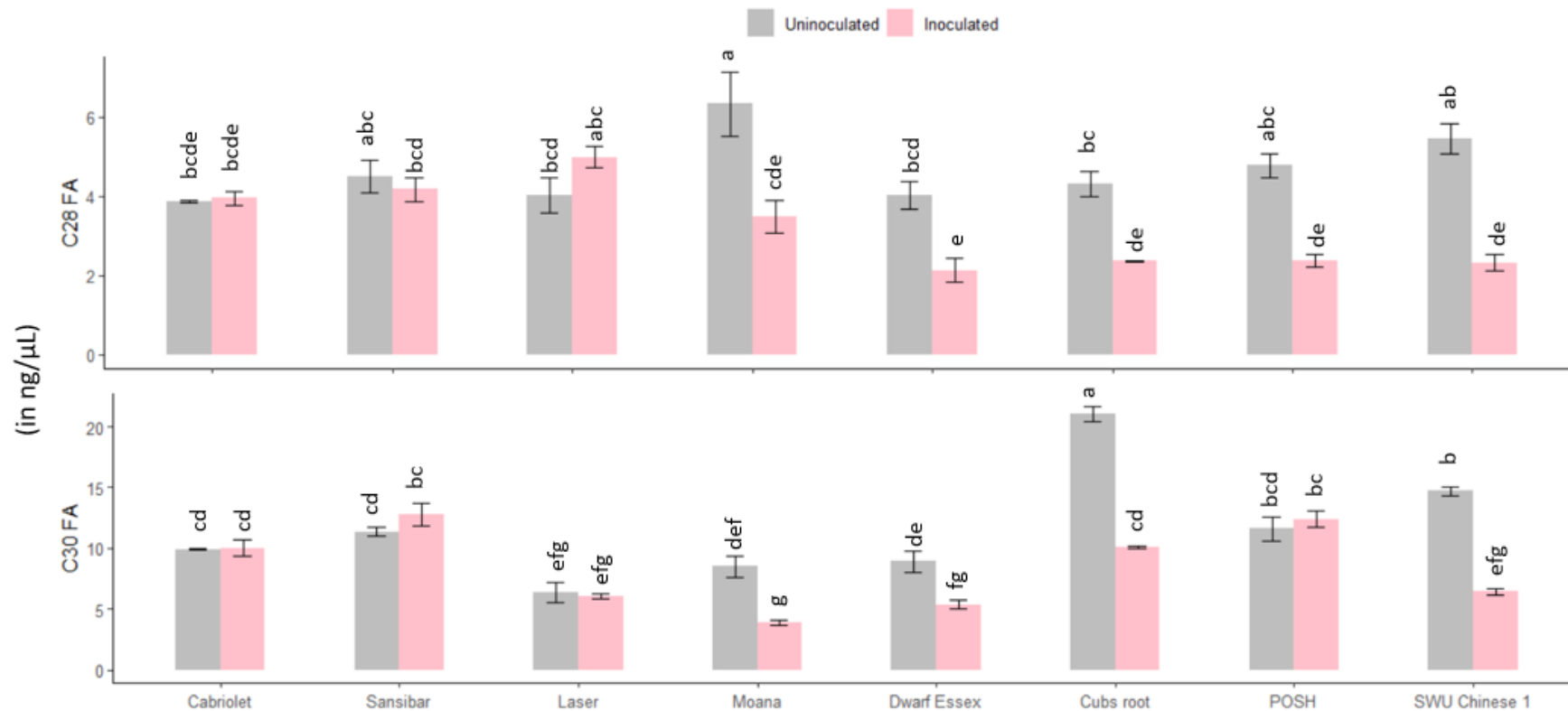
Individual compounds of fatty acid (FA) identified and quantified from *Brassica napus* lines spray inoculated with *Pyrenopeziza brassicae* (28 dpi) using GCMS. Error bars represent standard deviations of three replicates. Columns with the same letters are not significantly different (Wilcoxon, Anova and TukeyHSD) (df 7).

Appendix 21: Individual compounds of wax ester quantified from *Brassica napus* lines/cvs spray inoculated with *Pyrenopeziza brassicae* (28 dpi) using GCMS.
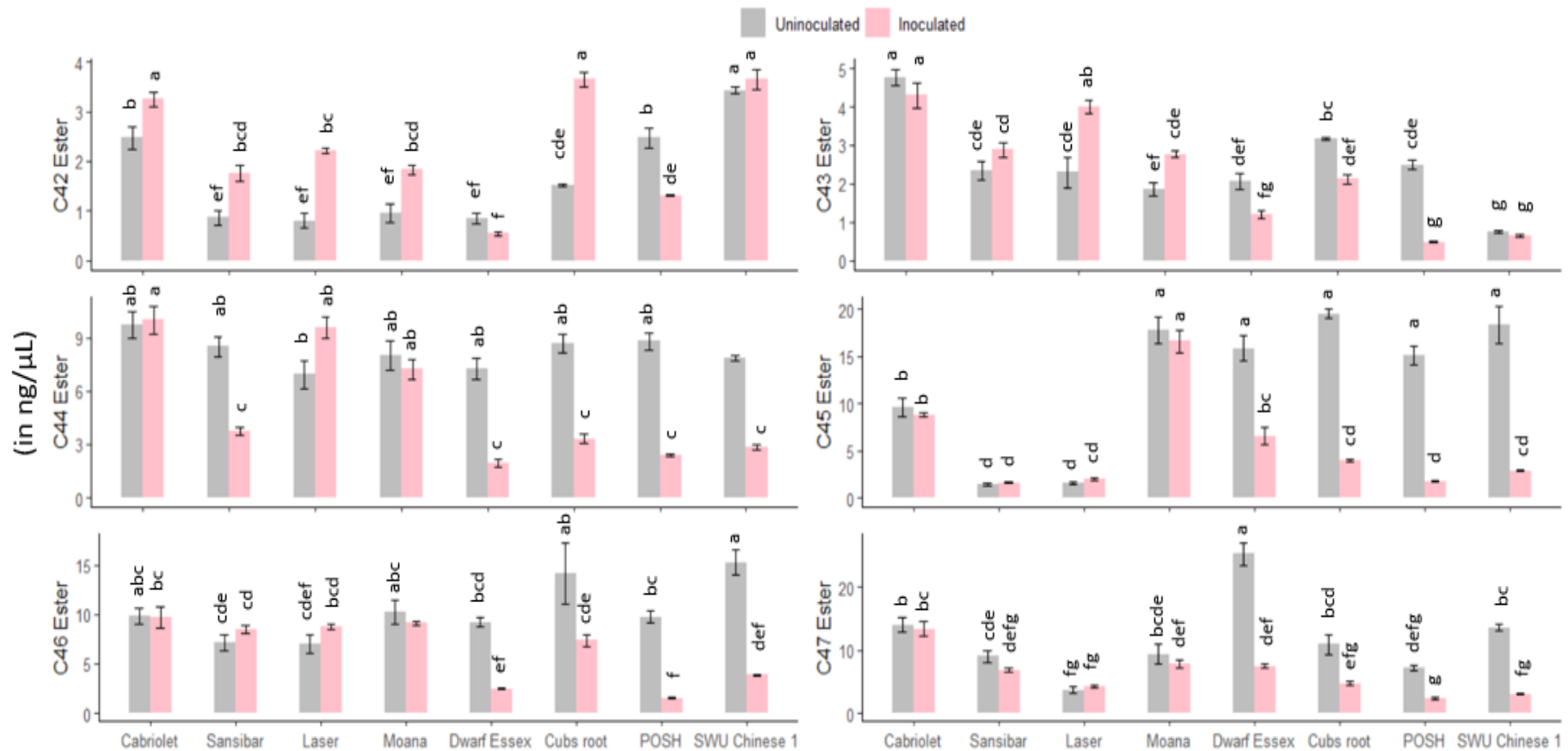
Individual compounds of ester identified and quantified from *Brassica napus* lines spray inoculated with *Pyrenopeziza brassicae* (28 dpi) using GCMS. Error bars represent standard deviations of three replicates. Columns with the same letters are not significantly different (Wilcoxon, Anova and TukeyHSD) (df 7).

Appendix 22: Percentage of individual intra-cuticular fatty acid compounds out of total cutin extracted from *Brassica napus* leaves spray inoculated with *Pyrenopeziza brassicae* (28 dpi) using GCMS.
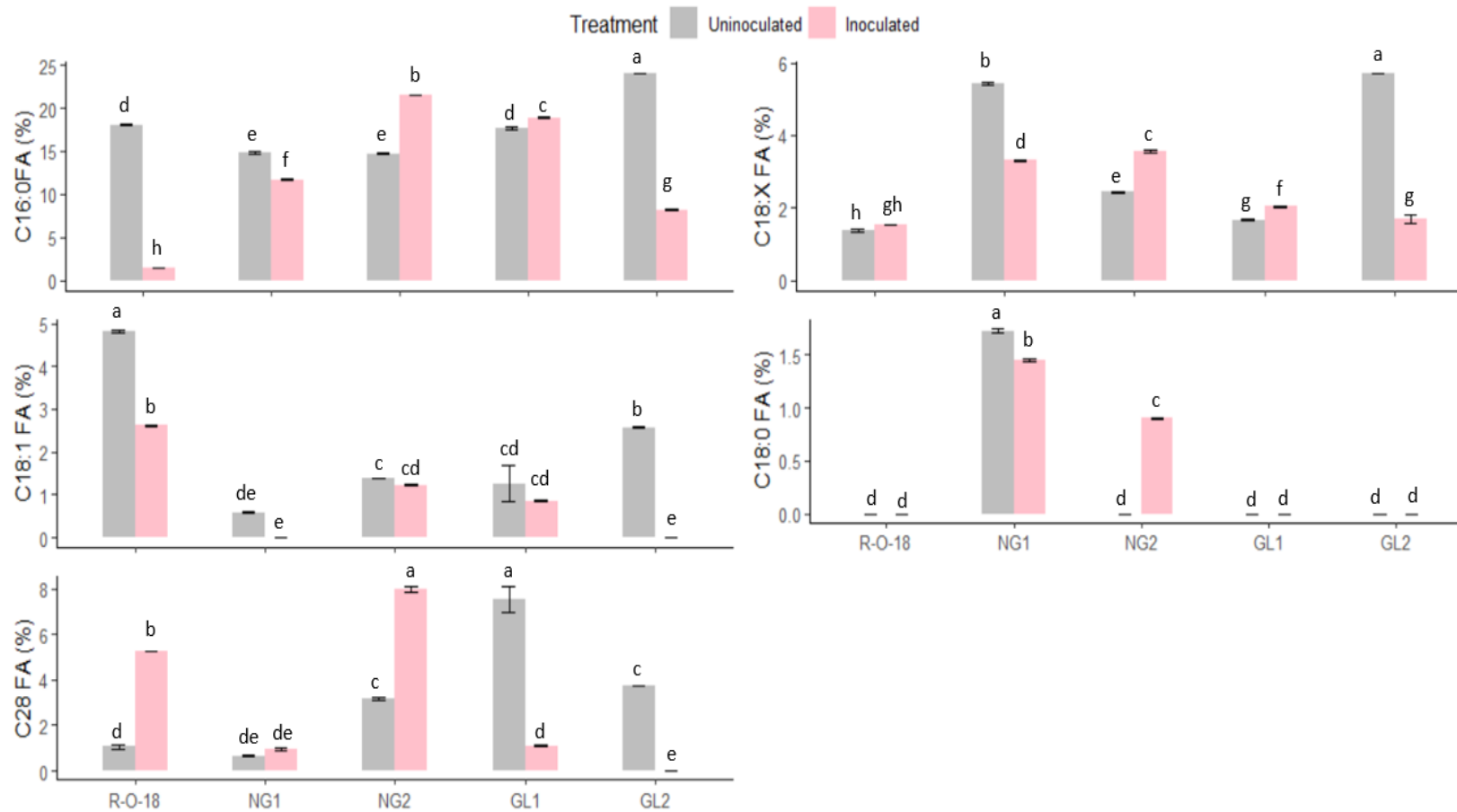
Percentage of individual compounds of intra cuticular fatty acids (FAs) out of total cutin extracted from *Brassica rapa* wax mutants spray inoculated with *Pyrenopeziza brassicae* (28 dpi) using GCMS. Error bars represent standard deviations of three replicates. Columns with the same letters are not significantly different (Wilcoxon, Anova and TukeyHSD) (df 4).

Appendix 23: Percentage of alcohol and fatty acid mixture, and ketone out of total cutin extracted from *Brassica napus* leaves spray inoculated with *Pyrenopeziza brassicae* (28 dpi) using GCMS.
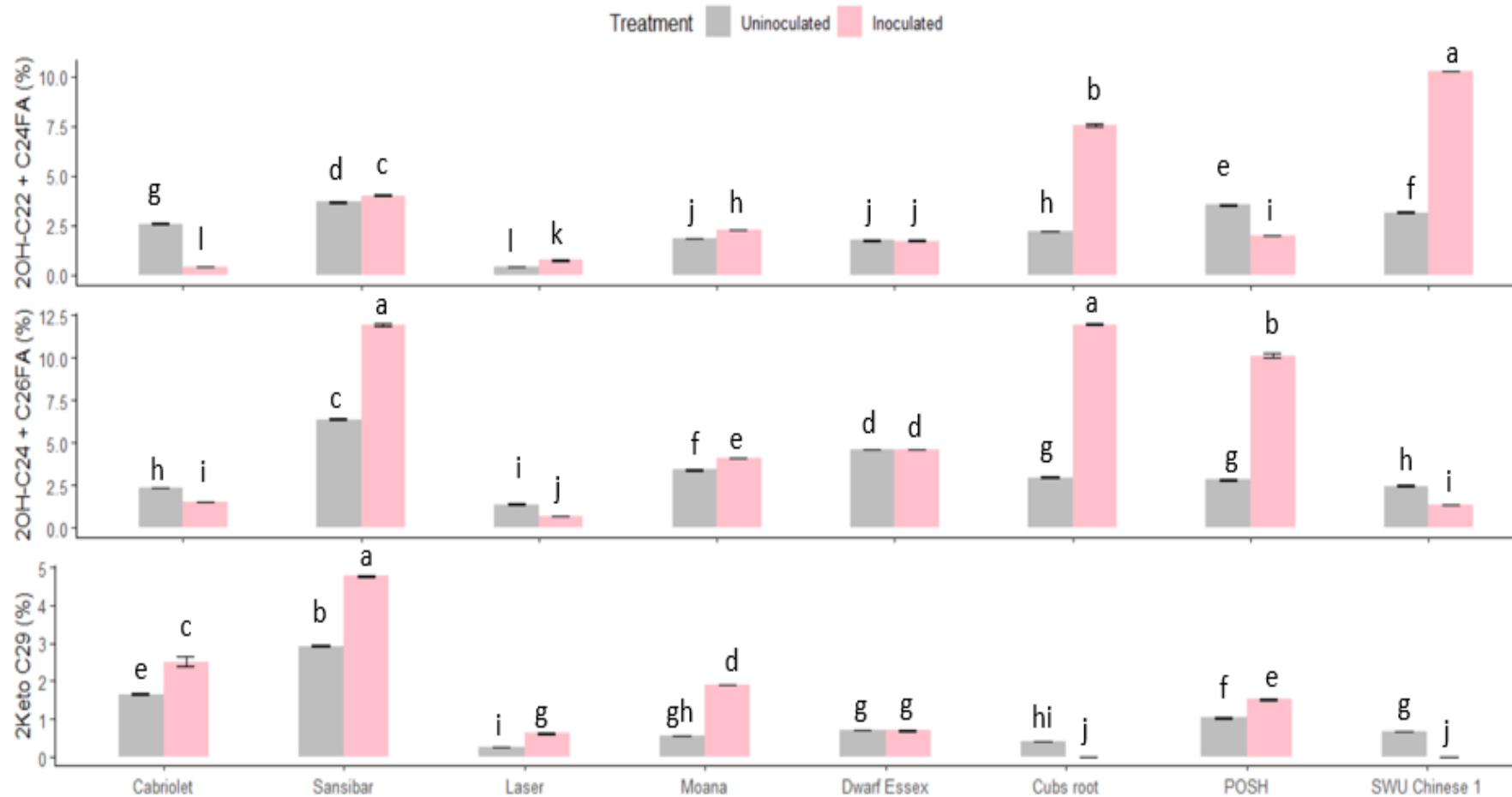
Percentage of alcohol and fatty acid mixture as well as ketone out of total cutin extracted from *Brassica napus* leaves spray inoculated with *Pyrenopeziza brassicae* (28 dpi) using GCMS. Error bars represent standard deviations of three replicates. Columns with the same letters are not significantly different (Wilcoxon, Anova and TukeyHSD) (df 7).

Appendix 24: Percentage of individual fatty acid compounds out of total cutin extracted from *Brassica napus* leaves spray inoculated with *Pyrenopeziza brassicae* (28 dpi) using GCMS.
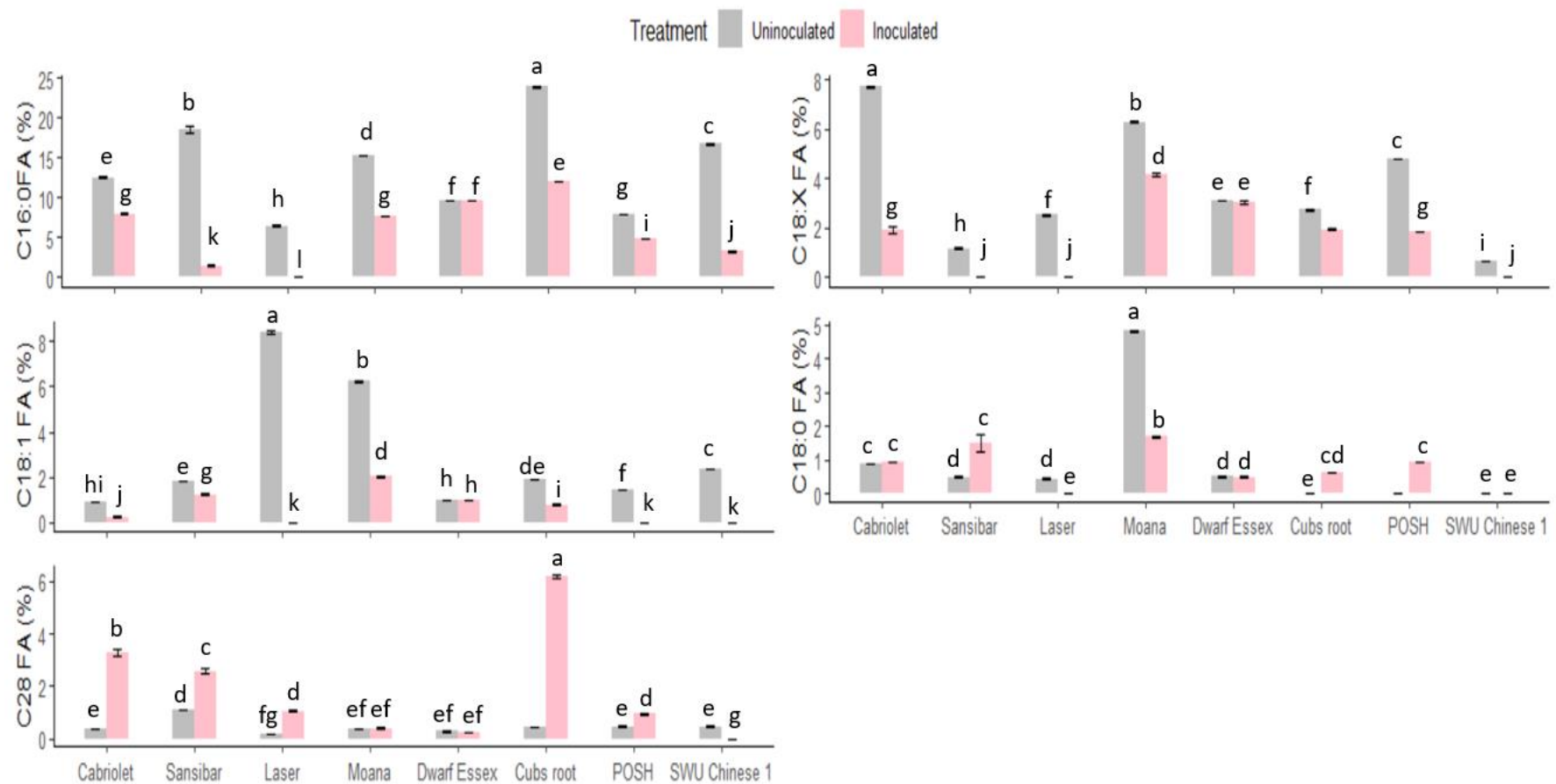
Percentage of individual fatty acids (FAs) out of total cutin extracted from *Brassica napus* leaves spray inoculated with *Pyrenopeziza brassicae* (28 dpi) using GCMS. Error bars represent standard deviations of three replicates. Columns with the same letters are not significantly different (Wilcoxon, Anova and TukeyHSD) (df 7).

Appendix 25: Wax content and composition of uninoculated *B. rapa* and *B. napus*. Colour formatted with green, yellow and red range (from higher to lower) for each molecular species and total wax.

Cultivar	Species	Alkane	Alcohol 1	Alcohol 2	Br Alcohol	Aldehyde	Fatty acid	Wax ester	Keto	Diol	Total wax
Cabriolet	*B napus*	598.4536	52.05378	60.67154	45.97359	39.5109	13.799916	50.41167739	200.6317	26.19694	1087.70367
Sansibar	*B napus*	676.7213	72.50563	61.7431	50.60176	54.39817	15.8577089	29.31804619	233.7692	12.61769	1207.53262
Laser	*B napus*	380.2625	43.22641	65.50371	61.21868	36.56413	10.4526299	22.2498129	177.1915	31.68294	828.352298
Moana	*B napus*	1106.985	71.82818	115.2102	79.09208	54.36488	14.8681802	48.27636881	309.1146	17.53207	1817.2719
Dwarf Essex	*B napus*	718.3934	42.92755	137.4111	63.0634	40.39191	12.9895531	60.51650222	243.4665	26.33538	1345.49533
Cubs Root	*B napus*	843.5264	52.07591	169.4178	54.38072	50.19317	25.3218743	58.01832433	337.5403	46.782	1637.25643
POSH	*B napus*	922.3955	63.5396	144.5212	68.35308	44.53036	16.3780074	45.82328257	281.8756	40.20255	1627.61926
SWU Chinese 1	*B napus*	917.1818	57.24261	114.5236	64.45979	60.66504	20.1777469	59.2459333	239.5605	27.78897	1560.84597
R-O-18	*B rapa*	478.8521	33.61019	95.28846	6.681298	7.852367	8.31484974	18.36774293	77.06196	4.851181	730.880176
NG1	*B rapa*	372.0328	28.7705	108.8934	9.921531	12.08636	4.94708359	4.200153457	143.9983	5.468527	690.318697
NG2	*B rapa*	876.9052	38.76713	100.5273	10.27821	10.92569	5.57492042	12.03021267	196.9811	8.440237	1260.43
GL1	*B rapa*	50.14705	92.75215	48.97868	52.44906	66.57926	5.11407194	14.80003095	1.693635	0.78088	333.294813
GL2	*B rapa*	36.76322	79.06307	20.90485	36.67464	41.84017	3.01533018	12.6356711	1.125859	1.021236	233.044051

Appendix 26: Screening for resistance against *Pyrenopeziza brassicae* in *Arabidopsis thaliana* using trypan blue staining.

A. thaliana ecotypes Ws-0, Nd-1, Columbia (Col-0), N22651, N22652, N22653, N22654, N22655, N22656 and N22658 were ordered from http://arabidopsis.info. Ecotypes were grown in controlled environment cabinets for 21 days and spray inoculated with 10^5 spores/ml spore suspension of *Pyrenopeziza brassicae* (section 2.8). The pathosystem of *Arabidopsis thalaiana* and *Pyrenopeziza brassicae* was assessed using trypan blue staining (section 2.9) at 7dpi, 18dpi and 25dpi.
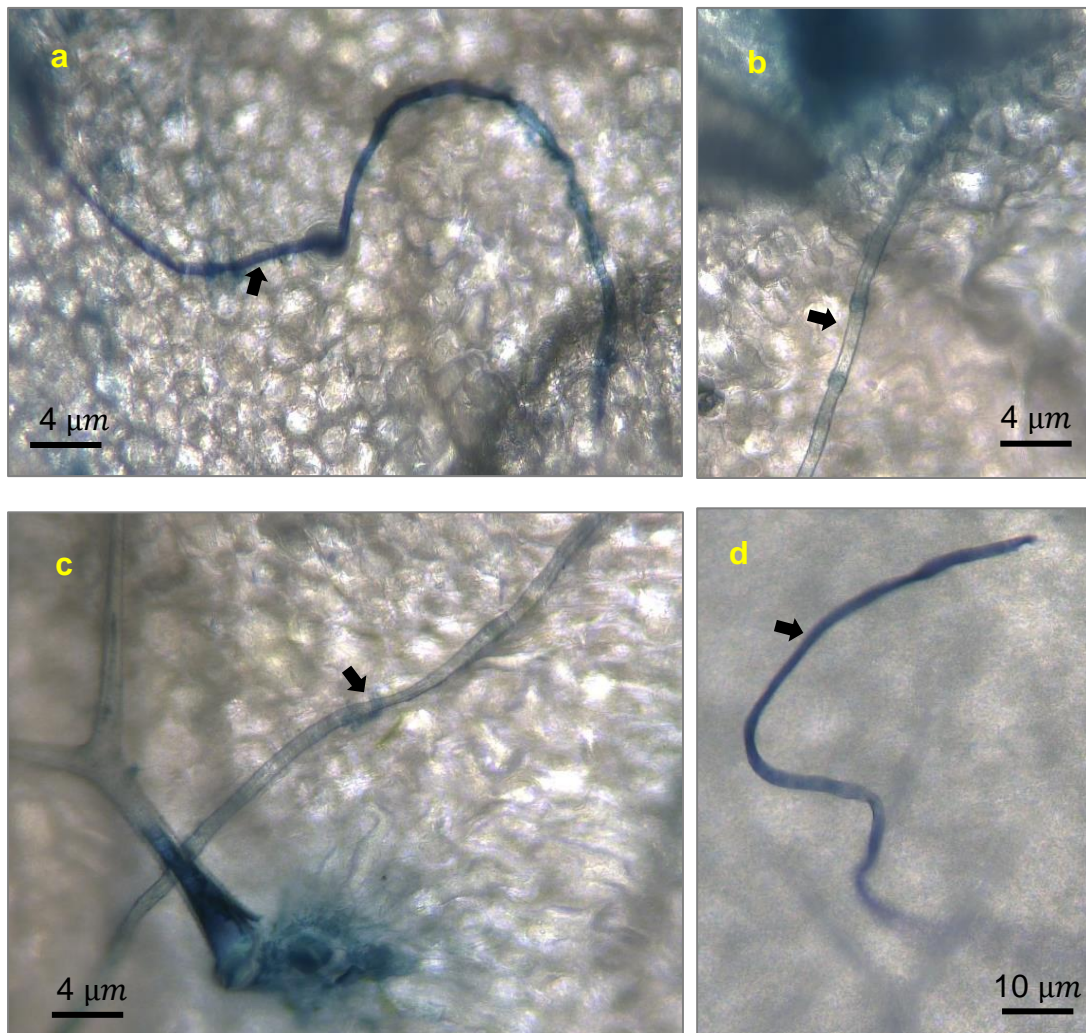
Trypan blue images of Nd-1 *A. thaliana* ecotype leaves with *P. brassicae* hyphal growth at 18dpi (a, b: Nd-1) and 25dpi (c, d: Nd-1). Minimal growth of hyphae was observed without any branching.
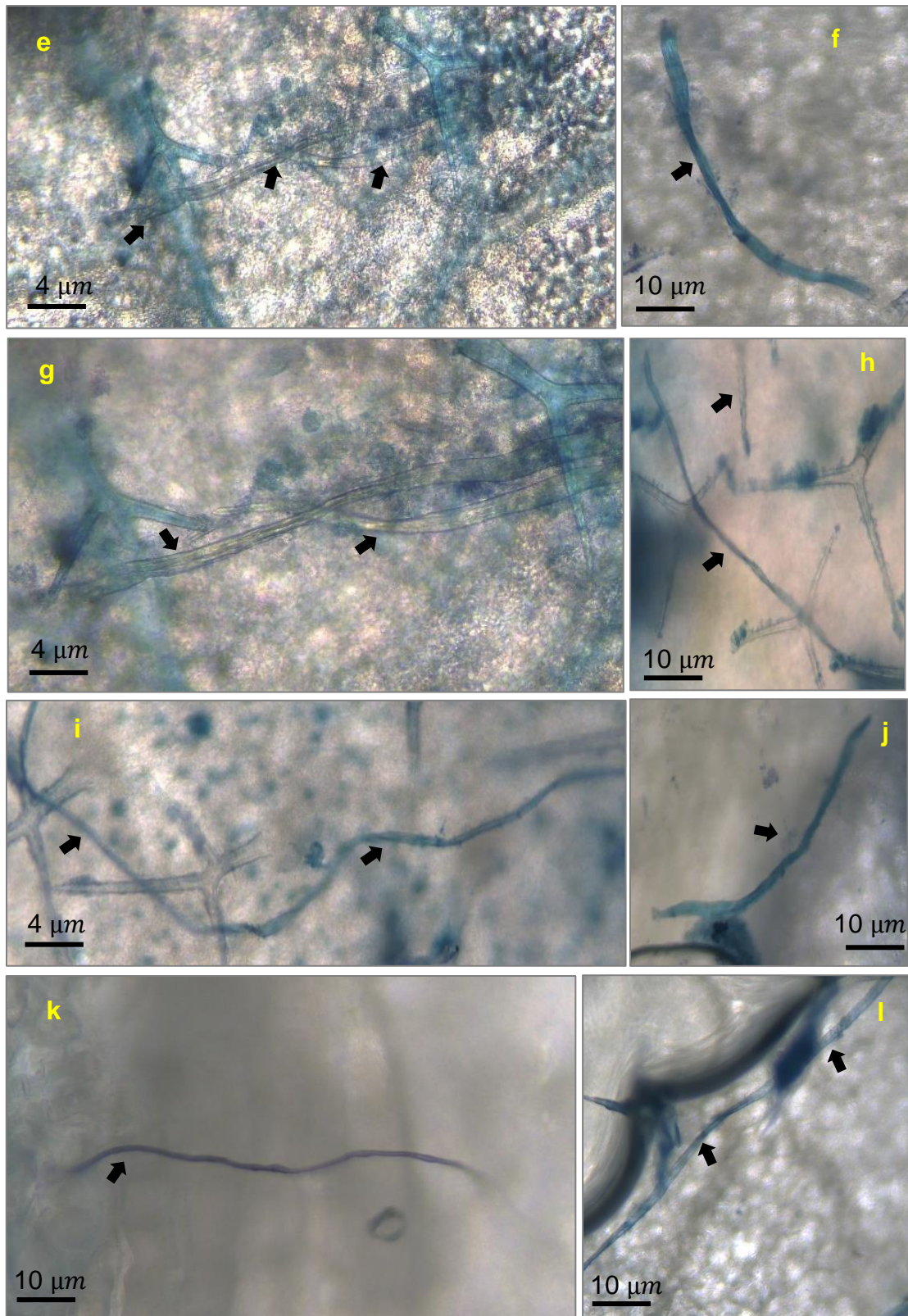
Trypan blue images of *Arabidopsis thaliana* ecotypes showing *Pyrenopeziza brassicae* hyphal growth at 25 dpi. N22651 (e), N22652 (f), N22653 (g), N22654 (h), N22655 (i), N22656 (j), N22658(k) and Ws-0 (l). No visible branching of hyphae was observed.

Appendix 27: Permeability test using toluidine blue staining

B. rapa control (R-0-18) and wax mutants (GL1, GL2: less wax and NG1, NG2: more wax) were grown in controlled environment cabinets (section 2.2) to assess the cuticle permeability using toluidine blue staining. Five biological replicates each were spot inoculated (section 2.7) respectively. Leaf discs from spot inoculated *Brassica rapa* wax mutants (1, 2, 4 and 8 dpi) were collected. Samples were immersed in a 0.05% (w/v) solution of toluidine blue for two min and any excess stain was washed with water (Pu *et al.*, 2013). Untreated leaves and leaf discs were used as controls.
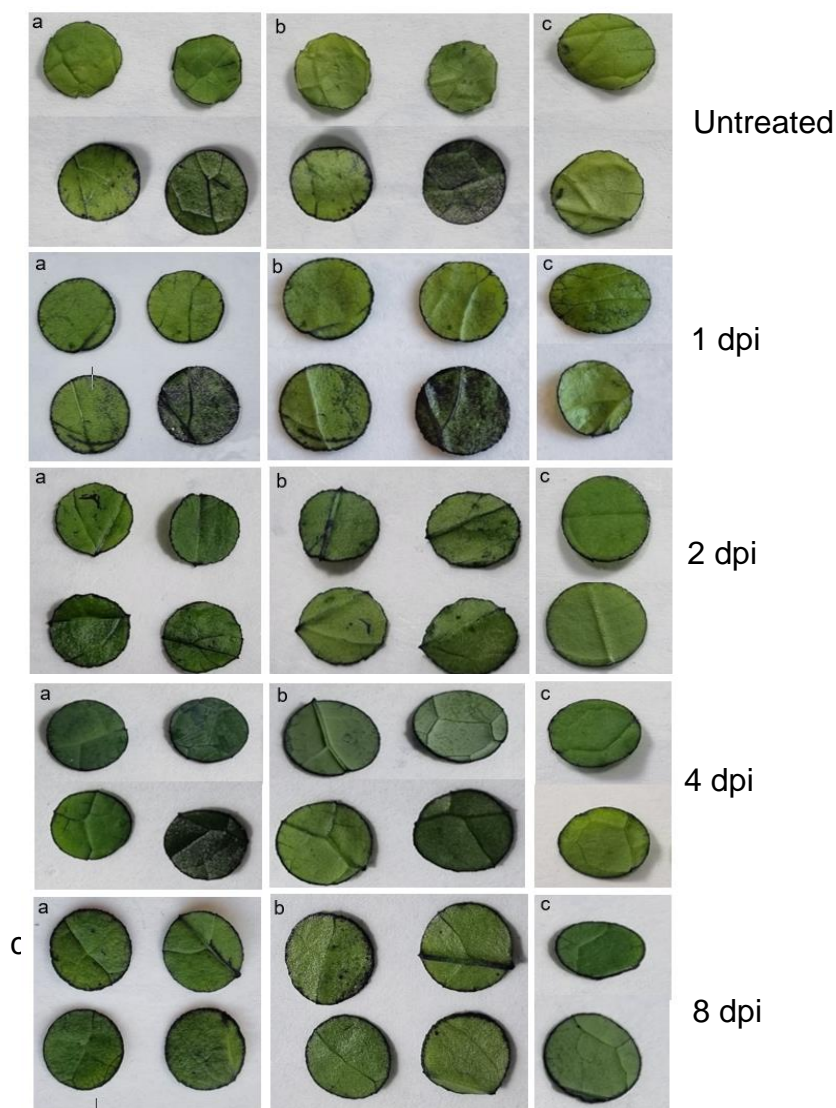
Toluidine blue staining images of *B. rapa* wax mutants spot inoculated with *P. brassicae* at 0dpi (untreated), 1dpi, 2dpi, 4dpi and 8dpi. (a) adaxial view of NG1and NG2 (top), GL1and GL2 (bottom) (b) abaxial view of NG1and NG2 (top), GL1and GL2 (bottom) (c) WT R-0-18 adaxial view (top) and abaxial view (bottom).

Appendix 28: Glasshouse and controlled environment experiments done during this PhD

Experiment condition	Number	Experiment	Chapter
Glasshouse	1,2,3	GWAS *B. napus* mapping - LLS scoring	4
Glasshouse	4,5	Commercial *B. napus* cvs/lines assessment- LLS scoring, *P. brassicae* spore counting and DNA content quantification	4
Glasshouse	6,7	Four resistant and four susceptible *B. napus* cvs/lines assessment - LLS scoring, *P. brassicae* spore counting and DNA content quantification	4
Glasshouse	8, 9	*B. rapa* wax mutants and *B. napus* screening – LLS scoring and *P. brassicae* spore counting	5
Glasshouse	8	*B. rapa* wax mutants and *B. napus* – cuticular wax and cutin extraction and analysis	5
Controlled experiment	1, 2	Regional pathogenicity variations of *P. brassicae* isolates	3
Controlled experiment	3, 4	Regional pathogenicity variations of *P. brassicae* populations	3
Controlled experiment	5	Cultivars Cabriolet and Cubs Root interaction with *P. brassicae* -trypan blue visualisation	4
Controlled experiment	6	Scanning electron microscopy (SEM) – Susceptible cv. Cabriolet and *P. brassicae* interaction study	4
Controlled experiment	7	Scanning electron microscopy (SEM) – Susceptible cv. Cabriolet and resistant cv. Cubs Root interaction with and *P. brassicae*	4
Controlled experiment	8, 9	Taqman multiplex qPCR – GEMs analysis	4
Controlled experiment	10	Glucosinolate quantification- *B. napus*	4
Controlled experiment	11	Cutinase expression analysis - *B. rapa* wax mutants and *B. napus*	5

Appendix 29: Publications

1. (a) Research paper - Theoretical and Applied Genetics - Novel gene loci associated with susceptibility or cryptic quantitative resistance to *Pyrenopeziza brassicae* in *Brassica napus*. (2023)

    (b) Supplementary table – Gene expression markers (GEMs)

    (c) Supplementary table - Environmental conditions of glasshouse experiments

2. Research paper - Pest Management Science - *Leptosphaeria maculans* isolates with variations in *AvrLm*1 and *AvrLm4* effector genes induce differences in defence responses but not in resistance phenotypes in cultivars carrying the *Rlm7* gene. (2023)

3. Conference paper - The AgriFood Charities Partnership AFCP conference - Genetic basis of partial resistance against *Pyrenopeziza brassicae* in oilseed rape. (2021)

4. (a) Poster - School of Life and Medical Sciences Research Conference, University of Hertfordshire - Genetic basis of partial resistance against *Pyrenopeziza brassicae* in oilseed rape. (2019)

    Poster - International Rapeseed Congress, Berlin, Germany - Genetic basis of partial resistance against *Pyrenopeziza brassicae* in oilseed rape. (2019)

    Poster - Arms race, evolution of plant pathogens and their hosts, future British Society for Plant Pathology Conference - Genetic basis of partial resistance against *Pyrenopeziza brassicae* in oilseed rape. (2019)

    (b) Abstract

5   (a) Poster - School of Life and Medical Sciences Research Conference,
University of Hertfordshire - Genetic basis of partial resistance against
Pyrenopeziza brassicae in oilseed rape. (2021)

Poster and oral presentation - Genetic basis of partial resistance against
Pyrenopeziza brassicae in oilseed rape -Our plants, our future, British
Society for Plant Pathology Conference, University of Birmingham, UK. Oral
presentation. P13. (6th-8th December 2021)

Poster - The AgriFood Charities Partnership AFCP conference – Genetic
basis of partial resistance against *Pyrenopeziza brassicae* in oilseed rape.
(2019)

(b) Abstract

1a

ORIGINAL ARTICLE

Novel gene loci associated with susceptibility or cryptic quantitative resistance to *Pyrenopeziza brassicae* in *Brassica napus*

Heather Fell[1] · Ajisa Muthayil Ali[1] · Rachel Wells[2] · Georgia K. Mitrousia[1,4] · Hugh Woolfenden[3] · Henk-jan Schoonbeek[2] · Bruce D. L. Fitt[1] · Christopher J. Ridout[2] · Henrik U. Stotz[1]

Abstract
Key message Quantitative disease resistance (QDR) controls the association of the light leaf spot pathogen with *Brassica napus*; four QDR loci that were in linkage disequilibrium and eight gene expression markers were identified.
Abstract Quantitative disease resistance (QDR) can provide durable control of pathogens in crops in contrast to resistance (*R*) gene-mediated resistance which can break down due to pathogen evolution. QDR is therefore a desirable trait in crop improvement, but little is known about the causative genes, and so it is difficult to incorporate into breeding programmes. Light leaf spot, caused by *Pyrenopeziza brassicae*, is an important disease of oilseed rape (canola, *Brassica napus*). To identify new QDR gene loci, we used a high-throughput screening pathosystem with *P. brassicae* on 195 lines of *B. napus* combined with an association transcriptomics platform. We show that all resistance against *P. brassicae* was associated with QDR and not *R* gene-mediated. We used genome-wide association analysis with an improved *B. napus* population structure to reveal four gene loci significantly ($P = 0.0001$) associated with QDR in regions showing linkage disequilibrium. On chromosome A09, enhanced resistance was associated with heterozygosity for a cytochrome P450 gene co-localising with a previously described locus for seed glucosinolate content. In addition, eight significant gene expression markers with a false discovery rate of 0.001 were associated with QDR against *P. brassicae*. For seven of these, expression was positively correlated with resistance, whereas for one, a HXXXD-type acyl-transferase, negative correlation indicated a potential susceptibility gene. The study identifies novel QDR loci for susceptibility and resistance, including novel cryptic QDR genes associated with heterozygosity, that will inform future crop improvement.

✉ Henrik U. Stotz
  h.stotz@herts.ac.uk

[1] Centre for Agriculture, Food and Environmental Management, School of Life and Medical Sciences, University of Hertfordshire, Hatfield AL10 9AB, UK

[2] Crop Genetics Department, John Innes Centre, Norwich Research Park, Norwich NR4 7UH, UK

[3] Computational and Systems Biology, John Innes Centre, Norwich Research Park, Norwich NR4 7UH, UK

[4] Present Address: Communication and Engagement Office, Science Innovation Engagement Partnerships, Rothamsted Research Ltd, West Common, Harpenden AL5 2JQ, UK

Introduction

Quantitative disease resistance (QDR) is predominant in natural plant populations and provides robust and durable protection from pathogens in ecosystems (Delplace et al. 2020). Although QDR could potentially provide more durable resistance in crop plants, it is not routinely selected for in breeding since the underlying gene loci are poorly characterised and contribute partial but additive resistance which is difficult to track in breeding programmes (Nelson et al. 2018). Understanding the molecular basis of QDR will provide novel opportunities for introducing durable disease resistance into crops and reducing the use of pesticides. Our investigation uses a pathosystem which, combined with an association genetics platform, establishes a novel approach to identify candidate QDR genes for crop improvement in *Brassica napus*.

Plants have evolved layers of immunity for defence against various pathogens with different modes of infection

🍏 Springer

and life styles. Although the layers of plant immunity are not distinct and may overlap to some extent (Ngou et al. 2021; Yuan et al. 2021), the first is considered to be the rapid detection of microbial patterns usually described as pattern-triggered immunity (PTI). Adapted pathogens secrete effectors that suppress PTI as they colonise the host plant and cause disease (Jones and Dangl 2006). Effectors can be recognised by resistance proteins, typically nucleotide-binding, leucine-rich repeat (NLR) immune receptors, which provide the second layer of immunity to protect the plant. When operating against cell-penetrating pathogens, this effector-triggered immunity (ETI) is the principal mechanism in qualitative, or *R* gene-mediated, resistance and provides a powerful defence response (Jones & Dangl 2006). However, operating against extracellular pathogens, *R* gene-mediated resistance, termed effector-triggered defence (ETD) acts more slowly and is not an immune but a resistance response (Stotz et al. 2014). Pathogen populations can mutate or lose effectors so that they are no longer recognised, leading to resistance breakdown in crops. This contrasts with QDR, which is predicted to provide durable protection against pathogens. Although less well-studied, mechanisms of QDR can include enhanced cell wall thickening, modified signalling processes and enhanced secondary metabolism (Cowger and Brown 2019). Interestingly, studies with the apoplastic (extracellular) fungal pathogen *Leptosphaeria maculans* have shown that ETD may also contribute to QDR in *B. napus*, reinforcing the concept of overlap between layers of defence in plants (Jiquel et al. 2021).

After soybean, oilseed rape (OSR; *Brassica napus*) is economically the second most important vegetable oil crop in the world. Amongst the biotic threats that challenge OSR production, light leaf spot (LLS), caused by the apoplastic ascomycete *Pyrenopeziza brassicae* (anamorph *Cylindrosporium concentricum*), ranks in the top 10 most damaging diseases on the crop in Europe (Zheng et al. 2020); note that *P. brassicae* is the perfect stage of *C. concentricum*. Yield losses are due to seedling death at the rosette stage, stunting of susceptible cultivars and floral infection, leading to malformed pods and seeds, premature pod senescence and pod shattering prior to harvest (Gilles et al. 2000). This pathogen has a widespread geographic distribution, occurring in the United Kingdom (UK) and, increasingly, continental Europe, the Pacific Northwest of the United States, Asia (Japan, Philippines) and New Zealand (Carmody et al. 2019; Karandeni Dewage et al. 2018). *P. brassicae* epidemics are initiated by wind-dispersed ascospores. Acervuli then produce asexual conidia in infected plant parts; these conidia are rain splash-dispersed to establish the polycyclic stage of the LLS disease epidemic.

LLS has become the most damaging disease of OSR in the UK. The disease accounts for up to £160 million yield loss annually in England, despite expenditure of £20 M on fungicides. The severity of the disease is greater in Scotland than in England (Karandeni Dewage et al. 2018). However, LLS has progressively become a greater problem in parts of the UK other than Scotland over more than a decade and may now be considered a national emergency. Simultaneously, *P. brassicae* has become a problem on Brassica vegetables in the UK and other places, causing market losses due to surface blemishes on crops like Brussels sprouts. Besides *B. napus* and *B. oleracea*, *P. brassicae* has been observed on mustard rape (*B. juncea*) and *B. rapa* (Carmody et al. 2019).

One of the limitations of studying QDR in crop species is that resistance of individual QDR loci is only partial and can be masked by *R*-gene-mediated resistance. *P. brassicae* on *B. napus* is an ideal pathosystem to study QDR because there are no known *R* genes effective against the pathogen. Moreover, one study has indicated the presence of QDR for LLS. Six environmentally stable quantitative trait loci (QTL) for resistance against *P. brassicae* were mapped in a doubled haploid (DH) population of *B. napus* derived from a cross between moderately resistant Darmor-*bzh* and susceptible Yudal cultivars (Pilet et al. 1998). Four new QTL for resistance against *P. brassicae* were identified on linkage groups C01, C06 and C09 (Karandeni Dewage et al. 2022). Two major loci for resistance against *P. brassicae* were identified (Bradburne et al. 1999), and one was mapped to the bottom of chromosome A1 of *B. napus* (Boys et al. 2012). This locus could be a QDR locus since it was associated with substantial decrease in LLS hyphal growth rather than death of the pathogen typical of *R* gene-mediated resistance (Boys et al. 2012; Stotz et al. 2014). However, apart from these examples, little is known about QDR for resistance against *P. brassicae* in *B. napus*.

P. brassicae and *Rhynchosporium commune* are closely related discomycetes (Goodwin 2002; Penselin et al. 2016) that occupy a subcuticular apoplastic niche in their respective brassica and barley hosts (Stotz et al. 2014). It is therefore relevant to compare resistance mechanisms that operate against these related pathogens. The major resistance locus *Rrs1*, containing wall-associated kinases, controls resistance against *Rhynchosporium commune* in barley (Looseley et al. 2020). *Rrs1* is the only *R* gene against *R. commune* that has a corresponding *Avr* gene, *NIP1*, that encodes a necrosis-inducing protein (Rohe et al. 1995). Additionally, multiple quantitative resistance loci were found to be involved in resistance of barley against *R. commune* (Buttner et al. 2020).

The development of association genetics and transcriptomics has enabled the identification of pathogen resistance loci that was not possible in biparental mapping populations (Bartoli and Roux 2017). The approaches take advantage of recombination events that have accumulated in natural populations to identify genetic polymorphisms associated with phenotypes of interest. The method requires genomic

or transcriptomic sequences from a diversity collection and phenotypic data for the trait of interest. The approach has been used to identify new resistance loci operating against *Sclerotinia sclerotiorum* stem rot and potential *R* genes for resistance in *B. napus* against *Plasmodiophora brassicae* (clubroot) (Hejna et al. 2019; Wu et al. 2016). However, no such studies have been done to identify QDR against *Pyrenopeziza brassicae*.

The aim of this study was to characterise genomic regions associated with QDR against *P. brassicae* in *B. napus* under glasshouse conditions. To achieve this, we performed association genetic analysis with a *B. napus* diversity set developed through the OREGIN initiative (https://www.herts.ac.uk/oregin) combined with genotype and expression data (Havlickova et al. 2018) and phenotypic measurement of *P. brassicae* infection that we developed for the study. This study provides new insights into QDR mechanisms and supports breeding efforts to generate durable disease-resistant crops.

Methods

Glasshouse growth conditions

Glasshouses at the Bayfordbury campus, University of Hertfordshire, and Rothamsted Research were utilised for experiments scored for partial resistance against *P. brassicae* with baseline temperatures set to 16 °C during the day and 14 °C during the night (see diurnal cycles below). Actual temperatures recorded were outside this baseline range, however, due to fluctuations in temperature and light during the experimental period (Supporting Information Table S1). At Bayfordbury, supplemental lighting was used for 12 h per day using sodium high pressure lamps (Sylvania SHP-TS 400 W GroLux), which automatically switched on once natural daylight decreased to < 115 μmol m^{-2} s^{-1}. Supplemental lighting (LEDs, 175 W m^{-2}) was used for 12 h and 14.5 h at Rothamsted Research for experiments 8 and experiments 9 and 10, respectively (Supporting Information Table S1). The intensity of supplemental lighting was 200 μmol m^{-2} s^{-1}. Humidity levels were variable as they cannot be controlled in a glasshouse situation, although they were monitored at Rothamsted Research.

Isolation of *P. brassicae* populations

Two populations of *P. brassicae* were used. The first population was amplified having obtained infected leaves from KWS SAAT SE & Co. KGaA (Einbeck, Germany) from field experiments on the island in Fehmarn, Germany (54.4701, 11.1329) in 2016. The second population was obtained from infected leaves of KWS-grown *B. napus* genotypes, including reference cultivars Cuillin and Express, at a

Rothamsted Research field site (51.813125, − 0.382005) in 2019. Populations obtained in 2016 and 2019 were used for seven and three glasshouse experiments at Bayfordbury and Rothamsted Research, respectively (Supporting Information Table S2).

Leaves of *B. napus* with the greatest amount of *P. brassicae* sporulation already present were sampled from the field experiments and placed into polyethylene bags for transportation back to the University of Hertfordshire. The spores were dislodged from the leaves by pipetting sterile distilled water over the leaf, and the run-off was collected in a glass beaker. This spore suspension was filtered using Miracloth (Merck Millipore, Watford, U.K.) and the spore concentration determined using a haemocytometer slide under a stereo-microscope (GX Microscopes, XTC-3A1). The concentration was adjusted to 10^5 spores ml^{-1} and dispensed into 50 ml aliquots for use as inoculum in the experiments or stored at − 20 °C.

Quantification of *P. brassicae* sporulation on leaves of *B. napus* accessions

Each of 10 experiments tested 24 accessions, each with five inoculated replicates with the exception of experiments 1 and 3, which each tested only 23 accessions (Supporting Information Table S2). In total, there were 195 accessions in these experiments. The replicates were arranged in a randomised alpha block design, so that each block included one replicate plant from each of the 24 accessions. All of the lines screened could not be grown at the same time; therefore, seven experiments were done at Bayfordbury from 2016 to 2018 with the cultivars Tapidor, Imola (resistant), Bristol (susceptible) and Temple included in each experiment to act as references for normalising symptom severity between experiments. In 2019, another three experiments were done at Rothamsted Research with the susceptible one of the replicated reference cultivars being Cabriolet instead of Bristol due to seed availability.

Seeds were stratified for 2 days at 4 °C prior to germination on damp filter paper in Petri dishes in the dark. The successfully germinated seeds were then planted into 8 × 5 cell seed trays with a 50:50 mixture of John Innes No.3 compost and multipurpose compost (Miracle Gro). The seedlings were left to grow in the glasshouse for approximately 2 weeks until the first and second true leaves had emerged. Established plants were transplanted into 9 cm diameter individual pots using the same potting mix. Additional fertiliser was not used. Seedlings were irrigated from below daily using capillary matting. Once potted, plants were checked each day and top-watered when the first 2.5 cm of soil was dry.

After a further 2 weeks, a total of 120 plants at growth stage 1,5 (Sylvester-Bradley 1985), i.e. seedlings with five true leaves, were sprayed with 100 ml of *P. brassicae* spore suspension, at a concentration of 10^5 spores ml^{-1} water containing 0.05% Silwet (Spiess-Urania Chemicals GmbH, Hamburg, Germany) as a wetting agent. A hand sprayer on fine mist setting was used to sufficiently cover all leaves of all plants. Subsequently, plants were incubated for 48 h under a clear polyethylene sheet over a plastic frame, $2 \times 1 \times 0.5$ m in dimension. The plants were grown for another 3 weeks before the whole plant was sampled by cutting at the base of the stem just above the soil surface, wrapped in a paper towel, and placed into a labelled polyethylene freezer bag to preserve the whole plant. As all plants were harvested at the same time, growth stages slightly varied amongst different lines. On average, plants reached growth stage 1,9. The inside of the bag and the paper towel were sprayed with sterile distilled water to create humidity, and then, sampled plants were incubated at 4 °C in a cold room. After 5 and 10 days of incubation, the sampled plants were assessed visually for the presence of *P. brassicae* sporulation using a modified LLS 1–6 severity scale (Karandeni Dewage et al. 2021). Specifically, score = 1 (no sporulation), score = 2 (< 10% leaf area with sporulation), score = 3 (10–25% leaf area with sporulation), score = 4 (25–50% leaf area with sporulation), score = 5 (50–75% leaf area with sporulation) and score = 6 (75–100% leaf area with sporulation). Each of three to six leaves per plant was given a score, and then, these scores were averaged to give a disease severity rating.

Statistical analysis of phenotypic traits

The quantitative resistance work consisted of 10 glasshouse experiments. A total of 195 accessions were scored for *P. brassicae* sporulation. Reference genotypes replicated in each of the ten experiments were used to determine normality of the data with the Shapiro–Wilk test and lack of effect of experiment for the entire study. Phenotypic data were analysed in R using a package for nonlinear mixed-effects models (nlme). The function for the model had the following structure: model = lme(Score – Genotype, data = LLS, random = – 1|Experiment/Genotype). Adjusted means were generated and ordered according to the scores of the genotypes. A Wilcoxon signed-rank test was used for pair-wise comparisons of the adjusted means of genotypes. A significance threshold of $P < 0.05$ was used to assess pair-wise differences in disease score. Data were visualised in R using ordered means dotchart and hist functions.

Association transcriptomics

The phenotyping datasets of the diversity set for LLS resistance scores were analysed using an association transcriptomics pipeline based on programs used to map traits in *B. napus* previously with minor modifications (Harper et al. 2012; Wells et al. 2013). Genotype and expression level datasets used were published (Havlickova et al. 2018) and available from York Knowledgebase (http://yorknowledgebase.info). This dataset was reduced to include only the accessions within this study.

Gene expression marker (GEM) associations were determined by linear regression using Reads Per Kilobase of transcript, per Million mapped reads (RPKM) to predict a quantitative outcome of the trait value. All markers with an average expression less than 0.5 RPKM were removed before analysis.

An updated population structure was calculated for the accessions used within this study using a Bayesian clustering approach. A Markov Chain Monte Carlo (MCMC) algorithm was implemented in the population-genetic software STRUCTURE V2.3.1. One of the requirements of STRUCTURE is unlinked markers; therefore, the single nucleotide polymorphism (SNP) file was adjusted before the analysis using the following criteria: SNPs were required to be biallelic, with a minor allele frequency (MAF) > 0.05 and a minimum distance of 500 kb between markers. Markers within 100 kb of the centromeres, based on published findings (Cheng et al. 2013; Mason et al. 2016), were excluded. STRUCTURE was run using the admixture model with uncorrelated allele frequencies with a burn-in period of 100,000 iterations and MCMC analyses of 100,000 permutations. The accessions were not assigned to a given population. Ten iterations were run for each value of K, the number of subpopulations estimated to make up the total population. STRUCTURE HARVESTER (Earl and vonHoldt 2012) was used to determine the optimal K value, by generating a series of ΔK values, which represent the mean likelihood of K divided by the standard deviation of K, for the population. To further investigate population clusters, TASSEL v5 was used to construct a phylogenetic tree, using the Neighbour Joining method and all SNPs with MAF > 0.05. A cluster matching and permutation program (CLUMPP) was used from STRUCTURE HARVESTER for $K = 6$ to generate the Q matrix input (Jakobsson and Rosenberg 2007).

Genome-wide association (GWA) mapping was performed using TASSEL v5 using SNP markers with an allele frequency > 0.05. Analysis was conducted using generalised linear models (GLM) and mixed linear models (MLM) to determine the optimal model. Kinship data were calculated using TASSEL's 'centered IBS' method. Optimum compression level and P3D variance component estimation were used as MLM options. The false discovery rate (FDR) was determined using the Shiny implementation of the q-value R package (Storey et al. 2020). GEM and GWA results were visualised using R (https://github.com/BRAVO-research-project/pyrenopeziza-resistance). The most significantly

associated SNP markers were selected for further analysis, including distribution within the population and allelic effect.

The level of linkage disequilibrium (LD) varies between and across chromosomes depending on the position and level of selection. To determine the specific level of LD at each locus, the mean pair-wise r^2 for all markers on a chromosome to each of the 11 significantly associated markers was calculated within TASSEL v5 using the site by all analysis option. Markers were considered in LD when $r^2 > 0.15$.

Results

LLS scoring system

Percentage of leaf area with *P. brassicae* sporulation observed on infected leaves was the most consistent measurement of disease severity across all accessions (Karandeni Dewage et al. 2021) and was therefore used as the basis for the scoring system. Disease severity was scored on a scale of 1 to 6, with a score of 1 for no sporulation and 6 for the most sporulation (Fig. 1A, Supporting Information Figure S1). The image of part of an infected cv. Tapidor leaf (Fig. 1A, score 2) shows why *P. brassicae* is referred as to *C. concentricum* in its imperfect stage; this pathogen produces concentric rings of acervuli on its hosts. Patchy sporulation was observed on leaf laminas of 'couve-nabiça' and cv. Capitol with scores of 3 to 4, respectively (Fig. 1A). The entire leaf laminas of cv. Musette and cv. Daichousen were covered with acervuli and scored 5 and 6, respectively.

Variation in sporulation of *P. brassicae* on leaves of diverse *B. napus* accessions

A diversity set of 195 accessions was tested in glasshouse experiments for the amount of pathogen sporulation after spray inoculation of *B. napus* seedlings with local *P. brassicae* populations. The distribution of disease scores showed wide variation in *P. brassicae* sporulation among diverse *B. napus* accessions with an approximately normal distribution of this trait (Fig. 1B).

The glasshouse screen consisted of 10 independent experiments, each with 23 or 24 *B. napus* accessions with four reference cultivars per experiment (Supporting Information Table S2). The first seven experiments were done at the Bayfordbury campus of the University of Hertfordshire and the last three experiments at Rothamsted Research. Instead of cv. Bristol, cv. Cabriolet was used as a susceptible reference cultivar for the experiments at Rothamsted Research. All other reference cultivars were identical between both sites. Irrespective of the location, there were significant differences between reference cultivars in disease score. No significant

effects of experiment and experiment-by-cultivar interaction on disease score were observed (Supporting Information Notes S1). Combination of all 10 experiments and comparison of the shared reference cultivars Imola, Tapidor and Temple resulted in significant effects of both cultivar and experiment, but no significant experiment-by-cultivar interactions on disease score (Supporting Information Table S2). The disease scores of all three reference cultivars were less at Rothamsted Research than at Bayfordbury, with cv. Temple differing the most between these two environments (Supporting Information Figure S2). Restricting the analysis to cv. Imola and cv. Tapidor eliminated the significant effect of experiment. Differences in disease scores between Rothamsted Research and Bayfordbury could have resulted from different environmental conditions, different pathogen inoculum and/or different assessors at the two sites.

Nonlinear mixed model analysis established that *B. napus* cv. Cabriolet and cv. Imola scored as the most susceptible and most resistant cultivars amongst the five reference cultivars tested, respectively (Supporting Information Table S2). Intermediate scores were observed for the other three cultivars Temple, Tapidor and Bristol. While cv. Cabriolet scored as the most susceptible cultivar amongst all 195 accessions tested, 60 accessions scored less sporulation than cv. Imola; half of these 60 accessions scored significantly less than cv. Imola, including all 11 accessions that supported the least *P. brassicae* sporulation. These data clearly show that quantitative resistance present in 30 diverse accessions resulted in less *P. brassicae* sporulation than in cv. Imola, which has a major QDR locus against this pathogen.

GWA mapping of quantitative resistance against *P. brassicae*

SNP data for 200 lines from the Renewable Industrial Products from Rapeseed (RIPR) genotype dataset from the resources page of York Knowledgebase (http://yorknowledgebase.info) were used for this study. Following analysis with STRUCTURE, calculation of ΔK divided the population into two clusters (Fig. 2); cluster one mainly comprising of winter OSR and fodder types and cluster two comprising of other crop types (Supporting Information Table S3). It was shown that $K = 2$ is a common outcome when using the ΔK method (Janes et al. 2017). ΔK frequently identifies $K = 2$ as the top level of hierarchical structure, and further analysis is required to determine whether more subpopulations are present. Our analysis identified a further maximum in ΔK at $K = 6$. This divided the population into groups comprising the different crop types; cluster one—winter and fodder; cluster two—swede; cluster three—spring OSR; clusters four and five—Siberian kale types, and six semi-winter (Chinese) OSR (Supporting Information Table S3). Subsequent

228

Fig. 1 Phenotypic assessment of *P. brassicae* sporulation on *B. napus* leaves, following 10 days of incubation at high humidity after sampling. **A** Sporulation structures (acervuli) can be visualised macroscopically. Acervuli were best visualised using greyscale images to improve contrast. The percentage leaf area with sporulation is assessed as the disease score and expressed on a scale of 1 to 6; numbers above images refer to these disease scores. Accessions/cultivars Bristol (1, no sporulation), Tapidor (2, < 10% leaf area with sporulation), 'couve-nabiça' (3, 10–25% leaf area with sporulation), Capitol (4, 25–50% leaf area with sporulation), Musette (5, 50–75% leaf area with sporulation) and Daichousen (6, 75–100% leaf area with sporulation) are shown. **B** Distribution of disease scores, representing the percentage leaf area with *P. brassicae* sporulation among 195 diverse *B. napus* accessions on a scale of 1 to 6. The data represent a total of 1190 assessments in 10 glasshouse experiments, each with 24 accessions and five replicates, with the exception of two experiments that contained only 23 accessions (Table S1). Note that the data are approximately normally distributed. The scores are adjusted means after analysis of a linear mixed model. Ten bins (red bars) were created for the histogram. The blue density curve is a kernel density estimate and provides a smoother description of the distribution. The rug plot below is a one-dimensional representation of adjusted means for individual accessions
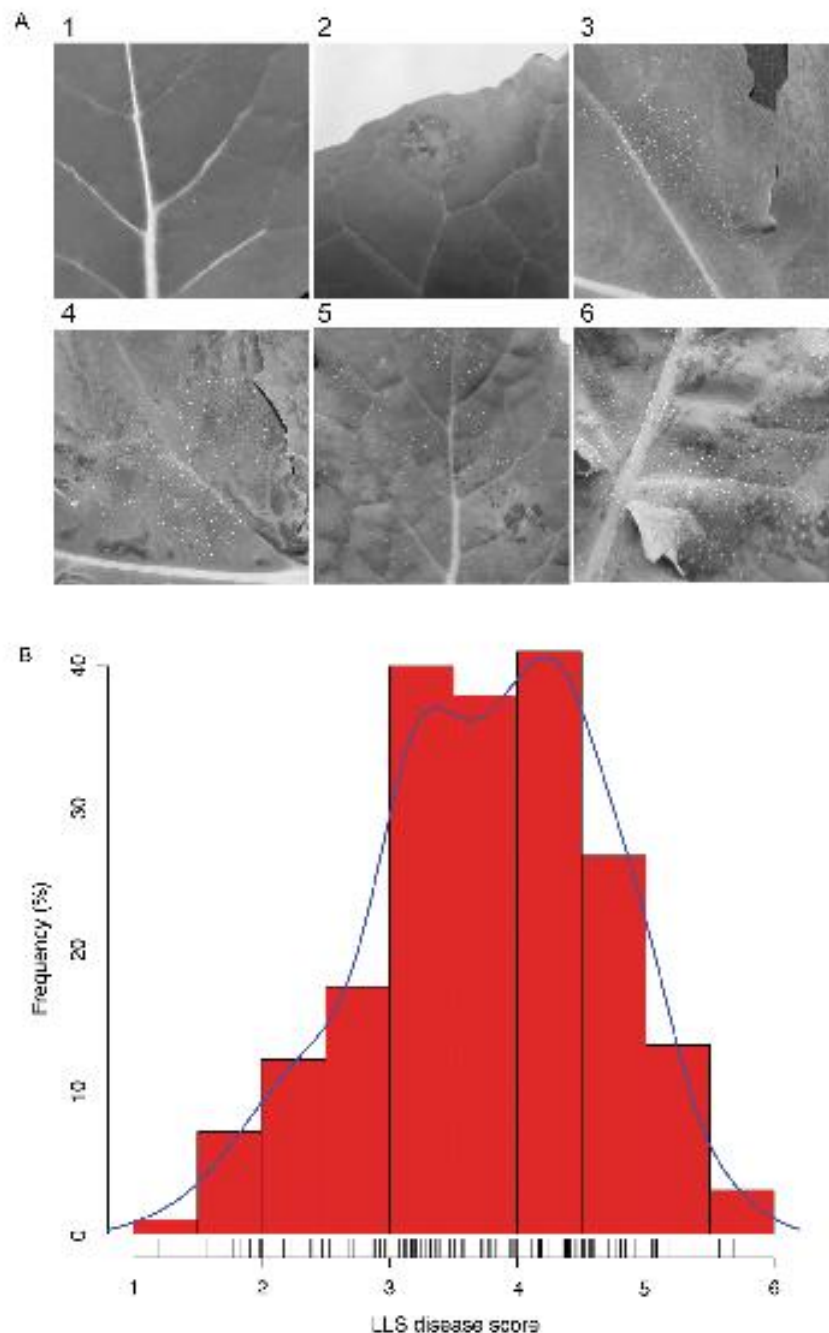
phylogenetic analysis showed a delineation of these crop types (Fig. 2), with the different crop types forming clear subgroups within the tree. A number of accessions did not cluster with their given crop types. However, bar diagram outputs from STRUCTURE (Supporting Information Figure S4) showed a level of admixture within these accessions. Given the evidence for population substructure

beyond $K = 2$, a structure of $K = 6$ was taken forward for use in association mapping.

Only lines with both population structure and phenotypic data were used for GWA mapping. Of the 200 lines used for generating population structure, 182 were used for GWA mapping. TASSEL identified a generalised linear modelling approach as an optimal fit for the phenotypic
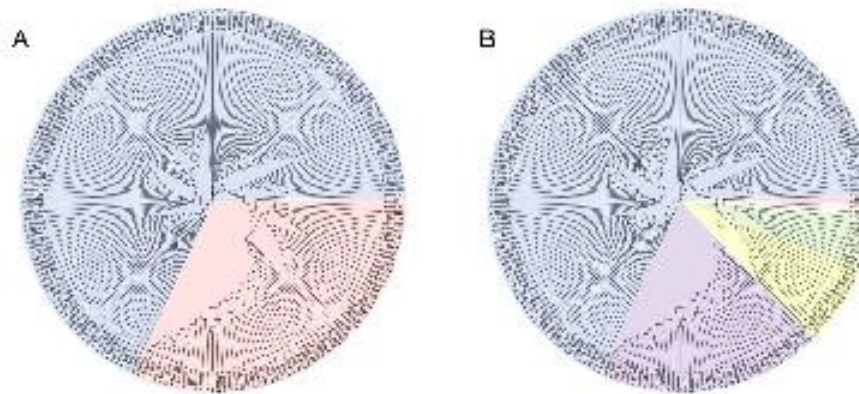
Fig. 2 Phylogenetic tree showing the distribution of clusters from STRUCTURE analysis; A K=2, divides the population into two main clusters comprising winter oilseed rape (OSR) and late winter/ fodder types (blue) and other crop types (red). B K=6, provides finer population structure identifying subpopulations of crop types comprising winter OSR and late winter/fodder types (blue), spring OSR (purple), semi-winter OSR (yellow), swede (green), Siberian kale group 1 (light orange), Siberian kale group 2 (red). For both A and B, some lines do not cluster phylogenetically with their crop type groups as observed in STRUCTURE due to a high degree of admixture. Detailed population structure is given in Supporting Information Figure S4 and Supporting Information Table S3

data (Supporting Information Figure S5). Eleven significant marker associations with LLS infection score were observed at $P < 0.0001$ (Table 1); however, none of these were significant at the FDR < 0.05. This is not unexpected as resistance against *P. brassicae* is a highly quantitative trait, with no known *R* gene loci.

The allelic effects of identified GWA maxima were determined (Table 2). The distribution of alleles contributing to resistance was not determined by crop type or phylogenetic relationship. Due to sequence similarities, cross alignment of transcriptome reads occurs between homeologous loci in the A and C genomes. This means that allelic calls can be the same in each genome or carry alternate alleles in the A and C genomes, referred to as a hemi-SNP, resulting in an ambiguity call during SNP calling. Three loci, *LLSC01*, *LLSA09a* and *LLSC02*, showed the strongest resistance when present as hemi-SNPs, suggesting a resistance benefit linked to carrying an alternative allele at the homeologous locus. Loci *LLSA01* and *LLSC04* showed that the majority of OSR in the panel carried the resistant allele; therefore, these may have already been selected for during breeding. Lines carrying alternate alleles at the homeologous position were also present, suggesting some breeding lines may not be optimised for these potential resistance loci. Loci *LLSA02*, *LLSA07*, *LLSA09b* and *LLSC08a* carried both A and C genome resistance alleles in a small number of lines, with most lines carrying alternate alleles at the homeologous loci. For locus *LLSC08a*, only one line carried susceptible alleles in both sub-genomes, resulting in an elevated disease score. For loci *LLSC05* and *LLSC08b*, resistant alleles at the two homeologous loci were not present within winter-OSR (WOSR) or in the case of *LLSC08b*, within the panel tested.

Although the 11 GWA markers detail the genetic variation most significantly associated with resistance against *P. brassicae* within this analysis, transcriptome sequencing does not provide all potential genetic variants present across the panel. Genetic polymorphisms close to the causal variation will be associated on the basis of genetic linkage or LD. In the case of LD, the GWA markers may not be indicative of the causal gene. Instead, causal genes will be more or less closely linked to the GWA marker. Each GWA marker was tested for LD against all other markers on a chromosome. Four of the 11 significantly associated markers, loci *LLSA02*, *LLSA09a*, *LLSC02*, *LLSC08b*, exhibited LD with $r^2 > 0.15$, thus defining the region where the causal gene is likely to be situated (Table 3, Fig. 3).

Eight gene expression markers are associated with resistance or susceptibility to *P. brassicae* infection

The transcriptomes of the 195 accessions were used to analyse the disease scores as a function of the expression of all gene models using a general linear model with an FDR of 0.001. A list of eight genes with P-values $< 1.6 \times 10^{-7}$ was selected for further analysis (Table 4). Linear regressions of the disease score versus the expression of each gene generated different slopes (Supporting Information Figure S3); the expression of seven genes was negatively correlated with the

Table 1 Genome-wide association (GWA) markers for resistance against *Pyrenopeziza brassicae* in *Brassica napus*

Locus	Brassica ID[a]	Chromosome	Marker position[b]	Reference base	Position (bp)	TAIR ID	Gene descriptor	*P*-value	−Log10P
LLSA01	BnaA01g25830D	A01	549	T	25,905,850	AT1G70980.1	Class II aminoacyl-tRNA and biotin synthetases superfamily protein SYNC3	1.41E−05	4.85
LLSC01	Bo1g123690.1	C01	471	T	37,055,696	AT3G16150.1	*N*-terminal nucleophile aminohydrolases (Ntn hydrolases) superfamily protein	1.58E−05	4.80
LLSA09a	Cab037694.1	A09	1371	C	175,592	AT4G00360.1	Cytochrome P450, family 86, subfamily A, polypeptide 2	1.68E−05	4.77
LLSA02	Cab039409.2	A02	406	C	1,016,409	AT5G06060.1	NAD(P)-binding Rossmann-fold superfamily protein	3.05E−05	4.52
LLSC08b	Bo8g108400.1	C08	610	G	38,642,478	AT1G12120.1	Plant protein of unknown function (DUF863)	5.24E−05	4.28
LLSA07	Cab020822.1	A07	852	G	27,411,592	AT1G77760.1	Nitrate reductase 1	6.29E-05	4.20
LLSC05	Bo5g150110.1	C05	1257	A	46,163,251	AT3G03250.1	UDP-GLUCOSE PYROPHOSPHORYLASE 1	7.16E−05	4.15
LLSA09b	Cab000353.1	A09	336	G	33,133,915	AT3G51370.1	Protein phosphatase 2C family protein	8.35E−05	4.08
LLSC02	Bo2g163990.1	C02	1694	G	51,188,221	AT5G62190.1	DEAD box RNA helicase (PRH75)	8.85E−05	4.05
LLSC04	Bo4g006960.1	C04	1050	A	690,146	AT3G61940.1	Cation efflux family protein (MTPA1)	9.33E−05	4.03
LLSC08a	Bo8g004430.1	C08	993	C	899,480	N/A	N/A	9.33E−05	4.03

[a]Markers showing association ($P < 0.0001$) with light leaf spot infection score as determined using the GLM model
[b]Position in bp given from pseudomolecule V11 (Havlickova et al. 2018)

disease score. Thus, expression was greatest when the least sporulation was observed. These seven GEMs may therefore contribute to partial resistance against *P. brassicae*. Another gene, encoding an HXXXD-type acyl-transferase (Table 4), had the opposite expression pattern with an expression positively correlated with the disease score. This is therefore a candidate gene for susceptibility to *P. brassicae*.

Discussion

QDR is the defence mechanism against *P. brassicae* in *B. napus*

Our pathosystem combined with association genetics enabled identification of candidate QDR gene loci for resistance

Table 2 Allelic effects of identified genome-wide association (GWA) markers for resistance against *Pyrenopeziza brassicae* in *Brassica napus*

Locus	Brassica ID	Marker position	Allele	N	Allelic effect	Resistant allele	Presence in WOSR[a]	Notes
LLSA01	BnA01g25830D	549	A/T or T/A	41	0.00	T	Common	Some accessions heterozygous, i.e. breeding potential
			TT	132	−0.62			
LLSC01	Bo1g123690	471	C/T or T/C	7	0.00	Mix	Rare	Unusual heterozygote advantage
			TT	66	1.31			
			CC	84	1.36			
LLSA09a	Cab037694	1371	G/C or C/G	12	0.00	Mix	Rare	Unusual heterozygote advantage
			CC	123	1.24			
			GG	41	1.20			
LLSA02	Cab039409	406	C/T or T/C	9	0.00	C	Rare	Seven WOSR accessions, but no modern ones
			TT	137	−0.39			
			CC	32	−1.14		Heterozygote	
LLSC08b	Bo8g108400	610	G/T or T/G	52	0.00	T	common	No homozygotes for T
			GG	110	0.56			
LLSA07	Cab020822.1	852	G/C or C/G	150	0.00	G	Rare	Nine WOSR accessions, including modern ones
			CC	12	0.67			
			GG	19	−0.47			
LLSC05	Bo5g150110	1257	A/C or C/A	158	0.00	A	Rare	AA not present in WOSR
			CC	16	−0.68			
			AA	7	−1.44			
LLSA09b	Cab000353	336	G/T or T/G	133	0.00	G	Rare	Present within WOSR
			GG	48	−0.63			
LLSC02	Bo2g163990	1694	AA	78	0.70	Mix	Common	Unusual heterozygote advantage
			GG	28	0.60			
			A/G or G/A	44	0.00			
LLSC04	Bo4g006960	1050	AA	103	−0.42	A	Common	AA common in WOSR
			GG	1	2.79			
			A/G or G/A	48	0.00			
LLSC08a	Bo8g004430	993	C/G or G/C	140	0.00	G	Rare	GG rare but present in two WOSR accessions
			GG	6	−0.10			
			CC	1	4.43			

[a]WOSR: Winter oilseed rape

Table 3 Linkage disequilibrium of markers associated with resistance against *Pyrenopeziza brassicae* in *Brassica napus*

Locus	Brassica ID	Position (bp)	*P*-value	LD upper marker bound	Pseudomolecule position[a]	LD lower marker bound	Pseudomolecule position[a]	LD Spread (Mb)
LLSA09	Cab037694.1	175,592	1.68E−05	Cab037721.1	A09_000021078_000020391	Cab042612.1	A09_001395929_001397818	1.38
LLSA02	Cab039409.2	1,016,409	3.05E−05	Cab039419.4	A02_000954941_000946007	Cab039323.2	A02_001448258_001444400	0.49
LLSC08	Bo8g108400.1	38,642,478	5.24E−05	Bo8g108400.1	C08_038642478_038643814	Bo8g108420.1	C08_038666739_038667339	0.02
LLSC02	Bo2g163990.1	51,188,221	8.85E−05	Bo2g161630.1	C02_050925826_050930832	BnaC02g43790D	C02_052872282_052871472	1.95

[a]Position in bp given from pseudomolecule V11 (Havlickova et al. 2018)
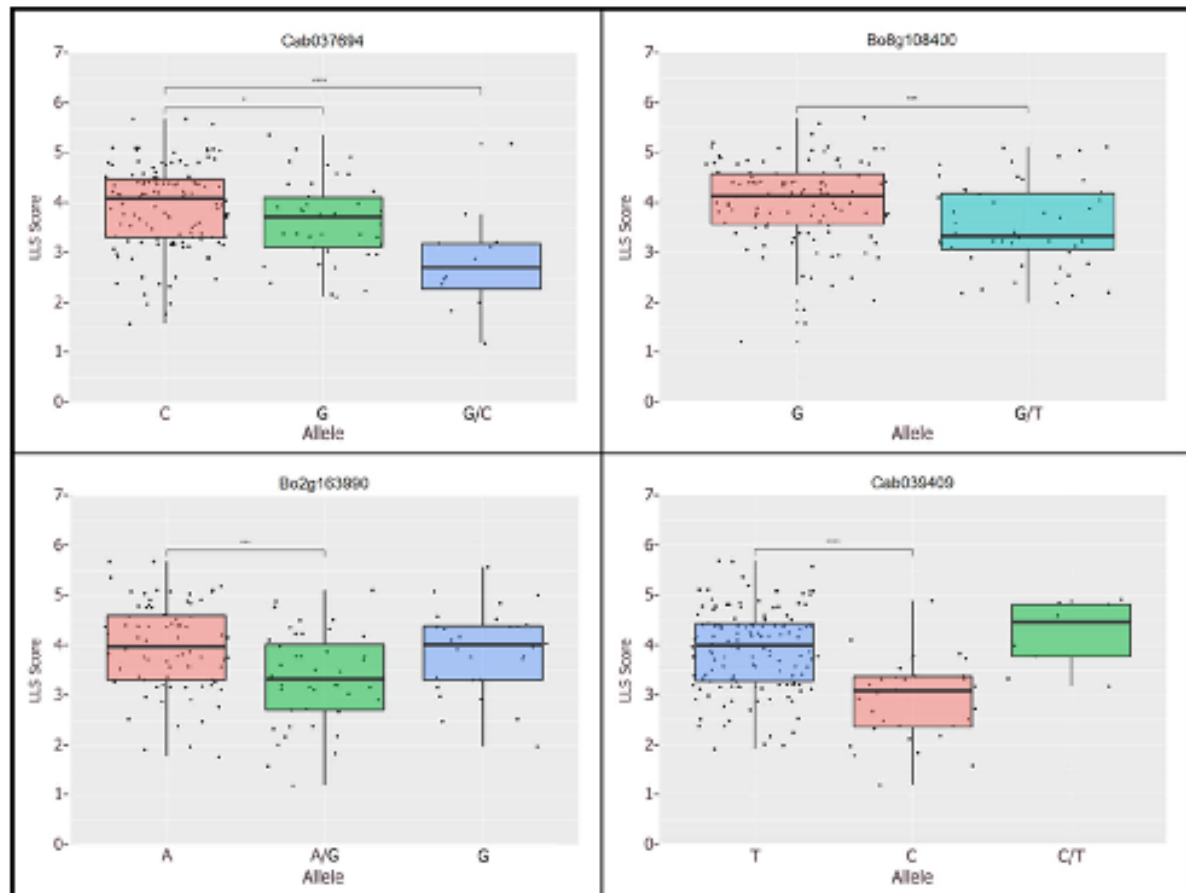
Fig. 3 Effects of SNPs at GWA markers that were in linkage disequilibrium on QDR against *P. brassicae*. Box plots were generated in R. The box represents the lower (25%) and upper (75%) quartiles with the median shown as a bar. The whiskers extend to the most extreme data point that is no more than 1.5 times the interquartile distance from the box. Outliers may extend beyond the whiskers. Jitters illustrate individual measurements. Resistance alleles were heterozygous in three cases or homozygous in one case. Asterisks indicate significant differences at $P < 0.05$ (*), 0.001 (***) or $P < 0.0001$ (****)

or susceptibility to *P. brassicae*. GWA mapping clearly demonstrated the existence of multiple genes contributing to QDR, confirming that combinations of genes with relatively minor effects are the predominant mechanism of resistance against *P. brassicae*. This contrasts to resistance against *L. maculans*, which is controlled by both *R* genes (Larkan et al. 2013, 2020) and quantitative resistance loci (Huang et al. 2019). We could associate enhanced resistance with hemi-SNPs at some loci, indicating the presence of previously unknown cryptic QDR. Importantly, accessions were identified that were more resistant to *P. brassicae* than the well-characterised cv. Imola, which contains a single major QDR locus for resistance against this pathogen (Boys et al. 2012). Our investigation reveals novel QDR loci that are the primary mechanisms of resistance against *P. brassicae*. Our findings could also provide insight into mechanisms of QDR

against other closely related apoplastic fungal pathosystems, including *R. commune* and *Venturia inaequalis*, for durable disease control (Stotz et al. 2014).

Population structure analysis reflects history of OSR cultivation

The origin of cultivated OSR has been considered to be Europe (Lu et al. 2019). Spring cultivars that are commonly grown in North America and Australia were developed in the late eighteenth century, and semi-winter cultivars were introduced into China in the twentieth century. Moreover, distinct morphotypes and subspecies of swedes (*B. napus* subsp. *rapifera*) and kale (*B. napus* subsp. *pabularia*) were developed as root and leaf crops (An et al. 2019).

Table 4 Gene expression markers (GEMs); expression of the genes listed is highly correlated with light leaf spot disease scores

Brassica ID[a]	Chromosome[b]	$Log_{10}P$[c]	P-alue[d]	TAIR ID	Custom annotation[f]
Cab002134.1	A03	7.324	4.75E-08	AT4G23460.1	Adaptin β1/2-subunit of AP-1 and AP-2; sorting at endosome and TGN in conjunction with clathrin
Bo5g052100.1	C05	7.314	4.85E-08	AT2G30490.1	Cinnamate-4-hydroxylase (C4H), CYP73A5; cinnamic acid—>4-coumaric acid; involved in lignification
Cab042707.1	A10	7.300	5.01E-08	AT5G51120.1	Cab042707 (AT5G51120): Polyadenylate-binding protein 1, controls length of poly(A) tail; localised to nuclear speckles, involved in pre-mRNA splicing
Cab000575.1	A09	6.997	1.01E-07	AT3G53990.1	Universal stress protein; localised to nucleus and cytoplasm; RNA chaperone, oxidative stress-related, antifungal activity
Bo2g028420.1	C02	6.958	1.10E-07	AT5G58700.1	Phosphatidylinositol-specific phospholipase C (PLC4); Ca2+signalling; *in vitro* interaction with PEN3
BnaA04g20860D	A04	6.862	1.37E-07	N/A	HXXXD-type acyl-transferase
Cab046181.1	A05	6.822	1.51E-07	AT3G01090.3	SNF1 kinase homolog 10 (KIN10); stress-related energy deprivation response, autophagy activation
Bo7g093320.1	C07	6.798	1.59E-07	AT5G28060.1	40S ribosomal protein S24

[a]Pan-transcriptome gene ID, http://yorknowledgebase.info

[b]*Brassica napus* chromosome location

[c]Based on Manhattan plot analysis; false discovery rate (FDA)=0.001

[d]Based on analysis of variance (ANOVA); disease score used as the dependent variable, gene expression (RPKM) as the independent variable

[e]The Arabidopsis Information Resource gene ID

[f]Consensus of web-based annotation and literature review

The population structure analysis using more than a thousand SNPs suggested genetic subdivisions into winter, spring, semi-winter and fodder OSR as well as swedes, and Siberian kale types are consistent with other published data based on *B. napus* genome sequences (An et al. 2019; Lu et al. 2019). The phylogenetic comparison reported here may be biased by the *B. napus* accessions that were used, but it suggests WOSR to be ancestral to kales, with spring OSR, swedes and semi-spring OSR being more derived (Fig. 2). The established population structure was used with associative transcriptomics to identify GWA markers and GEMs linked to quantitative resistance against *P. brassicae*.

GWA mapping indicates four QDR loci against *P. brassicae*

GWA mapping identified four loci in LD, showing multiple markers within a region associated with the infection score, and therefore, more likely linked to QDR against *P. brassicae* than single associated SNP markers. The loci on chromosomes A02, A09, C02 and C08 were not located in regions previously identified for resistance against *P. brassicae* (Boys et al. 2012; Bradburne et al. 1999; Karandeni Dewage et al. 2022; Pilet et al. 1998). The LD observed on chromosome A09 coincides with a homeologous QTL for seed glucosinolate content (Qian et al. 2014). The spread of the LD on chromosomes A02, A09 and C02 was too large to identify candidate gene loci that might be responsible

for QDR against *P. brassicae*. In contrast, the LD spread on chromosome C08 was narrow. The GWA marker Bo8g108400, corresponding to BnaC08g41550D, encodes an Cys-rich protein of unknown function. The hemi-SNP results in Gly204Cys substitution, which could be functionally significant (Perry et al. 2009). Of note, this codon is otherwise conserved in *B. oleracea*, *B. rapa* and for the homeolog *BnaA09g47370D*. Collectively, this could point to an important novel gene involved in host–pathogen interactions.

An alternative explanation could be that this gene was located right next to an ortholog of the *Arabidopsis thaliana* flavin-containing monooxygenase gene FMO_{GS-OX5} (At1g12140) that converts methylthioalkyl to methylsulfinylalkyl (MS) glucosinolates. MS glucosinolates are precursors to MS isothiocyanates that are toxic to phytopathogenic fungi (Stotz et al. 2011b). Importantly, FMO_{GS-OX5} has a preference for long-chain aliphatic glucosinolates (Li et al. 2008), which release isothiocyanates that are most toxic to phytopathogenic fungi like *S. sclerotiorum* (Stotz et al. 2011b). Notably, a mutation in the FMO_{GS-OX5} gene also altered cytokinin and jasmonate levels (Garrido et al. 2020), which is of significance considering that *P. brassicae* is a cytokinin-producing pathogen (Ashby 1997). Although the impact of jasmonates on infections by *P. brassicae* has not yet been studied, jasmonates are known to influence many pathosystems (Stotz et al. 2011a; Zheng et al. 2012). The FMO_{GS-OX5} gene is also part of an *FMO* cluster and the paralog At1g12200 that corresponds to BnaC08g41500D is

induced after inoculation with *S. sclerotiorum* or *B. cinerea* (Stotz et al. 2011b). The role of this chrC08 locus in resistance against *P. brassicae* is therefore worth investigating.

The hemi-SNP for GWA marker Bo2g163990, encoding a nuclear localised DEAD box ATP-dependent RNA helicase, would result in a Gly565Asp substitution. However, in *B. rapa* and *B. napus*, a Ser and Asn are found in the same position, respectively. The amino acid substitutions would occur in the GUCT domain of these types of helicases. As these helicases are involved in development and abiotic stress responses (Liu et al. 2016; Perroud et al. 2021), it is not immediately obvious whether this helicase or another gene within LD are responsible for QDR at this locus.

The disclosed GWA markers will assist with the development of molecular markers for marker-assisted selection, plant breeding and crop improvement.

Putative function of GEMs in QDR

The expression of eight GEMs was correlated with resistance against or susceptibility to *P. brassicae*. Amongst them were three genes that were previously reported to be involved in host pathogen interactions, including a gene encoding a cinnamate-4-hydroxylase (C4H). *C4H* genes are induced after infection of *B. napus* with *S. sclerotiorum* or *L. maculans* (Becker et al. 2017; Wu et al. 2016) and infection of the liverwort *Marchantia polymorpha* with the oomycete *Phytophthora palmivora* (Carella et al. 2019). The product 4-coumarate feeds into phenylpropanoid, flavonoid and lignin biosynthesis. Mutations in the *C4H* gene of *A. thaliana* have pleiotropic developmental defects (El Houari et al. 2021). Multiple corresponding *C4H* genes occur in *B. napus*, which may have developed specialised functions, including involvement in resistance against *P. brassicae*.

Another gene, *PLC4*, is involved in resistance against pathogens. Expression of the tomato gene *SlPLC4* is tightly regulated in response to the apoplastic fungal pathogen *Cladosporium fulvum* with a tenfold increase in expression 7 days after infection (Vossen et al. 2010). *SlPLC4* contributes to *R* gene-mediated resistance against *Cladosporium fulvum* (Vossen et al. 2010). Unlike *SlPLC6*, *SlPLC4* is not involved in resistance against *Verticillium dahliae* or *Pseudomonas syringae*. PLC4 of *A. thaliana* interacts with PEN3 (Campe et al. 2016), which is involved in resistance to penetration and export of protective metabolites against microbial invasion (Lu et al. 2015; Stein et al. 2006).

Moreover, *KIN10* recently emerged as a gene involved in resistance against the clubroot pathogen in *A. thaliana* (Chen et al. 2021). *KIN10* is a central regulator in response to energy deprivation, facilitating survival under stress conditions (Baena-Gonzalez et al. 2007) including pathogen challenge (Chen et al. 2021). These findings are consistent with the correlated of *KIN10* expression and resistance against *P. brassicae* that we observed (Supporting Information Figure S3). All of these examples suggest that the GEMs we identified are of significance and potential breeding targets. Importantly, it also implicates other, less characterised genes, in resistance against pathogens (Table 1).

Conclusion

All resistance against *P. brassicae* found in 195 accessions of *B. napus* results from QDR with no evidence of *R* gene-mediated resistance. For genome-wide association studies, we developed an improved population structure with six phylogenetic groups based on *B. napus* crop types. We identified four gene loci significantly ($P = 0.0001$) associated with QDR and in LD. On chromosome A09, enhanced resistance was associated with a cryptic heterozygous locus for a cytochrome P450 gene co-localising with a previously described QTL for seed glucosinolate content. The expression of seven gene expression markers were positively correlated with resistance, whereas one, a HXXXD-type acyltransferase, was negatively correlated and so is a potential susceptibility gene. The results provide new insight into QDR against *P. brassicae* in *B. napus* and can be used for marker-assisted breeding in crop improvement.

Declarations

Conflict of Interest The authors have no relevant financial or non-financial interest to disclose.

References

An H, Qi X, Gaynor ML, Hao Y, Gebken SC, Mabry ME, McAlvay AC, Teakle GR, Conant GC, Barker MS, Fu T, Yi B, Pires JC (2019) Transcriptome and organellar sequencing highlights the complex origin and diversification of allotetraploid *Brassica napus*. Nat Commun 10:2878

Ashby AM (1997) A molecular view through the looking glass: the *Pyrenopeziza brassicae Brassica interaction*. Adv Bot Res 24:31–70

Baena-Gonzalez E, Rolland F, Thevelein JM, Sheen J (2007) A central integrator of transcription networks in plant stress and energy signalling. Nature 448:938–942

Bartoli C, Roux F (2017) Genome-wide association studies In plant pathosystems: toward an ecological genomics approach. Front Plant Sci 8:763

Becker MG, Zhang X, Walker PL, Wan JC, Millar JL, Khan D, Granger MJ, Cavers JD, Chan AC, Fernando DWG, Belmonte MF (2017) Transcriptome analysis of the *Brassica napus-Leptosphaeria maculans* pathosystem identifies receptor, signaling and structural genes underlying plant resistance. Plant J 90:573–586

Boys EF, Roques SE, West JS, Werner CP, Kinga GJ, Dyer PS, Fitt BDL (2012) Effects of *R* gene-mediated resistance in *Brassica napus* (oilseed rape) on asexual and sexual sporulation of *Pyrenopeziza brassicae* (light leaf spot). Plant Pathol 61:543–554

Bradburne R, Majer D, Magrath R, Werner CP, Lewis B, Mithen R (1999) Winter oilseed rape with high levels of resistance to *Pyrenopeziza brassicae* derived from wild *Brassica* species. Plant Pathol 48:550–558

Buttner B, Draba V, Pillen K, Schweizer G, Maurer A (2020) Identification of QTLs conferring resistance to scald (*Rhynchosporium commune*) in the barley nested association mapping population HEB-25. BMC Genom 21:837

Campe R, Langenbach C, Leissing F, Popescu GV, Popescu SC, Goellner K, Beckers GJ, Conrath U (2016) ABC transporter PEN3/PDR8/ABCG36 interacts with calmodulin that, like PEN3, is required for Arabidopsis nonhost resistance. New Phytol 209:294–306

Carella P, Gogleva A, Hoey DJ, Bridgen AJ, Stolze SC, Nakagami H, Schornack S (2019) Conserved biochemical defenses underpin host responses to oomycete infection in an early-divergent land plant lineage. Curr Biol 29(2282–2294):e2285

Carmody SM, King KM, Ocamb CM, Fraaije BA, West JS, du Toit LJ (2019) A phylogenetically distinct lineage of *Pyrenopeziza brassicae* associated with chlorotic leaf spot of Brassicaceae in North America. Plant Pathol 69:518–537

Chen W, Li Y, Yan R, Ren L, Liu F, Zeng L, Sun S, Yang H, Chen K, Xu L, Liu L, Fang X, Liu S (2021) SnRK1.1-mediated resistance of *Arabidopsis thaliana* to clubroot disease is inhibited by the novel *Plasmodiophora brassicae* effector PBZF1. Mol Plant Pathol 22:1057–1069

Cheng F, Mandakova T, Wu J, Xie Q, Lysak MA, Wang X (2013) Deciphering the diploid ancestral genome of the Mesohexaploid *Brassica rapa*. Plant Cell 25:1541–1554

Cowger C, Brown JKM (2019) Durability of quantitative resistance in crops: Greater than we know? Annu Rev Phytopathol 57:253–277

Delplace F, Huard-Chauveau C, Dubiella U, Khafif M, Alvarez E, Langin G, Roux F, Peyraud R, Roby D (2020) Robustness of plant quantitative disease resistance is provided by a decentralized immune network. Proc Natl Acad Sci U S A 117:18099–18109

Earl DA, vonHoldt BM (2012) STRUCTURE HARVESTER: a website and program for visualizing STRUCTURE output and implementing the Evanno method. Conserv Genet Res 4:359–361

El Houari I, Van Beirs C, Arents HE, Han H, Chanoca A, Opdenacker D, Pollier J, Storme V, Steenackers W, Qureshy M, Napier R, Beeckman T, Friml J, De Rybel B, Boerjan W, Vanholme B (2021) Seedling developmental defects upon blocking CINNAMATE-4-HYDROXYLASE are caused by perturbations in auxin transport. New Phytol 230:2275–2291

Garrido AN, Supijono E, Boshara P, Douglas SJ, Stronghill PE, Li B, Nambara E, Kliebenstein DJ, Riggs CD (2020) Flasher, a novel mutation in a glucosinolate modifying enzyme, conditions changes in plant architecture and hormone homeostasis. Plant J 103:1989–2006

Gilles T, Evans N, Fitt BDL, Jeger MJ (2000) Epidemiology in relation to methods for forecasting light leaf spot (*Pyrenopeziza brassicae*) severity on winter oilseed rape (*Brassica napus*) in the UK. Eur J Plant Pathol 106:593–605

Goodwin SB (2002) The barley scald pathogen *Rhynchosporium secalis* is closely related to the discomycetes *Tapesia* and *Pyrenopeziza*. Mycol Res 106:645–654

Harper AL, Trick M, Higgins J, Fraser F, Clissold L, Wells R, Hattori C, Werner P, Bancroft I (2012) Associative transcriptomics of traits in the polyploid crop species *Brassica napus*. Nat Biotechnol 30:798–802

Havlickova L, He Z, Wang L, Langer S, Harper AL, Kaur H, Broadley MR, Gegas V, Bancroft I (2018) Validation of an updated Associative Transcriptomics platform for the polyploid crop species *Brassica napus* by dissection of the genetic architecture of erucic acid and tocopherol isoform variation in seeds. Plant J 93:181–192

Hejna O, Havlickova L, He Z, Bancroft I, Curn V (2019) Analysing the genetic architecture of clubroot resistance variation in *Brassica napus* by associative transcriptomics. Mol Breed 39:112

Huang YJ, Paillard S, Kumar V, King GJ, Fitt BDL, Delourme R (2019) Oilseed rape (*Brassica napus*) resistance to growth of *Leptosphaeria maculans* in leaves of young plants contributes to quantitative resistance in stems of adult plants. PLoS One 14:e0222540

Jakobsson M, Rosenberg NA (2007) CLUMPP: a cluster matching and permutation program for dealing with label switching and multimodality in analysis of population structure. Bioinformatics 23:1801–1806

Janes JK, Miller JM, Dupuis JR, Malenfant RM, Gorrell JC, Cullingham CI, Andrew RL (2017) The K = 2 conundrum. Mol Ecol 26:3594–3602

Jiquel A, Gervais J, Geistodt-Kiener A, Delourme R, Gay EJ, Ollivier B, Fudal I, Faure S, Balesdent MH, Rouxel T (2021) A gene-for-gene interaction involving a "late" effector contributes to quantitative resistance to the stem canker disease in *Brassica napus*. New Phytol 231:1510–1524

Jones JDG, Dangl JL (2006) The plant immune system. Nature 444:323–329

Karandeni Dewage CS, Klöppel CA, Stotz HU, Fitt BDL (2018) Host–pathogen interactions in relation to management of light leaf spot disease (caused by *Pyrenopeziza brassicae*) on *Brassica* species. Crop Pasture Sci 69:9–19

Karandeni Dewage CS, Qi A, Stotz HU, Huang Y-J, Fitt BDL (2021) Interactions in the *Brassica napus–Pyrenopeziza brassicae* pathosystem and sources of resistance to *P. brassicae* (light leaf spot). Plant Pathol 70:2104–2114

Karandeni Dewage CS, Qi A, Stotz HU, Huang Y-J, Fitt BDL (2022) QTL mapping for resistance against *Pyrenopeziza brassicae* derived from a *Brassica napus* secondary gene pool. Front Plant Sci 13:786189. https://doi.org/10.3389/fpls.2022.786189

Larkan NJ, Lydiate DJ, Parkin IA, Nelson MN, Epp DJ, Cowling WA, Rimmer SR, Borhan MH (2013) The *Brassica napus* blackleg resistance gene *LepR3* encodes a receptor-like protein triggered by the *Leptosphaeria maculans* effector AVRLM1. New Phytol 197:595–605

Larkan NJ, Ma L, Haddadi P, Buchwaldt M, Parkin IAP, Djavaheri M, Borhan MH (2020) The *Brassica napus* wall-associated kinase-like (WAKL) gene *Rlm9* provides race-specific blackleg resistance. Plant J 104:892–900

Li J, Hansen BG, Ober JA, Kliebenstein DJ, Halkier BA (2008) Subclade of flavin-monooxygenases involved in aliphatic glucosinolate biosynthesis. Plant Physiol 148:1721–1733

Liu Y, Tabata D, Imai R (2016) A cold-Inducible DEAD-Box RNA helicase from *Arabidopsis thaliana* regulates plant growth and development under low temperature. PLoS One 11:e0154040

Looseley ME, Griffe LL, Buttner B, Wright KM, Bayer MM, Coulter M, Thauvin JN, Middlefell-Williams J, Maluk M, Okpo A, Kettles N, Werner P, Byrne E, Avrova A (2020) Characterisation of barley landraces from Syria and Jordan for resistance to rhynchosporium and identification of diagnostic markers for *Rrs1 Rh4*. Theor Appl Genet 133:1243–1264

Lu X, Dittgen J, Pislewska-Bednarek M, Molina A, Schneider B, Svatos A, Doubsky J, Schneeberger K, Weigel D, Bednarek P, Schulze-Lefert P (2015) Mutant allele-specific uncoupling of PENETRATION3 functions reveals engagement of the ATP-binding cassette transporter in distinct tryptophan metabolic pathways. Plant Physiol 168:814–827

Lu K, Wei L, Li X, Wang Y, Wu J, Liu M, Zhang C, Chen Z, Xiao Z, Jian H, Cheng F, Zhang K, Du H, Cheng X, Qu C, Qian W, Liu L, Wang R, Zou Q, Ying J, Xu X, Mei J, Liang Y, Chai YR, Tang Z, Wan H, Ni Y, He Y, Lin N, Fan Y, Sun W, Li NN, Zhou G, Zheng H, Wang X, Paterson AH, Li J (2019) Whole-genome resequencing reveals *Brassica napus* origin and genetic loci involved in its improvement. Nat Commun 10:1154

Mason AS, Rousseau-Gueutin M, Morice J, Bayer PE, Besharat N, Cousin A, Pradhan A, Parkin IA, Chevre AM, Batley J, Nelson MN (2016) Centromere locations in *Brassica* A and C genomes revealed through half-tetrad analysis. Genetics 202:513–523

Nelson R, Wiesner-Hanks T, Wisser R, Balint-Kurti P (2018) Navigating complexity to breed disease-resistant crops. Nat Rev Genet 19:21–33

Ngou BPM, Ahn HK, Ding P, Jones JDG (2021) Mutual potentiation of plant immunity by cell-surface and intracellular receptors. Nature 592:110–115

Penselin D, Munsterkotter M, Kirsten S, Felder M, Taudien S, Platzer M, Ashelford K, Paskiewicz KH, Harrison RJ, Hughes DJ, Wolf T, Shelest E, Graap J, Hoffmann J, Wenzel C, Woltje N, King KM, Fitt BD, Guldener U, Avrova A, Knogge W (2016) Comparative genomics to explore phylogenetic relationship, cryptic sexual potential and host specificity of *Rhynchosporium* species on grasses. BMC Genom 17:953

Perroud PF, Demko V, Ako AE, Khanal R, Bokor B, Pavlovic A, Jasik J, Johansen W (2021) The nuclear GUCT domain-containing DEAD-box RNA helicases govern gametophytic and sporophytic development in Physcomitrium patens. Plant Mol Biol 107:307–325

Perry J, Brachmann A, Welham T, Binder A, Charpentier M, Groth M, Haage K, Markmann K, Wang TL, Parniske M (2009) TILLING in Lotus japonicus identified large allelic series for symbiosis genes and revealed a bias in functionally defective ethyl methanesulfonate alleles toward glycine replacements. Plant Physiol 151:1281–1291

Pilet ML, Delourme R, Foisset N, Renard M (1998) Identification of QTL involved in field resistance to light leaf spot (*Pyrenopeziza brassicae*) and blackleg resistance (*Leptosphaeria maculans*) in winter rapeseed (*Brassica napus* L.). Theor Appl Genet 97:398–406

Qian L, Qian W, Snowdon RJ (2014) Sub-genomic selection patterns as a signature of breeding in the allopolyploid *Brassica napus* genome. BMC Genom 15:1170

Rohe M, Gierlich A, Hermann H, Hahn M, Schmidt B, Rosahl S, Knogge W (1995) The race-specific elicitor, NIP1, from the barley pathogen, Rhynchosporium secalis, determines avirulence on host plants of the Rrs1 resistance genotype. EMBO J 14:4168–4177

Stein M, Dittgen J, Sanchez-Rodriguez C, Hou BH, Molina A, Schulze-Lefert P, Lipka V, Somerville S (2006) Arabidopsis PEN3/PDR8, an ATP binding cassette transporter, contributes to nonhost resistance to inappropriate pathogens that enter by direct penetration. Plant Cell 18:731–746

Storey JD, Bass AJ, Dabney A, Robinson D (2020) Q-value estimation for false discovery rate control. 2.22.0 edn, Bioconductor open source software for bioinformatics, p R package

Stotz HU, Jikumaru Y, Shimada Y, Sasaki E, Stingl N, Mueller MJ, Kamiya Y (2011a) Jasmonate-dependent and COI1-independent defense responses against *Sclerotinia sclerotiorum* in *Arabidopsis thaliana*: auxin is part of COI1-independent defense signaling. Plant Cell Physiol 52:1941–1956

Stotz HU, Sawada Y, Shimada Y, Hirai MY, Sasaki E, Krischke M, Brown PD, Saito K, Kamiya Y (2011b) Role of camalexin, indole glucosinolates, and side chain modification of glucosinolate-derived isothiocyanates in defense of Arabidopsis against *Sclerotinia sclerotiorum*. Plant J Cell Mol Biol 67:81–93

Stotz HU, Mitrousia GK, de Wit PJ, Fitt BDL (2014) Effector-triggered defence against apoplastic fungal pathogens. Trends Plant Sci 19:491–500

Sylvester-Bradley R (1985) Revision of a code for stages of development in oilseed rape (*Brassica napus* L.). Asp Appl Biol 10:395–400

Vossen JH, Abd-El-Haliem A, Fradin EF, van den Berg GC, Ekengren SK, Meijer HJ, Seifi A, Bai Y, ten Have A, Munnik T, Thomma BP, Joosten MH (2010) Identification of tomato phosphatidylinositol-specific phospholipase-C (PI-PLC) family members and the role of PLC4 and PLC6 in HR and disease resistance. Plant J 62:224–239

Wells R, Trick M, Fraser F, Soumpourou E, Clissold L, Morgan C, Pauquet J, Bancroft I (2013) Sequencing-based variant detection in the polyploid crop oilseed rape. BMC Plant Biol 13:111

Wu J, Zhao Q, Liu S, Shahid M, Lan L, Cai G, Zhang C, Fan C, Wang Y, Zhou Y (2016) Genome-wide association study identifies new loci for resistance to sclerotinia stem rot in *Brassica napus*. Front Plant Sci 7:1418

Yuan M, Jiang Z, Bi G, Nomura K, Liu M, Wang Y, Cai B, Zhou JM, He SY, Xin XF (2021) Pattern-recognition receptors are required for NLR-mediated plant immunity. Nature 592:105–109

Zheng XY, Spivey NW, Zeng W, Liu PP, Fu ZQ, Klessig DF, He SY, Dong X (2012) Coronatine promotes *Pseudomonas syringae* virulence in plants by activating a signaling cascade that inhibits salicylic acid accumulation. Cell Host Microbe 11:587–596

Zheng X, Koopmann B, Ulber B, von Tiedemann A (2020) A global survey on diseases and pests in oilseed rape—current challenges and innovative strategies of control. Front Agron 2:590908

1b

Table 4. Gene expression markers (GEMs); expression of the genes listed is highly correlated with light leaf spot disease scores.

Brassica Ida	Chromosome[b]	Log_{10}P[c]	P-value[d]	TAIR ID	Custom annotation[f]
Cab002134.1	A03	7.324	4.75E-08	AT4G23460.1	Adaptin β1/2-subunit of AP-1 and AP-2; sorting at endosome and TGN in conjunction with clathrin
Bo5g052100.1	C05	7.314	4.85E-08	AT2G30490.1	Cinnamate-4-hydroxylase (C4H), CYP73A5; cinnamic acid -> 4-coumaric acid; involved in lignification
Cab042707.1	A10	7.300	5.01E-08	AT5G51120.1	Cab042707 (AT5G51120): Polyadenylate-binding protein 1, controls length of poly(A) tail; localised to nuclear speckles, involved in pre-mRNA splicing
Cab000575.1	A09	6.997	1.01E-07	AT3G53990.1	Universal stress protein; localised to nucleus and cytoplasm; RNA chaperone, oxidative stress-related, antifungal activity
Bo2g028420.1	C02	6.958	1.10E-07	AT5G58700.1	Phosphatidylinositol-specific phospholipase C (PLC4); Ca2+ signalling; *in vitro* interaction with PEN3
BnaA04g20860D	A04	6.862	1.37E-07	N/A	HXXXD-type acyl-transferase
Cab046181.1	A05	6.822	1.51E-07	AT3G01090.3	SNF1 kinase homolog 10 (KIN10); stress-related energy deprivation response, autophagy activation
Bo7g093320.1	C07	6.798	1.59E-07	AT5G28060.1	40S ribosomal protein S24

[a] Pan-transcriptome gene ID, http://yorknowledgebase.info

[b] *Brassica napus* chromosome location

[c] Based on Manhattan plot analysis; false discovery rate (FDA) = 0.001

[d] Based on analysis of variance (ANOVA); disease score used as the dependent variable, gene expression (RPKM) as the independent variable

[e] The Arabidopsis Information Resource gene ID

[f] Consensus of web-based annotation and literature review

1c

Table S1. Environmental temperature conditions during 10 glasshouse experiments studying susceptibililty of *Brassica napus* to *Pyrenopeziza brassicae*.

Location	Experiment	Germination[1]			Transplanting[1]			Innoculation[1]			Sampling[1]		
Bayfordbury	1	N/A[2]			7th December 2016			20th December 2016			13th January 2016		
		N/A	N/A	N/A	Max °C[3]	Avg °C	Min °C	Max °C	Avg °C	Min °C	Max °C	Avg °C	Min °C
		N/A	N/A	N/A	11	9.6	9	5	3.6	2	4	1.3	0
Bayfordbury	2	3rd January 2017			17th January 2017			13th February 2017			9th March 2017		
		Max °C	Avg °C	Min °C	Max °C	Avg °C	Min °C	Max °C	Avg °C	Min °C	Max °C	Avg °C	Min °C
		4	1.6	-2	4	1.2	-1	9	4.3	2	14	10.4	6
Bayfordbury	3	N/A			24th March 2017			3rd April 2017			27th April 2017		
		N/A	N/A	N/A	Max °C	Avg °C	Min °C	Max °C	Avg °C	Min °C	Max °C	Avg °C	Min °C
		N/A	N/A	N/A	12	6.9	3	16	9.4	3	9	5.5	0
Bayfordbury	4	21st April 2017			9th May 2017			22nd May 2017			15th June 2017		
		Max °C	Avg °C	Min °C	Max °C	Avg °C	Min °C	Max °C	Avg °C	Min °C	Max °C	Avg °C	Min °C
		13	11	9	10	7.7	5	23	15.8	8	21	17	12
Bayfordbury	5	8th December 2017			21st December 2017			8th January 2017			1st February 2017		
		Max °C	Avg °C	Min °C	Max °C	Avg °C	Min °C	Max °C	Avg °C	Min °C	Max °C	Avg °C	Min °C
		3	1.1	-1	11	9.6	8	3	1.4	-2	6	4.1	2
Bayfordbury	6	15th December 2017			2nd January 2018			22nd January 2018			15th February 2018		
		Max °C	Avg °C	Min °C	Max °C	Avg °C	Min °C	Max °C	Avg °C	Min °C	Max °C	Avg °C	Min °C
		4	2.8	1	12	6.3	3	9	7.1	5	8	6	3
Bayfordbury	7	2nd February 2018			19th February 2018			12th March 2018			5th April 2018		
		Max °C	Avg °C	Min °C	Max °C	Avg °C	Min °C	Max °C	Avg °C	Min °C	Max °C	Avg °C	Min °C
		6	3.9	3	10	7.9	6	10	7.1	5	11	6.7	3
Rothamsted	8	14th October 2019			21st October 2019			11th November 2019			5th December 2019		
		Max °C	Avg °C	Min °C	Max °C	Avg °C	Min °C	Max °C	Avg °C	Min °C	Max °C	Avg °C	Min °C
		15	11.1	9	11	9.8	9	8	5.6	4	8	5.1	1
Rothamsted	9	14th November 2019			21st November 2019			12th December 2019			5th January 2020		
		Max °C	Avg °C	Min °C	Max °C	Avg °C	Min °C	Max °C	Avg °C	Min °C	Max °C	Avg °C	Min °C
		6	4.2	2	6	3.4	2	8	4.3	0	7	6.3	5
Rothamsted	10	17th December 2019			22nd December 2019			12th January 2020			5th February 2020		
		Max °C	Avg °C	Min °C	Max °C	Avg °C	Min °C	Max °C	Avg °C	Min °C	Max °C	Avg °C	Min °C
		6	5.1	4	7	6.5	5	10	7.5	3	7	3.6	0

[1] Germination, transplanting, inoculation and sampling refer to the stages in experiments with *B. napus* seedlings.

[2] Not available

[3] Information about temperature was obtained from United Kingdom Weather History in Luton, U.K. (51.88 °N, 0.36 °W)

2

Leptosphaeria maculans isolates with variations in *AvrLm1* and *AvrLm4* effector genes induce differences in defence responses but not in resistance phenotypes in cultivars carrying the *Rlm7* gene

Henrik Uwe Stotz,[a][*] Ajisa Muthayil Ali,[a] Lucia Robado de Lope,[a] Mohammed Sajid Rafi,[b] Georgia Konstantinou Mitrousia,[a][†] Yong-Ju Huang[a] and Bruce David Ledger Fitt[a]

Abstract

BACKGROUND: The phoma stem canker pathogen *Leptosphaeria maculans* is one of the most widespread and devastating pathogens of oilseed rape (*Brassica napus*) in the world. Pathogen colonization is stopped by an interaction of a pathogen *Avr* effector gene with the corresponding host resistance (R) gene. While molecular mechanisms of this gene-for-gene interaction are being elucidated, understanding of effector function remains limited. The purpose of this study was to determine the action of *L. maculans* effector (*AvrLm*) genes on incompatible interactions triggered by *B. napus* noncorresponding *R* (*Rlm*) genes. Specifically, effects of *AvrLm4-7* and *AvrLm1* on *Rlm7*-mediated resistance were studied.

RESULTS: Although there was no major effect on symptom expression, induction of defence genes (e.g. *PR1*) and accumulation of reactive oxygen species was reduced when *B. napus* cv. Excel carrying *Rlm7* was challenged with a *L. maculans* isolate containing *AvrLm4-7* and a point mutation in *AvrLm4-7* (*AvrLm1, avrLm4-AvrLm7*) compared to an isolate lacking *AvrLm1* (*avrLm1, AvrLm4-AvrLm7*). *AvrLm7*-containing isolates, isogenic for presence or absence of *AvrLm1*, elicited similar symptoms on hosts with or without *Rlm7*, confirming results obtained with more genetically diverse isolates.

CONCLUSION: Careful phenotypic examination of isogenic *L. maculans* isolates and *B. napus* introgression lines demonstrated a lack of effect of *AvrLm1* on *Rlm7*-mediated resistance despite an apparent alteration of the *Rlm7*-dependent defence response using more diverse fungal isolates with differences in *AvrLm1* and *AvrLm4*. As deployment of *Rlm7* resistance in crop cultivars increases, other effectors need to be monitored because they may alter the predominance of *AvrLm7*.
© 2023 The Authors. *Pest Management Science* published by John Wiley & Sons Ltd on behalf of Society of Chemical Industry.

Supporting information may be found in the online version of this article.

Keywords: apoplast; effector; gene expression; reactive oxygen species; *R* gene-mediated resistance; symptoms

1 INTRODUCTION

Leptosphaeria maculans (syn. *Plenodomus lingam*, anamorph: *Phoma lingam*) causes phoma stem canker of oilseed rape (*Brassica napus*) and annual yield losses of approximately US$1 billion globally.[1] The species name *L. maculans* is preferred here because the alternative species name has not been universally adopted.[2,3] This apoplastic fungal pathogen spreads disease through release of air-borne ascospores.[4,5] Once ascospores land on the surface of *B. napus* cotyledons or leaves, they germinate and subsequently penetrate the surface through stomatal pores.[6,7] Upon entry into the substomatal cavity, the pathogen colonizes the apoplastic space of the foliar mesophyll layer. Following a period of

*   Correspondence to: H Stotz, Centre for Agriculture, Food and Environmental Management, University of Hertfordshire, Hatfield, Hertfordshire, AL10 9AB, UK. E-mail: h.stotz@herts.ac.uk

‡   This manuscript is destined for the special issue on "Integrated Pest Control in Oilseed Crops".

†   Present address: Rothamsted Research Ltd, West Common, Harpenden, Hertfordshire, AL5 2JQ, UK

a   Centre for Agriculture, Food and Environmental Management, University of Hertfordshire, Hertfordshire, UK

b   Khalifa Center for Genetic Engineering and Biotechnology, United Arab Emirates University, Al Ain, PO Box 15551, United Arab Emirates

symptomless growth for more than a week, lesions with pycnidia, capable of releasing asexual spores, develop within 2 weeks after infection.[6] During incompatible interactions, single dominant *R* genes control foliar resistance by recognizing corresponding pathogen *Avr* genes (that encode effectors) to prevent pathogen growth from the leaf to the stem.[8,9] During compatible interactions, the pathogen continues asymptomatic colonization of the leaf petiole and subsequently the stem for months, before finally causing severe stem canker and yield loss.[10,11]

More than 19 *R* genes against *L. maculans* have been identified in *B. napus* and five of them have been cloned.[12–16] Conversely, the *L. maculans* genome contains >14 genes encoding effectors, 12 of which have been cloned, including *AvrLm1* and *AvrLm4-7*.[17–21] The number of putative effectors is far greater.[22] *Rlm1* and *LepR3* resistance genes, operating against *AvrLm1*, have been rendered ineffective in France and Australia, respectively;[23,24] this breakdown was caused by a decrease in frequencies of avirulent *AvrLm1* in *L. maculans* populations in both France and Australia.[23,25] Conversely, discontinuation of use of *Rlm1* or *LepR3* has resulted in an increase in *AvrLm1* frequencies, suggesting that there is a fitness penalty for the loss of this *AvrLm1* function, confirming previous studies.[25,26] Whereas *AvrLm4-7* and most other effector genes code for cysteine-rich peptides, *AvrLm1* encodes only a single Cys residue.[17] Recognition of AvrLm1 by LepR3 occurs outside the plant cell, not requiring the first 40 amino acids following the signal peptide.[27]

AvrLm1 triggers defence responses in *B. napus* cv. Columbus (carrying *Rlm1*), including salicylic acid (SA) and hydrogen peroxide (H_2O_2) production as well as induction of *ICS1*, a SA biosynthetic gene, *WRKY70* and *PR-1* expression.[28] Pathogen effectors are known to suppress innate immune responses, such as pattern-triggered immunity (PTI).[29] This may explain that *AvrLm4-7* transiently reduces SA production, *PR-1* expression and H_2O_2 accumulation during compatible interactions with susceptible *B. napus* cvs Eurol and ES Astrid.[30] While the AvrLm1 effector is recognized by the receptor-like protein (RLP) LepR3 outside the plant cell,[8] AvrLm1 interacts with the cytosolic signal transducer mitogen-activated protein kinase 9 (MPK9) of *B. napus* to increase host susceptibility.[31] Conversely, documented evidence for suppression of *R* gene-mediated resistance by noncorresponding pathogen effectors is less frequent.[32] In the case of *AvrLm5-9*, *AvrLm3* and *AvrLm4-7*, however, evidence for interference with effector recognition has been obtained; *AvrLm4-7* suppresses both *Rlm3*- and *Rlm9*-mediated resistance.[33,34] These types of epistatic interactions have altered crop protection and rotation strategies to adjust to *L. maculans* isolates carrying multiple *Avr* genes because a simple gene-for-gene model does not always determine the outcome of a particular host–pathogen interaction.[13]

The purpose of this study was to determine the action of *L. maculans* effectors on incompatible interactions triggered by noncorresponding *R* genes. Of particular interest were the effects of *AvrLm1* and *AvrLm4* on the defence responses mediated by the noncorresponding *R* gene *Rlm7*. Hence, the effects of *AvrLm4-7* and presence or absence of *AvrLm1* on *Rlm7*-mediated resistance were tested. Attention was given to effector-triggered defence (ETD) responses – defence-related gene expression and reactive oxygen species (ROS) production.[5] While *AvrLm1* had no effect on *Rlm7*-mediated resistance, *AvrLm4* had a subtle effect in

enhancing ETD, although background effects of *L. maculans* isolates could not be excluded.

2 MATERIALS AND METHODS

2.1 Plant, pathogen growth and inoculation

Spring (Topas DH16516, Topas-*LepR3*, Topas-*Rlm4*, Topas-*Rlm7*) and winter (Capitol with *Rlm1* and Excel with *Rlm7*) oilseed rape cultivars/lines were used (Table 1). Seedlings were pre-germinated on filter paper and grown using a mixture of general-purpose compost (Miracle-Gro; Evergreen Garden Care, Cardiff, UK) and John Innes No 3 compost (J Arthur Bowers; Westland Horticulture Ltd, Huntingdon, UK) as described.[35] Controlled environment (CE) chambers (Fitoclima 1200; Aralab, Rio de Mouro, Portugal) were set to a 12 h:12 h, light: dark photoperiod with a light intensity of 250 μmol m^{-2} s^{-1}. Seedlings were grown for 10 days before inoculation.

Leptosphaeria maculans isolates were grown from conidial glycerol stocks stored at –80 °C. The isolates used were v23.11.9 (*AvrLm1*, *avrLm4-AvrLm7*) and v23.2.1 (*avrLm1*, *AvrLm4-AvrLm7*), derived from a single cross,[36] v29.3.1 (*avrLm1*, *avrLm4-AvrLm7*) and its transformed isogenic strains v29.3.1-T2 and v29.3.1-T3 (*AvrLm1*, *avrLm4-AvrLm7*),[17] and isolate 99–79 (*avrLm1*, *AvrLm2*, *AvrLm4-AvrLm7*)[11] (Table 1). Conidial suspensions were prepared from sporulating cultures on V8 agar.[37] A conidial suspension (10^5 mL^{-1}) was used to infiltrate the abaxial surface of cotyledons with a volume of 10 μL on both sides of the midrib. Inoculated seedlings were kept for 24 h in darkness at 100% humidity in CE chambers (Conviron, Isleham, USA) before re-establishing standard growth conditions.[35] To investigate gene expression, cotyledons were sampled and immediately frozen in liquid nitrogen (N_2) at the same time of the day as the inoculation occurred to avoid diurnal fluctuations.

Table 1. *Brassica napus* cultivars and *Leptosphaeria maculans* isolates used in this study

Cultivar/line or isolate	Description (*Rlm/AvrLm* genes)	Reference
B. napus		
Capitol	Winter oilseed rape; *Rlm1*	Gout et al. (2006)
Excel	Winter oilseed rape; *Rlm7*	Mitrousia et al. (2018)
Topas DH16516	Spring oilseed rape	Larkan et al. (2016)
Topas-*LepR3*	Introgression line with *LepR3*	Larkan et al. (2016)
Topas-*Rlm4*	Introgression line with *Rlm4*	Larkan et al. (2016)
Topas-*Rlm7*	Introgression line with *Rlm7*	Haddadi et al. (2022)
L. maculans		
v23.2.1	*avrLm1*, *avrLm2*, *AvrLm4-AvrLm7*, *AvrLm5*, *AvrLm6*, *AvrLm8*	Rouxel et al. (2003)
v23.11.9	*AvrLm1*, *avrLm2*, *avrLm4-AvrLm7*, *AvrLm5*, *AvrLm6*, *AvrLm8*	Balesdent et al. (2001)
v29.3.1	*avrLm1*, *AvrLm2*, *avrLm4-AvrLm7*	Gout et al. (2006)
v29.3.1-T2	*AvrLm1*, *AvrLm2*, *avrLm4-AvrLm7*	Gout et al. (2006)
v29.3.1-T3	*AvrLm1*, *AvrLm2*, *avrLm4-AvrLm7*	Gout et al. (2006)
99–79	*avrLm1*, *AvrLm2*, *AvrLm4-AvrLm7*	Mitrousia et al. (2018)

241

Seedlings also were wound-inoculated, following standard procedures.[7] For this purpose, plants were grown in a CE chamber (Conviron A1000) with a 16 h:8 h, light:dark photoperiod. Each cotyledon was marked, removing a small plug of leaf tissue with a sterile Pasteur pipet. Cotyledons then were wounded to the left and right of the midrib and inoculated with a droplet of conidial suspension (10^7 mL^{-1}). Incubation and further plant growth were as described. Disease was scored on a scale of 1 to 9 as reported previously.[11]

2.2 Phenotypic assessment and image analysis

A GXM XTC3A1 stereo microscope (GT Vision, Stansfield, UK) was used to obtain images of cotyledons with pycnidia. Numbers of pycnidia were determined using the Cell Counter Plugin for ImageJ;[38] two individuals counted pycnidia independently and a consensus was made. Lesions observed on the abaxial surface of cotyledons were photographed and analyzed using ImageJ.[38] All images were processed equally after conversion to 8-bit. A ruler was used to set a scale of 1 cm. A light background of 20 was used for background subtraction. Threshold was set from 0 to 225. Particles were analyzed from 100 to infinity; circularity was 0.4 to 1.0. Numbers of lesions per cotyledon were determined as was total lesion area per cotyledon; F-tests and Student's t-tests were used to determine statistically significant differences.

2.3 qPCR experiments for gene expression

Plant tissue was ground to a powder in liquid N_2 and total RNA was extracted using TRI Reagent (Sigma-Aldrich, St Louis, MO, USA). RNA was quantified using NanoDrop 1000 (Thermo Fisher Scientific, Waltham, MA, USA), and RNA quality was assessed using agarose gel electrophoresis.[39] RNA was treated with RNase-Free DNase (Promega, Madison, WI, USA) and reverse-transcribed using M-MLV RT (H-) Point Mutant (Promega) using oligo-dT$_{15}$-VN. Sequences of the primers to amplify *PR-1*, *PDF1.2*, *WRKY70* and actin transcripts are listed in Supporting Information, Table S1.

Calibration standards were generated by amplifying cDNA and purifying products. Yeast tRNA (Sigma-Aldrich) was used as a carrier to generate dilution series of PCR products. Each 96-well plate contained calibration standards and samples analysed for a specific experiment. A Stratagene Mx3005P qPCR System (Agilent Technologies, Santa Clara, CA, USA) was used for PCR amplification and analysis. Two-step PCR parameters were: 95 °C for 15 s, 60 °C for 1 min for 40 cycles. The Relative Standard Curve Method was used to quantify gene expression because gene-specific differences in amplification efficiencies were observed. A minimum of three biological and two technical replicates was used. For all analyses, the same gene-specific thresholds were used for separate experiments. Relative differences in expression were Log_2-transformed for statistical analysis; the Shapiro–Wilk test for normality and the Bartlett's test for homogeneity of variances were used before ANOVA; alternatively, Student's t-tests were used. Nonparametric tests also were done using the Wilcoxon rank sum exact test and the Kruskal–Wallis rank sum test.

2.4 Histochemistry

3,3'-Diaminobenzidine (DAB)- and p-nitroblue tetrazolium (NBT)-staining were used for detection of H_2O_2 and superoxide radicals, respectively, following published procedures[40] with some modifications. Following DAB staining, tissues were cleared with lactic acid/glycerol/ethanol (1/1/1, v/v/v). ImageJ was used to convert images to 8-bit. Background was subtracted using a rolling ball

radius of 30 pixels. The threshold was adjusted from 0 to 220. Particles were analyzed with circularity from 0.2 to 1.0. Statistical analysis was done using ANOVA in Spss.

NBT-stained cotyledons were analyzed using ImageJ. Background was removed by adjusting the colour threshold to determine the total area of the cotyledons. Particles were analyzed with circularity values of 0.2 to 1.0. A colour threshold of 120 to 180, corresponding to blue colour, was applied to quantify the total area stained and subtract the green colour. Spss was used for statistical analysis using ANOVA.

3 RESULTS

3.1 Phenotypic analyses of resistance to *AvrLm1* isolates in *B. napus*

Leptosphaeria maculans isolates were used to differentiate the effects of *AvrLm1* and *AvrLm4-7* during incompatible interactions between *B. napus* genotypes and specific races of the pathogen (Table 1). The *L. maculans* isolates used were v23.2.1 (*avrLm1*, *AvrLm4-AvrLm7*) and v29.3.1 (*avrLm1*, *avrLm4-AvrLm7*) without *AvrLm1* and v23.11.9 (*AvrLm1*, *avrLm4-AvrLm7*) and transformed v29.3.1-T2 and v29.3.1-T3 with *AvrLm1*. The Topas DH16516 line (simply referred to as Topas), with no known *R* genes against *L. maculans*, was compared to resistant cv. Capitol, carrying *Rlm1*, cv. Excel, carrying *Rlm7*, and introgression lines Topas-
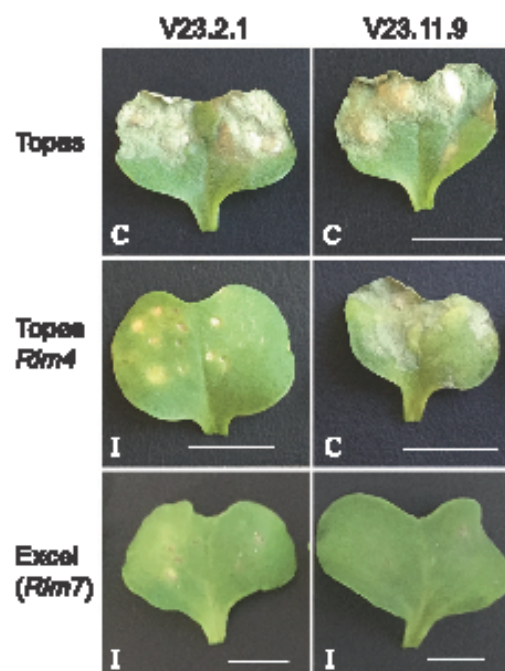
Figure 1. Phenotypic assessment of *Brassica napus* seedlings challenged with *Leptosphaeria maculans*. *L. maculans* isolates v23.2.1 (*avrLm1*, *AvrLm4-AvrLm7*) and v23.11.9 (*AvrLm1*, *avrLm4-AvrLm7*) and host genotypes Topas, Topas-*Rlm4* and cv. Excel (with *Rlm7*) were used. Both cotyledons of each seedling were infiltrated on both sides of the midrib. For illustration, cotyledons with average phenotypes were selected from a total of 10 cotyledons. Compatible (C) and incompatible (I) interactions are indicated. Scale bars are 1 cm; the size of the upper left cotyledon was not determined.

Pest Manag Sci 2023
© 2023 The Authors.
wileyonlinelibrary.com/journal/ps

Pest Management Science published by John Wiley & Sons Ltd on behalf of Society of Chemical Industry.

242
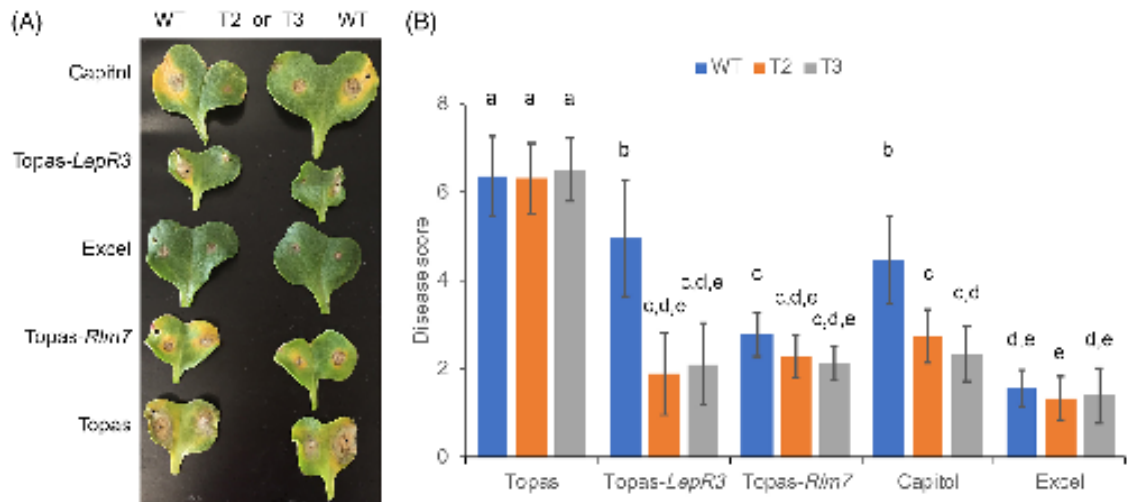
Figure 2. Phenotypic assessment of *Brassica napus* seedlings challenged with *Leptosphaeria maculans*. Isogenic *L. maculans* isolates used were v29.3.1 (*avrLm1, avrLm4-AvrLm7*) wild-type (WT) and isolates transformed with *AvrLm1*, v29.3.1-T2 (T2) and v29.3.1-T3 (T3); host genotypes used were Topas, Topas-LepR3, Topas-Rlm7, cv. Capitol (*Rlm1*) and cv. Excel (*Rlm7*). (A) Cotyledons of each seedling were wounded and inoculated with a droplet of conidia of WT, T2, T3 or WT at four sites. (B) Quantitative analysis of disease scores on a scale of 1 to 9. Means and standard deviations (*n* > 7) are indicated. Differences between means are based on Tukey's honestly significant difference with α < 0.05; different letters indicate significant differences.

LepR3, Topas-Rlm4 and Topas-Rlm7. Inoculation of susceptible Topas with isolates v23.11.9 or v23.2.1 resulted in spreading lesions (Fig. 1) and production of many pycnidia (Fig. S1). As predicted, Topas-Rlm4 was resistant against isolate v23.2.1 but susceptible to v23.11.9 (Fig. 1). The incompatible interaction in Topas-Rlm4 expressed itself on the adaxial leaf surface as discrete lesions (Fig. 1). The incompatible reaction of cv. Excel was less dramatic, resulting in resistance against both isolates v23.11.9 and v23.2.1 (Fig. 1). Despite incompatibility of cv. Excel against both v23.11.9 and v23.2.1, isolate-specific differences in size and frequencies of discrete lesions were observed (Fig. S2). Both frequency and size of discrete lesions on the abaxial leaf surface of cv. Excel were increased after infection with isolate v23.2.1 compared to isolate v23.11.9 (Fig. S2), but these isolate-specific effects were not statistically significant. Cotyledons subsequently were incubated under high humidity to determine the frequency of asexual sporulation. No significant differences between the incompatible interactions were observed regarding pycnidial numbers per inoculation or the frequency of asexual sporulation as determined by the production of cirrhi (Fig. S1). Thus, only subtle and not statistically significant phenotypic differences were observed between inoculations with isolates v23.2.1 and v23.11.9.

In order to determine whether these phenotypic findings were a result of using isolates with several genetic differences, isogenic isolates v29.3.1, v29.3.1-T2 and v29.3.1-T3 that differed only in a single effector gene as a result of transformation with *AvrLm1*[17] were used. The expression of symptoms [Fig. 2(A)] was consistent with that observed with genetically more diverse isolates (Fig. 1); both cv. Excel (with *Rlm7*) and Topas-Rlm7 were resistant against isolates v29.3.1 (without *AvrLm1*) and v29.3.1-T2 and v29.3.1-T3 (with *AvrLm1*) [Fig. 2(B)]. Statistical analysis of all different host genotypes clearly showed that significant differences in effector-dependent resistance were observed only when Topas-LepR3 and Capitol (*Rlm1*) were inoculated with isolates v29.3.1-T2 and v29.3.1-T3 that contained the corresponding *AvrLm1* effector (Fig. 2).

3.2 Isolate-dependent modulation of Rlm7-mediated defence gene expression

Induction of plant defence genes was studied 3, 5 and 7 days postinfiltration with pathogen (dpi) in Topas, introgression line Topas-Rlm4 and cv. Excel (with *Rlm7*). Three separate experiments to test defence gene expression were done (Table S2).

Expression of neither *PR-1* nor *WRKY70* was elevated at 3 dpi in Topas and cv. Excel (Fig. S3). Although a significant increase in *PR-1* expression was observed at 5 dpi, expression of this defence gene increased still further at 7 dpi, particularly when Topas-Rlm4 was challenged with *AvrLm4-AvrLm7*-containing isolate 99–79 (Fig. S4). *WRKY70* expression was significantly induced at 7 dpi when resistant cv. Excel was inoculated with isolate v23.2.1 (*avrLm1, AvrLm4-AvrLm7*) but not with v23.11.9 (*AvrLm1, avrLm4-AvrLm7*) (Fig. S3). In separate experiments, *PR-1* expression was significantly increased in resistant cultivars at 7 dpi [Figs 3(A) and S3]. *PR-1* expression was particularly strongly induced in Topas-Rlm4 when it was challenged with isolates containing the corresponding *AvrLm4-AvrLm7* gene [Figs 3(A) and S4]. Reproducibly, induction of *PR-1* expression was less when cv. Excel was challenged with v23.11.9 compared to v23.2.1, suggesting isolate-specific effects on the *Rlm7*-mediated defence response [Figs 3(a) and S3]. However, whereas induction of *PR-1* expression was less for v23.11.9 than for v23.2.1 when Topas-Rlm4 was inoculated [Fig. 3(A)], *PR-1* expression was not significantly different when cotyledons of cv. Excel were inoculated with either isolate (Student's *t*-test, *P* = 0.194; Wilcoxon, *P* = 0.229). Analysis of actin and *PR-1* expression revealed cultivar- ($F_{2,31}$ = 22.608, *P* < 0.001) and treatment-specific differences ($F_{3,31}$ = 9.423, *P* < 0.001), respectively. No cultivar-dependent differences in *PR-1* expression were observed ($F_{2,31}$ = 1.510, *P* = 0.237). Conversely, no treatment effects on actin expression were observed ($F_{2,31}$ = 0.722, *P* = 0.546). Of note, although pathogen inoculation with either v23.11.9 or v23.2.1 did not induce *PDF1.2* expression at 7 dpi in Topas, Topas-Rlm4 or cv. Excel, the expression of this gene was reduced when cv. Excel was challenged with v23.11.9 as compared to v23.2.1 [Fig. 3(B)].

(A)

(B)
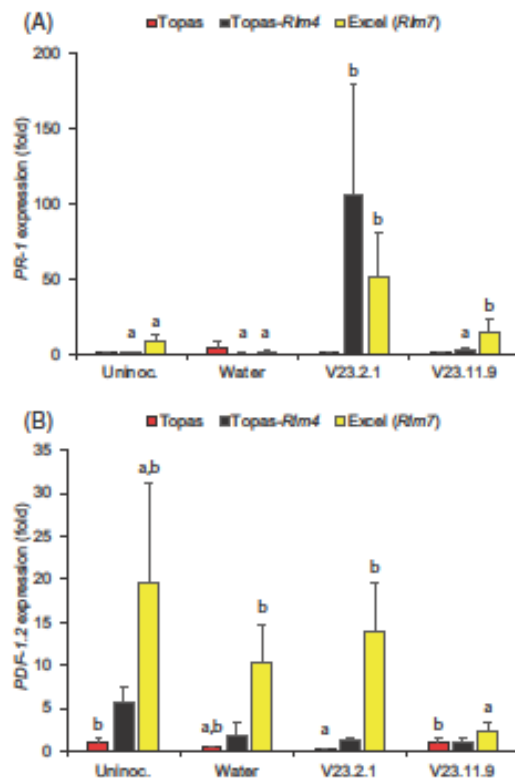
Figure 3. Defence-related gene expression in *Brassica napus* cotyledons challenged with *Leptosphaeria maculans*. RNA was extracted from cotyledons 7 days postinoculation for qPCR analysis. Topas, Topas-*Rlm4* and cv. Excel (*Rlm7*) were infiltrated with isolate v23.2.1 (*avrLm1*, *AvrLm4-AvrLm7*) or v23.11.9 (*AvrLm1*, *avrLm4-AvrLm7*), mock-infiltrated with water or not inoculated (Uninoc.). Relative quantification was used to determine (A) *PR-1* or (B) *PDF1.2* expression relative to actin as a control. Means and standard errors are shown (*n* = 3 to 4). Significant differences in *PR-1* expression between pathogen- and water-inoculation within cultivars were detected after log$_2$-transformation of relative expression values. A Student's *t*-test of log$_2$-transformed data was used to determine significant differences in *PDF1.2* expression. Different letters within genotype comparisons illustrate statistically significant differences (*P* < 0.05).

Collectively, data from independent experiments provide evidence that isolate-specific differences in effector composition modulate the defence-related gene expression; *PDF1.2* expression differs between those isolates in cv. Excel carrying the *Rlm7* gene, whereas *PR-1* expression significantly differs only in Topas-*Rlm4* (Fig. 3).

3.3 Isolate-specific modulation of *Rlm7*-mediated reactive oxygen species production

Dyes were used to monitor the production of ROS after inoculation of *B. napus* cultivars with *L. maculans* isolates v23.2.1 (*avrLm1*, *AvrLm4-AvrLm7*) or v23.11.9 (*AvrLm1*, *avrLm4-AvrLm7*). Little change in DAB staining, indicative of H$_2$O$_2$ production, occurred at 3 dpi in cotyledons of Topas or cv. Excel inoculated with either of these *L. maculans* isolates (Fig. S5). Likewsie, only a minor increase in DAB staining was evident

(A)

	Topas	Excel (*Rlm7*)
Water		
V23.2.1		
V23.11.9		

(B)
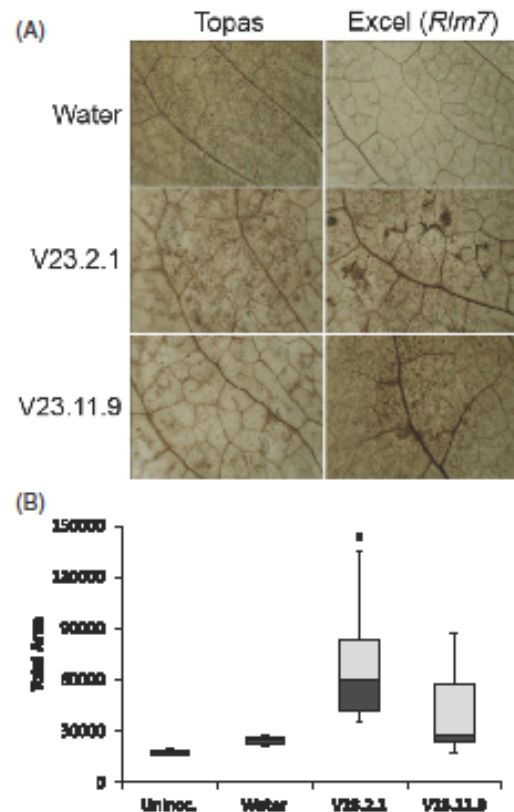
Figure 4. Diaminobenzidine staining of *Brassica napus* cotyledons challenged with *Leptosphaeria maculans*. (A) Micrographs of stained cotyledons at 7 days postinfiltration with water or *L. maculans* isolates v23.2.1 (*avrLm1*, *AvrLm4-AvrLm7*) or v23.11.9 (*AvrLm1*, *avrLm4-AvrLm7*). (B) Box plot of the staining intensity in uninoculated, water- or *L. maculans*-challenged cotyledons of cv. Excel (*Rlm7*). ImageJ was used measure total area (pixels). Sample sizes for controls (*n* = 6) and pathogen treatments (*n* = 12) are given. Asterisk indicates statistical significance (*P* < 0.05).

at 7 dpi of susceptible Topas with either *L. maculans* isolate [Figs 4(A) and S5]. A clearer indication of elevated H$_2$O$_2$ production was evident after inoculation with either isolate in stained cotyledon tissues of resistant cv. Excel [Fig. 4(A) and S5]. In the case of inoculation with *L. maculans* isolate v23.2.1 (*avrLm1*, *AvrLm4-AvrLm7*), a quantitatively significant increase in DAB staining was observed in cotyledons of cv. Excel at 7 dpi [Fig. 4(B)].

Infected cotyledons also were stained using NBT staining, indicative of superoxide formation. No changes in NBT staining were observed at 3 dpi with *L. maculans* but increases in NBT staining occurred in resistant cv. Excel at 7 dpi (Fig. S6). The largest increase in NBT staining was observed when cv. Excel was challenged with *L. maculans* isolate v23.2.1, but this suggestive increase in superoxide formation was not statistically significant. Together, however, these data imply that an oxidative burst occurs in response to *L. maculans* infection, especially when cv. Excel is challenged with *L. maculans* isolate v23.2.1 (*avrLm1*, *AvrLm4-AvrLm7*).

Table 2. Interactions between pathogen isolates and host genotypes

Pathogen isolate	Avr genes	Host genotype	R genes	Interaction
v23.2.1	avrLm1, AvrLm4-AvrLm7	Topas	None	Compatible
v23.2.1	avrLm1, AvrLm4-AvrLm7	Topas-Rlm4	Rlm4	Incompatible
v23.2.1	avrLm1, AvrLm4-AvrLm7	Excel	Rlm7	Incompatible
v23.11.9	AvrLm1, avrLm4-AvrLm7	Topas	None	Compatible
v23.11.9	AvrLm1, avrLm4-AvrLm7	Topas-Rlm4	Rlm4	Compatible
v23.11.9	AvrLm1, avrLm4-AvrLm7	Excel	Rlm7	Incompatible
v29.3.1	avrLm1, avrLm4-AvrLm7	Topas	None	Compatible
v29.3.1	avrLm1, avrLm4-AvrLm7	Topas-LepR3	LepR3	Compatible
v29.3.1	avrLm1, avrLm4-AvrLm7	Topas-Rlm7	Rlm7	Incompatible
v29.3.1	avrLm1, avrLm4-AvrLm7	Capitol	Rlm1	Compatible
v29.3.1-T2 or T3	AvrLm1, avrLm4-AvrLm7	Topas	None	Compatible
v29.3.1-T2 or T3	AvrLm1, avrLm4-AvrLm7	Topas-LepR3	LepR3	Incompatible
v29.3.1-T2 or T3	AvrLm1, avrLm4-AvrLm7	Topas-Rlm7	Rlm7	Incompatible
v29.3.1-T2 or T3	AvrLm1, avrLm4-AvrLm7	Capitol	Rlm1	Incompatible
99–79	avrLm1, AvrLm2, AvrLm4-AvrLm7	Topas	None	Compatible
99–79	avrLm1, AvrLm2, AvrLm4-AvrLm7	Topas-Rlm4	Rlm4	Incompatible

4 DISCUSSION

Our results show that irrespective of use of the diverse isolates v23.2.1 (*avrLm1, AvrLm4-AvrLm7*) and v23.11.9 (*AvrLm1, avrLm4-AvrLm7*) or transgenic isolates expressing *AvrLm1* in the background of v29.3.1 (*avrLm1, avrLm4-AvrLm7*), no significant phenotypic differences in recognition by the noncorresponding receptor *Rlm7* were observed (Figs 1 and 2; Table 2). However, defence gene expression (e.g. *PR1*) and production of ROS were greater when cv. Excel was challenged with v23.2.1 rather than v23.11.9 (Figs 3 and 4); this could have been caused by differences in effector gene composition or genetic background effects (Table 3).

It is unlikely that *AvrLm1* would have been responsible for these differences in defence responses because isogenic isolates with or without this effector gene did not influence resistance phenotypes in cv. Excel or Topas-*Rlm7*. Nevertheless, it should be mentioned that transformation of *Arabidopsis thaliana* with *AvrLm1* reduced *PR1* expression *in planta*.[31] Consequently, *AvrLm1*-transformed *A. thaliana* plants were more susceptible to the virulent *Pseudomonas syringae* strain Pst DC3000.[31]

It is more likely that *AvrLm4* triggered a stronger defence response in cv. Excel to isolate v23.2.1 than to isolate v23.11.9. In this context, near-isogenic isolates with *AvrLm4* were more aggressive than *avrLm4* mutants on susceptible host cultivars lacking *Rlm4*, suggesting a fitness penalty for virulent strains.[41] However, a single amino acid change resulting in loss of *AvrLm4-7* recognition by *Rlm4*[18] maintained effector function of *avrLm4-AvrLm7* isolates; *avrLm4-AvrLm7* isolates also containing *AvrLm3* or *AvrLm5-9* were virulent on *B. napus* lines with *Rlm3* or *Rlm9*, respectively.[34,42] The subtle differences in defence gene expression and ROS production reported here also could be the result of a combination of effects based on differences in *AvrLm1* and *AvrLm4* effector composition. Alternatively, different genetic backgrounds of v23.2.1 and v23.11.9 could have been responsible for the observed differences in defence responses.

A reduction in *PDF1.2* expression was observed when the v23.11.9 isolate was used for infection of cv. Excel relative to

isolate v23.2.1 [Fig. 3(B)]. The combination of jasmonic acid (JA) and ethylene regulates *PDF1.2* expression.[43,44] JA signalling was suppressed when *AvrLm1* was expressed in *A. thaliana*, although upregulation of JA signalling was observed when MPK9 was overexpressed in *B. napus*.[31]

Our results also show that ROS production is increased postinoculation with isolate v23.2.1 relative to v23.11.9 (Fig. 4). *AvrLm1* activates *PR1* expression, salicylic acid (SA) production and ROS accumulation during the incompatible interaction of *L. maculans* with cv. Columbus carrying the *Rlm1* gene.[30] Contrary to suppression of *PR1* expression by *AvrLm1*, activation of MPK9 leads to increased ROS production, cell death and disease susceptibility.[31] Our finding of less ROS production after inoculation with isolate v23.11.9 is therefore not in conflict with the finding that MPK9 increases ROS concentrations.[31] Although analysis of *Rlm7*-dependent defence responses with isogenic isolates differing in *AvrLm1* composition would be desirable, this was not justified because no phenotypic differences in disease resistance were observed (Fig. 2).

Alteration of host plant defence responses by noncorresponding effectors, such as *AvrLm1* on *Rlm7*-mediated resistance, may be of concern to the plant-breeding industry, considering the increased use of oilseed rape cultivars containing the *Rlm7* gene. In addition to *AvrLm7*, it is recommended to monitor other effector genes in *L. maculans* populations to avoid breakdown of *Rlm7* resistance. We recently noted that a reduction of the *AvrLm7* allele in *L. maculans* populations was correlated with a corresponding increase of the *AvrLm1* allele in *L. maculans* populations.[45,46] Disease management may therefore require development of *LepR3* cultivars to compensate for the decline in *Rlm7*-mediated resistance or use of different *R* genes for crop rotation.[13] Increases in *AvrLm1* have been observed previously after deployment of corresponding *LepR3*-mediated resistance was suspended in Australian cultivars[25]; both *AvrLm1* and *AvrLm4* incur fitness costs.[26,41] As a note of caution, because the correlations to previous studies were not strong (Table 3), different genetic backgrounds used for analysis of defence responses may have contributed to

Table 3. Comparison of different studies on the effects of Avrlm1 and Avrlm4 in enhancing susceptibility to or triggering resistance against *Leptosphaeria maculans* in susceptible and resistant hosts

	SA pathway			ET/JA pathway		JA pathway						
R genes and noncorresponding effectors[†]	PR1	WRKY70	SA	PDF1.2	HEL, CHI	JA	LOX2	AOS	H2O2	Susceptibility	Interaction	Reference
avrlm1,Avrlm4	Increase	Increase	N/A	Increase	N/A*	N/A	N/A	N/A	Increase	Level	Incompatible	This study
Avrlm1,avrlm4	Decrease	N/A	N/A	Decrease	N/A	N/A	N/A	N/A	Decrease	Level	Incompatible	This study
Avrlm1	Increase	Increase	Increase	N/A	Increase	Level	N/A	N/A	Increase	Decrease	Incompatible	Saek et al., 2012
Avrlm1	N/A	N/A	N/A	N/A	N/A	N/A	N/A	N/A	N/A	N/A	Compatible	Saek et al., 2012
Avrlm1 OE At[†]	Decrease	N/A	N/A	N/A	N/A	N/A	Decrease	Decrease	N/A	Increase	Heterologous system	Ma et al., 2018
Avrlm1 transient Nb[†]	N/A	N/A	N/A	N/A	N/A	N/A	N/A	N/A	N/A	N/A	Heterologous system	Ma et al., 2018
BnMPK9 OE Bn[†]	Decrease	Decrease	N/A	N/A	N/A	N/A	N/A	Increase	Increase	Increase	Compatible	Ma et al., 2018
Avrlm4	N/A	N/A	N/A	N/A	N/A	N/A	N/A	N/A	N/A	Increase	Compatible	Huang et al., 2006
Avrlm4	Decrease	N/A	Decrease	N/A	Decrease	Level	N/A	N/A	Decrease	Increase	Compatible	Novakova et al., 2016

*Not available.
† *Arabidopsis thaliana* (At), *Nicotiana benthamiana* (Nb), *Brassica napus* (Bn), overexpression (OE), transient expression (transient).

the observed molecular changes in isolates varying in *AvrLm1* and *AvrLm4*.

CONFLICT OF INTEREST

The authors have no conflict of interest to declare.

DATA AVAILABILITY STATEMENT

The data that support the findings of this study are available from the corresponding author upon reasonable request.

SUPPORTING INFORMATION

Supporting information may be found in the online version of this article.

REFERENCES

1 Stotz HU, Mitrousia GK, PJ de Wit and Fitt BDL, Effector-triggered defence against apoplastic fungal pathogens. *Trends Plant Sci* **19**: 491–500 (2014).
2 Spatafora JW, Aime MC, Grigoriev IV, Martin F, Stajich JE and Blackwell M, The fungal tree of life: from molecular systematics to genome-scale phylogenies. *Microbiol Spectrum* **5**:1–34 (2017).
3 de Gruyter J, Woudenberg JH, Aveskamp MM, Verkley GJ, Groenewald JZ and Crous PW, Redisposition of phoma-like anamorphs in Pleosporales. *Stud Mycol* **75**:1–36 (2013).
4 Fitt BDL, Hu BC, Li ZQ, Liu SY, Lange RM, Kharbanda PD et al., Strategies to prevent spread of *Leptosphaeria maculans* (phoma stem canker) onto oilseed rape crops in China; costs and benefits. *Plant Pathol* **57**:652–664 (2008).
5 Huang YJ, Fitt BDL, Jedryczka M, Dakowska S, West JS, Gladders P et al., Patterns of ascospore release in relation to phoma stem canker epidemiology in England (*Leptosphaeria maculans*) and Poland (*Leptosphaeria biglobosa*). *Eur J Plant Pathol* **111**:263–277 (2005).
6 Elliott CE, Harjono and Howlett BJ, Mutation of a gene in the fungus *Leptosphaeria maculans* allows increased frequency of penetration of stomatal apertures of *Arabidopsis thaliana*. *Mol Plant* **1**:471–481 (2008).

7 Huang YJ, Toscano-Underwood C, Fitt BDL, Hu XJ and Hall AM, Effects of temperature on ascospore germination and penetration of oilseed rape (Brassica napus) leaves by A- or B-group Leptosphaeria maculans (phoma stem canker). Plant Pathol 52:245–255 (2003).

8 Larkan NJ, Lydiate DJ, Parkin IA, Nelson MN, Epp DJ, Cowling WA et al., The Brassica napus blackleg resistance gene LepR3 encodes a receptor-like protein triggered by the Leptosphaeria maculans effector AVRLM1. New Phytol 197:595–605 (2013).

9 Rouxel T and Balesdent MH, From model to crop plant-pathogen interactions: cloning of the first resistance gene to Leptosphaeria maculans in Brassica napus. New Phytol 197:356–358 (2013).

10 Fitt BDL, Brun H, Barbetti MJ and Rimmer SR, World-wide importance of phoma stem canker (Leptosphaeria maculans and L. biglobosa) on oilseed rape (Brassica napus). Eur J Plant Pathol 114:3–15 (2006).

11 Huang YJ, Mitrousia GK, Sidique SNM, Qi A and Fitt BDL, Combining R gene and quantitative resistance increases effectiveness of cultivar resistance against Leptosphaeria maculans in Brassica napus in different environments. PLoS One 13:e0197752 (2018).

12 Raman H, Raman R and Larkan N, Genetic dissection of blackleg resistance loci in rapeseed (Brassica napus L.), in Plant Breeding from Laboratories to Fields, ed. by Andersen SB. InTech, pp. 85–120 (2013). http://doi.org/10.5772/53611

13 Van de Wouw AP and Howlett BJ, Advances in understanding the Leptosphaeria maculans - Brassica pathosystem and their impact on disease management. Can J Plant Pathol 42:149–163 (2020).

14 Raman H, Raman R, Qiu Y, Zhang Y, Batley J and Liu S, The Rlm13 gene, a new player of Brassica napus-Leptosphaeria maculans interaction maps on chromosome C03 in canola. Front Plant Sci 12:654604 (2021).

15 Larkan NJ, Ma L, Haddadi P, Buchwaldt M, Parkin IAP, Djavaheri M et al., The Brassica napus wall-associated kinase-like (WAKL) gene Rlm9 provides race-specific blackleg resistance. Plant J 104:892–900 (2020).

16 Haddadi P, Larkan NJ, Van de Wouw A, Zhang Y, Neik TX, Beynon E et al., Brassica napus genes Rlm4 and Rlm7, conferring resistance to Leptosphaeria maculans, are alleles of the Rlm9 wall-associated kinase-like resistance locus. Plant Biotechnol J 20:1229–1231 (2022).

17 Gout L, Fudal I, Kuhn M-L, Blaise F, Eckert M, Cattolico L et al., Lost in the middle of nowhere: the AvrLm1 avirulence gene of the Dothideomycete Leptosphaeria maculans. Mol Microbiol 60:67–80 (2006).

18 Parlange F, Daverdin G, Fudal I, Kuhn ML, Balesdent MH, Blaise F et al., Leptosphaeria maculans avirulence gene AvrLm4-7 confers a dual recognition specificity by the Rlm4 and Rlm7 resistance genes of oilseed rape, and circumvents Rlm4-mediated recognition through a single amino acid change. Mol Microbiol 71:851–863 (2009).

19 Degrave A, Wagner M, George P, Coudard L, Pinochet X, Ermel M et al., A new avirulence gene of Leptosphaeria maculans, AvrLm14, identifies a resistance source in American broccoli (Brassica oleracea) genotypes. Mol Plant Pathol 22:1599–1612 (2021).

20 Xiang Neik T, Ghanbarnia K, Ollivier B, Scheben A, Severn-Ellis A, Larkan NJ et al., Two independent approaches converge to the cloning of a new Leptosphaeria maculans avirulence effector gene, AvrLmS-Lep2. Mol Plant Pathol 23:733–748 (2022).

21 Jiquel A, Gervais J, Geistodt-Kiener A, Delourme R, Gay EJ, Ollivier B et al., A gene-for-gene interaction involving a 'late' effector contributes to quantitative resistance to the stem canker disease in Brassica napus. New Phytol 231:1510–1524 (2021).

22 Rouxel T, Grandaubert J, Hane JK, Hoede C, van de Wouw AP, Couloux A et al., Effector diversification within compartments of the Leptosphaeria maculans genome affected by repeat-induced point mutations. Nat Commun 2:202 (2011).

23 Rouxel T, Penaud A, Pinochet X, Brun H, Gout L, Delourme R et al., A 10-year survey of populations of Leptosphaeria maculans in France indicates a rapid adaptation towards the Rlm1 resistance gene of oilseed rape. Eur J Plant Pathol 109:871–881 (2003).

24 Sprague SJ, Marcroft SJ, Hayden HL and Howlett BJ, Major gene resistance to blackleg in Brassica napus overcome within three years of commercial production in southeastern Australia. Plant Dis 90:190–198 (2006).

25 Marcroft SJ, Elliott VL, Cozijnsen AJ, Salisbury PA, Howlett BJ and Van de Wouw AP, Identifying resistance genes to Leptosphaeria maculans in Australian Brassica napus cultivars based on reactions to isolates with known avirulence genotypes. Crop Pasture Sci 63:338–350 (2012).

26 Huang YJ, Balesdent MH, Li ZQ, Evans N, Rouxel T and Fitt BDL, Fitness cost of virulence differs between the AvrLm1 and AvrLm4 loci in Leptosphaeria maculans (phoma stem canker of oilseed rape). Eur J Plant Pathol 126:279–291 (2010).

27 Ma L and Borhan MH, The receptor-like kinase SOBIR1 interacts with Brassica napus LepR3 and is required for Leptosphaeria maculans AvrLm1-triggered immunity. Front Plant Sci 6:933 (2015).

28 Sasek V, Novakova M, Jindrichova B, Boka K, Valentova O and Burketova L, Recognition of avirulence gene Avr.Lm1 from hemibiotrophic ascomycete Leptosphaeria maculans triggers salicylic acid and ethylene signaling in Brassica napus. Mol Plant Microbe Interact 25:1238–1250 (2012).

29 Chisholm ST, Coaker G, Day B and Staskawicz BJ, Host-microbe interactions: shaping the evolution of the plant immune response. Cell 124:803–814 (2006).

30 Novakova M, Sasek V, Trda L, Krutinova H, Mongin T, Valentova O et al., Leptosphaeria maculans effector AvrLm4-7 affects salicylic acid (SA) and ethylene (ET) signalling and hydrogen peroxide (H₂O₂) accumulation in Brassica napus. Mol Plant Pathol 17:818–831 (2016).

31 Ma L, Djavaheri M, Wang H, Larkan NJ, Haddadi P, Beynon E et al., Leptosphaeria maculans effector protein AvrLm1 modulates plant immunity by enhancing MAP kinase 9 phosphorylation. iScience 3:177–191 (2018).

32 Houterman PM, Cornelissen BJ and Rep M, Suppression of plant resistance gene-based immunity by a fungal effector. PLoS Pathog 4:e1000061 (2008).

33 Plissonneau C, Blaise F, Ollivier B, Leflon M, Carpezat J, Rouxel T et al., Unusual evolutionary mechanisms to escape effector-triggered immunity in the fungal phytopathogen Leptosphaeria maculans. Mol Ecol 262:183–2198 (2017).

34 Ghanbarnia K, Ma L, Larkan NJ, Haddadi P, Fernando WGD and Borhan MH, Leptosphaeria maculans AvrLm9: a new player in the game of hide and seek with AvrLm4-7. Mol Plant Pathol 19:1754–1764 (2018).

35 Sewell TR, Hawkins NJ, Stotz HU, Huang Y, Kelly SL, Kelly DE et al., Azole sensitivity in Leptosphaeria pathogens of oilseed rape: the role of lanosterol 14alpha-demethylase. Sci Rep 7:15849 (2017).

36 Balesdent MH, Attard A, Ansan-Melayah D, Delourme R, Renard M and Rouxel T, Genetic control and host range of avirulence toward Brassica napus cultivars Quinta and Jet Neuf in Leptosphaeria maculans. Phytopathology 91:70–76 (2001).

37 Ansan-Melayah D, Balesdent MH, Buree M and Rouxel T, Genetic characterization of AvrLm1, the first avirulence gene of Leptosphaeria maculans. Phytopathology 85:1525–1529 (1995).

38 Schneider CA, Rasband WS and Eliceiri KW, NIH image to ImageJ: 25 years of image analysis. Nat Methods 9:671–675 (2012).

39 Sambrook J, Fritsch EF and Maniatis T, Molecular Cloning: A Laboratory Manual. Cold Spring Harbor, New York (1989).

40 Guo X and Stotz HU, Defense against Sclerotinia sclerotiorum in Arabidopsis is dependent on jasmonic acid, salicylic acid, and ethylene signaling. Mol Plant Microbe Interact 20:1384–1395 (2007).

41 Huang YJ, Li ZQ, Evans N, Rouxel T, Fitt BDL and Balesdent MH, Fitness cost associated with loss of the AvrLm4 avirulence function in Leptosphaeria maculans (phoma stem canker of oilseed rape). Eur J Plant Pathol 114:77–89 (2006).

42 Plissonneau C, Daverdin G, Ollivier B, Blaise F, Degrave A, Fudal I et al., A game of hide and seek between avirulence genes AvrLm4-7 and AvrLm3 in Leptosphaeria maculans. New Phytol 209:1613–1624 (2016).

43 Becker MG, Zhang X, Walker PL, Wan JC, Millar JL, Khan D et al., Transcriptome analysis of the Brassica napus-Leptosphaeria maculans pathosystem identifies receptor, signaling and structural genes underlying plant resistance. Plant J 90:573–586 (2017).

44 Zander M, La Camera S, Lamotte O, Metraux JP and Gatz C, Arabidopsis thaliana class-II TGA transcription factors are essential activators of jasmonic acid/ethylene-induced defense responses. Plant J 61:200–210 (2010).

45 Gajula LH, Understanding R Gene-Mediated Resistance against Leptosphaeria Maculans for Effective Control of Phoma Stem Canker in Oilseed Rape. PhD thesis. PhD. University of Hertfordshire, Hatfield AL10 9AB (2019).

46 Noel K, Qi A, Gajula LH, Padley C, Rietz S, Huang Y-J et al., Influence of elevated temperatures on resistance against phoma stem canker in oilseed rape. Front Plant Sci 13:785804 (2022).

3

Genetic basis of partial resistance against *Pyrenopeziza brassicae* in oilseed rape

AJISA M ALI, HEATHER FELL, BRUCE D L FITT, FREDERIC BEAUDOIN and
HENRIK U STOTZ

*Centre for Agriculture, Food and Environmental Management, School of Life and Medical
Sciences, University of Hertfordshire, Hatfield, AL10 9AB, UK*
Corresponding Author Email: a.muthayil-ali@herts.ac.uk

Introduction

Light leaf spot (LLS) caused by *Pyrenopeziza brassicae* is the most damaging disease of oilseed rape (*Brassica napus*) in the UK. The disease accounts for up to £160M yield loss annually in England, despite expenditure of £20M on fungicides, and the severity of the disease is much greater in Scotland (Karandeni Dewage *et al.*, 2018; Ashby, 1997). In the UK, the disease has been increasing as a national problem in recent decades, rather than just being confined to Scotland and northern England.

LLS is currently controlled by a combination of cultivar resistance, fungicide applications and cultural practices. However, resistance mechanisms of the oilseed rape plant against *P. brassicae* are not well understood. Furthermore, fungicide control is problematic as the pathogen has developed insensitivity to triazole and MBC fungicides (Carter *et al.*, 2013; Carter *et al.*, 2014). Thus, it is necessary to identify the genes involved in quantitative resistance of *Brassica napus* to design an improved and durable control strategy against LLS. The aim of this project is to better understand (i) the genes involved in quantitative resistance against *P. brassicae* in oilseed rape and (ii) the contribution of the host wax/cuticle to this host-pathogen interaction.

Materials and methods

A phenotypic screen for LLS susceptibility was done in glasshouse experiments using 195 accessions of *B. napus*. In collaboration with the John Innes Centre, this screen was used together with an associative transcriptomics pipeline (http://www.yorknowledgebase.info) to identify gene expression markers (GEMs). Experiments will be done using TILLING mutants to confirm the involvement of specific GEMs in quantitative resistance.

Trypan blue staining and scanning electron microscopy (SEM) were used to monitor the pathogen during the infection process and to determine time points for gene expression analysis. Wax and cutin were quantified and the components were compared to assess the role of these components in host resistance or susceptibility. *B. rapa* wax mutants and resistant and/or susceptible *B. napus* accessions were used for this purpose. Furthermore, toluidine blue staining was used to compare these accessions/mutants for cuticle permeability and host resistance. Cutinase expression will be analysed to determine whether wax/cutin components can affect the expression of this gene implicated in pathogenicity.

Results

Eight GEMs were expressed differently in accessions susceptible or resistant to *P. brassicae*; among these genes were cinnamate 4-hydroxylase, beta-adaptin and KIN10, a SNF1 kinase homolog. Genotyping and phenotyping of TILLING mutants which have been obtained (J130317a, J130819a, JI30010-b, J1320204a and JI31647b) will establish the role of these genes in resistance against *P. brassicae*. SEM showed that the pathogen germinates 1-day post-inoculation (dpi) on leaf surfaces, penetrates the cuticle by 2 dpi and colonises the subcuticular layer by 8 dpi.

Discussion

Wax and cutin analysis of wax mutants, together with cutinase expression in these mutant and wild-type plants, will provide host data corresponding to the role of cutinase in pathogenicity. Li *et al.*, (2003) have shown that a cutinase-deficient mutant of *P. brassicae* was unable to penetrate the cuticle and asexually propagate on oilseed rape. Together with the GEM data, this will help crop breeders to develop oilseed rape with better protection against *P. brassicae*.

References

Ashby AM. 1997. A molecular view through the looking glass: The *Pyrenopeziza brassicae-Brassica* interaction. *Advances in Botanical Research* **24**:31-70.

Carter HE, Cools HJ, West JS, Shaw MW, Fraaije BA. 2013. Detection and molecular characterisation of *Pyrenopeziza brassicae* isolates resistant to methyl benzimidazole carbamates. *Pest Management Science* **69**:1040–1048. https://doi.org/10.1002/ps.3585

Carter HE, Fraaije BA, West JS, Kelly S L, Mehl A, Shaw MW, Cools HJ. 2014. Alterations in the predicted regulatory and coding regions of the sterol 14α-deethylase gene (*CYP51*) confer decreased azole sensitivity in the oilseed rape pathogen *Pyrenopeziza brassicae*. *Molecular Plant Pathology* **15**:513–522. https://doi.org/10.1111/mpp.12106

Karandeni Dewage CS, Klöppel CA, Stotz HU, Fitt BDL. 2018. Host-pathogen interactions in relation to management of light leaf spot disease (caused by *Pyrenopeziza brassicae*) on *Brassica* species. *Crop and Pasture Science* **69**:9–19. https://doi.org/10.1071/CP16445

Li D, Ashby AM, Johnstone K. 2003. Molecular evidence that the extracellular cutinase *Pbc1* is required for pathogenicity of *Pyrenopeziza brassicae* on oilseed rape. *Molecular Plant-Microbe Interactions* **16**:545–552.

Acknowledgements

4a

Genetic basis of partial resistance against *Pyrenopeziza brassicae* in Oilseed Rape

Ajisa Ali[1] Bruce D.L Fitt[2] and Henrik U. Stotz[3]

1. PhD student, Centre for Agriculture, Food and environmental Management, University of Hertfordshire, Hatfield, UK AL10 9AB
2. Professor, Centre for Agriculture, Food and environmental Management, University of Hertfordshire, Hatfield, UK AL10 9AB
3. Reader in Crop Protection, Centre for Agriculture, Food and environmental Management University of Hertfordshire, Hatfield, UK, AL10 9AB

University of Hertfordshire **UH**

Life and Medical Science

Introduction

❖ Light leaf spot (LLS), caused by the hemi-biotrophic pathogen *Pyrenopeziza brassicae*, is the most damaging disease of oilseed rape in the UK.

❖ Many studies indicate that wet and cold weather favours pathogen development. However, a recent LLS disease survey (Figure 1) by Agriculture and Horticulture Development Board (AHDB) shows that the severity of the disease has increased across UK despite an increase in temperature.

Figure 1: LLS survey map by AHDB from 2013-2018 in UK.

Aim

❖ To study the *Brassica napus* and *P. brassicae* pathosystem.

Objectives

❖ To study crop resistance mechanisms against *P. brassicae*.

❖ To analyse pathogen population diversity and dynamics.

Materials and Methods

Spray inoculated 21 days old susceptible cultivars Marathon, Cabriolet, Apex, Bristol and Eurol with 10^5 ml of *P. brassicae* spore suspension produced from original stock collected on 23/05/2017 from Rothamsted, UK.

↓

Incubated at 16^0 for 12 hours with day light and 14^0C for 12 hours in darkness for 21 days.

↓

Stored harvested plants at 4^0C for 10 days.

Results

Figure 2a: Marathon showing leaf deformation

Figure 2b: Green island formation in Cabriolet.

Figure 2c: Apex (1), Bristol (2) and Eurol (3) with visible conidiospores.

Discussion

Visible progression of pathogen growth in *B. napus* cultivars
❖ Leaf deformation (Figure 2a) and green island formation (Figure 2b) by 7dpi suggests possible involvement of cytokinins (Ashby, 1997).

❖ Conidiospores appearance on leaf surface (from 16dpi) suggests that the pathosystem colonises susceptible hosts.

Works in progress

❖ Analysis of *P. brassicae* extracellular vesicles from media.

❖ Screening the model plant *Arabidopsis thaliana* for any resistance against *P. brassicae*.

❖ Field study to understand the genetic basis of host resistance and compare the genetic variations of pathogen populations.

250

4b

Genetic basis of partial resistance against *Pyrenopeziza brassicae* in oilseed rape

Ajisa **ALI**, Bruce D L Fitt, Henrik U Stotz

School of Life and Medical Sciences, University of Hertfordshire, Hatfield, AL10 9AB, UK

Light leaf spot (LLS) caused by the hemibiotroph *Pyrenopeziza brassicae* is the most damaging disease of oilseed rape (*Brassica napus*) in UK. The disease is accountable for up to £160M yield loss annually in England, despite spending of £20M on fungicides, and the severity of the disease is much greater in Scotland. In the UK, the disease has been increasing and has become a national problem in last decades rather than just being confined to Scotland and Northern England. LLS is currently controlled by a combination of cultivar resistance, fungicide applications and cultural practices. However, the resistance mechanism of the oilseed rape plant against *P. brassicae* is not understood well. Furthermore, fungicide control is problematic as the pathogen has developed insensitivity to methyl benzimidazole carbamate and triazole fungicides (Carter et al., 2013). Therefore, this study aims to achieve a greater understanding of crop resistance mechanisms against *P. brassicae* and pathogen population diversity and dynamics, to design a sustainable control strategy against LLS.

References: Carter HE et al. (2013). *Pest Management Science*, 69 (9), 1040–1048; Dewage CSK et al. (2018). *Crop and Pasture Science*, 69 (1), 9–19.

a.muthayil-ali@herts.ac.uk

5a

University of Hertfordshire UH

Life and Medical Science

Genetic basis of partial resistance against *Pyrenopeziza brassicae* in oilseed rape

Ajisa Ali[1] Bruce D.L. Fitt[2] Frederic Beaudoin[3] Henrik U. Stotz[4]

1. PhD student, Centre for Agriculture, Food and Environmental Management, University of Hertfordshire, Hatfield, UK AL10 9AB
2. Professor, Centre for Agriculture, Food and Environmental Management, University of Hertfordshire, Hatfield, UK AL10 9AB
3. Senior Scientist, Rothamsted Research, West Common, Harpenden AL5 2JQ
4. Reader in Crop Protection, Centre for Agriculture, Food and Environmental Management University of Hertfordshire, Hatfield, UK, AL10 9AB

Introduction

❖ Light leaf spot (LLS), caused by the pathogen *Pyrenopeziza brassicae*, is the most damaging disease of oilseed rape in the UK.

❖ LLS accounts for up to £160M annual yield loss despite expenditure of £20M on fungicides.

❖ This disease is controlled by fungicide applications and partially resistant cultivars (AHDB recommendation lists).

❖ *P. brassicae* has developed fungicide insensitivity.

❖ Better understanding of quantitative resistance (QR) against *P. brassicae* in oilseed rape is important in designing improved and durable control strategy against LLS.

Aim

❖ To study genes involved in QR in oilseed rape against *P. brassicae*.
❖ To understand the contribution of host wax/cuticle to this pathosystem.

Objectives

❖ To screen *B. napus* accessions and *B. rapa* wax mutants under glasshouse conditions.
❖ To assess cuticle permeability of *B. rapa* wax mutants using toluidine blue staining.

Materials and Methods

❖ 195 *B. napus* cultivars were spray inoculated with a *P. brassicae* spore suspension. Disease were scored on a scale of 1-6 (Fig.1).
❖ Associative transcriptomics was used to identify 8 genes that were differently expressed in partially resistant and susceptible accessions.
❖ Scanning electron microscopy was done to track pathogen and decide future gene expression works.
❖ Toluidine blue staining were done before and after inoculation with pathogen on *B. rapa* wax mutants.

Results
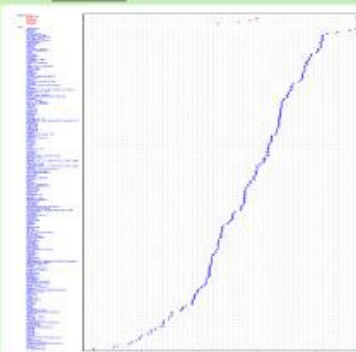
Figure 1: LLS disease scoring of 195 *B. napus* accessions
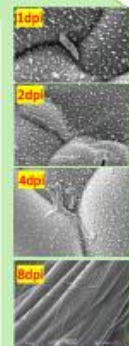
Figure 2: SEM results on susceptible *B. napus* cabriolet

Figure 3: Toluidine blue staining with wild type R-O-18, two glaucous (GL) and non-glaucous (NG) mutants of *B. rapa* from top left to bottom

Untreated / Water and Silwet / Inoculated

Discussion

❖ The four most susceptible (Dwarf Essex, Laser, Sansibar and Cabriolet) and resistant (POSH, SWU Chinese1, Cubs Root and Moana) cultivars were chosen from glasshouse results for further experiments.
❖ R-O-18 and NG (more wax) showed more permeability and susceptibility.
❖ GL (less wax) was less permeable and more resistant.

Works in progress

❖ Gene expression using multiplex Taqman qPCR to study the expression of GEMs during the interaction with *P. brassicae*.
❖ KASP primer analysis of *B. rapa* TILLING mutants to confirm the involvement of GEMs in partial resistance against *P. brassicae*.
❖ Quantification of pathogen DNA.
❖ Analysis of wax and cutin quantities and compositions in pathogen challenged *B. napus* leaves with differences in susceptibility to *P. brassicae* and in and *B. rapa* wax mutants.

Acknowledgements

5b

POSTER   amuthayil-ali@herts.ac.uk

Genetic basis of partial resistance against *Pyrenopeziza brassicae* in oilseed rape

Ajisa Muthayil ALI, Stotz, H

University of Hertfordshire

Light leaf spot (LLS) caused by *Pyrenopeziza brassicae* is the most damaging disease of oilseed rape (*Brassica napus*) in the UK. The disease accounts for up to £160M yield loss annually in England and Wales, despite expenditure of £20M on fungicides, and the severity of the disease is much greater in Scotland. In the UK, the disease has been increasing as a national problem in recent years rather than just being confined to Scotland and Northern England. LLS is currently controlled by a combination of cultivar resistance, fungicide applications and cultural practices. However, resistance mechanisms of the oilseed rape plant against P. brassicae are not well understood. Furthermore, fungicide control is problematic as the disease remains asymptomatic from autumn until spring and the pathogen has developed insensitivity to triazole and MBC fungicides. Thus, it is necessary to identify the genes involved in quantitative resistance of B. napus to design an improved and durable control strategy against LLS. The aim of this project is to better understand the genes involved in quantitative resistance against *P. brassicae* in oilseed rape. A phenotypic screen for LLS susceptibility was done in glasshouse experiments using 195 accessions of B. *napus*. In collaboration with the John Innes Centre, this screen was used together with an associative transcriptomics pipeline to identify gene expression markers (GEMs). Scanning electron microscopy (SEM) were used to monitor the pathogen during infection process and to determine time points for gene expression analysis. SEM showed that the pathogen germinates 1-day post-inoculation (dpi) on leaf surfaces, penetrates the cuticle by 2dpi and colonises the subcuticular layer by 8 dpi. Eight GEMs were expressed differently in accessions susceptible or resistant to P. brassicae. Characterisation of gene expression and function will aid crop breeders to develop oilseed rape with better protection against *P. brassicae*.